Integrated studies of the interactions of macrophages with synthetic hydrogels

Submitted as part of the requirements for the award of the degree of Doctor of Philosophy

Andrew D. McKenzie

Acknowledgements

This PhD project has been a long journey and I could not have made it without the help of a great many people. To everyone who has helped in any small or large part or given me advice, wisdom or even just encouraged me when I needed help, thank you. From the bottom of my heart, this work is dedicated to you, your contributions, in whatever part will always be greatly appreciated and cherished and I hope I can somehow show my gratitude.

I would also like to single out a few people for special thanks.

Firstly I would like to thank the EPSRC for funding me and this project.

To Professor Steve Rimmer, thank you for your patience and supervision that you have given me throughout this project.

To the University of Sheffield for being a home to me for many, many years.

To Professors Ingham and Southgate, Sam Bullers and the research groups in Leeds and York thank you for getting me started with the biology aspect, for sound advice and technical tips, for putting up with my constant questioning and supervising my amateurish early attempts at cell culture.

To the members of F-floor past and present, thank you for making work not seem like a chore, for making the office an enjoyable place to be and for making me fear for my life every time I set foot in the lab. I shall cherish these memories forever.

To Pauline, thank you for providing me, on a daily basis, with a hot cup of tea and a friendly smile to help me get through the day.

To my friends for all of your understanding and trying to figure out what exactly it is that I do each day, your frequent questions about this nearly matched my own.

To Will, Nev and Fred thank you for keeping me well entertained with your company and reminding me what is important in life.

To my family for your love and support throughout, especially to my wife Amy. Thank you. I couldn't have done it without you I will be eternally grateful and appreciative.

And finally I would like to give my everlasting thanks to the millions upon millions of cells that laid down their lives so that this thesis may live.

Abstract

In this project a glycerol methacrylate hydrogel surface was synthesised, which acted as a biomaterial. This biomaterial was used as a surface on which fibroblast and macrophage type cells were grown. The hydrogels were synthesised from glycerol methacrylate, a hydrophilic monomer, cross-linked with glycerol dimethacrylate using chiefly thermal polymerisation methods. The hydrogels were shown to have similar water contents of around 75-85% mass and similar physical structures. Polystyrene latex particles were also synthesised using emulsion polymerisation. Latex particles were synthesised in 3 sizes: 100 nm, 250 nm and 720 nm. These particles were produced easily and in large quantities in the three sizes and with good control. The particles were incorporated into the hydrogel structures to give three sets of hydrogels with surfaces of varying roughnesses but identical surface chemistry. The surfaces were analysed with electron microscopy and white light interferometry to gain an understanding of the roughness and appearance of the surfaces. These latex hydrogels were optimised for cell culture and shown to be non-cytotoxic by the culture of 3T3 fibroblast cells on their surfaces. Normal human dermal fibroblast cells were also grown on the hydrogels and were shown to have survived on the surface for at least 48 hours with some evidence of proliferation. A simple staining and imaging method using Giemsa nuclear stain, PicoSirius red cellular collagen stain and upright inverted light microscopy was demonstrated. Optimisation of the hydrogels for the culture of THP-1 macrophage like cells was demonstrated and ruled out epifluorescence imaging for these materials due to excessive autofluorescence generated by the hydrogels. It was shown that it was possible to induce differentiation of the THP-1 cells using PMA and for the cells to adhere to the hydrogel surface, however an experimental attempt to investigate to what extent the hydrogel surfaces caused an activation of the macrophages was inconclusive.

Using ELISA it was shown that the detection of very small levels of inflammatory cytokines was a possible.

Alongside these investigations, a set of water swollen core-shell particles was synthesised from a protected monomer in water using emulsion polymerisation. These particles were shown to swell with water on the removal of a protecting acetonide group. The particles increased in size from around 100-300 nm to 5-6 µm. This water swelling is a key indication of hydrogel function. The core shell particles were shown to be able to adsorb protein molecules (lysozyme, albumin and fibrinogen) onto their surfaces and the change of surface charge, measured by zeta potential was shown. Higher adsorbed protein concentration had a more marked effect on the elevation of charge on the particles and the particles with a smaller shell diameter showed the largest change in zeta potential with adsorbed proteins. Total protein content adsorbed to the particles was measured using the BCA assay. The protein adsorption showed that these particles may have potential used in a biological context and could be investigated further in the area of drug or biomolecule uptake and release.

Contents

Table of figures

1 Introduction

1.1 Tissue engineering

This thesis is part of an interdisciplinary project which aims to create a better understanding of various scientific and engineering disciplines enabling the betterment of all of these areas from the skills and experiences gleaned from working between them. This project encompasses aspects of polymer chemistry to create hydrogel materials, cell biology to culture cells on the polymer materials and a number of engineering techniques to analyse and understand the results. As such, it falls under the broad field of tissue engineering. Tissue engineering has been described as "An interdisciplinary field that applies the principles of engineering and life sciences toward the development of biological substitutes that restore, maintain or improve tissue function or a whole organ." [1] This definition is from Langer and Vacanti, two of the pioneers of the field. The definition itself is broad, reflecting the very wide ranging nature of the field. Tissue engineering encompasses elements of a number of disciplines including engineering, physics, chemistry, biology and biomaterials, as well as many others, but the emphasis of tissue engineering is to work with the body's own resources to help it out in times when it is injured or not functioning properly and of course this will require deep understanding of the science that underpins both cell biology and materials. This is achieved in a number of ways including the generation of tissue types in the lab, *ex vivo,* for example bone, skin and cartilage and also applying this knowledge to allow the re-growth and regeneration of the tissues in the body for example bone and tendon grafts. Ultimately this knowledge could be used to repair complex organs in the body, reducing the necessity for transplants.[2] Before this can happen, a better understanding of the mechanics, biological and chemical functions and

responses of the body's tissues needs to be found. Tissue engineering presents numerous opportunities to model and examine various tissue systems, ranging from skin and bone to cartilage and even whole organs, helping to gain a better understanding into the activities and pathways of stem cells, expression of genes in response to stimuli or the ways in which body cells and tissues degrade or fail as they age. Taking skin tissue engineering as an example, a large number of different problems can be modelled using lab produced tissue engineered skin cell cultures. These include full thickness burns and skin graft contraction,[3],[4, 5] models of melanoma infiltration[6] or models of skin pigmentation disorders including psoriasis.[7] Tissue engineered skin also has produced applications in the clinic for the past 25 years,[3] for example in burn healing,[8] which has also led to the development of the commercial products such as Apligraf[9] [10], which is used in the treatment of burns and chronic wounds, and also in the generation and clinical replacement of human buccal mucosa to repair damaged urethra.[11]

A further application of tissue engineered skin is in using *in vitro* cell cultures as an alternative for cosmetics testing. This allows a variety of cosmetic compounds to be tested on realistic human skin giving more accurate and representative results, without any of the cost or ethical issues involved in using animals for testing.[12, 13]

1.2 Macrophages

The main aim of the project is to gain an understanding of how macrophage and macrophage-like cells interact with polymer biomaterials. Macrophages are monocyte derived white blood cells which are part of both the non-specific, innate immunity and a member of the specific defence strategy employed as part of acquired immunity. Their roles in the immune system are to engulf (phagocytose) foreign cellular material or cellular debris

and break it down into harmless, or useful products and to stimulate other immune cells (including lymphocytes and T-cells) to help combat infections and foreign bodies. Much of the early understanding of macrophages and their immune activities comes from experiments by Mackaness and colleagues[14] in the 1960s. They investigated immunity to microbial infections through changes in the activity of macrophages in response to antigens. They found that when macrophages came in contact with pathogens, they developed immunity specific to the stimulus i.e. the pathogen, but not specific to antigen displayed by it.[15] This meant that the antimicrobial activities of the macrophages were greatly improved. They then surmised that this improved immunity was dependent upon an altered or activated state of the macrophage working with antigen and specific antibodies adsorbed onto the macrophage surface. It was later shown that this activation depended on the products of specifically activated T-helper cells (T_H1) and Natural Killer (NK) cells[16]. These cells themselves were activated through interactions with the antigen expressed on the surface of the macrophages. The products included interferon γ (IFNγ) and cytokine networks, including interleukin-12 (IL-12) and IL-18. After this work, interest in macrophages appeared to wane and not much research was conducted into their activities until the 1990s where Mackaness' work became known as the classical activation pathway of macrophages and his work helped open the door to research into the biochemistry of macrophage killing actions, cytokine biology and tumour immunology.[17]

1.2.1 Classical activation of macrophages

The classical activation pathway is a well-established sequence of cytokine activity which causes classical activation of macrophages, it is IFNγ dependent and results in the stimulation of T-helper type 1 immune (T_H1) responses and encourages pro-inflammatory activity in response to infections such as those caused by *mycobacterium tuberculosis* or by the human immunodeficiency virus (HIV).[15]

Classically activated macrophages are induced by a combination of two signals IFNγ, which primes the macrophage for action but does not actually activate it, and one or more of; tumour necrosis factors (TNF), an inducer of TNF including the cytokines IF-12 and IF-18, produced by T-cells or from exposure to microbe or microbial products.[18] In mice this activation is easily identified as nitric oxide (NO) is produced.[19] This identification is not as simple in humans as we do not produce NO as part of this macrophage response. Instead the response is identified by a variety of biochemical and macrophage functional criteria,[18] including increased ability to kill intracellular pathogens and the up-regulation of certain proteins, such as surface major histocompatibiliy (MHC) proteins. Following activation, macrophages will migrate to the sites of infection, following chemotaxis, where they will encounter pathogens and engulf and degrade them as well as stimulating inflammatory responses to the infection by releasing pro-inflammatory cytokines. Inflammatory responses are critical for the removal of pathogens and foreign extracellular material. During the response large numbers of immune system components including macrophages and dendritic cells rush into the infected area. A swelling action brought on by an increase in blood vessel permeability allowing the influx of immune cells to the tissue, blood plasma and proteins, as well as the associated increase in temperature, all help to kill invading pathogens.[18]

The action of cytokines is not the only way in which macrophage activity is modulated. Contact dependent interactions between T-cells and macrophages, though poorly understood and defined, have been shown to alter their activity.[20],[21] Macrophages are also said to able to induce changes in cell adhesion, migration and the secretion of various proteins of a number of cells including T-cells and fibroblasts.[15],[22],[23] In certain immune responses, large numbers of macrophages can be seen in tissues, organised into groups of cells called granulomas.[18] Granulomas form around foreign intrusions into the body which are then encapsulated by various immune cells including macrophages and T-cells. They form around a variety of particles which the immune system has recognised as foreign but is unable to degrade including; bacteria (such as *mycobacterium tuberculosis* [15]), fungi or inert non-biological material such as surgical sutures.[24] Macrophages in these structures are frequently surrounded by T-cells which produce a constant supply of activating, pro-inflammatory cytokines, lipid mediators and toxic radical molecules.[25] These granulomas can result in extensive tissue damage and are dangerous themselves as they could contain necrotic cells at their core, as is the case with some tuberculosis infections. Necrosis at the core is a result of the central cells being starved of nutrients by the surrounding cell layers, causing them to die off. Correct identification of necrotic granulomas is important as they often indicate that the cause of the granuloma is an infectious agent.

In recent years, the concept of an alternative activation of macrophages through T_H2 cytokines has gained credibility. This alternative activation presents as a distinctive macrophage phenotype with activities consistent with anti-inflammatory immune responses and possibly wound repair.[18],[26],[27]

1.2.2 Alternatively activated macrophages

The first description in the literature of an alternative method of macrophage activation, presented by Stein et al in 1992,[27] introduced them as 'macrophages which, when treated with IL-4 assume an alternative activation.' This was some of the first in-depth investigations into macrophages since Mackaness' work in the 1960s and lead to a large volume of work being undertaken in the next few years, to investigate and understand this new aspect of macrophage activity. The proposed alternative was found to be distinct and different to the classically described activation and behaviour of macrophages.[27] Further study by Goerdt and colleagues confirmed the diverse biological and immunological roles of the alternatively activated macrophages (AAMs) which distinguished them from classically activated macrophages (CAMs).[26] In Stein's study, the activation of murine macrophages followed induction with IL-4 which had previously been described as a macrophage activating factor.[27] [28] The activity of the macrophage was assessed by measuring the binding and degradation of radioactively labelled mannose serum albumin. They found that the macrophage mannose receptor (MMR) had been expressed ten-fold in response to IL-4 activation and that its activity had increased 15 fold [27]. Analysis of the macrophage gene showed that only MMR had been up-regulated whereas the regulation of lysosome and TNF had remained steady. He describes how mannose surface receptors are important for phagocytic binding and ingestion of pathogens, enhancing their activity and increasing their capacity to clear mannose ligands which leads to reduced pro-inflammatory cytokine production. MMR is also noted as not being a marker for IFNγ macrophage phenotypes. Later studies would show that IFNγ phenotype is an inflammatory response phenotype and so due to this IL-4 induced activity suppressing the response of IFNγ, the macrophage begins to express an alternative activation,[15] as well as releasing anti-inflammatory cytokines.

Whilst inflammatory responses are critical for the removal of pathogens and foreign extracellular material from the site of an infection, they also have a detrimental effect on tissues. An influx of immune cells and activity, can prove to be very damaging to tissues, ultimately resulting in necrosis of the tissue.[18] Therefore the induction of pro-inflammatory processes must be repressed to allow complete healing of the tissues. Experiments by Raes and colleagues[29] showed that markers for alternative expression of macrophages could be found on the inflammatory zone (FIZZ1) and Ym1 part of the macrophage gene and that they were dependent on IL-4. They also found that the inflammatory IFNγ antagonises the effect of IL-4 on these markers which would reduce its effectiveness in stimulating the markers.

AAMs are thought to able to suppress the inflammatory effects of CAMs, especially during apoptosis where CAMs will endocytose the cellular debris produced in the process. The AAMs will express an anti-inflammatory phenotype.[30]

Stein's paper is not the first example in the literature of investigations into the actions of IL-4 on macrophage activity,[28]′[31] but it does present the first evidence for a definitely identified, distinct phenotype of macrophages with anti-inflammatory actions. This paper encouraged a flurry of research into the activities of these new 'alternatively activated' macrophages.[17]

IL-4 and IL-13 are the main activators of AAMs[27] but their main sources are not particularly well defined, neither are the stimuli that induce their synthesis and release,[15] despite a large volume of papers which can be found in the literature, the activities induced by the cytokines IL-13 and IL-4 are less well defined than the activities brought about by cytokines recognised by the classically activated macrophages. Many papers report that cytokines are generally produced in T-helper type 2 immune (T_H2) responses especially in

allergic cellular and humoral responses to parasitic and pathogenic infections.[15] AAMs which induce T_H2 response is predominated by IL-4 signalling.[32]

The effects of IL-4 and IL-13 are virtually identical in their induction of AAMs[33] which include a weak proliferative effect and the inducement of macrophage cell fusion.[34],[35],[36] IL-4 and IL-13 may enhance the expression of an IL-1 decoy receptor which would act as a signal-less trap for other inflammatory cytokines thus counteracting pro-inflammatory actions.[37],[35] It has been found that glycans, for example chitin, lacto-N-fructapentose III initiate AAMs in mouse models and possibly in humans, this activation also increases arginase activity and promotes T_H2 responses and IL-10, IL-13 and IL-4 secretion from T-cells.[38],[39]

IL-4 and IL-13 share many common features including biochemical structural features, for example both proteins belong to the same α-helix family. They are also similar on a genetic level, sharing approximately 30% of similar sequences.[15] They have many sources, chief amongst them is T_H2 cells and as noted previously, their activity is nearly identical. They have also been reported to have immunostimulatory and immunosuppressive effects upon other immune cells including NK cells, neutrophils, mast cells and on smooth muscle cells, endothelial cells and fibroblasts.[15]

Some sources in the literature define CAMs and AAMs as M1 and M2 macrophages respectively,[15],[40],[23] however this can be misleading as it implies the macrophages are locked in theses phenotypes. It is also worth noting that there is no straight forward correspondence of CAM and AAM between subpopulations of other classes of immune cells.[15] There is evidence that macrophages are able to switch between the CAM and AAM phenotypes quickly and fully, thus inverting their phenotype. This means that the

same cell could initiate an inflammatory response then work to resolve this response by inverting to an anti-inflammatory phenotype due to appropriate stimuli.[41],[42]

In an interestingly light-hearted article, the action of polarised macrophages are directly compared to the 'light-side' and 'dark-side' of 'the force' from the film series 'Star Wars'.[23] This is an interesting analogy to make, as, in the article the inflammatory actions of classically activated macrophages are said to embody the evil spirit of the dark-side of the force, whereas the anti-inflammatory action and wound regenerative properties of alternatively activated macrophages act as the good, light-side of the force. Also in keeping with the observed activities of macrophages and with the star wars analogy, the balance of the force (the body in this case) is maintained by the ability of the macrophages to switch back and forth between the two phenotypes as required. In the article, the author Laskin states that M2 macrophages exert immunosuppressive activity and inhibit t-cell proliferation whilst down regulating pro-inflammatory M1 macrophage cells. She also states that M2 macrophages are capable of stimulating angiogenesis and inducing fibroblasts and macrophages to synthesise extra cellular matrix proteins in areas of tissue wounded by inflammation, thus bringing balance to the force. This article, not only served as a welcome break from the heavy reading usually expected when reviewing literature in most scientific disciplines, but also managed to succinctly describe the complex effects of macrophages in context with the fictitious plot elements of a film and acts as a competent review of the balancing act effected by macrophages as they go through their opposing inflammatory and anti-inflammatory actions. This article also is one of the few articles in the literature in general which makes reference to the wound healing abilities of which macrophages are thought to be capable. It even provides some detail into the signalling molecules thought to aid in the repair of wounds and tissues, with the example of the liver and the macrophage

dealing with hepatotoxins being given. These healing effects are all referred to in terms of 'weapons of the Jedi', to which ancient and noble order the healing alternatively activated macrophages are said to belong. The article concludes by stating that the inflammatory responses to injuries and the anti-inflammatory, healing responses are two sides of the same coin with complex interrelations which rely upon one another.

1.2.3 Alternatively activated macrophage assisted wound healing

Alternatively activated macrophages, as they became known, were shown to be unable to synthesise nitrogen monoxide (NO) due to the induction of arginase and as such are much less able to kill intracellular microbes.[43] However if the substrate for both arginase and the enzyme responsible for NO production, L-arginine, were to be added to IL-4 activated macrophages, after activation, NO production would be restored.[44] This reduced cytotoxic activity suggests a different mode of action.

AAMs express high levels of M2 markers Ym1 and Arginase 1 (Arg1) and on stimulation by IL-4 induce the production of lower levels of inflammatory cytokines.[40] AAMs produce several components which are known to be involved in the synthesis of the extra cellular matrix (ECM), suggesting that they have more of a role in the repair of tissue rather than microbe killing like the CAMs do.[18],[45] AAMs are not very efficient at antibody presentation and in many cases have been known actually to inhibit T-cell proliferation.[18] This would suggest that they have a decreased role in the management of intracellular pathogens and recent studies on this population of macrophages have begun to focus on the AAMs potential not only to reduce inflammation through the release of IL-10 and IL-4 agonists,[18] but also their potential to encourage wound healing, immunosuppression and tissue repair[18] through angiogenesis and extra cellular matrix (ECM) deposition. AAMs

are thought to produce high levels of fibronectin and other matrix associated proteins[45] and also promote fibrogenesis from fibroblastiod cells.[46] Thus repairing any damaged tissues at the site of previous inflammation. This action seems to be the polar opposite to the action of CAMs which will inhibit fibrogenesis by releasing anti-fibrogenesis or fibrolytic factors.[46] Through the strict induction of arginase, these cells may lead to the biosynthesis of polyamine and proline complexes which in turn would promote cell growth and collagen network formation, ultimately resulting in tissue repair,[47],[48] though CAMs could contribute to the dissolution of fibrin fibres present from blood clotting mechanisms and they would also have a role in the disposal of dead cells in the wound, therefore a low number of CAMs would likely be found in the site of the wound.

The alternative activation of macrophages by T_H2 cytokines and glucocortids is essential for the correct functioning of anti-inflammatory immune reactions. [45] The induction of AAMs by IL-4 also causes an over expression of prototype ECM protein fibronectin. This over expression suggests that the macrophages do indeed have a role in tissue remodelling and the healing of acute and chronic inflammatory reactions and diseases. AAMs are even found in the healing phase of acute inflammation reactions, for example in teeth after gingival infections [49]. They have also been shown to be major players in type 1 autoimmune responses[50] in the chronic inflammatory diseases; rheumatoid arthritis [51, 52] and psoriasis.[53]

Mantovani et al stated that 'M1 and M2 polarised macrophages are extremes of a continuum of functional states.' By this he was outlining the versatility of macrophages, that they can express different and varied functions in response to microenvrionmental signals.[54] This article describes how tumour and T-cell derived cytokines acquire polarised M2 (AAM) phenotypes which are able to act with anti-inflammatory responses as part of the

adaptive immunity. They are able to scavenge debris and promote angiogenesis, tissue remodelling and tissue repair.[40] Evidence in the literature of macrophages inducing tissue repair and remodelling is limited, indeed, many of the papers which make mention of the anti-inflammatory action of AAMs appear to be unaware of the proposed healing efforts of these macrophages. This could be due to a number of reasons including the obvious, that these healing effects are beyond the scope of investigations into the effects of cytokines on the macrophages, or possibly that they are difficult to detect. The papers that do make mention of tissue repair or remodelling effects seem to be unaware of the exact mechanisms at work or potential impact of these healing effects, particularly if considered from a tissue engineering stand-point. If these healing effects could be harnessed by deliberate induction of their phenotypes by a suitable biomaterial for example as suggested by Ratner and colleagues using patterned P(HEMA)[55], there would be the potential for a huge amount of research into the tissue remodelling activities of macrophages in response to wound stimuli or in ways to produce novel advanced forms of wound dressings which could directly affect curative action upon the wound, rather than merely protecting it from further damage and infection as many of today's dressings do.

1.2.4 An alternative alternative activation?

The definition of alternatively activated macrophages broadened with the proposal of type two alternatively activated macrophages[32], which despite activation by pro-inflammatory cytokines; appear to show a preference towards anti-inflammatory actions.[41]

Class II alternatively activated macrophages (CIIAAMs) are thought to release large amounts of the cytokine IL-10, which is a potent inhibitor of acute inflammatory responses to certain

bacterial endotoxins. This type of activation resulted from classically activating signals (IL-12, IL-18) in the presence of IgG immune complexes.[18],[56]

CIIAMs, similarly to CAMs require two induction signals, the first is ligation of Fcγ-receptors (FcγR) by non-activating IgG complexes and then by toll-like receptors (TLRs).[18] When activated, CIIAMs do not induce arginase and begin to produce many of the same cytokines as the classically activated macrophages, with the exception of IL-12 and IL-10.[18] Large amounts of IL-10 are produced by CIIAMs and act as anti-inflammatory agents. This action was shown in experiments by Gerber and Mosser.[56] In these experiments, macrophage Fcγ receptors were ligated by IgG complexes following stimulation by known pro-inflammatory agents. It was found that the ligation induced anti-inflammatory action in the macrophages and triggered a reduction in the amount of inflammatory cytokines, showing that effectively ligating the receptor with IgG could prevent inappropriate levels of inflammatory cytokine responses. This new kind of activity upon activation makes CIIAM distinct from alternatively activated macrophages and classically activated macrophages.

The literature is sparse in details on the existence of CIIAMs and in their possible activities. Many papers offer small hints of their existence but group the possible activity of the CIIAMs in with either of the other two phenotypes of macrophage or otherwise remain unaware of their existence. This makes assessing the validity of the existence of CIIAMs difficult as there is no real firm basis of literature on which to base a judgement. The main papers which reported the possible existence of CIIAMs did so in the early 2000s and this seems to be another area of research which has fallen out of favour. The general lack of any identifying references to these macrophages is possibly due to the marked similarity of their proposed actions with those of the established classical and alternatively activated phenotypes. This could mean that they fail to be identified as their actions appear

contradictory to those expected for either CAMs or AAMs or that any activity that is recorded possibly falls within the bounds of experimental error and is discounted as legitimate activity in terms of the study. It is also worth observing that there appears to be no definite consensus on whether CIIAMs are a distinct phenotype or one of the other two phenotypes acting in a different fashion to the expected way. Further study in this area could clear up this mysterious behaviour and also help shed some light on whether a new phenotype needs to be added to the family of macrophages.

1.2.5 Macrophages and hydrogels

The first in-depth study on biomaterials was by Lentz and colleagues[57] and concerned the adhesion of rat peritoneal macrophages to synthetic hydrogels. In this study the authors assessed the ability of the macrophages to adhere to various hydrogels. A range of hydrogels comprising a number of different proportions of hydroxyethyl methacrylate (HEMA) and ethyl methacrylate (EMA) were compared to sets of copolymers made up of styrene (S) and *para*hydroxystyrene (HS) repeat units. Both groups of copolymers contained hydroxyl functionality but the poly(EMA-co-HEMA) materials swell in aqueous media to a much higher degree than poly(HS-co-S) materials, as is suggested by their capacity as a hydrogel. These differences in swelling directly affected the adhesion of the macrophages and in general the macrophages adhered more preferentially to the copolymers which had swelled the least,[52] indicating a preference of the cells for materials with higher moduli. Other factors were also likely at work, for example the hydrogels would likely have different charges present at their surfaces, as the phenol hydroxyl groups will be partially deprotonated at neutral pH. Later studies by Smetana et al[58],[59] showed that monocyte

adhesion to polyHEMA hydrogels could be enhanced by incorporating functional groups with a charge or by templating precisely sized pores into the hydrogel matrix[60]. They found that macrophages preferred and spread over a wider area on tertiary amine functionalised hydrogels compared to carboxylic acid or sulphonic acid hydrogels. This is not surprising as the tertiary amines present would be partially protonated and therefore positively charged at physiological pH, therefore presenting a more attractive surface. In his paper, Rimmer[52] notes that Smetana did not investigate the activation of these cells, merely their adhesion. These studies were concerned with the key issue of cell adhesion to the surface of hydrogels, for when the cells are attached, they would then be free to grow and proliferate on these surfaces. This rational is at the centre of designing viable tissue engineering biomaterial constructs.

Having successfully adhered macrophages to hydrogel surfaces the hydrogels need to be assessed to see whether the macrophages can proliferate on their surfaces and that the hydrogels are not cytotoxic. If, on adhesion, the macrophages become activated and express inflammatory responses, they can sometimes form foreign body giant cells (FBGCs) in a sequence of events similar to that of granuloma formation[61]. The duration and magnitude of the inflammatory response has a direct bearing on the stability, compatibility and indeed the suitability of the biomaterial[62]. Macrophages can react to a huge variety of synthetic polymers[52], treating them as foreign objects. It therefore stands to reason that incorporating protein molecules into the structure could have a stabilising effect on the macrophages. In their study, Kao and colleagues[62] note that macrophages are able to recognise the protein molecules adsorbed onto the biomaterial surface and that macrophages can adhere to these proteins or become activated by them. They also noted that where FBGCs form on biomaterials, the biomaterial immediately underneath will

become degraded by them, meaning that this effect should be avoided where possible. A number of researchers have demonstrated that this is possible to grow macrophages on polymer surfaces without the activation of inflammatory responses, including Rimmer and colleagues[52], who used alkyl aminated hydrogels and found that they induced very low levels of pro-inflammatory cytokines and Jenny & Anderson,[63] who showed that it was possible to prevent FBGC formation by macrophages, by grafting polyethylene glycol (PEG) to amine modified glass. Ratner and colleagues has described how influencing the macrophage behaviour and expression by manipulating hydrogel properties is a key way to encourage an alternative and therefore healing activation, promoting tissue remodelling of implants and immune system pacification [64] [60]

The literature concerning macrophages interacting with biomaterials is very varied. There is a lot of attention paid to the assessment of macrophage adhesion and proliferation, as, for the obvious reasons that it is pointless to make a biomaterial upon which macrophages cannot grow. There is also a lot of work done on the assessment of the cytotoxicity of biomaterials in question, again for obvious reasons. It is often noted throughout the literature that macrophages can become 'activated' with response to the biomaterial[65],[62],[66], this can be either when the biomaterial is implanted into the body, or when macrophage cells are introduced directly to it. The activation referred to in the literature is almost exclusively classical activation and research is focused on developing biomaterials which will interact with macrophages without activating their pro-inflammatory responses, thus increasing the biomaterial's biocompatibility.

In terms of investigating macrophage interaction with polymers, specifically hydrogels, there is also little literature evidence. There have been studies on polymers tailored to encourage

cellular protein deposition and adhesion by macrophages reported by Godek et al,[67] as well as study into reactions of macrophages with polymer nano- and microparticles either directly synthesised or as wear or breakdown debris to investigate cellular uptake and inflammation,[68],[69], [70, 71] particularly with regards to drug delivery,[72],[73],[74] or as a means to assess macrophage differentiation.[75] However there has been a great deal of study into how to assess the various interactions of macrophages and other immune cells with biomaterials used in tissue engineering by using a number of assays[76], as well as studies of surface reactions between polymers and macrophages,[77] but those studies which have looked at macrophage interactions with hydrogels have lacked an overall systematic approach into different methods of causing and modulating macrophage responses[78]

There is almost no mention in the literature, of inducing alternative activation of macrophages in relation to biomaterials, and in the rare case when it is mentioned; AAMs on biomaterials tend to be the aim of future research[79]. It seems that this lack of directly induced alternative activation by biomaterials consists as a gap in the literature. The reasons for pursuing it include increasing the biocompatibility of biomaterials by the encouragement of an anti-inflammatory phenotype and also the encouragement of wound healing and angiogenesis, particularly when the biomaterial in question is being used in a tissue engineering context. This biomaterial, along with cultured tissue would likely be implanted into the body wherein it would encourage the body to integrate this new part of the tissue, effect tissue repair, hopefully joining existing native tissue with the engineered culture and encouraging the growth of blood vessels into the engineered tissue implant - described by some tissue engineers as the ‘holy grail of tissue engineering.’

1.2.6 Cell adhesion to surfaces

When a material encounters a living system, for example a biomaterial that is implanted, proteins are quickly found on the surface. Proteins rapidly adsorb to most surfaces and quickly form a monolayer.[80] Hydrophobic materials are preferred by cells, [81] likely due to the proteins changing conformation and unfolding on interaction with the surface, then releasing water molecules which would increase the entropy present in the system, making this a favourable interaction. The chemistry of the surface is therefore highly important in controlling the degree of cell adhesion. So control of properties such as charge and water swelling/wettability can alter the attractiveness of the surface for adhesion. Tailoring a biomaterial surface to encourage specific protein adsorptions can have a profound effect on the types of cells which will adhere.[81] Cells adhered to these proteins signal both internally and externally to other cells and can be induced to behave in a particular way, such as undergoing a phenotypic switch, or forming a particular tissue type. [82]

When cells arrive at the surface they interpret and recognise the surface as the protein monolayer therefore for successful cell adhesion, correct protein adsorption properties must be present. Once adhered, the cells are capable of altering their surroundings by depositing further proteins, proliferating on the surface and recruiting other cells. With the arrival of more cells, differentiation into new cell types is possible, as is the arranging into tissues, cells generate the extracellular matrix to aid with further adhesion and differentiation.[82]

Cells possess receptors which specifically recognise adhesion proteins present on surfaces. These receptors are known as integrins. Integrins are a large family of transmembrane proteins which bind to specific amino acid sequences on proteins especially adhesion

proteins.[83] Common adhesion proteins are fibronectin and vitronectin. These proteins contain binding sites comprised of a three amino acid sequence arginine-glycine-aspartic acid (RGD)[84]. Other integrins ($\alpha_m\beta_2$) facilitate macrophage adhesion to various proteins including fibrinogen and immunoglobin G (IgG), this adhesion is an important factor in inflammatory responses. [84-86] Control of this adsorption or the deliberate presence of desirable amino acid sequences can lead to directly tailorable surfaces which can encourage cell adhesion, spreading or differentiation.[84]

One typical role of integrin binding to adsorbed proteins is to encourage spreading out of the cells on the surface[87] and can be used as a key indicator of successful adhesion.

As well as surface chemistry, another important aspect of the cell's interaction with the surface is through the its response to surface topography, both at the nano- and micro-scale.[88] It has been shown that cells can recognise shapes and align their cytoskeletal structures with them accordingly.[89] It is not surprising that cells respond in three dimensions to their surroundings, as in their native environment they are usually connected on all sides to other cells, ECM components and are highly hydrated, giving access to soluble growth factors, hormones and other signalling molecules. Simple shapes can be introduced to surfaces artificially by using such techniques as lithography, a type of patterning which uses light to fix a material into a given pattern. By tailoring the shape or adding a desired adhesive or non-adhesive protein to the shape, it is possible to create areas of space which cells will fine more or less attractive.[90, 91] In addition to increasing the likelihood of adhesion, it is possible to use patterned surfaces or topographical features to induce desired cellular behaviour such as polarisation of macrophages into a tissue regenerative phenotype.[92, 93] By introducing features such as 2D grooves in the surface, polarisation of macrophages towards M2 type phenotypes can be achieved, encouraging the macrophages

to elongate,[93, 94] or by allowing them to interact with 3d pores which favoured M1 activation.[95]

Whilst well documented, the exact roles of integrin binding in three dimensional ECM environments is not yet fully understood and is a thriving area of research.

2 Aims and objectives

This project aims to determine and define a set of investigations into the activities of macrophage and macrophage-like cells. This will be achieved using synthetic hydrogels as a biomaterial platform. Hydrogels are a versatile material for tissue engineering purposes, they are also very customisable and the chemical methodology of synthesis and modification is well recorded in the literature and offers the potential for many variations to the surface, structure and properties. However, the chief advantage of using synthetic biomaterials such as hydrogels, over natural biomaterials is that synthetic hydrogels have little to no natural immunological properties.

The hydrogel materials and handling methods will be developed and optimised to first encourage fibroblast cells to adhere and recognise hydrogel surfaces then to encourage THP-1 macrophage like cells to adhere and to attempt to cause an activation response.

The next step would then be to introduce a surface modification which could modulate this activation, potentially reducing it and investigating whether the activation could be stimulated to change to the alternative activation, described above as a tissue remodelling form of macrophage cell action.

The optimisations and modifications will be directed at the surface of the hydrogels, as this is the area which native macrophages would first encounter, were the hydrogel to be introduced into the body, for example as a tissue construct or implant.

Testing of surface properties will reveal if macrophages are influenced directly by contacting a surface and to what effect these surfaces have on the action and continuing life cycle of the macrophage. The next phase of the investigation will be to trial different combinations of surface modifications to build up a library of surfaces and the corresponding affects upon

macrophage activity and activation. Surface modifications will include changes to hydrogel stiffness and water content or incorporating particles with different characteristics such as hydrogel-like properties.

The activity and activation of macrophages will be monitored and measured by analysing whether or not the macrophages will adhere to a surface, this can be assessed by visualising cells on the surfaces of hydrogels, whether adhered cells respond to the surface by modifying their morphology or activity. Changes in cellular activity can be measured by analysing the cell signalling molecules produced by the cells, these include cytokines. The signalling molecules can be analysed and quantified using assays such as ELISA.

3 Abbreviations

2-hydroxy-2-methylpropiophenone – HMPP

Analysis of variance - ANOVA

Atomic force microscopy – AFM

Azobisisobutyronitrile - AIBN

Benzoyl peroxide - BPO

Core-Shell – CS

Dichloromethane – DCM

Dimethylaminopyridine - DMAP

Dimethylsulphoxide - DMSO

Dulbecco's modified Eagle's media – DMEM

Enzyme-linked immunosorbant assay - ELISA

Ethylene diamine tetracetic acid – EDTA

Ethylene glycol dimethacrylate - (EGDMA)

Foetal bovine serum – FBS

Fourier transform infrared spectroscopy – FTIR

Glycerol dimethacrylate – GDMA

Glycerol methacrylate acetonide – GMAC

Glycerol monomethacrylate – GMMA

Hydrochloric acid – HCl

Hydroxyethylmethacrylate - HEMA

Isoelectric point - pI

L-Glutamine - LG

Lipopolysaccharide - LPS

Methacrylic anhydride – MA

Non-serum containing media soked gels - NSER

Normal human dermal fibroblasts - NHDF

Penicillin/streptomycin - pen/strep

Phorbol-12-myristate-13-acetate - PMA

Phosphate buffer solution - PBS

Poly(divinyl benzene) – PDVB

Poly(glycerol monomethacrylate) – PGMMA

Polyethylene terephthalate – PET

Polystyrene – PS

Polytetrafluoroethylene – PTFE

Potassium chloride - KCl

Roswell Park Memorial Institute medium- RPMI

Scanning electron microscopy – SEM

Serum containing media soaked gels - SER

Sodium dodecylsulphate – SDS

Sodium hydroxide – NaOH

Tissue culture plastic – TCP

White light interferometry - WLI

4 Synthesis and characterisation of polystyrene latexes

4.1 Introduction

Emulsion polymerisation is a form of radical polymerisation which incorporates an aqueous phase, a monomer phase, surfactants and a radical initiator. Emulsion polymerisations can be one of two types: oil-in-water or water-in-oil emulsions.

Emulsion polymerisation was first utilised as a method of producing synthetic rubbers. This was due to the high demand for natural rubbers which come from *Hevea Brasiliensis,* or the Rubber Tree. Demand was particularly high during the first and second world wars. The first patent for synthetic rubber was submitted by Friedrich Hoffman (German Patent No. 250690) in September 1909, while working at Bayer in Germany.

The process and kinetics of emulsion polymerisation was first understood and developed by Fryling[96] in 1944, Harkins[97] in 1947 and Smith & Ewart[98],[99] in 1948. Harkins developed the understanding of where the loci of polymerisation were to be found, while Smith described the kinetics of styrene polymerisation, detailing how free radicals in solution migrated into monomer droplets and micelles to form small droplets of polystyrene. Smith, working with Ewart, then developed the mechanism in some more detail and described it as undergoing the following general stages, illustrated Figure 4-1 below.

1. A monomer droplet is dispersed in the bulk phase, typically, but not always, water. Surfactant molecules adsorb to the surface of the droplet. Micelles form in the bulk phase.
2. Initiator molecules dissolve into the micelles and start polymerisation, these micelles can now be thought of as monomer swollen polymer particles. Polymerisation is terminated when another radical enters the micelle.

3. When all of the monomer droplets have disappeared and any remaining free monomer is located in the particles the reaction eventually terminates. The particles can then be considered latex particles or colloidal polymers. Additional monomer and initiator could be added to the system if desired to continue particle growth.

Micelles, monomer droplets and empty micelles can all be found at the same time dispersed in the bulk phase and the numbers of which will vary as polymerisation continues.

The final colloidal polymers can be of very high molecular weight due to the very small number of propagating chains present in the micelles and polymer particles.

Latexes produced by emulsion polymerisation have a number of uses in many industries, including: the creation of artificial rubbers, which find uses in the automotive industry, amongst others; in the creation of plastics, particularly polystyrene and in situations where polymer dispersions are desired, such as the paints industry.

The sizes of latex particles can very easily be tailored by altering the concentration of surfactant, allowing a high degree of control over the latex product. Particles can be made in sizes ranging from a few tens of nanometres up to the micron scale. Due to this size range,

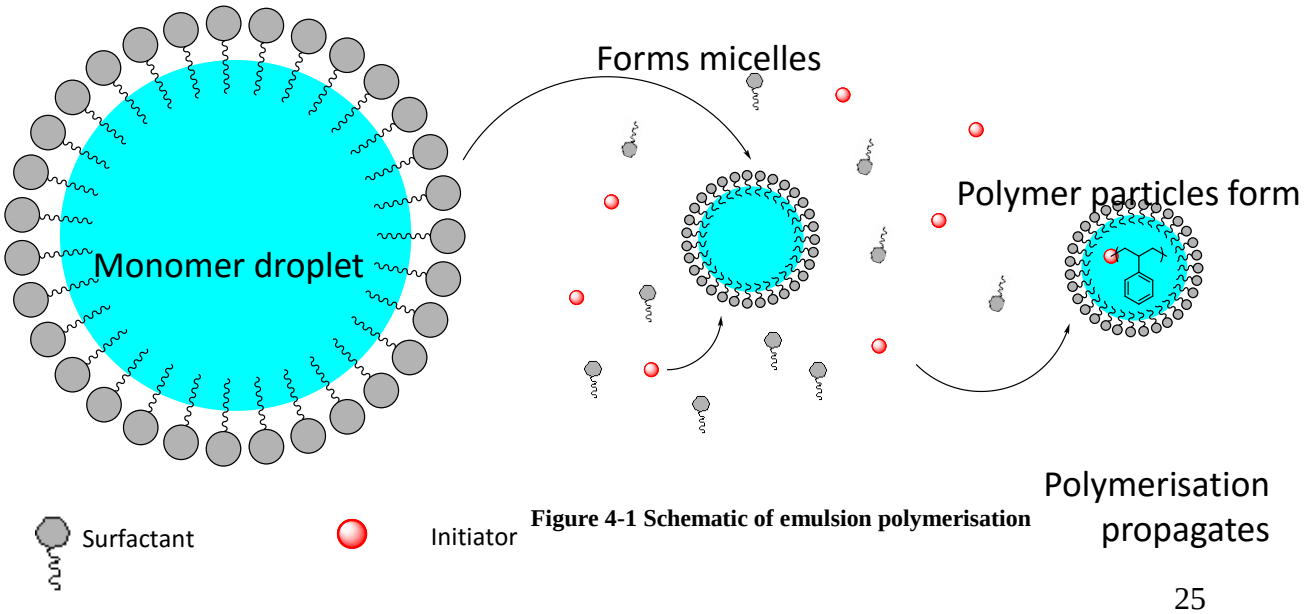

Figure 4-1 Schematic of emulsion polymerisation

latexes are finding many applications in the field of nanotechnology.

One key application of nanoparticles is in drug delivery. Their ability to encapsulate drug molecules or have them adsorb onto their surface, make nanoscale particles an attractive target for a large body of research.[100],[101],[102] The small size of the particles enables them to penetrate deep into tissues and be transported across cell membranes as well as delivering drugs or active biomolecules directly to the desired site of action.[103] Nanoparticles can have long circulation times in the body[104] and their ability to target specific tissues or cells mean that drug levels in the whole body can be reduced but effectiveness is potentially increased.

In the scope of this research, latex particles are of interest in the guise of being an immune system agonist. The immune system protects the body against invasion from without, whether this is in the form of pathogens such as bacteria and viruses or as synthetic implants such as hip or knee replacement joints. One of the first responders to an insult to the immune system is the macrophage. Macrophages are monocyte derived white blood cells, which are part of both the non-specific, innate immunity and a member of the specific defence strategy employed as part of acquired immunity. Their roles in the immune system are to engulf (phagocytose) foreign cellular material or cellular debris and break it down into harmless, or useful products and to stimulate other immune cells (including lymphocytes and T-cells) to help combat infections and foreign bodies.

Due to their roles as first responders in the body, macrophages usually encounter nanoparticles before other immune system components,[68] there can therefore be adverse interactions between the macrophages and the nanoparticles, caused by the body inadvertently identifying them as foreign, causing localised or systemic inflammation or

even stimulating autoimmune disorders, which could in turn increase a person's susceptibility to further infection.

A key location where synthetic nanoparticles are generated in the body is at the site of joint replacements. In these situations, age and wearing or bodily defects have necessitated a joint such as the knee or hip to be replaced by a synthetic analogue. These synthetic implants may cause an acute inflammatory response from the immune system when they are initially implanted but a chronic inflammatory response can be caused by debris formed when the implants wear. The wear is caused by moving components rubbing on one another creating small particulate debris with each movement. Many of these particles are on the nanoscale and when they are encountered by the immune system, particularly by macrophages, contribute to the inflammatory response, causing localised tissue damage and pain and discomfort to the patient.[105],[106] Gaining a better understanding of the cellular reaction to nanoparticles will lead to better methods of reducing inflammation and improving the quality of life of those patients affected by ageing joint prostheses.

4.2 Experimental

4.2.1 Emulsion polymerisation of styrene

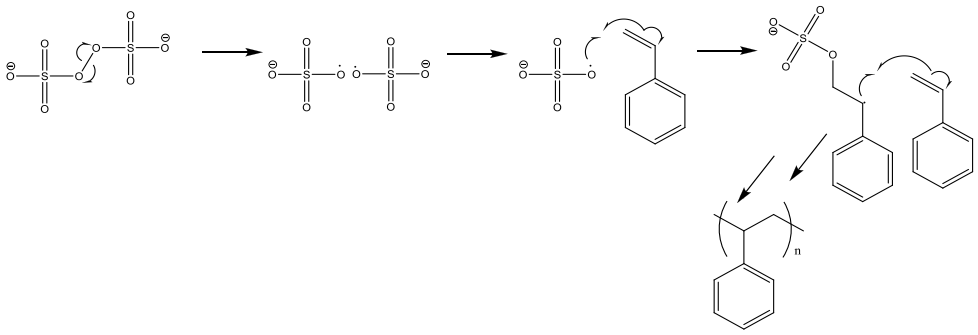

4.2.1.1 Materials

Styrene, sodium dodecyl sulphate (SDS), potassium persulphate and potassium dihydrogen phosphate were obtained from Sigma and used without further purification, distilled and deionised water was used throughout.

4.2.1.2 Polymerisation

Batch polymerisations were conducted in a 1.0L jacketed glass reaction vessel (Radleys, UK) which was equipped with a mechanical stirrer, a nitrogen inlet, a reflux condenser and a temperature probe. For typical preparation, water (600g), SDS (10g) and potassium dihydrogen phosphate (0.3g) were charged to the vessel. The mixture was deoxygenated by bubbling under nitrogen with agitation for one hour, whilst hot water was circulated through the jacket of the vessel to maintain the temperature of the mixture at 70°C. After this styrene (300g) was slowly added dropwise to the reaction, when addition was completed potassium persulphate (1.5g) was added in water (20 cm^3) and the polymerisation was stirred for 4 hours. At the end of 4 hours, the temperature of the circulated water was increased to 80°C for 1 hour to ensure total monomer conversion. The latex was discharged from the vessel, allowed to cool and stored at room temperature.

4.2.1.3 Variations to method

To produce larger latex particles the above formulation, formulation **1**, was varied as shown: Formulation **2**: styrene (300g), SDS (0.5g), potassium hydrogen phosphate (0.3g), water (600 cm^3), potassium persulphate (0.5g) and formulation **3**: styrene (300g), SDS (0.1g), potassium hydrogen phosphate (0.3g), water (600g), potassium persulphate (0.5g). The polymerisation was followed as described above.

4.2.1.4 Analysis of latex

Particle size and zeta potential data were obtained using the ZetaPals zeta potential analysis instrument (Brookhaven Instruments Corporation) and the provided ZetaPals and light scattering particle size analysis software.

The pH of the latex was obtained using a Hannah Instruments pH meter and the latex solids content was assessed by solvent evaporation under vacuum.

4.2.2 Emulsion polymerisation of styrene-co-divinylbenzene

4.2.2.1 Materials

Styrene, sodium dodecyl sulphate (SDS), potassium persulphate and potassium dihydrogen phosphate were obtained from Sigma and used without further purification, distilled and deionised water was used throughout. Divinyl benzene (DVB) was obtained from sigma and cleaned as described below. Sodium hydroxide and magnesium sulphate were obtained from Fisher.

4.2.2.2 Polymerisation

DVB was cleaned prior to polymerisation to remove the storage stabiliser, with 5% sodium hydroxide (NaOH) (3x100 cm^3) and washed with deionised water (3x300 cm^3) before drying over magnesium sulphate.

20 mol % DVB was added to the latex monomer feed.

A typical preparation was as follows:

Water (100g), SDS (1.66g) and potassium dihydrogen carbonate (0.33g) were charged to the vessel. The mixture was deoxygenated by bubbling under nitrogen with vigorous stirring for one hour, whilst hot water was circulated through the jacket of the vessel to maintain the temperature of the mixture at 70°C. After this styrene (25g) and DVB (6.249g) were slowly added dropwise to the reaction, when addition was completed potassium persulphate (0.25g) was added in water (5 cm^3) and the polymerisation was stirred for 4 hours. At the end of 4 hours, the temperature of the circulated water was increased to 80°C for 1 hour to ensure total monomer conversion. The latex was discharged from the vessel, allowed to cool and stored at room temperature.

4.2.2.3 Analysis of latex

Zeta potential and particle size analysis were performed to characterise the latex, as described above using the ZetaPals instruments. pH was recorded and solids contents were determined by solvent evaporation under vacuum.

4.3 Results and Discussion

4.3.1 Emulsion polymerisations

Latex nanoparticles were polymerised as an emulsion in order to produce a large number of spherical particles of a given size. Styrene was chosen as the latex particles produced in the polymerisation are hard spheres. This hardness is relevant to investigate whether macrophage cells can detect the physical shape of the particles but any difference in chemical composition between particles and hydrogels, and whether this difference leads to any differing behaviour of the macrophages. The particles are envisaged as an easily synthesised material which are analogous to hard wear particles in joint replacement environments. These particles are known to cause macrophage-related inflammation, as noted previously.

4.3.2 Emulsion polymerisation of styrene

4.3.2.1 Polymerisation

The emulsion polymerisation of styrene produced a milky white latex suspension. This is due to the size of the polystyrene particles produced. Laser light scattering from the particle sizing apparatus gave the average particle size to be 102 ± 1.5 nm with an average polydispersity of 0.037. The technique of light scattering, or quasi-elastic light scattering (QELS), analyses the scattering of laser light caused by particles in suspension. The particles, which are undergoing Brownian motion scatter incoming light and create constructive or destructive interference patterns, depending on the distance of the light travelling to the detector, resulting in an average intensity of scattered light with superimposed fluctuations. The decay times of the fluctuations are related to the diffusion constants of the particles

and therefore, the sizes of the particles. The instrument and software are then able to interpret these fluctuations and give a measure of the particle size.

The pH of the latex was found to be 2.42. Following the polymerisation, no significant coagulum was found and the latex was stable at room temperature for a number of months. The charge on the particles, given by the zeta potential was -29 ± 1 mV at 25 °C. The average solids content of the latex was found to be around 30% Formulation **2** was found to have particle size of 248 ± 2 nm. The zeta potential for these particles was -29 ± 1 mV. The average particle size of formulation **3** was 712 ± 7 nm and the zeta potential was -28 ± 1 mV. The average solids content of formulations 2 and 3 was 21% and 23% respectively. The three formulations are distinct in size giving three different variables, yet the charge on the particles is very similar meaning that any effects the charge will remain constant over all of the sets. The zeta potential measurements all being around -30 mV which is an indicator of colloidal stability. The physical data is summarised in the table below

LATEX FORMULATION	PARTICLE SIZE / NM	ZETA POTENTIAL / MV	SOLIDS CONTENT
1	102 ± 2	-28.9 ± 1	30 %
2	247.5 ± 2	-29.4 ± 1	21%
3	712.8 ± 7	-27.6 ± 2	23%

Table 4-1 Particle size, zeta potential and solids content of the three latex formulations

4.3.3 Emulsion polymerisation of styrene-CO-divinylbenzene

4.3.3.1 Polymerisation

The initial latex comprised of PS-CO-DVB was white as were previous latexes. The initial particle size was 75 ± 1 nm and zeta potential of -19 ± 4 mV. This particle size is significantly smaller than the smallest formulation of pure styrene nanoparticles but there will be a small

degree of particle cross linking due to the bifunctional nature of the DVB molecule. This will decrease some particle sizes in the latex, giving a broader dispersity. The inclusion of DVB means that a further monomer can be coupled to the surface of each particle allowing for the synthesis of core-shell particles.

4.4 Conclusion

In this chapter three formulations of polystyrene latex particles were synthesised using batch emulsion polymerisation. The particles were readily synthesised and with good size control by varying initiator and buffer concentrations. The particle sizes were approx. 100 nm, 250 nm and 710 nm. The latexes were analysed by zeta potential measurements and shown to be colloidally stable, the latexes were stable at room temperature for many months. Also synthesised was a smaller PS-CO-DVB latex which has dual vinyl functionality. This latex will be investigated in later chapters for coupling to another monomer to produce a core-shell particle with PS-CO-DVB at the core.

5 Synthesis and characterisation of glycerol methacrylate hydrogels

5.1 Introduction

5.1.1 Biomaterials

There is much potential for the development of biomaterials, which could influence macrophage phenotype activity and could possibly encourage the action of favourable, wound healing type macrophages. Research and development in this area would be classed as tissue engineering as enhancement of wound healing and regeneration may be achieved by considering how environments that influence macrophage differentiation could be produced. Promising materials for study in this field are hydrogels. [52]

5.1.2 Hydrogels

Hydrogels are extended three dimensional networks of polymer chains with hydrophilic and hydrophobic moieties, the chains are often crosslinked. The dispersion medium of the gel is water. The hydrophobic components of the gel comprise the bulk of the chains making the hydrogels insoluble in water. However, the hydrophilic components, chiefly side groups on the chains, attract and hold a large number of water molecules giving the overall hydrogel structure a high water content but the gel overall remains insoluble. The gel is given a permanent physical structure by incorporating crosslinking groups, usually a second, bifunctional monomer. It is therefore possible to tailor hydrogel rigidity by varying the amount of crosslinking agent. As well as providing permanent structural support, the crosslinks in the gel can cause it to be highly porous. The water content of a hydrogel can, in some cases be as high as 99% of its total weight. These structures are described as being ‘water swollen’. Due to their high water content, swollen hydrogels can be very flexible and bear many similarities to tissues, in particular, hydrogels can be compared to the

extracellular matrix (ECM) of tissues[107]. Indeed the matrixes of soft tissues are bicomponent hydrogels composed predominately of crosslinked collagen fibres, with charged polysaccharides providing increased osmotic pressure and thus high swelling. These similarities to natural tissues make hydrogels excellent candidates for scaffolds and biomaterials in tissue engineering constructs. Another key aspect in which hydrogels mimic the ECM of tissues is their extended porous, three dimensional structure which has been shown to be beneficial to the culturing of cells on hydrogel surfaces and throughout hydrogel networks.[108] In order for a synthetic hydrogel to be a viable biomaterial for *in-vivo* testing it must be non-cytotoxic but if the biomaterial were ever to be viable for implantation into the body, it must also be biocompatible. This means that it would not trigger an immune response in the body, chiefly an inflammatory response from macrophages.

5.1.3 White light interferometry

An interferometer is an optical device that divides a beam of light produced by a single source into two or more beams, then recombines them to create an interference pattern. A typical interferometer setup has a light beam from a source, which is split into two, one beam hits a sample and the other hits a reference mirror. The light beams are recombined and which creates an interference pattern. However if the mirror is tilted, the interference pattern will form in light and dark bands called fringes and as the mirror is tilted, the fringes will move across the sample which has been analysed. The spatial arrangement of these fringes can give details about the three dimensional shape of the sample for example arranged in parallel lines, fringes correspond to a flat surface whereas fringes which form concentric circles around a point indicate that the surface is curved or spherical. Minute variations in the fringes allow the instrument detecting them to recognise minute variation

in surface topography down to the tens of nanometre scale and the surface data produce can compare favourably with electron microscopy and atomic force microscopy.[109-111] White light interferometry (WLI) finds applications in a number of fields where surface analysis is required including polymer paints and coatings,[112] and the assessment of the surfaces of bioimplants.[113]

5.2 Experimental

5.2.1 Synthesis of poly(glycerol monomethacrylate)

Poly(glycerol methacrylate) (PGMMA) hydrogels were synthesised by two methods: thermal and UV curing.

5.2.1.1 Thermal curing materials

Glycerol monomethacrylate (GMMA) was obtained from Cognis and used without further purification. Glycerol dimethacrylate (GDMA) was obtained from Sigma and used without further purification. Reagent grade ethanol was obtained from Fisher scientific. Potassium persulphate was obtained from Sigma. Deionised and distilled water was used throughout.

5.2.1.1.1 Thermal polymerisation

GMMA (4g), GDMA (0.2g) and water (4g) were mixed. Two soda glass plates were lined with poly(ethylene terephthalate) (PET) sheets and a poly(tetrafluoroethylene) (PTFE) spacer (250μm thickness) was placed between the sheets and the apparatus was held in place with bulldog clips. Potassium persulphate (0.06g) was added to the polymerisation mixture, mixed well, any bubbles were removed by brief sonication. The mixture was quickly injected between the sheets into the spacer. The apparatus was heated in a 70°C oven for 24 hours.

The resulting hydrogels were washed and stored in ethanol at room temperature in a sealed container.

5.2.1.1.2 Analysis of hydrogels

Hydrogels were characterised with FTIR using a Perkin Elmer FTIR instrument

5.2.1.2 UV curing materials

GMMA and GDMA were used as before with the addition of UV initiator 2-hydroxy-2-methylpropiophenone (HMPP) which was obtained from Sigma.

5.2.1.2.1 UV Polymerisation

GMMA (4g), GDMA (0.2g) and water (4g) were mixed. Two quartz glass plates were lined with polyethylene terephthalate (PET) sheets and a polytetrafluoroethylene (PTFE) spacer (250µm thickness) was placed between the sheets and the apparatus was held in place with bulldog clips. HMPP (0.6g) was added to the polymerisation mixture and mixed well, any bubbles were removed by brief sonication. The mixture was quickly injected between the sheets into the space. The apparatus was placed in a UV oven (Dymax Corporation) for 6 minutes, turning over at the end of each minute. The resulting hydrogels were washed and stored in ethanol at room temperature in a sealed container.

5.2.1.2.2 Analysis of hydrogel

Hydrogels were characterised with Fourier transform infrared spectroscopy (FTIR) using a Perkin Elmer FTIR instrument

5.2.2 Incorporation of latex nanoparticles to PGMMA hydrogels

5.2.2.1 Materials

GMMA and GDMA were used as before and PS latexes were incorporated during the polymerisation steps. The latexes synthesised previously had different particle diameters and were used to produce hydrogels with differing distributions of particles and therefore different surface profiles. The particles had approximate diameters of 100, 250 and 715 nm respectively and were incorporated to give 3 different hydrogel formulations. **Formulation 1** was 50% w/w latex: GMMA monomer, **formulation 2** was 25% w/w latex: GMMA and **formulation 3** was 1% w/w latex: GMMA

5.2.2.2 Polymerisation

The latex hydrogels were produced using the thermal curing method described above. GMMA (4g) and GDMA (0.2g) were added to the latex, amounts of which were varied according to the desired formulation and the remaining mass was made up with water. 50% w/w latex hydrogels comprised 4g of latex and no further water (**Formulation 1**), 25% w/w latex hydrogels comprised 2g latex, 2g water (**Formulation 2**) and 1% w/w latex hydrogels comprised 0.8g latex and 3.2g water (**Formulation 3**). The monomers and latexes (and water) were mixed well and potassium persulphate (0.06g) was added and mixed. Again any bubbles were removed by brief sonication. The polymerisation mixture was injected into the cavity between the glass sheets made by the spacer and cured in an oven at 70° C for 24 hours then removed, washed and stored in ethanol in a sealed container at room temperature.

5.2.2.3 Analysis of hydrogel

Hydrogels were characterised with Fourier transform infrared spectroscopy (FTIR) using a Perkin Elmer FTIR instrument, and imaged using scanning electron microscopy (SEM) and a Calibre atomic force microscopy (AFM) instrument. The hydrogels were imaged with SEM on the bulk flat surface and also as a cross-section, which was made by snapping the hydrogel. The cross section served to analyse whether the latex particles were incorporated throughout the hydrogel matrix or on the surface.

5.2.2.4 White light interferometry

A measure of the roughness of the hydrogel surfaces of dried samples was obtained using a white light interferometer instrument, made by Bruker, model NPFLEX. Dried hydrogel samples were analysed with the instrument and corresponding Vision 64 software. Dried samples were used as the interferometer makes very sensitive measurements, when the wetted hydrogel samples are exposed to the air, they begin to dry which changes their shape and causes the gels to curl. This causes difficulties with obtaining accurate measurements of surface profiles.

5.2.3 Contact cytotoxicity testing of hydrogels with 3T3 cells

To test whether the surfaces of the hydrogels were toxic to cells, a robust and adherent cell line was cultured on their surfaces.

5.2.3.1 3T3 cell culture media materials

RPMI 1640 media, Dulbecco's modified Eagle's media (DMEM), ethylene diamine tetracetic acid (EDTA) and trypsin solution were obtained from Sigma. FBS and L-glutamine (LG) were obtained from Sigma and aliquoted from stock solutions.

DMEM and RPMI were mixed in a Sterilin pot, to which, 1% LG and 10% FBS were added and were well mixed.

5.2.3.2 Culturing 3T3 cells

3T3 murine fibroblast cells were kindly provided by Sam Bullers (Jack Birch Unit, Dept. of biology, University of York) and cultured in media described above. The cells were cultured to confluence in 100ml Nunc brand flasks, obtained from Fisher Scientific. Cells were incubated at 37°C, 10% CO_2. Cells were passaged when they reached confluence.

5.2.3.3 Passaging 3T3 cells

Cell culture media was removed and 5-10 ml EDTA was added. Flasks were then incubated at 37°C for 5-7 minutes (maximum). EDTA was removed and 1 ml trypsin was added to lift the cells from the surface of the flask. The flask was vigorously agitated to aid lifting and cells were washed with 5-10 ml fresh culture media. The cell solution was centrifuged at 1400 RPM for 4 minutes and the resulting cell pellet was resuspended in 9 ml fresh media, from which 1ml was removed and added to a fresh Nunc flask and topped up with 14 ml fresh media. The flask was then returned to the incubator.

5.2.3.4 Culturing 3T3 cells on hydrogels

5.2.3.4.1 Materials

Media equilibrated 50% latex hydrogel disks comprising of 100nm particles and 3T3 cell stocks were placed in 24 well plates (Corning® CellBIND® cell culture plates) obtained from Sigma. Solvent grade ethanol was obtained from Fisher and diluted to 70% with deionised water and was used for general disinfection, formalin 10% solution was obtained from Sigma and used without further dilution. Hoechst staining solution (1 in 10000 dilution) was kindly provided by the Southgate research group (Jack Birch Unit, Dept. of biology,

University of York), and was diluted with PBS where necessary. PBS and Triton-X solution (0.1%) were obtained from Sigma.

5.2.3.4.2 Cell culture

Cells were seeded onto prepared hydrogels into steel seeding rings (10ml internal diameter) at concentrations of 10^6, 10^5, 10^4, 10^3, 10^2 cells/ml to test optimal seeding densities. The cell solutions were allowed to soak into the hydrogels before the volume of media in the wells was raised to 200µl in the seeding rings. The plates were covered and incubated at 37°C, 10% CO_2 for 24 hours. At the end of the experiment the cell media was aspirated from the wells and Phosphate buffer solution (PBS) was added to wash, each well was mixed well and the PBS was then removed. 10% formalin was then added to each well and the plate was covered and left for 24 hours at room temperature. After 24 hours the formalin was removed and 70% ethanol was added to the wells to fix the cells. The wells were sealed and stored in a refrigerator.

5.2.3.5 Epifluorescence imaging of 3T3 cells on hydrogel surfaces

Following fixation, ethanol was removed from the wells containing the hydrogels and a 0.1% Triton-X solution in PBS was added to the wells to permeabilise the cell membranes. The wells were covered and placed on a rocker plate for 15 minutes. After 15 minutes, the solution was removed and the wells were treated with a 1 in 10000 (v/v) solution of Hoechst stain in PBS and placed on a rocker for 10 minutes. Following this the solution was removed and the gels were washed with PBS for 3x5 minutes on the rocker. After washing the gels were removed from the wells and mounted on glass microscope slides, antifade solution was added to the surfaces and a cover slip was placed on top.

The gels were imaged using a mercury burner lamp in the blue fluorescent channel. The ImagePro plus software was used to obtain images of cell nuclei on the surface of the hydrogel. The cells were imaged at x20 magnification using a non-oil lens.

5.3 Results and discussion

5.3.1 Hydrogel synthesis

Hydrogels were synthesised to produce a surface upon which cells could be cultured. As noted previously, hydrogels bear many similarities to native tissue due to characteristics such as their high water content and porosity. A number of hydrogels were synthesised to give a range of surfaces for the cells to interact with. These surfaces possessed varying surface profiles from latex particles embedded in the surface. Bare hydrogels with no particles incorporated were synthesised as a control. Shown schematically below

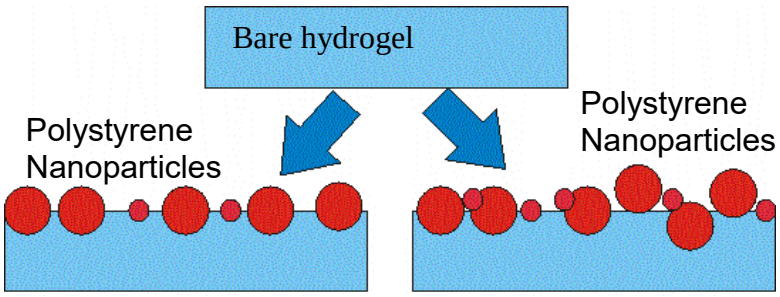

Figure 5-1 Schematic of producing rough surfaced hydrogels

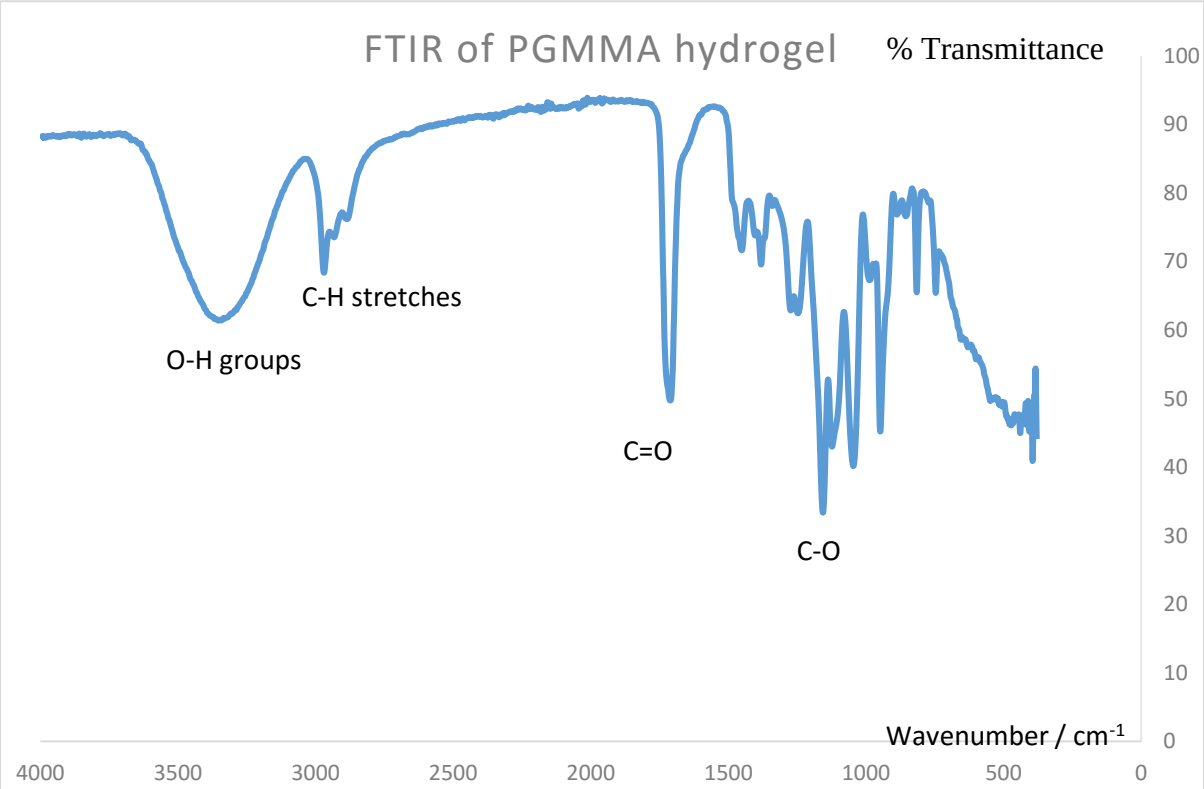

Figure 5-2 FTIR spectrum of PGMMA hydrogel

5.3.2 Synthesis of poly(glycerol monomethacrylate)

The hydrogels produced by both the thermal and UV curing methods were thin, transparent gels. They were flexible and somewhat fragile, tearing easily when manipulated.

The IR spectra (shown in Figure 5-2 above) showed peaks at approximately 3380 cm^{-1} (broad) representing –OH stretching vibrations, 2960 cm^{-1} signifying –C-H stretches, 1700 representing C=O stretches, 1100 representing C-O stretches.

The hydrogels were stored in ethanol, this was due to their eventual use as a biomaterial, the ethanol served as a disinfectant to kill any microorganisms currently present on the surface and stop any further infection.

The surface of the hydrogel was imaged using SEM and found to be very flat and mostly featureless, any features of note were due to defects in the surface, and for example where

the hydrogel had stuck to the PET sheet during curing and torn during removal or manipulation. The mostly featureless surface is due to the curing of the hydrogel on a flat PET covered glass surface and is to be expected. The following images are SEM micrographs of the hydrogel surface (Figure 5-3 below).

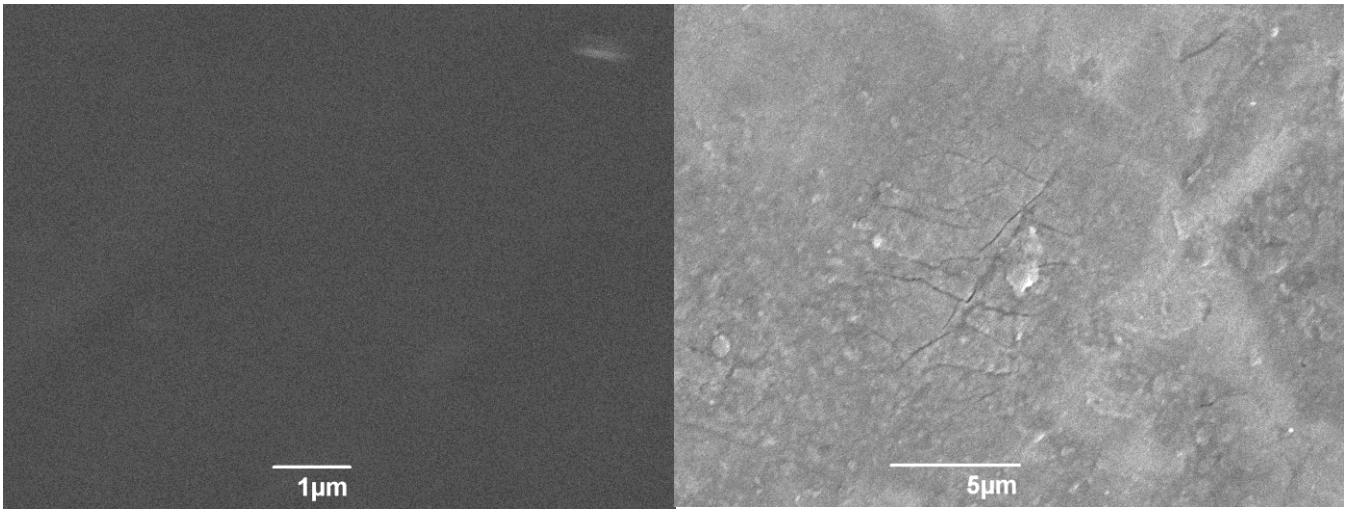

Figure 5-3 SEM image of PGMMA hydrogel surface

5.3.3 Incorporation of latex nanoparticles to PGMMA hydrogels

The hydrogels with incorporated PS nanoparticles were produced using thermal induced radical polymerisation in water. The gels produced were white and opaque. When the gels had finished curing they were firmer than the bare PGMMA, when dry they were very brittle and would tear and break easily when manipulated. Following curing the gels were transferred to ethanol. In general the gels containing the larger particle size latex (550 and 715 nm, formulations 2 & 3 respectively) were tougher than the 150 nm latex gels. The equilibrium water contents (EWC) of the latex hydrogels are shown in the following table. (Table 5-1). The EWCs of the gels are all around the same value despite there being a relatively large volume of latex particles incorporated into the gel structure. This is possibly due to the low solids content of the latex solutions and increasing water contents of the

hydrogels meaning that water swelling effects will dominate over possible reduction in swelling caused by hydrophobic latex particles.

LATEX FORMULATION WITH % LATEX CONTENT OF HYDROGEL (W/W)	% EQUILIBRIUM WATER CONTENT
50-1	75.48 ± 3.1
25-1	76.82 ± 3.1
1-1	78.91 ± 2.6
50-2	73.46 ± 3.4
25-2	79.56 ± 5.1
1-2	80.25 ± 3.6
50-3	77.69 ± 3.0
25-3	75.28 ± 3.7
1-3	79.61 ± 3.0
0	77.62 ± 3.4

Table 5-1 Table of equilibrium water content of PS latex embedded hydrogels

The FTIR spectra (Figure 5-4 below) obtained for the 50% latex composition of formulation 1 contained peaks at approximately 3320 cm^{-1} (broad) representing –OH stretching vibrations, 2900 cm^{-1} signifying –CH stretches, and C=O stretches around 1700 cm^{-1}, aromatic C-C stretches around 1450 and also an increase of peaks in the fingerprint region representing aromatic bond stretches from the polystyrene particles present.

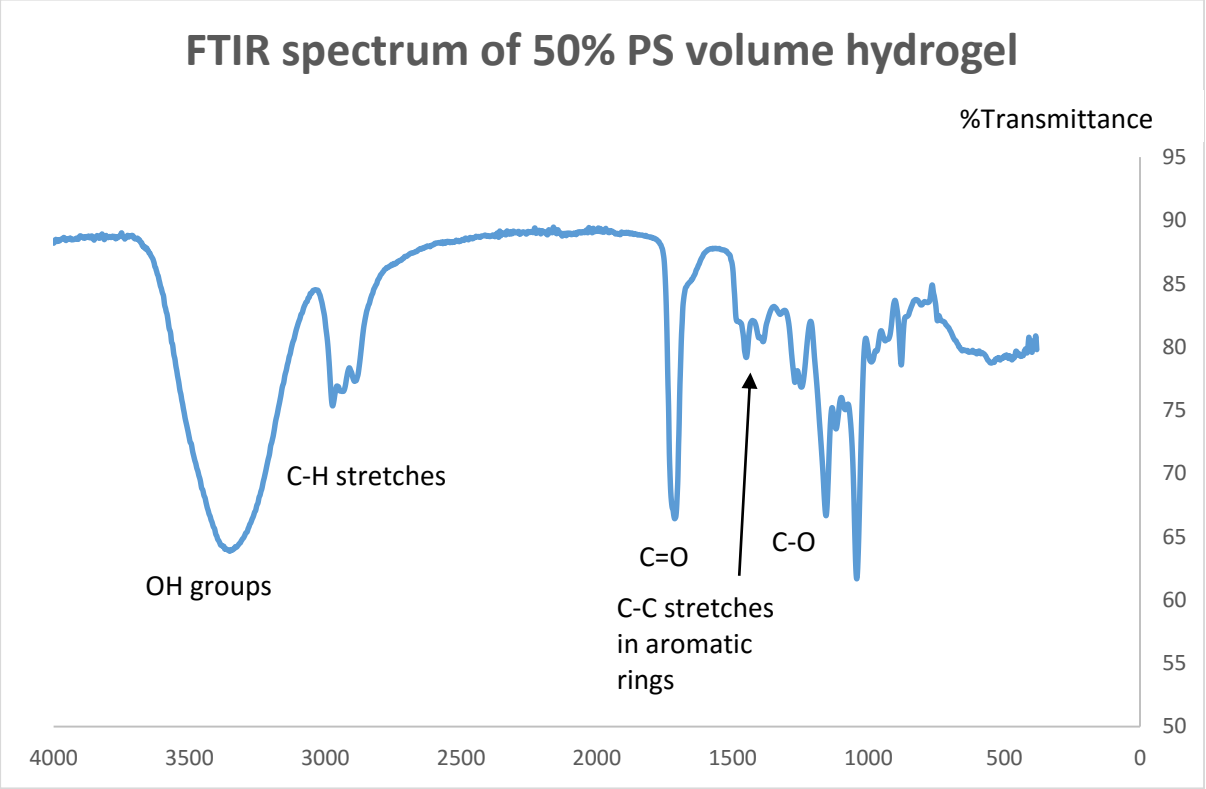

Figure 5-4 FTIR spectrum of 50% PS volume hydrogel

The surfaces of these hydrogels were intended to be rougher than the bare PGMMA hydrogel and were imaged using both AFM and SEM. The following SEM micrographs illustrate the surface topography. Hydrogels containing all three particle sizes were imaged and are presented at similar scales. It is possible to discern the differences in size of the particles and their different surface densities.

The cross sectional images show that PS nanoparticles are present throughout the hydrogel structure and that they are not just found on the surface of the gel. Figure 5-11 and Figure 5-16 show the transition between the top surface and the cross sectional area and show that the particles continue to be distributed into the interior of the structure and that there is much more than a surface monolayer of PS particles.

5.3.4 Scanning electron microscope images of hydrogel surfaces

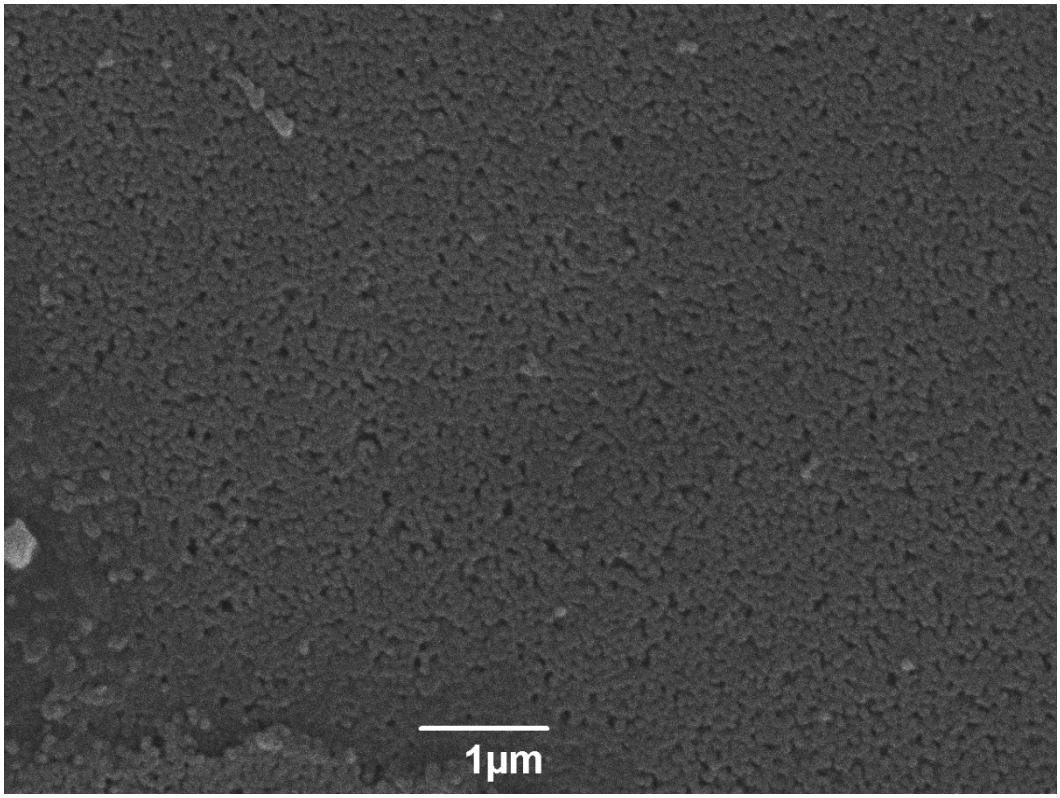

Figure 5-5 SEM image of hydrogel 50-1

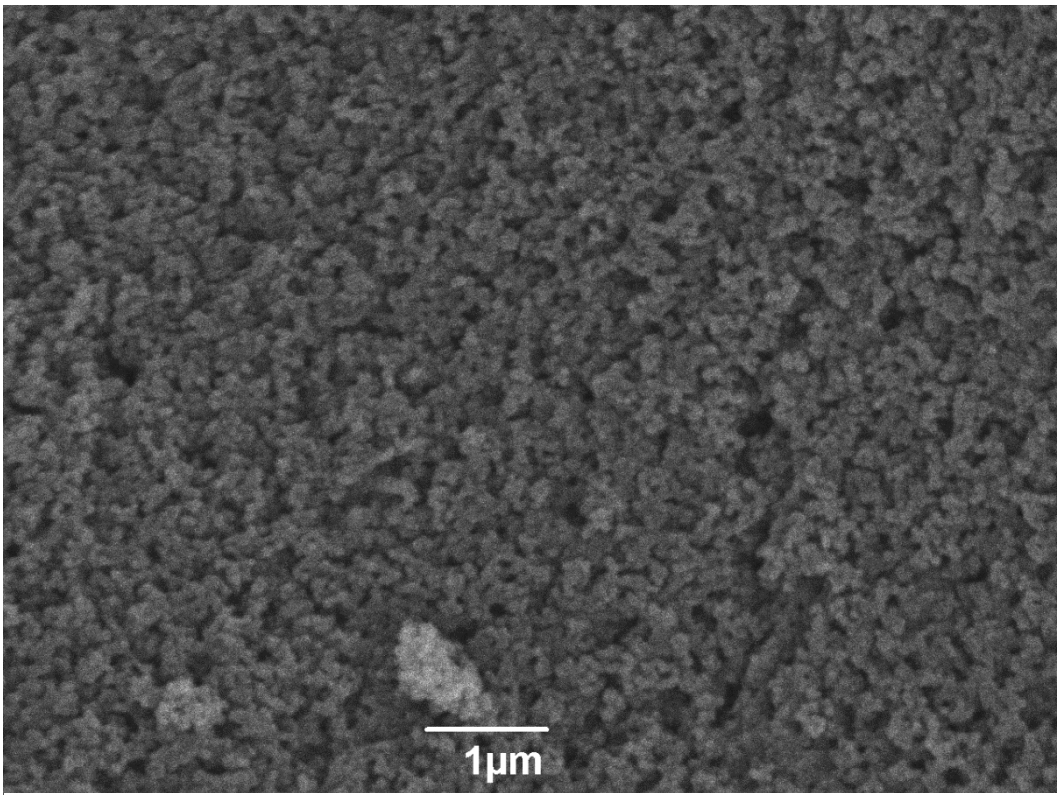

Figure 5-6 SEM image of hydrogel 1-1,

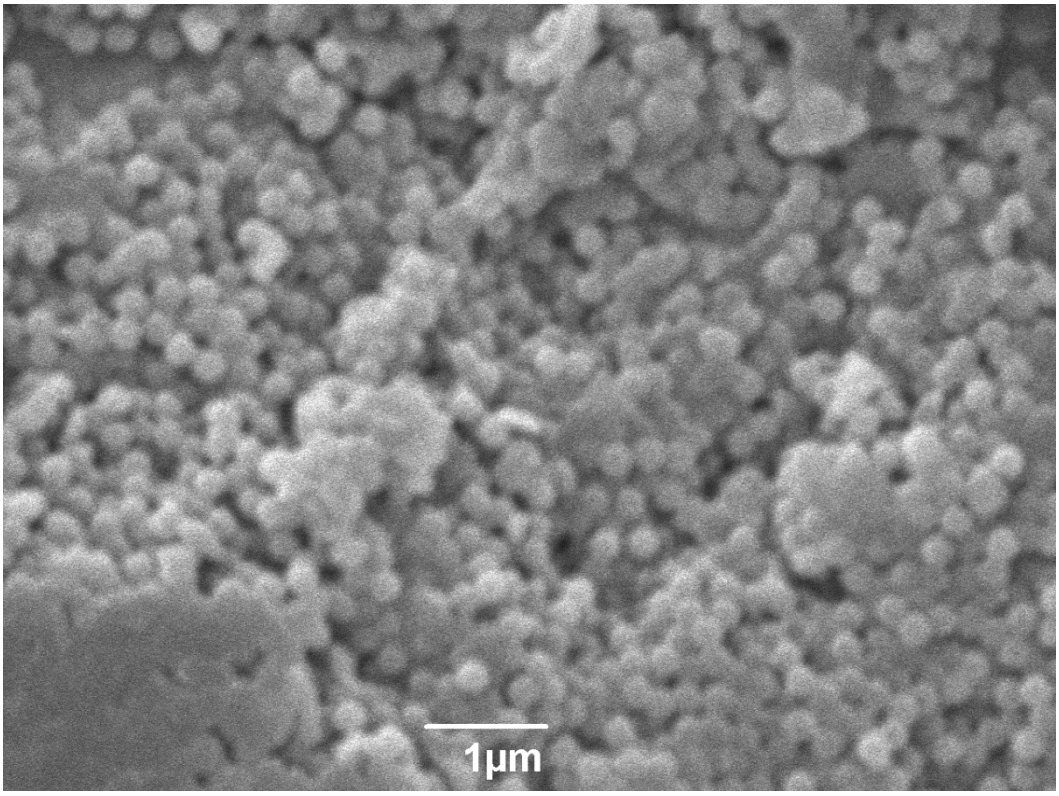

Figure 5-7 SEM image of hydrogel 50-2

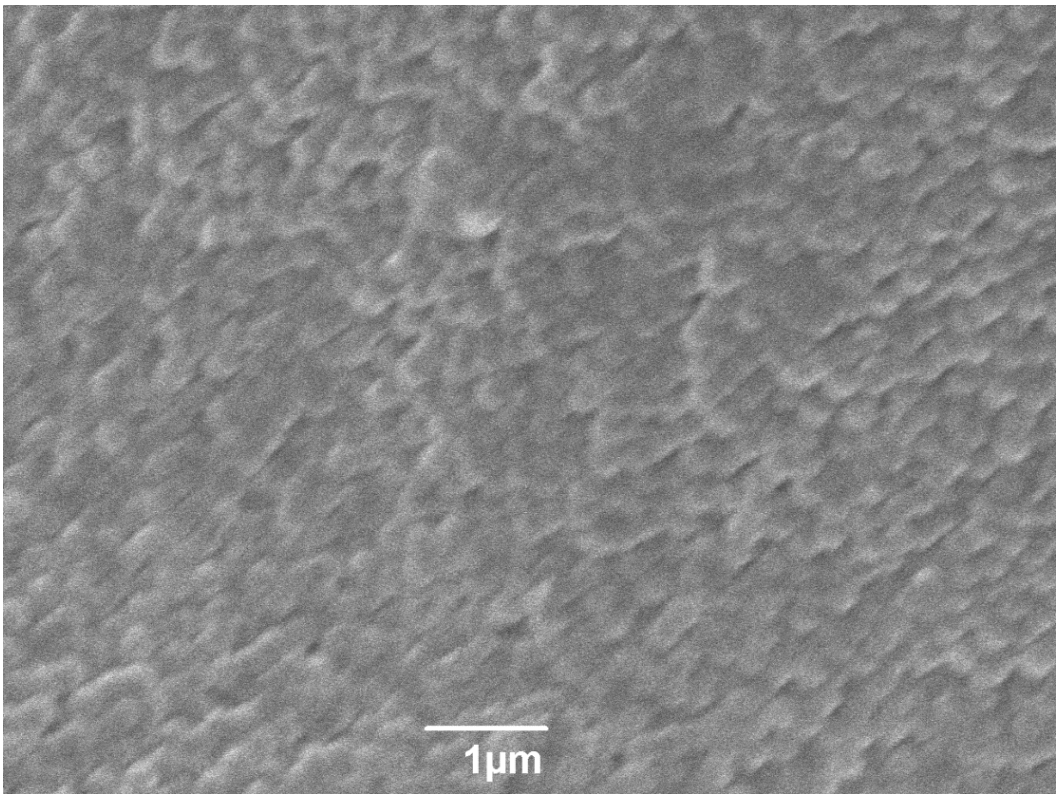

Figure 5-8 SEM image of the surface of hydrogel 50-1

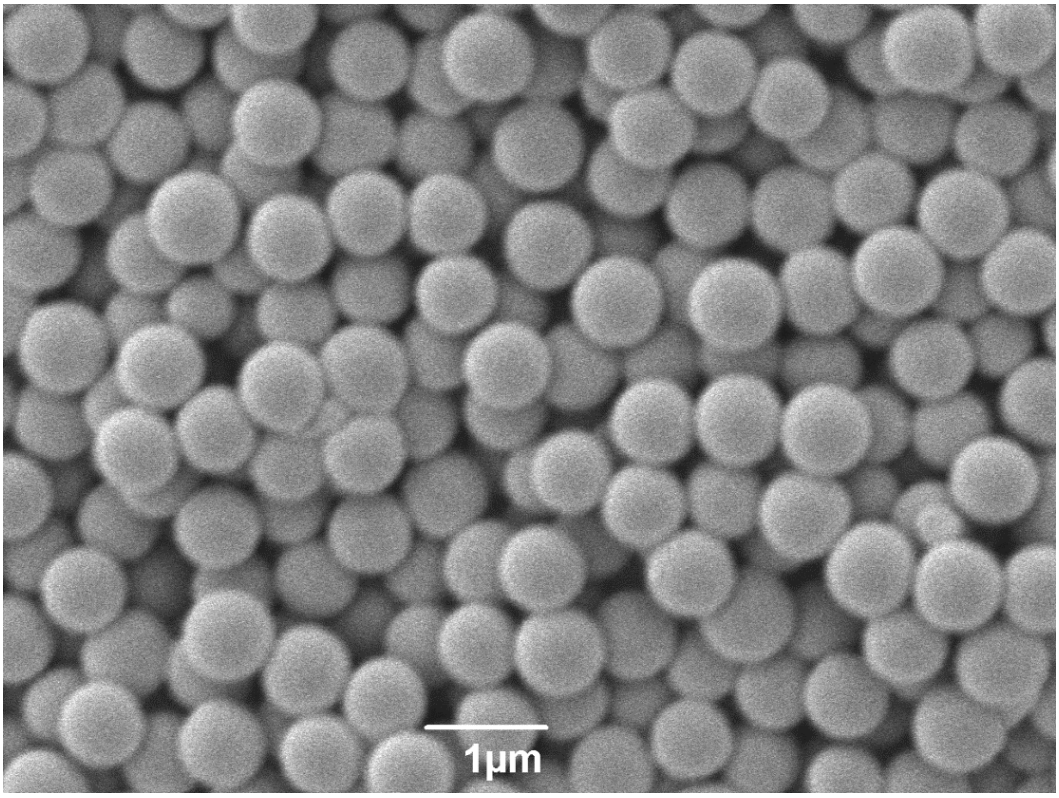

Figure 5-9 SEM of hydrogel 50-3 surface

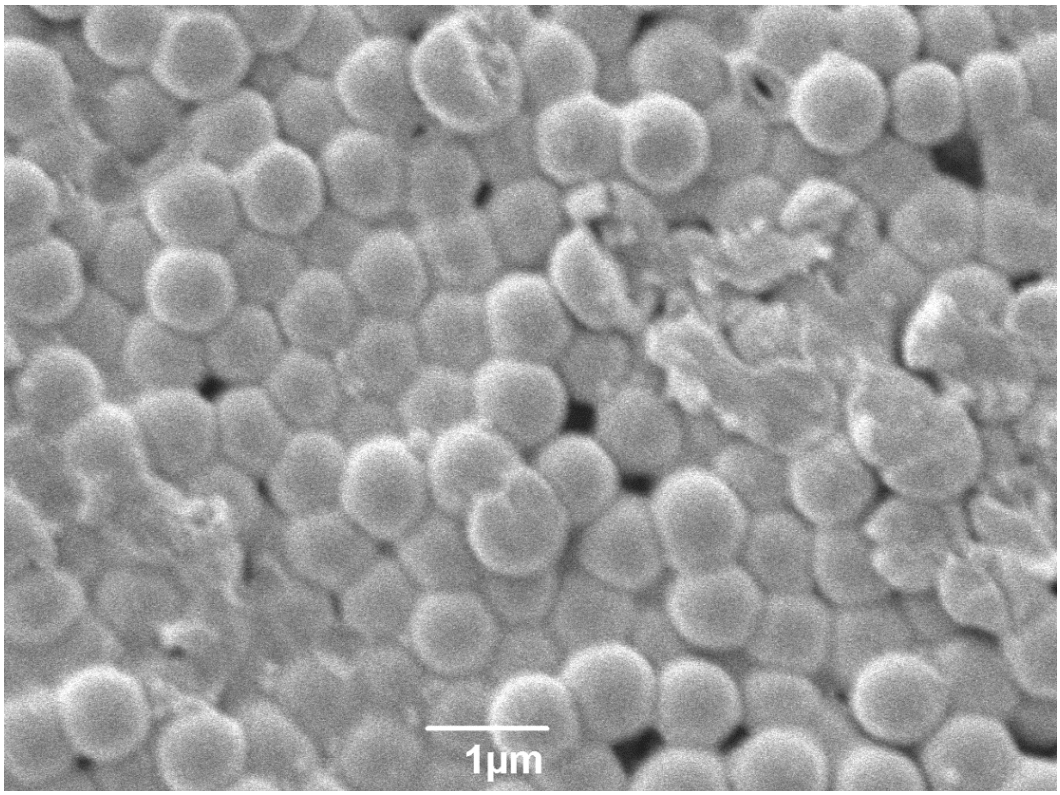

Figure 5-10 SEM image of hydrogel 1-3

The SEM images above show that the latex particles are present and visible on the surfaces of the hydrogels. The physical distribution of the particles does change according to the amount of particles present and the size of the particles.

The 50-1 hydrogel (Figure 5-8), appears to have a somewhat even spread of PS nanoparticles across the surface. It is possible that the THP-1 cells, when they encounter the surface of this hydrogel will not be able to discern much roughness due to the small particle size. Cells will be around 10µm across (approximately the width of Figure 5-8). For this reason, it was decided to fabricate larger particles.

The SEM of the surface of hydrogel 1-1 (Figure 5-6), appears to show a more convoluted surface which could be indicative of a rougher appearance than the 50% hydrogel, this is somewhat surprising as this hydrogel contained a lower concentration of particles. It is suspected that the lower concentration caused the particles to aggregate to a degree, creating an uneven, rougher surface with different aggregations on top of one another. This clustering of aggregations may be caused by the repulsion of the hydrophobic PS particles by the continuous water phase. The PS particles may then aggregate to lessen their overall surface area and these new larger colloidal particles cluster together at the surface of the gel producing the observed rougher surface.

The SEMs of 50% latex content for formulations 2(Figure 5-7) also showed this crowded, convoluted arrangement of particles whereas when the lower proportion of particles were present (Figure 5-8 & Figure 5-10), they appeared to pack more closely together and give a smoother appearance. This is perhaps due to that as their size increased, the charge on the particles did not significantly change (as shown by zeta potentials, previously), therefore, the overall charge per unit of surface area will have decreased as size increased meaning the particles could pack together better giving a better arrangement at lower concentrations. At

higher concentrations, the larger number of particles in a similar area causes them to stack up on top of each other.

To investigate whether the particles were present throughout the matrix of the gel or simply on the surface, images of cross sections of the gels were images with SEM, shown in the following figures.

5.3.5 Cross section images of latex hydrogels

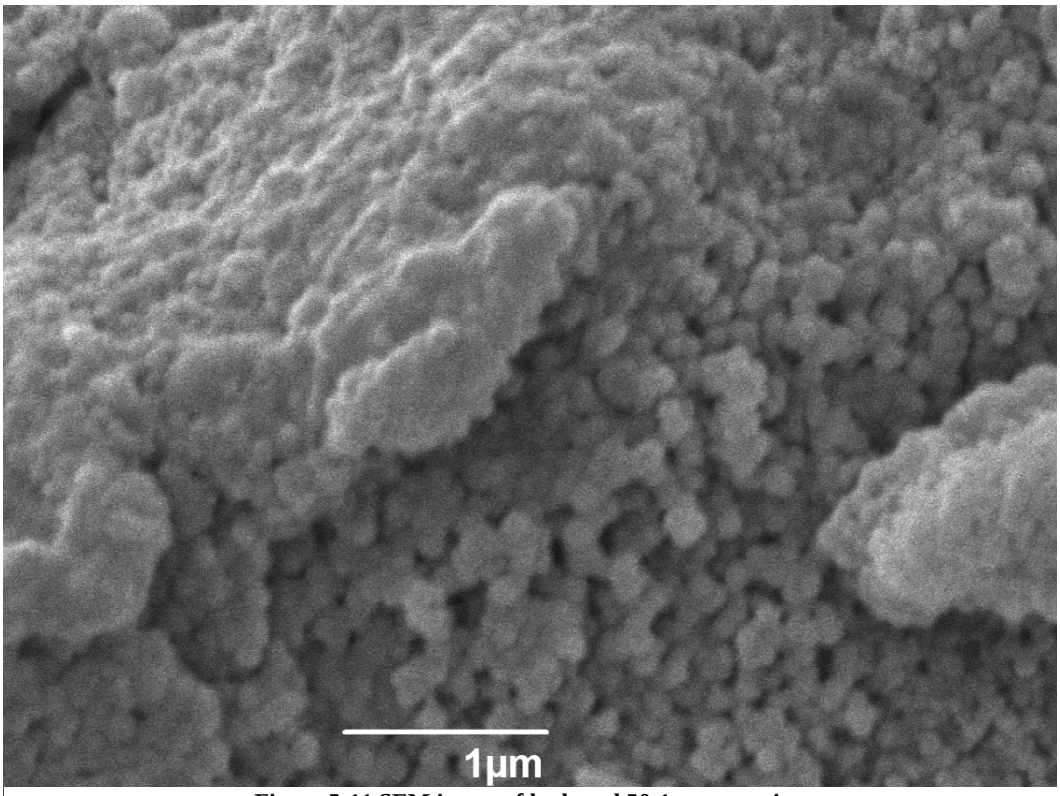

Figure 5-11 SEM image of hydrogel 50-1 cross section

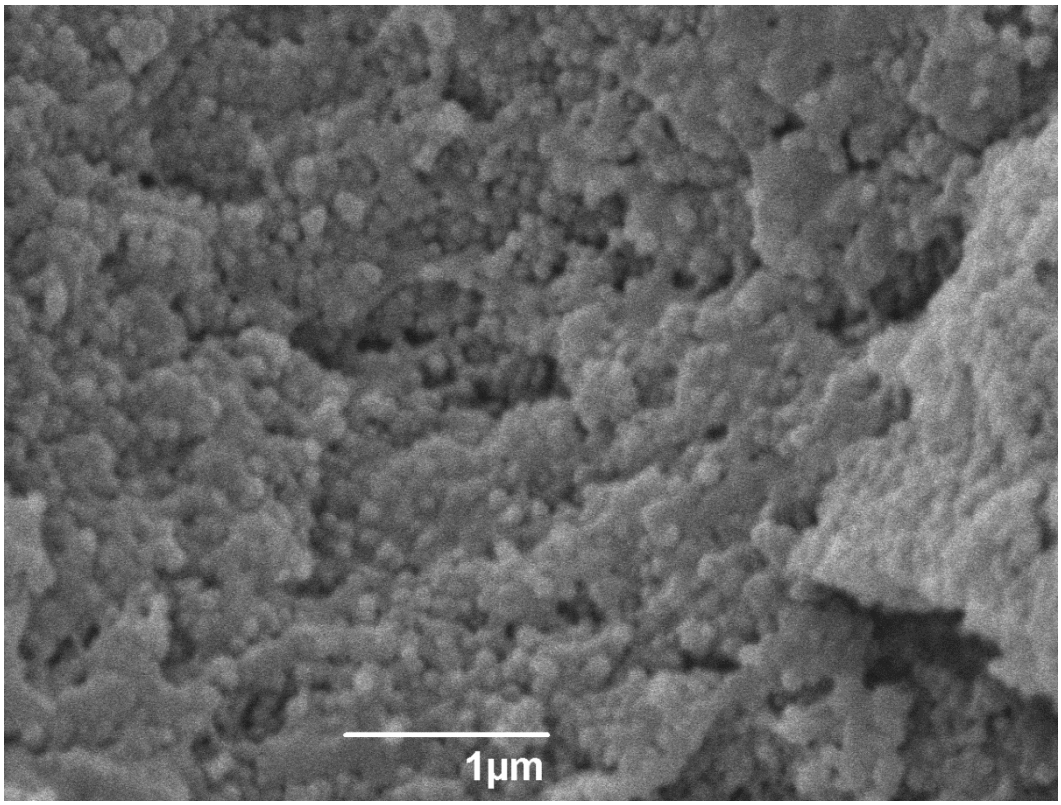

Figure 5-12 SEM image of hydrogel 50-1 cross section

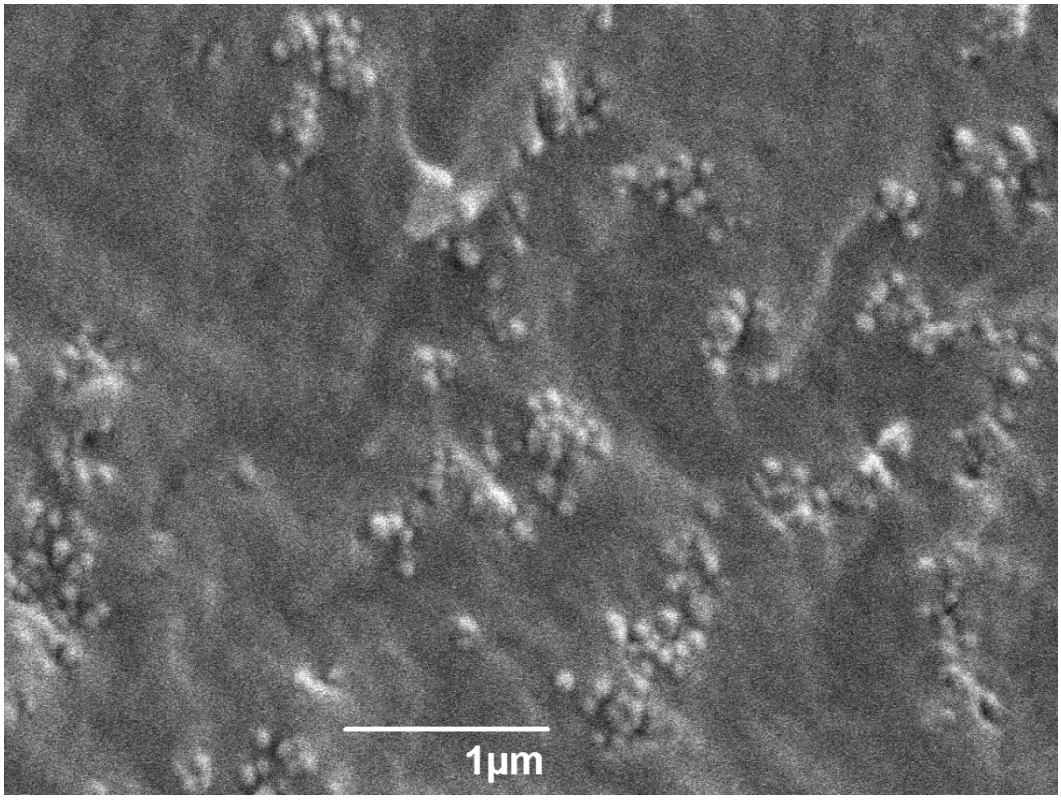

Figure 5-13 SEM image of hydrogel 1-1 cross section

In order to image the cross section, the hydrogels were snapped and torn lengthways between two pairs of forceps. The exposed surface was then examined using SEM. The above figures show formulation 1 hydrogels. Figure 5-11 & Figure 5-12 show SEM images of the 50% latex content hydrogel, Figure 5-13 shows 1% latex content. The decrease in latex particle density is immediately apparent. The first image shows the boundary between the flat surface (top left of the image) and the internal surface exposed in cross section. In the image, the flat surface descends into the plane of the page in the upper left hand corner of the image while the cross sectional surface is shown parallel to the plane of the page. Exposed latex particles can easily be seen on the cross section near the surface, still giving the appearance of roughness. The larger areas of uniform material are parts of the bulk hydrogel matrix. This view is consistent in the second image which was taken nearer the centre of the cross sectional area. Particles are shown to be present throughout the

structure of the hydrogel and not just clustered at the surfaces. The third image shows the hydrogel with the lowest distribution of particles. There are clearly fewer particles present which is why the appearance of the hydrogel matrix appears to dominate.

The following images are of the other two formulations of latex particles which show similar distributions of particles despite increasing particle size.

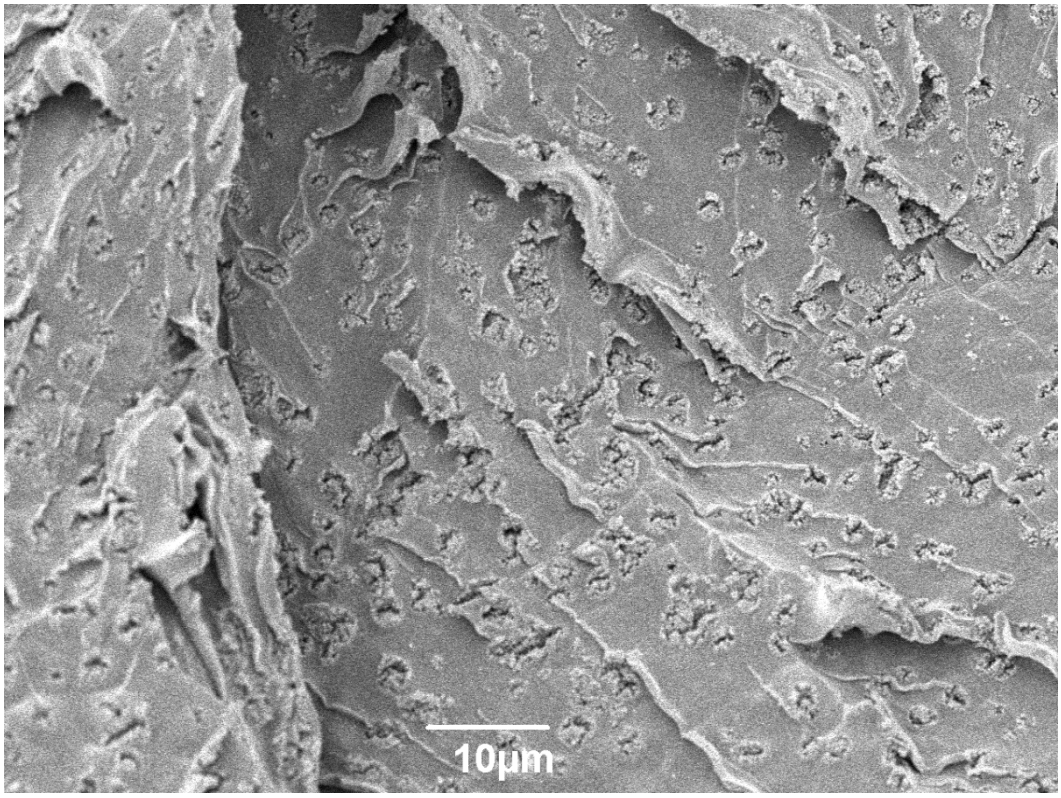

Figure 5-14 SEM image of hydrogel 50-2 cross section

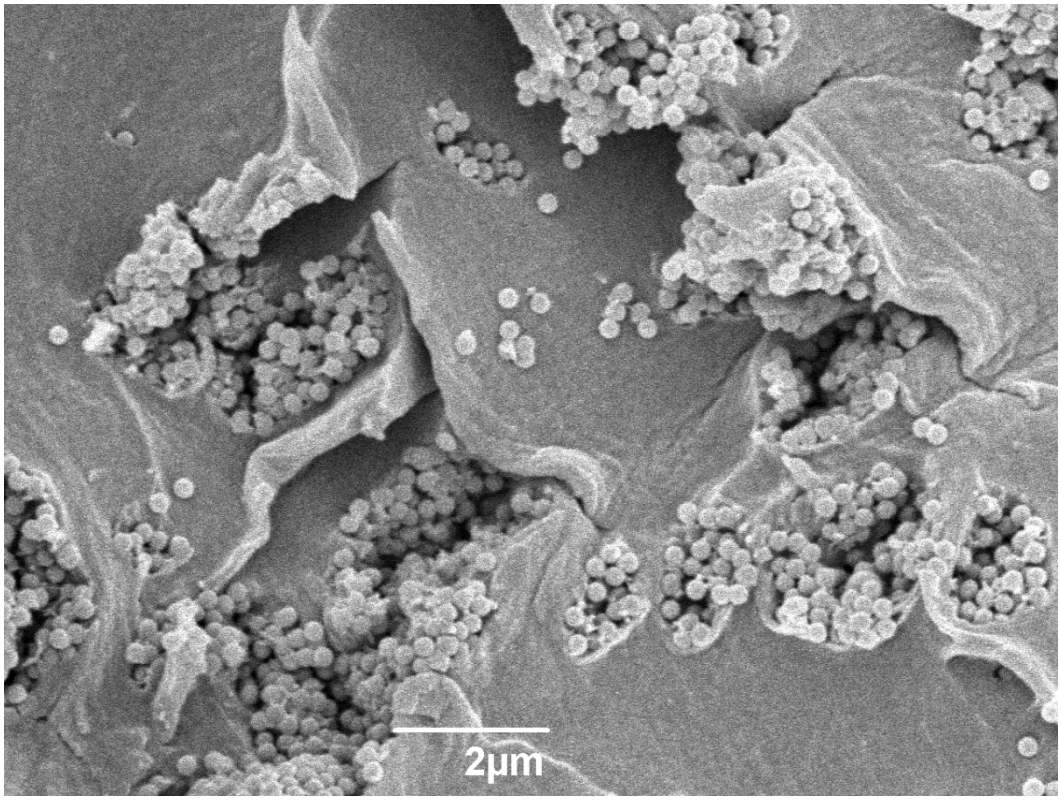

Figure 5-15 SEM image of hydrogel 50-2, cross section

The above images (Figure 5-14 & Figure 5-15) are of the formulation 2 latex particles present at 50% composition of the hydrogel taken from the middle of the cross sectional area. The second is a closer view of the first they show particles present in small clefts in the hydrogel matrix. This is due to the random nature of the tearing of the hydrogel. The clefts are areas where the matrix surrounding the particles has been torn away. Again the images show that the particles are present throughout the structure of the gel. The second image with its increased magnification shows the large distribution of particles, with many crowding on top of one another. This is consistent with the previous image of the surface of this gel, again showing that the particles are distributed throughout the gel.

These particle characteristics are again visible in the cross section of the hydrogel containing 50% formulation 3 latex particles (Figure 5-16 Figure 5-17below). Again the first image is taken at the edge of the flat portion and the cross section. The flat surface extends into the plane of the page and it is possible to see a great many particles clustered on the surface. This again agrees with the flat surface images seen previously. The following images show the clefs visible in previous images. Again large numbers of the particles can be seen clustered in these windows into the bulk hydrogel matrix (Figure 5-18).

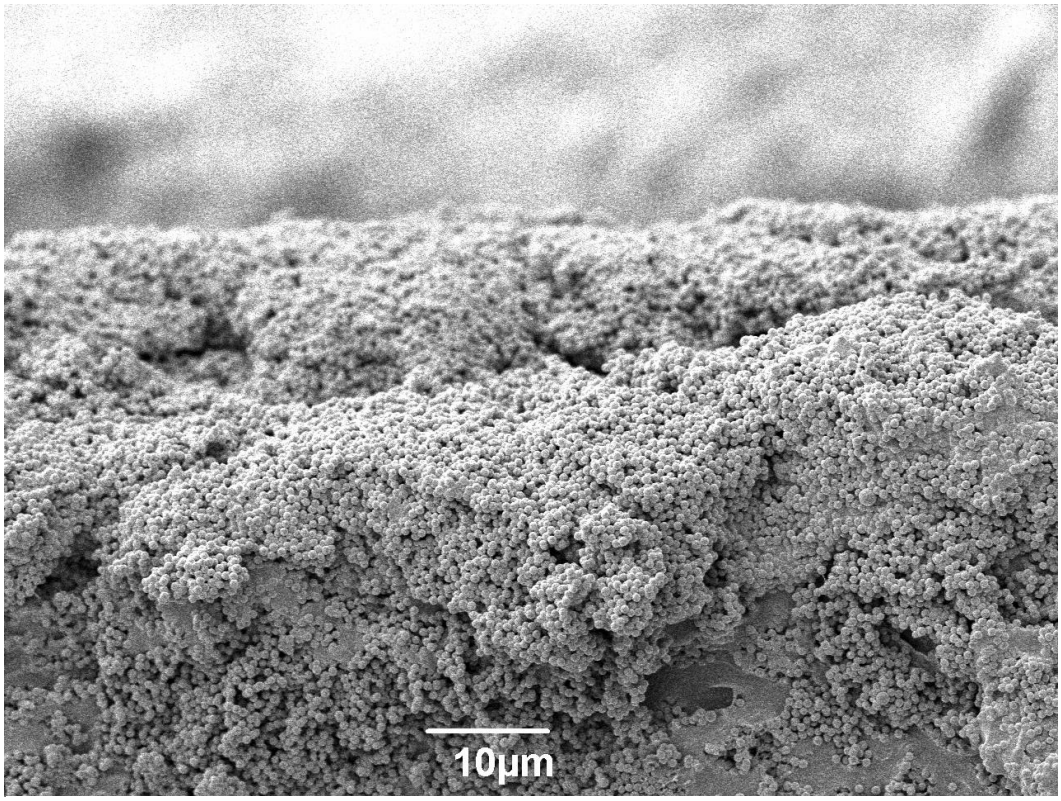

Figure 5-16 SEM image of hydrogel 50-3, cross section

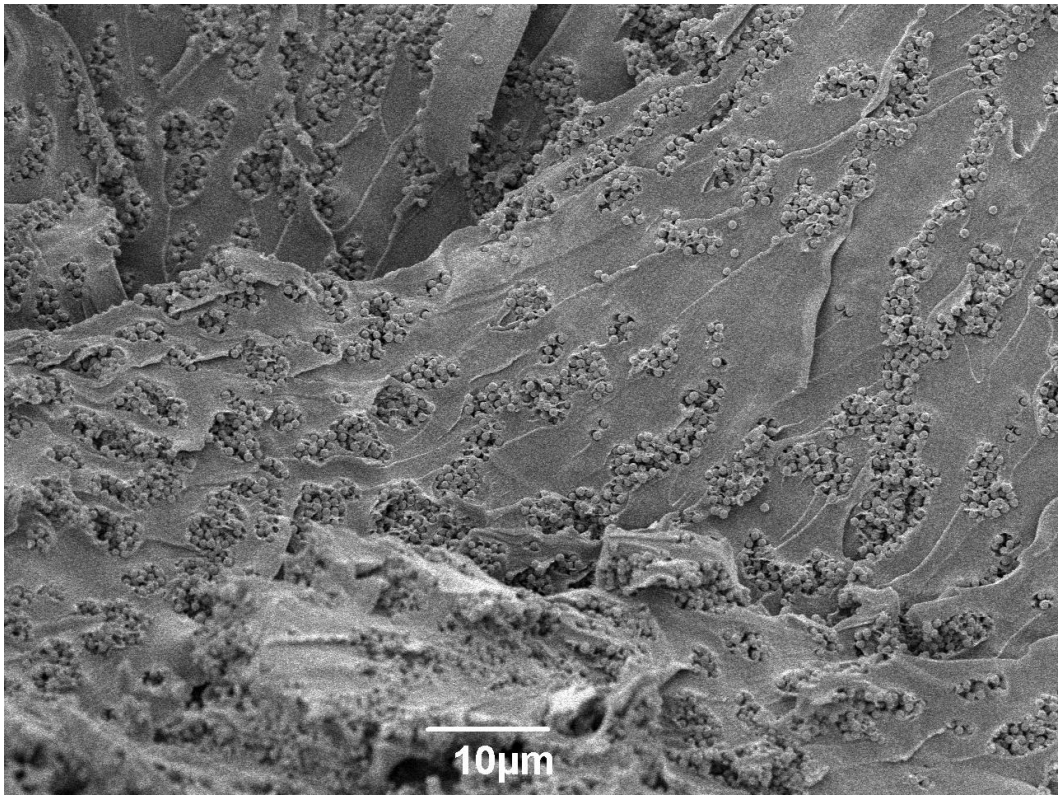

Figure 5-17 SEM image of hydrogel 50-3, cross section

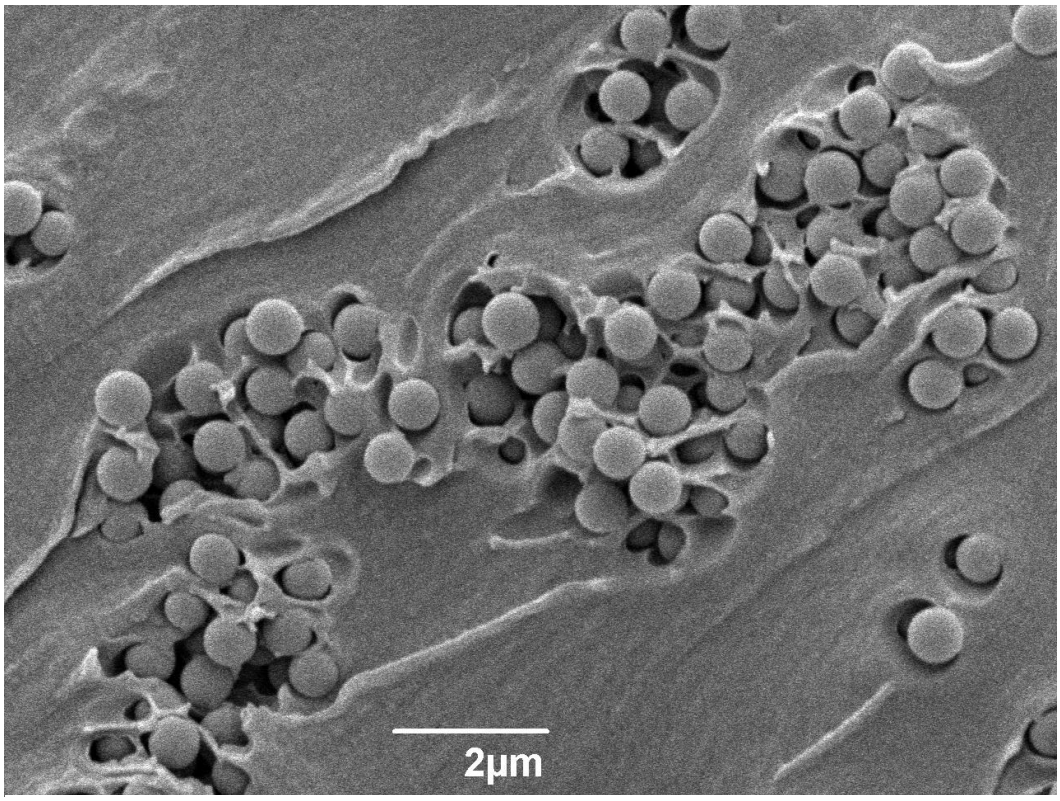

Figure 5-18 SEM image of hydrogel 50-3, cross section

5.3.6 Culturing 3T3 cells

3T3 cells are a cancer cell line derived from murine fibroblasts. They are static culture cells and grow in a monolayer on the base surface of a culture flask. They are regarded as a hardy cell line and will grow on most surfaces, which was why they were used as a test to see whether any cells can grow on the surface of the hydrogels and whether the surfaces are inherently cytotoxic.

5.3.7 Culturing 3T3 cells on hydrogels

The cells were cultured directly onto the surface of the hydrogels in order to assess the possibility of the hydrogels as a biomaterial. The cells were cultured for 48 hours and then fixed using formalin. During the fixation, the cells were treated with Triton-X, a detergent which permeabilise the cellular membrane. The subsequent treatment with Hoechst stain then stained the nucleus of the cells allowing them to be viewed using a fluorescence microscope. The following images (Figure 5-19 -Figure 5-30) show the 3T3 cells, seeded at the various concentrations described above, on the hydrogel surfaces. The hydrogels are formulations 50-1, 1-1 and 0. The images show that 3T3 cells are present on the surface of the gels and that these surfaces have not killed the cells before the end of the 48 hour experiment meaning that the 3T3 cells adhered to the surface of the gels. The images are a qualitative assessment of viability and serve as a positive indicator for the usefulness of the hydrogel surfaces for further culturing of cells.

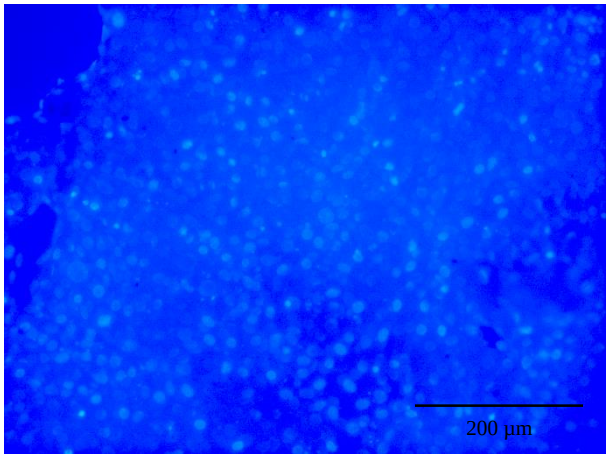

Figure 5-19 Fluorescent micrograph of 1x10^6 3T3 cells seeded onto hydrogel 50-1

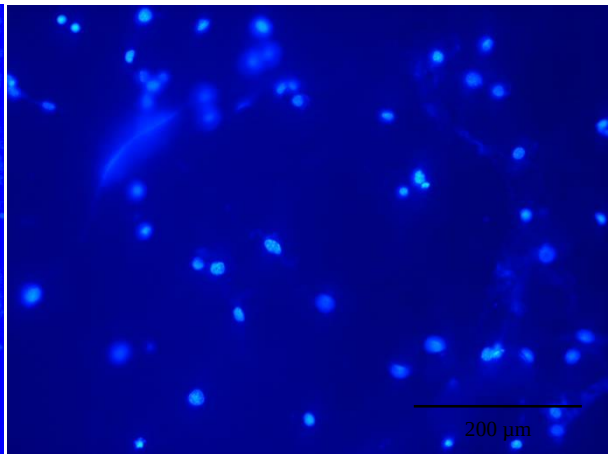

Figure 5-20 Fluorescent micrograph of 1x10^6 3T3 cells seeded onto hydrogel 1-1

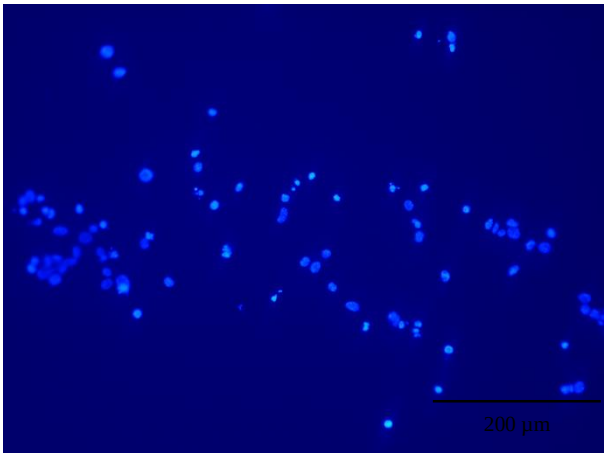

Figure 5-21 Fluorescent micrograph of 1x10^6 3T3 cells seeded onto hydrogel 0

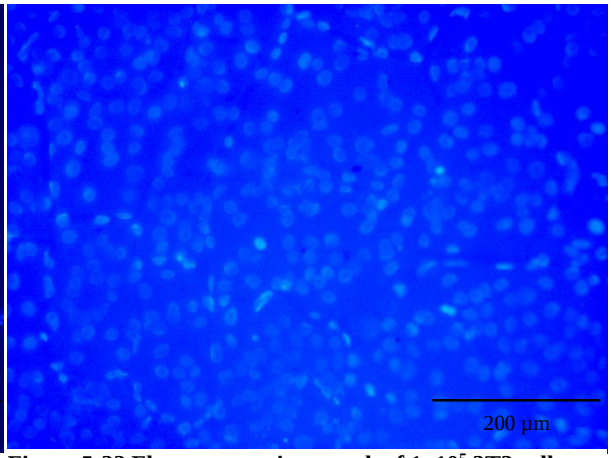

Figure 5-22 Fluorescent micrograph of 1x10^5 3T3 cells seeded onto hydrogel 50-1

Figure 5-23 Fluorescent micrograph of 1x10^5 3T3 cells seeded onto hydrogel 25-1

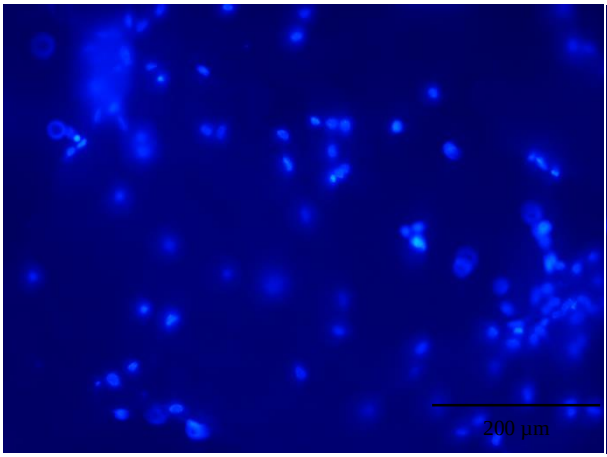

Figure 5-24 Fluorescent micrograph of 1x10^5 3T3 cells seeded onto hydrogel 0

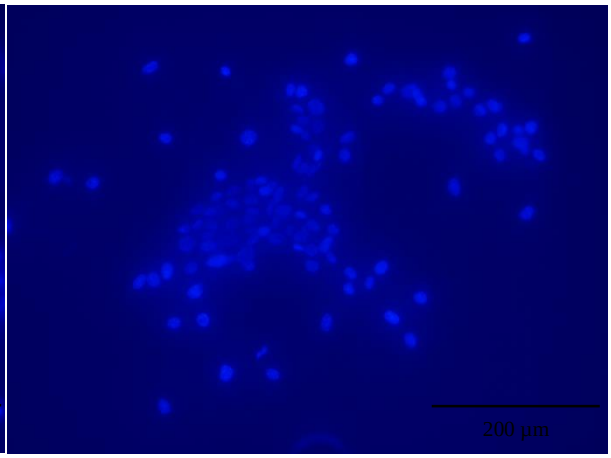

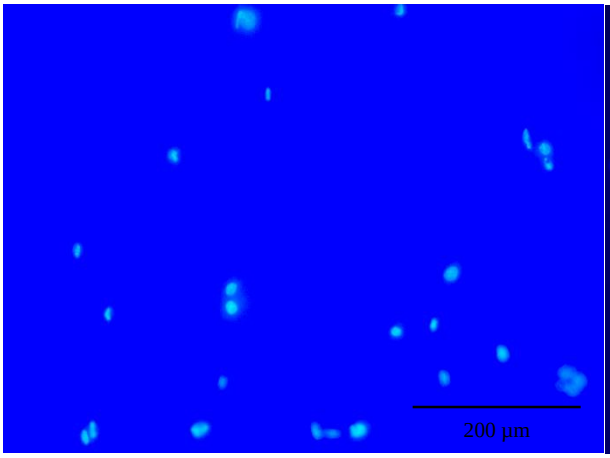

Figure 5-25 Fluorescent micrograph of $1x10^4$ 3T3 cells seeded onto hydrogel 50-1

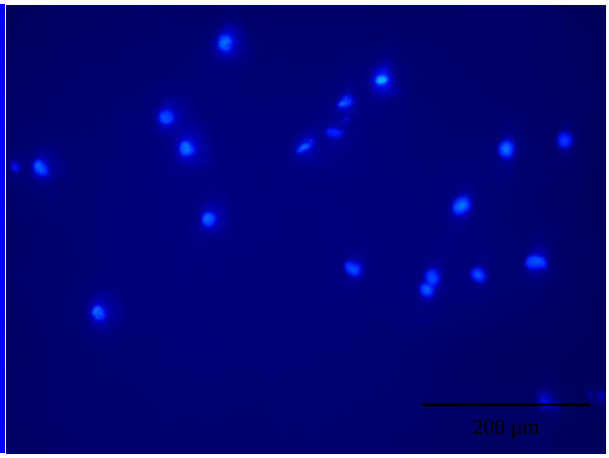

Figure 5-26 Fluorescent micrograph of $1x10^4$ 3T3 cells seeded onto hydrogel 25-1

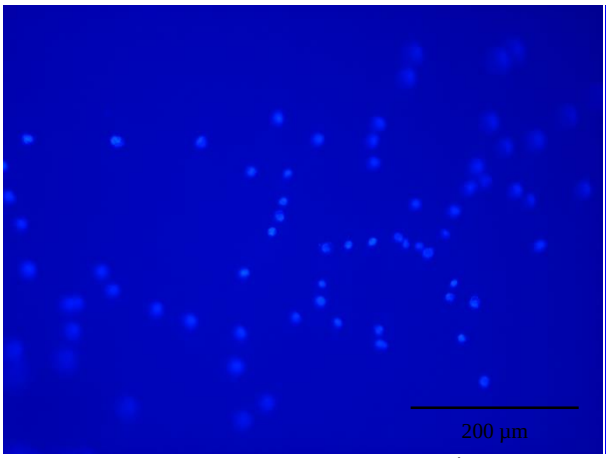

Figure 5-27 Fluorescent micrograph of $1x10^4$ 3T3 cells seeded onto hydrogel 0

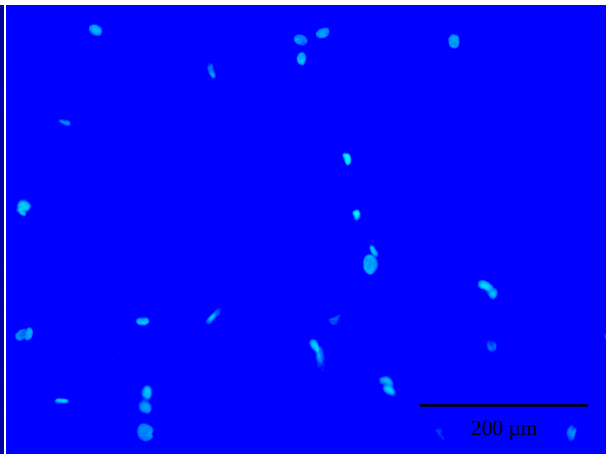

Figure 5-28 Fluorescent micrograph of $1x10^3$ 3T3 cells seeded onto hydrogel 50-1

Figure 5-29 Fluorescent micrograph of $1x10^3$ 3T3 cells seeded onto hydrogel 25-1

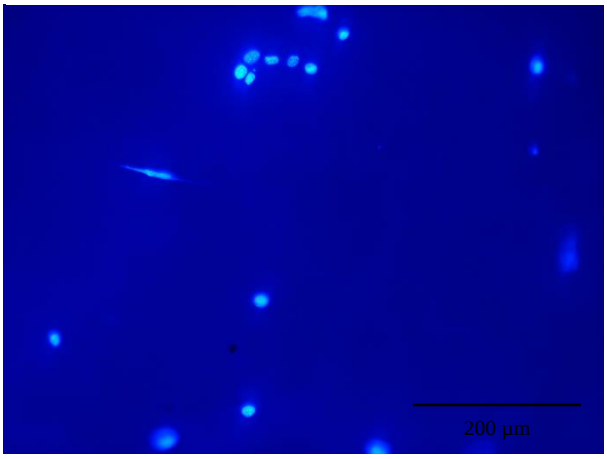

Figure 5-30 Fluorescent micrograph of $1x10^3$ 3T3 cells seeded onto hydrogel 0

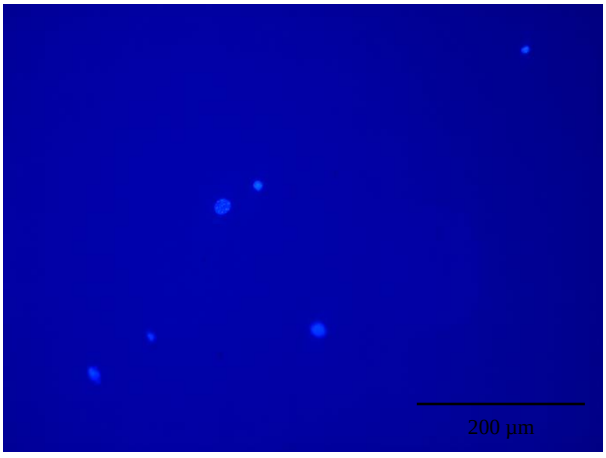

The micrographs shown above show typical views of cellular placement across the surface of the gels, from them it can be seen that cells are present on all surfaces used in this experiment and all concentrations. However as the cell concentration is reduced, qualitatively it is seen that the number cells adhering to the surface appears to decrease. This is shown as a decrease in cell nucleus density and also that a higher number of cells may be present on the 50% PS particle surfaces. This would indicate that the cells prefer the surface with the higher particle density to the surface with fewer particles. This could be due to the hydrophobicity of the surface. As the 50% gel surface has a higher particle surface area and the cells will be in much more contact with more hydrophobic regions on this hydrogel. It should also be noted that although the cells appeared present on the surface of the bare PGMMA hydrogel, there are fewer cells present than the hydrogels containing PS particles indicating that the surfaces of these gels may be unsuitable for the cells to properly adhere. Any cells that were non-adherent will have died and been washed off the surface during fixation. It is not known whether the cells remaining on the surface have also died but are still slightly adherent. A possible probe for this would be to use a cytoskeletal dye to highlight cell morphology or a metabolic activity indicator such as the AlamarBlue® assay.

The intensity of the background indicates the amount of autofluorescence given off by the hydrogels, there is much less autofluorescence given off by the 1% PS hydrogel and bare GMMA hydrogel which makes the individual nuclei and their features easier to distinguish. This strong autofluorescence makes interpreting the endpoints of cell adhesion studies on hydrogels difficult and therefore alternate visualising methods will be utilised in further experiments.

5.3.8 White light interferometry

White light interferometry (WLI) is a method of non-contact surface analysis and characterisation using light. It enables detailed three dimensional analysis of a surface giving measurements of surface characteristics ranging from the submicron scale to the centimetre scale. In this experiment, dried hydrogel samples were used because in the short space of time (approx. 90 seconds), that the samples were under the instrument's light beam being analysed, they were beginning to dry out due to localised heating from the light beam. A similar problem was described when using upright microscopy to visualise hydrogel surfaces, described in later chapters.

This drying caused them to curl on one side or both and caused problems for the instrument as it was measuring very sensitive surface characteristics which were changing rapidly. As the samples were dried out, the measurements only give an indication of the roughness of the wetted samples which are experienced by cells during culture. Dried samples are slightly smaller in all dimensions, than when they are fully wetted.

The WLI instrument measured surface topography parameters and gave a value for roughness, Sa, which is measured as an average of surface height deviation from an ideal mean. The WLI software measures Sa and other surface parameters over the whole of the hydrogel sample. It gave surface data and three dimensional images which illustrate this data. The surface data is summarised in the following table. Three individual samples were measured for each hydrogel and the error is reported as the standard error where n=3.

HYDROGEL	S_A / µm
50-1	0.62±0.03
25-1	0.40±0.08
1-1	0.21±0.04
50-2	0.47±0.02
25-2	1.78±0.21
1-2	0.73±0.04
50-3	1.15±0.08
25-3	1.45±0.07
1-3	1.022±0.04
0	0.30±0.11

Table 5-2 A table showing the average surface roughness of the hydrogels

This data is represented graphically in the following Figure 5-31

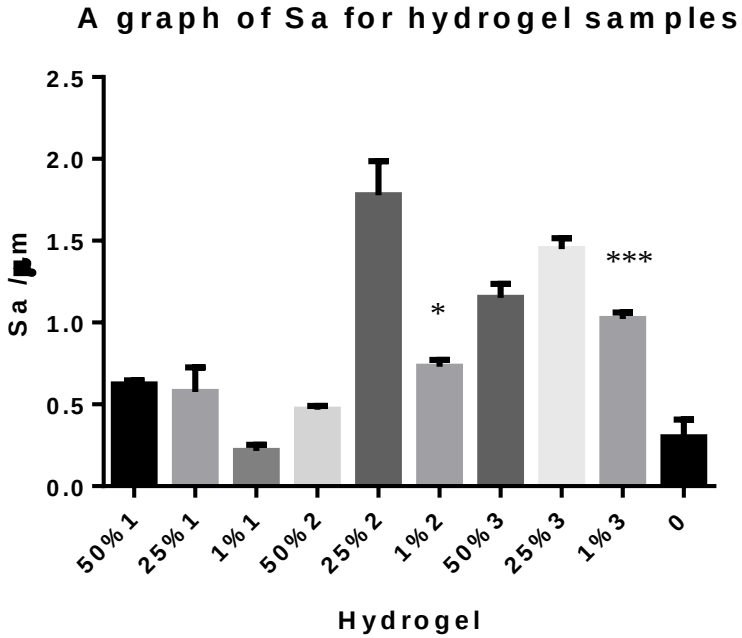

Figure 5-31 A graph of surface roughness for the hydrogel samples with statistical significance level indicated

From the data presented above, it is clear that the 25-2 hydrogel is an anomaly. It appears to be much rougher than the other hydrogel samples. The reason for this becomes clear when the visual representation of the samples is examined, shown below (Figure 5-32 Figure 5-35). These 25-2 samples measured had more voids from air bubbles in the surface which the instrument recorded as larger variations from its average structure. This is understandable, however the holes themselves are sub millimetre in size. Later chapters will investigate cells cultured on the surfaces of hydrogels to examine whether large scale features like these holes and voids has an effect on cell adhesion on the gels.

The roughness measurements were analysed with one-way analysis of variance (ANOVA) and Dunnett's multiple comparison test using the GraphPad Prism programme which compared the average roughness values of the latex hydrogels against the values for the bare PGMMA gel. It found that gels 25-2, 1-2, 50-3, 25-3 and 1-3 were significantly rougher than the bare hydrogel, the level of statistical significance is indicated on the graph above. This is understandable as these gels contain larger particles which increase in roughness. The relatively smoother value for the formulation 1 hydrogels which had the smallest diameter particles, appears to tally well with the visual information available from SEMs taken of the gels shown above. There is a relatively large error value associated with the bare PGMMA hydrogel, this is because the surface of this hydrogel is quite smooth and featureless and any small surface deviations such as those caused by cracks or debris too small to be seen with the human eye can cause a large degree of variation across the whole hydrogel surface

.Repeated measurements of a larger sample of gels would give a more complete picture with less error in the samples. Unfortunately time constraints prevented a repeat of this experiment.

The following figures are a selection of the three dimensional representations of the hydrogel surfaces generated by the WLI software.

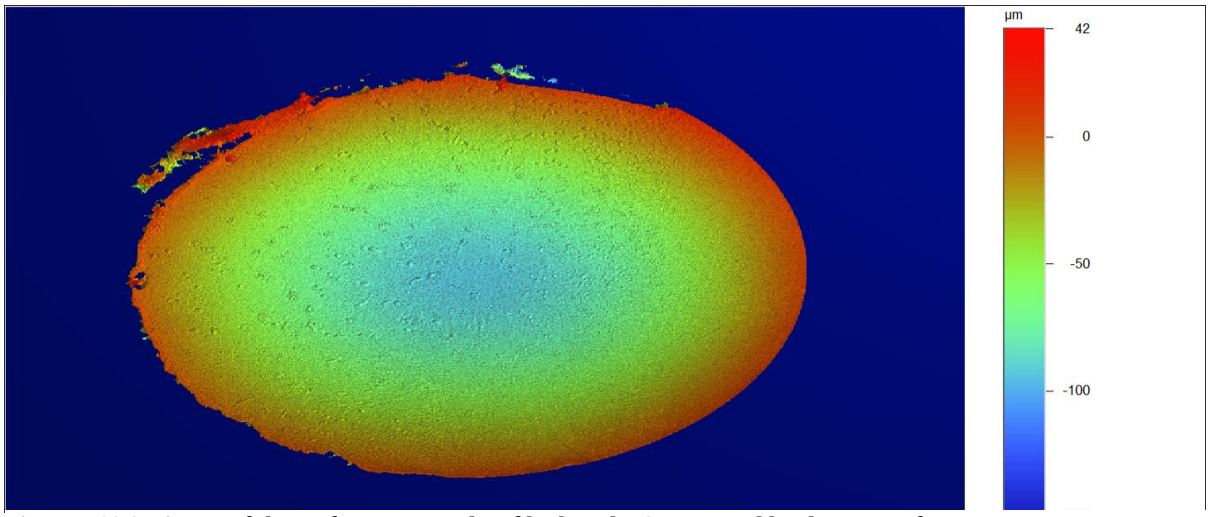

Figure 5-32 3D image of the surface topography of hydrogel 1-2 generated by the WLI software

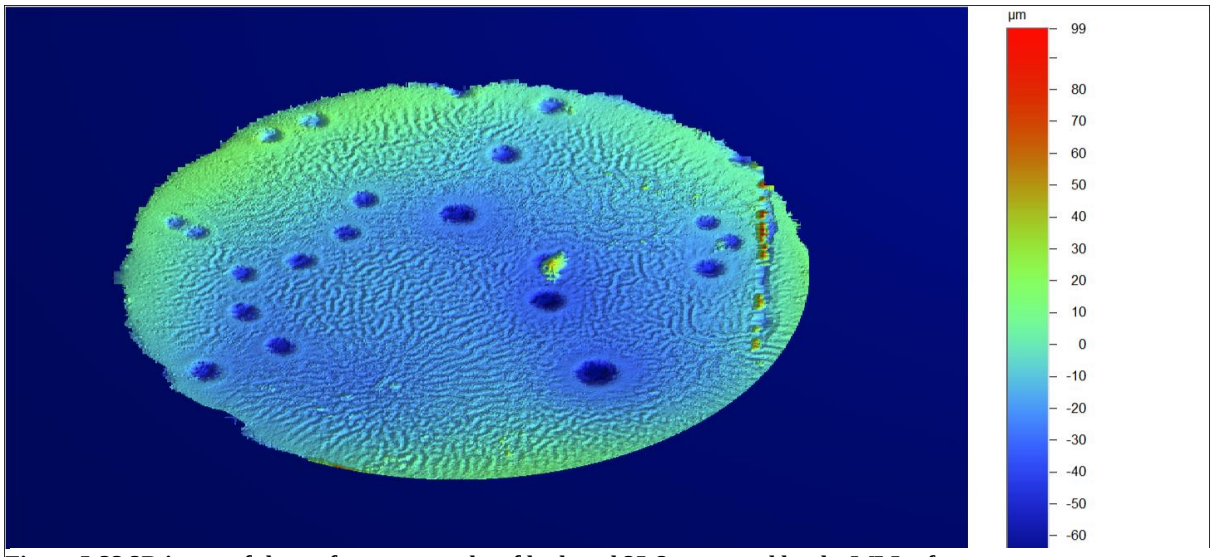

Figure 5-33 3D image of the surface topography of hydrogel 25-2 generated by the WLI software

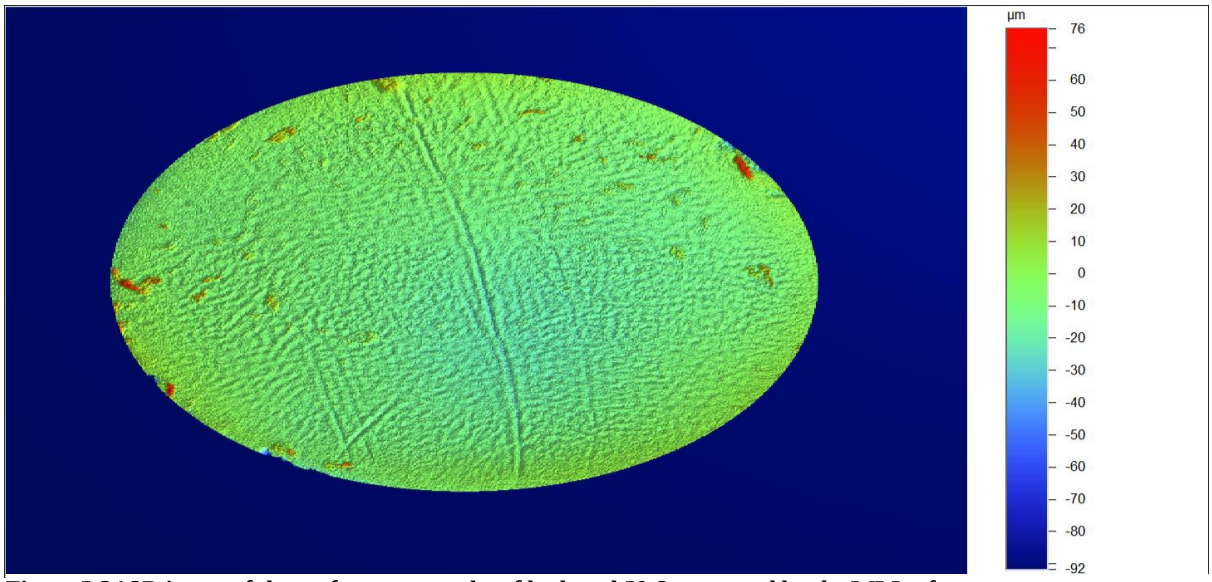

Figure 5-34 3D image of the surface topography of hydrogel 50-2 generated by the WLI software

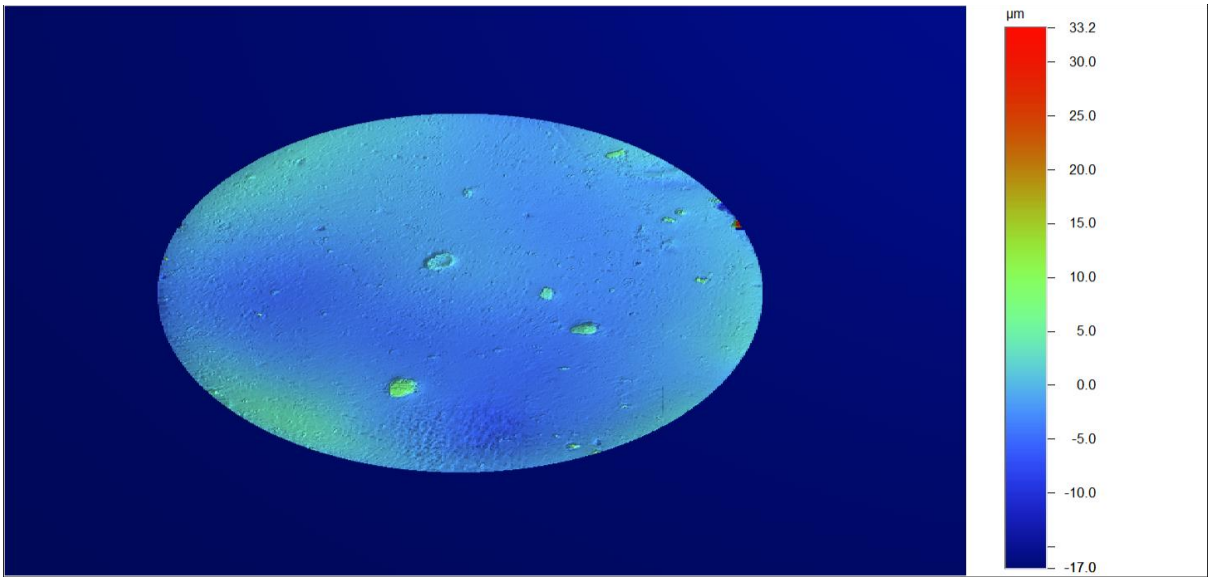

Figure 5-35 3D image of the surface topography of hydrogel 0 generated by the WLI software

The images above show the 3D representations of the hydrogels taken from the WLI software. Figure 5-32 3D image of the surface topography of hydrogel 1-2 generated by the WLI softwareshows a red colour around the edges of the gel and blue in the middle which that the hydrogel is slightly curved and concave in shape with the centre being the lowest point. Figure 5-33 shows the many holes that feature in the hydrogel surfaces as well as a rippling effect across the surface which is likely caused when the gel dried and contracted. These holes are a large feature that skews the measured value for roughness but due to their size in comparison to cells which will likely occupy the surfaces during culturing experiments, cells are unlikely to interact directly with the holes and their overall effect could be reduced, if not discarded especially when considering that aside from the holes in the surface, the bulk surface colour contours change little overall. Figure 5-34 shows a crack in the surface running along the length of the gel. Cracks like these occur during the polymerisation of the hydrogels and are random and unavoidable. Later chapters will investigate how these cracks will affect cell behaviour. Finally figure 5-35 shows the surface of the bare PGMMA gel. The image shows little colour variation which indicates that the gel is very flat and mostly featureless. The prominent features seen on the gel are deviations from the average surface of approximately 5-10 μm which is a very small value. The crater like feature in the centre is likely a bubble, which formed during polymerisation and deformed the surface while the other bright features are likely debris these debris and surface deviations had a large effect on the average roughness and may have skewed the reading.

Generally speaking the surface roughness data of the dried samples shows that the three sets of hydrogels with increasing particle size increase in roughness, the aberrant nature of

25-2 makes this hard to see but the general trend is one of increasing roughness with particle size.

5.4 Conclusion

In this chapter the synthesis of a set of glycerol methacrylate hydrogel materials is presented. These hydrogels are able to be synthesised quickly and easily and it is possible to synthesise them in large quantities. The gels show easy incorporation of latex particles into the hydrogel matrix which give surfaces of different apparent roughness but identical chemistry. Physical roughness is caused by the embedded polystyrene particles and deviations in surface topography.

It has been shown that these gels are non-cytotoxic from the culture of 3T3 cells on their surfaces for 24 hours. This shows that these hydrogels have potential as a biomaterial.

6 Synthesis and analysis of Core-Shell particles

6.1 Introduction

Core-Shell (CS) particles are particulate materials with layered multi-domain morphologies in which the layers have different compositions. Particles of this type have found a large number of uses and uses in a wide variety of applications including in the biomedical field: such as for drug and growth factor delivery, as biomechanical implants, as biomaterials and in tissue engineering [114-125]. Core-shell particles also find broad application in other areas such as catalysis [126, 127], imaging [128-130] and in paints and coatings [131-133].

One key benefit of creating CS particles over other ways of combining polymer mixtures, such as polymer blends, are their increased physical and chemical properties [134, 135]. There are large numbers of examples in the literature that highlight the usefulness of exploiting magnetic properties of some types of particles, for example as a means of virus-free gene delivery[136], or targeted drug delivery [137] or as a way of easily separating and collecting the particles when their intended role had been completed, such as when used as a catalyst[138]

However, the synthesis of particles with aqueous swollen shells (hydrogel shells) and hydrophobic cores is very difficult if water soluble monomers are used. [139] The difficulty arises because the hydrophilic monomers tend to polymerise in the aqueous phase and do not form the shell on existent core particles instead forming a macrogel in the bulk solvent. One strategy is to polymerise with amphiphilic macromonomers at the shell stage[140] or by adsorbing shell monomers with opposite charge onto the cores and polymerising in-situ [141] or by simply encapsulating a porous core in the shell [142]. Another possibility is to use hydrophilic macro-initiator and macro-transfer agents [143-145] Our quest to prepare

hydrogels with differing degrees of surface roughness used embedded particles as the source of the roughness and this strategy involved introduction of another variable: the hydrophobicity/hydrophilicity of the particle surface. In order to account for the current and future biological studies we prepared both hydrophobic poly(styrene-co-divinyl benzene) particles and core-shell particles with hydrogel shells composed of poly(1,2-propandiol-3-monomethacrylate-co-ethandiol dimethacrylate) (poly(GMMA-co-EGDMA). In order to achieve the core-hydrogel shell particles an alternative strategy was used. This involved the copolymerisation of hydrophobic derivative of GMA, which can be polymerised successfully using conventional emulsion polymerisation. By incorporating a comonomer with multi-functionality cross-linked shells can be prepared. Then removal of the hydrophobic (acetonide) group provides a cross-linked hydrogel shell that swells in water. [146]

6.2 Experimental

6.2.1 Synthesis of dihydroxypropan-1-methacrylate acetonide (glycerol methacrylate acetonide, GMAC)

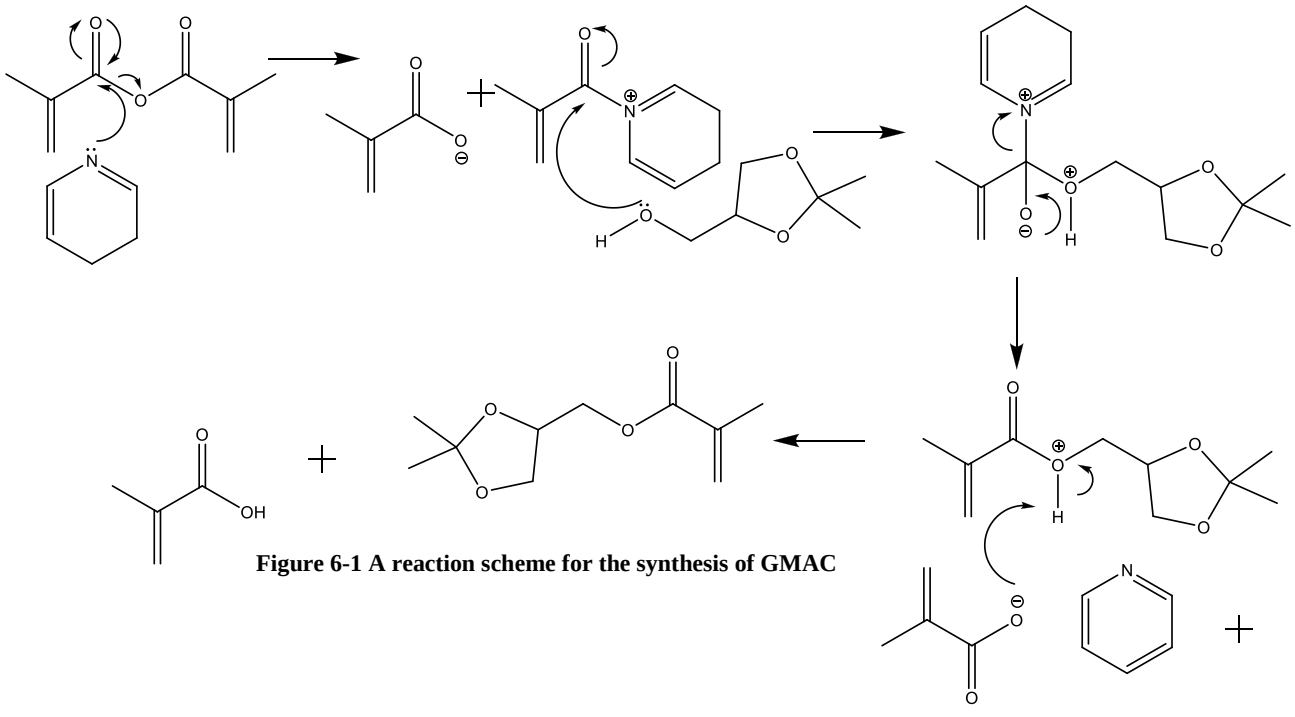

Figure 6-1 A reaction scheme for the synthesis of GMAC

6.2.1.1 Materials

The dry solvents dichloromethane (DCM) and toluene were obtained from Grubbs dry solvent system and used as received, dry pyridine, methacrylic anhydride (MA) solketal and Amberlite 402 resin were obtained from Sigma. Deionised and distilled water was used throughout.

6.2.1.2 Method

The core-shell particles were prepared by a two stage emulsion polymerisation as follows; Solketal (66.08g) was dried by azeotropic distillation with dry toluene at 70°C using a rotary evaporator.

Dry solketal, dry pyridine (63.28g) and dry DCM (500ml) were mixed in a 3 necked round bottom flask in an ice bath with a stirrer bar, nitrogen inlet and reflux condenser. DMAP (6.08g, 0.05 mol) was added to the reaction vessel and dissolved with stirring, MA (92.49g) was added dropwise under nitrogen. When addition was completed, reaction was raised to room temperature and stirred for typically 24 hours. Finally water (250 cm^3) was added to quench the reaction. The organic phase was washed with water (3x300 cm^3) and concentrated using a rotary evaporator.

A gel-type basic anion exchange resin was used to remove the by-product acrylic acid from the concentrated liquid. The Amberlite IRA 402 resin was activated by treating with 1.0 M NaOH for 2-4 hours then repeatedly washed with water and then acetone and was finally added to the concentrated crude liquid GMAC. The mixture was shaken gently for 2-4 hours, or overnight before being filtered and fresh activated resin was added, again for 2-4 hours

or overnight. When completed the liquid was distilled and collected at 60-70° C under reduced pressure of approximately 1mm Hg. Yield 66.09g, 66.01% based on solketal.

6.2.1.3 Analysis and characterisation

Analytical data for GMAC ^{1}H NMR (d6 DMSO): δ= 1.35, 1.40 (2x s, **1**), 1.85 (s **5**), 3.75 (m, **2**), 4.05 (m, **3**), 4.20 (m, **4**), 5.70 (d, **6**), 6.05 (s **7**)

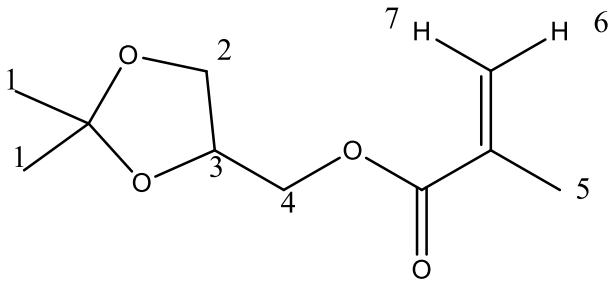

Figure 6-2 Labelled structure of GMAC

6.2.2 Creating a core-shell particle latex by coupling GMAC with PS-CO-PDVB

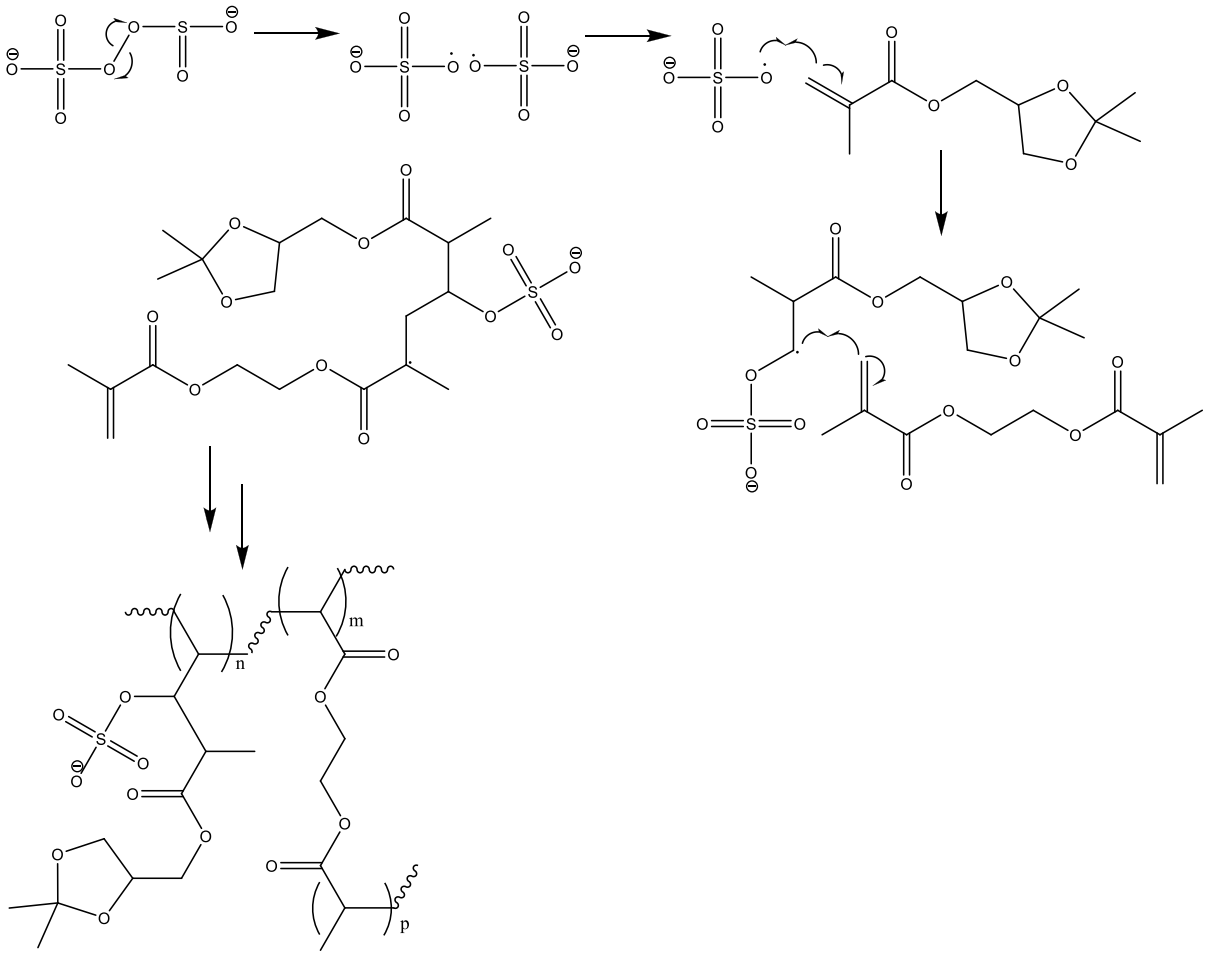

Figure 6-3 A reaction scheme showing the polymerisation of GMAC and EGDMA

6.2.2.1 Materials

Styrene, potassium carbonate, potassium persulphate, SDS, and ethylene glycol dimethacrylate (EGDMA) were obtained from Sigma and used without further purification. DVB was obtained from Sigma and washed as described previously. Distilled and deionised water was used throughout.

6.2.2.2 Polymerisation

Batch polymerisations were conducted in a 1.0L jacketed glass reaction vessel (Radleys, UK) which was equipped with a mechanical stirrer, a nitrogen inlet, a reflux condenser and a temperature probe. To produce the cores, a typical reaction was as follows: water (100g),

SDS (1.6g) and potassium carbonate (0.33g) were charged to the vessel. The mixture was deoxygenated by bubbling under nitrogen with agitation for one hour, whilst hot water was circulated through the jacket of the vessel to maintain the temperature of the mixture at 70°C. After this styrene (25g) and DVB (18.5g) were slowly added dropwise to the reaction. When addition was completed potassium persulphate (0.25g) was added in water (5 cm^3) and the mixture was stirred for 3 hours.

Five formulations were devised for the shells. The quantities represent 5, 10 & 15 mol% of GMAC with respect to the molar quantity of styrene, to produce 3 particles with varying shell monomer concentrations and 5, 10 & 15 mol% EGDMA with respect to the molar quantity of GMAC, to produce particles with varying shell cross-link density. Preparations with increasing shell monomer concentration had the same cross-link density (5%). As the shell cross-link density was increased, the amount of monomer in the stage 2 feed was maintained at 5%.

The preparations were as follows:

LABEL	GMAC MASS / G	EGDMA MASS / G
1A	2.402	0.1189
2A	4.8055	0.1189
3A	7.2083	0.1189
1B	2.402	0.2379
1C	2.402	0.3569

Table 6-1 A table showing the GMAC and EGDMA contents for the CS particle formulations

The GMAC and EDGMA were mixed and added dropwise to the reaction and the mixture was stirred for a further 3 hours. At the end of 3 hours, the temperature was raised to 80°C

for 1 hour to ensure total monomer conversion. The latex was discharged from the vessel and stored at room temperature.

6.2.2.3 Analysis of latex

As described previously; the particle sizes and zeta potentials of the latexes were obtained using the Brookhaven instrument.

6.2.2.4 Deprotection of shell molecules

A sample of the core-shell (CS) latex particles was taken (25 cm^3), added to 1.0 M hydrochloric acid (HCl) (100 ml) and heated to 60°C in a water bath for 4-8 hours.

6.2.2.5 Analysis of deprotection

Particle size data was obtained with the Brookhaven instrument as described previously.

6.2.3 Protein adsorption of Core-Shell particles

As a means of analysing the surfaces and properties of the CS particles, samples of the particles were introduced to protein solutions to assess and analyse how their properties changed with proteins adsorbed onto the surface.

6.2.3.1 Materials

CS particles were deprotected as above and further purified as follows. The proteins lysozyme, fibrinogen and albumin were obtained from Sigma and used without further purification. Ultrapure water was obtained using Millipore Direct Q ultrapurification system, water purity was given as 18 Ω. Potassium chloride (KCl) was obtained from Sigma.

Servapore dialysis tubing was obtained from Fisher Scientific and had a mol wt. cut off of 12000-14000, The Pierce BCA assay was also obtained from Fisher Scientific.

6.2.3.2 Purification of latexes

The deprotected latexes were centrifuged and resuspended in KCl to wash out the acid used for the deprotection. Multiple washes were required (3-5) to fully wash out all of the acid and to reach the pH of KCl (approx. 7.4). When the particles were washed, they were stirred with activated Amberlite 402 resin to remove surfactant molecules bound to the surface from the emulsion polymerisation steps. Again multiple interactions with the resin were required and the latex solutions were stirred for approximately 4 hours to overnight at each wash. Following the washing with the resin, the particles were filtered to remove the resin and again washed with KCl. The latexes were then dialysed in ultrapure water to remove any remaining surfactant. The dialysis took place over 3-5 days with the water changed daily. Successful removal is confirmed by Zeta potential measurements.

6.2.3.3 Protein adsorption

The protein solutions were made up in the following quantities: 50, 25, 10, 5, 1 mg/ml in ultrapure water.

Following the successful washing and removal of surfactant, the bulk solids contents of the latexes were determined by solvent evaporation and the latex concentration was adjusted to give 10 mg/ml. 1ml samples of latex were taken and pipetted into ependorf tubes then centrifuged to remove the bulk water. The protein solutions were then added and the solutions were incubated at 37°C for 24 hours. At the end of 24 hours, the latex solutions

were centrifuged, the protein solutions removed and the latexes washed twice with KCl. The adsorbed proteins on the particle surface were then analysed with by Zeta potential measurements.

6.2.3.4 BCA assay

The total protein content adsorbed to the surface of the particles was analysed using the BCA assay. Following the washing stage the protein was extracted from the surface of the CS particles using a solution of 50:49.8:0.2 water: acetonitrile: trifluoroacetic acid (TFA). 1 cm^{-3} of the extraction solution was added to the samples and incubated for 1 hour. At the end of an hour, the extraction solution was removed and analysed using the bicinchoninic acid (BCA) assay.

The assay is supplied with a 'working reagent' comprised of 50 parts of solution A to 1 part of solution B. 100 µl of the working reagent was added to a well in a 96 well plate and 5µl of sample was well mixed. The solution was incubated at 37°C for 30 min then cooled to room temperature. Protein content is assessed against a standard containing known amounts. The colour change of this solution was measured using absorbance at 562 nm.

6.3 Results and discussion

6.3.1 Synthesis of dihydroxypropan-1-methacrylate acetonide (glycerol methacrylate acetonide, GMAC)

Acrylic acid was produced as a by-product of this reaction, as an impurity, it interfered with the overall quality of the final GMAC product which made it more difficult to distil and further purify GMAC, also since acrylic acid is capable of polymerisation, the presence of this impurity would continue into the later steps of the intended polymerisation of the GMAC. Acrylic acid was removed using the ion exchange resin Amberlite 402, as described above. Multiple washes with the resin were required to fully remove all of the acrylic acid and any residual pyridine which also lowered purity. The resulting crude GMAC solution was distilled twice to purify further. A good vacuum is required to achieve the distillation (around 1mm Hg). If it was not possible to distil the crude GMAC, further ion exchange was required to remove impurities. The pure GMAC appeared as a clear, slightly viscous liquid.

The NMR data showed that GMAC had been successfully produced, shown by key peaks at δ= 1.35, 1.40 corresponding to the acetonide group and at δ=5.70 & 6.05 corresponding to the terminal carbons of the methacrylate group.

6.3.2 Creating a core-shell particle latex by coupling GMAC with PS-CO-PDVB

The latex was produced from the emulsion polymerisation of styrene and DVB to produce the cores, as described previously. This latex was white and opaque and was composed of particles of average diameters of 75 ± 1.0 nm and a zeta potential of -46 ± 2 mV. These particles are referred to as the cores.

When the cores were coupled with GMAC and EGDMA the latex remained white but the particle sizes and zeta potentials of the particles changed. The results are summarised in the following table.

LATEX	PARTICLE SIZE / NM	ZETA POTENTIAL / MV
CORES	70 ±1	-47±2.8
1A	97±3	-44±1.5
2A	215±2	-40±0.5
3A	333±41	-38±0.9
1B	223±14	-39±0.3
1C	289±5	-41±0.2

Table 6-2 A table showing the particle size and zeta potentials of protected GMAC CS particles

Following coupling, all of the particles had increased in size, relative to the cores as expected. An aspect to always consider in core-shell emulsion polymerisation is the possibility of the production of new smaller particles at the second stage monomer feed as a result of polymerisation at secondary nucleation points. This produces a reduction in average size and bimodality in the particle size distributions but in this process neither of these effects were observed. It appears that as the shell monomer concentration increased, the particle size also increases by a significant degree. However, as cross-link monomer concentration increases, the overall increase of particle size is less pronounced: increased cross-linker tends to increase the volume shrinkage observed on polymerisation. Each of these observations were expected and tend to, at least indirectly, confirm the presence of the second stage polymer as a shell on the core particles.

The zeta potentials of the particles became less negative upon the coupling with the shells compared to the bare cores. However, the change in zeta potential on producing core-shell

particles from the cores is quite small and the change is likely to have little effect on colloidal stability The particles at this stage of the process are still protected and the charges present on the surfaces are due to the surfactant molecules used in the emulsion polymerisation so it is unsurprising that the zeta potential would be dominated by the adsorbed surfactant. The concentration of the surfactant should not have changed the surface area over which they are spread has increased thus slightly reducing the overall charge felt across the whole surface. The zeta potential values of all of the particles are shown to be over -30 mV, which is a key indicator that all of the latexes are colloidally stable.

The acetonide protecting group was removed upon reacting with HCl and heating. Following this hydrolytic deprotection, the particle sizes of the latexes increased. This is shown in the table below and repeated in graphical format in figures 3 & 4 below The error bars present on the graphs and the errors reported in the tables below and those that follow show the standard error (n=3 for the following particle size data) .

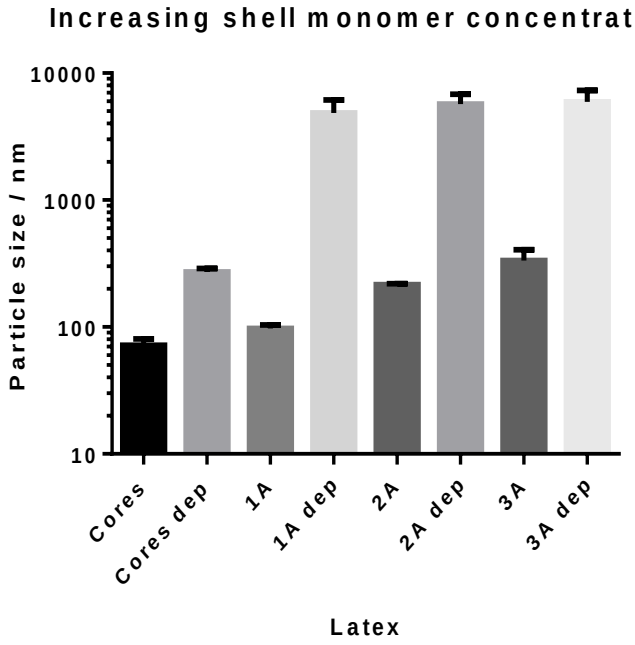

Figure 6-4 A graph showing increasing particle size of CS latexes on deprotection as shell monomer concentration increases

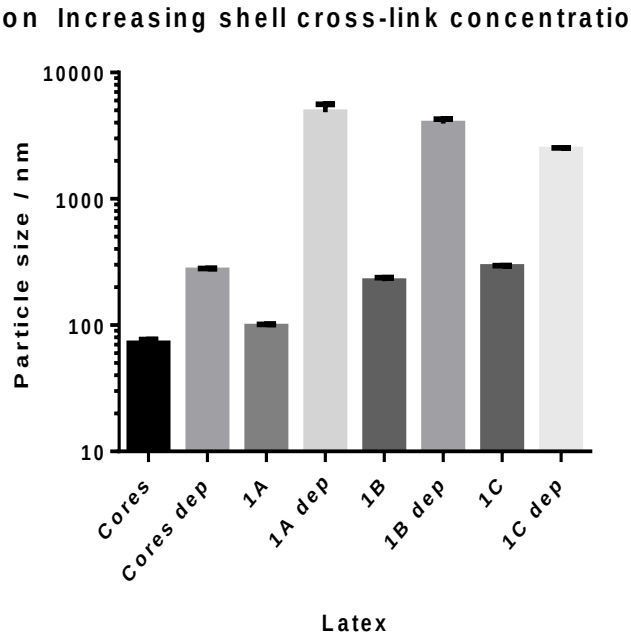

Figure 6-5 A graph showing increasing particle size of CS latexes on deprotection as shell cross-link concentration increases

LATEX	PARTICLE SIZE / NM
CORES	270±10
1A	4800±350
2A	5900±600
3A	6000±500
1B	4000±200
1C	2500±100

Table 6-3 A table showing particle size for the deprotected GMAC CS particles

All of the particles have increased in size, indicating that the deprotection had been successful. This size increase is due to the GMAC molecules present on the surface losing the hydrophobic acetonide group and exposing hydrophilic glyceryl groups. As they became

hydrophilic the molecules swelled with water. Therefore, this increase in size is a useful indication of the success of the deprotection. It is also worth noting that the core particles have also increased in size. This is likely due to these particles losing some of the surfactant molecules present on their surfaces during deprotection. The reduced number of surfactant molecules can be observed as a decrease in colloidal stability of all of the particles following deprotection. When left in sealed containers at room temperature, the latex particles will slowly begin to settle out of solution within one day. This instability most likely has two sources. Firstly, the increased swelling produces a more hydrophilic interface, which will result in surfactant desorption and a decreased electrostatic component to the stability. This is shown in Table 6-4 A table showing the change in zeta potential of the GMAC CS particles before and after deprotection and removal of surfactant. Secondly, a substantial increase in particle size will also decreases particle Brownian velocity at constant momentum so that gravitational sedimentation forces become more significant.

After deprotection, the particles have all dramatically increased in size (shown in Table 6-3), as core monomer concentration increased, the size of the deprotected particles increased. This is due to the higher concentration of hydrophilic groups now available to swell with solvent. The inverse is observed as shell cross-link concentration is increased. As crosslink density is increased, the deprotected particles decrease in size. This is because the increased number of crosslinks in the shell chains increases the mechanical stress developed on swelling, so that at equilibrium reduced swelling is observed.

It is possible that the large increase in the particles sizes was caused by hydrolysis of the ester bond in the crosslink molecule EGDMA. The conditions of the hydrolysis could have caused this further breakdown which would have led to more hydrophilic OH groups being present and contributing to a greater degree of solvent swelling than would expected with

merely the acetonide hydrolysis. The decrease in particle size observed as the cross-link density was increased would suggest that the hydrolysis of the cross-link agent is not the dominant effect on the increase of particle size. If this were the case, the particle sizes would be expected to increase as cross-link concentration increase. This is not observed. Further investigation is required to determine the extent of this effect.

6.3.3 Protein adsorption on Core-Shell particles

The particle performance in contact with proteins was examined using a model set of blood derived proteins. The rationale for the design these experiments was as follows:

i. Lysozyme-A medium molar mass (~40 kDa) highly charged (+ve) proteins
ii. Fibrinogen-A high molar mass (~340 kDa) protein, adsorption of which is one of the first events in the thrombus formation.
iii. Albumin-A medium molar (~66 kDa) mass protein that is in high concentration in many biofluids. Adsorption of albumen can often pacify the immune response.

During the washing, deprotection and surfactant removal steps in preparation for introducing the particles to the protein solutions, the particles appeared to become less colloidally stable and would settle out in the order of hours rather than days, forming flocs. This was most apparent in the purified core samples, in which the flocs of particles could reach approximately 5mm across. However, the flocs could be redispersed if the samples were vigorously shaken, showing that removal of surfactant, whilst reducing colloidal stability did not induce coagulum formation.

The bulk deprotected particles solutions appeared grainier looking and settled out much more readily than samples containing surfactant. The cleaned samples also did not produce

soap bubbles when shaken unlike samples prior to purification. However the ultimate success of removing the surfactant was determined by zeta potential. The following table summarises the results of the zeta potential analysis of the particles after multiple washes with the resin and dialysis. The errors reported below are the standard error, where n=6 sample repeats, each comprising of 5 runs as measured by the zeta potential machine.

LATEX	ZETA POTENTIAL BEFORE DEPROTECTION / MV	ZETA POTENTIAL AFTER DEPROTECTION /MV
CORE	-47±2.8	-23±1.6
1A	-44±1.5	-28±1.8
2A	-40±0.5	-26±1.4
3A	-38±0.9	-29±0.7
1B	-39±0.3	-23±1.2
1C	-41±0.2	-23±2.0

Table 6-4 A table showing the change in zeta potential of the GMAC CS particles before and after deprotection and removal of surfactant

From the above table it can be seen that the zeta potential is significantly reduced by the deprotection and removal of surfactant. Analysis of variance (ANOVA) showed no significance between the samples and cores when grouped by increasing shell monomer concentration ($p=0.1110$) and increasing shell cross-link concentration ($p=2.112$). The zeta potential values for the particles following deprotection could be due in part, to the presence of an increased number of hydrophilic groups caused by the hydrolysis of the cross-link molecules, however this would not seem to be the dominant effect as there is no significant difference between any of the zeta potentials of the particles, particularly those where the concentration of cross-links was increased.

Following incubation with protein solutions of varying concentrations the zeta potential (in mV) of the particles were again analysed. This is summarised in the following tables. It is worth considering that as zeta potential becomes less negative and values approach 0 mV, electrophoretic mobility is decreased and the particles are becoming less stable, sedimentation effects may begin to predominate. This gives purely qualitative information on the effects of protein adsorption on the surfaces of the particles.

Lysozyme	Protein concentration / mg/ml						
Latex		50	25	10	5	1	0
	Core	2±0.9	-2±1.5	-14±1.4	-15±2.3	-15±1.6	-23±1.7
	1A	-8±1.6	-11±1.4	-20±1.4	-20±2.0	-26±2.3	-28±2.2
	2A	-14±1.4	-24±3.0	-22±2.3	-23±1.5	-21±0.9	-25±2.1
	3A	-24±0.6	-18±2.2	-27±1.3	-25±1.5	-25±2.6	-29±0.7
	1B	-5±1.0	-13±0.6	-15±1.7	-20±1.2	-21±0.8	-23±1.2
	1C	-6±0.4	-13±1.7	-19±1.3	-17±2.1	-23±2.1	-24±2.0

Table 6-5 A table of zeta potentials of the CS particles as lysozyme concentration is increased

Fibrinogen	Protein concentration / mg/ml						
Latex		50	25	10	5	1	0
	Core	-9±1.0	-3±2.1	-3±1.3	-5±1.5	-12±1.9	-23±1.7
	1A	-11±1.2	-4±3.1	-6±2.3	-7±1.5	-22±1.6	-28±2.2
	2A	-11±1.2	-8±2.6	-12±2.1	-13±1.0	-17±1.5	-25±2.1
	3A	-16±1.1	-14±1.4	-14±1.3	-16±1.3	-20±1.3	-29±0.7
	1B	-9±0.6	-9±0.6	-6±1.8	-7±1.4	-12±1.3	-23±1.2
	1C	-11±1.6	-8±1.5	-5±1.4	-9±1.3	-15±1.8	-24±2.0

Table 6-6 A table of zeta potentials of the CS particles as fibrinogen concentration is increased

Albumin	Protein concentration / mg/ml						
Latex		50	25	10	5	1	0
	Cores	-18±2.8	-22±1.7	-19±3.8	-16±1.4	-20±0.8	-23±1.7
	1A	-24±2.2	-25±1.8	-27±2.0	-23±1.7	-26±2.1	-28±2.2
	2A	-24±1.2	-22±2.0	-26±2.4	-24±1.8	-23±1.8	-25±2.1
	3A	-23±3.7	-18±2.1	-22±1.2	-28±1.3	-24±2.9	-29±0.7
	1B	-19±0.6	-22±1.4	-20±0.9	-19±1.9	-18±5.0	-23±1.2
	1C	-18±2.4	-20±2.0	-18±1.5	-23±0.7	-20±1.7	-24±2.0

Table 6-7 A table of zeta potentials of the CS particles as albumin concentration is increased

The zeta potential data presented above is presented graphically in the following figures which highlight the zeta potentials as trends of increasing shell monomer concentration and increasing shell cross-link concentration.

Figure 6-6 A graph showing the zeta potentials of latex particles with increasing shell monomer concentration, as adsorbed lysozyme increases with the statistical significance level indicated

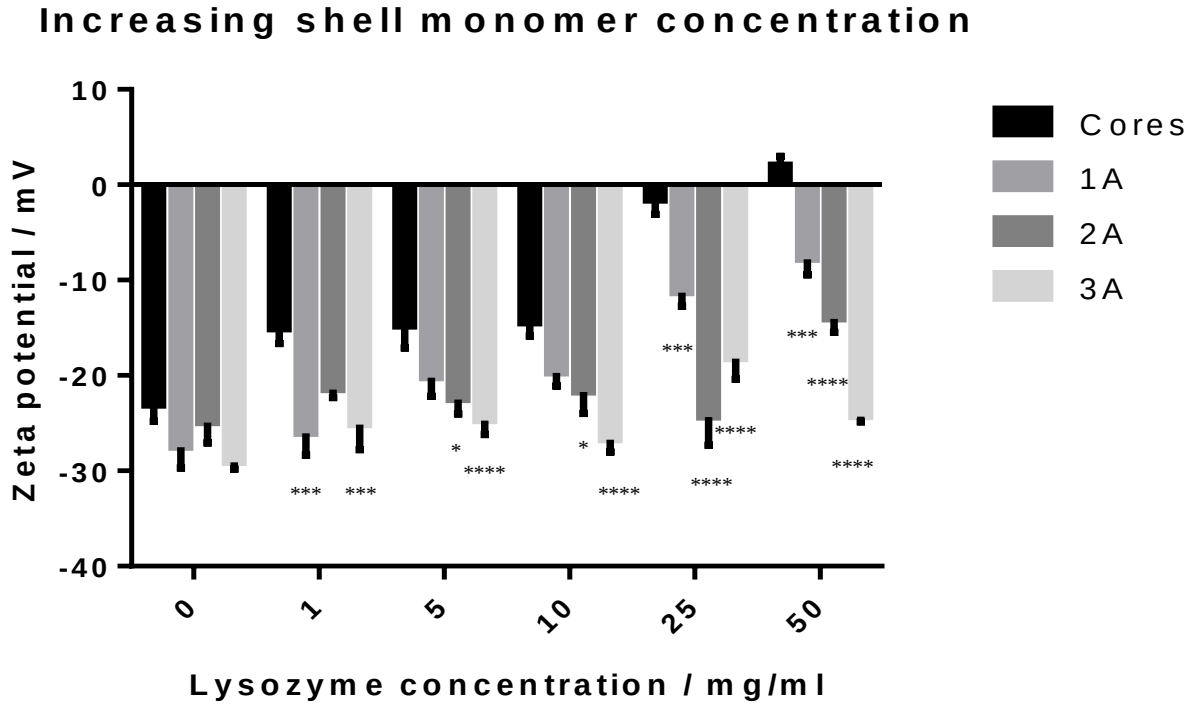

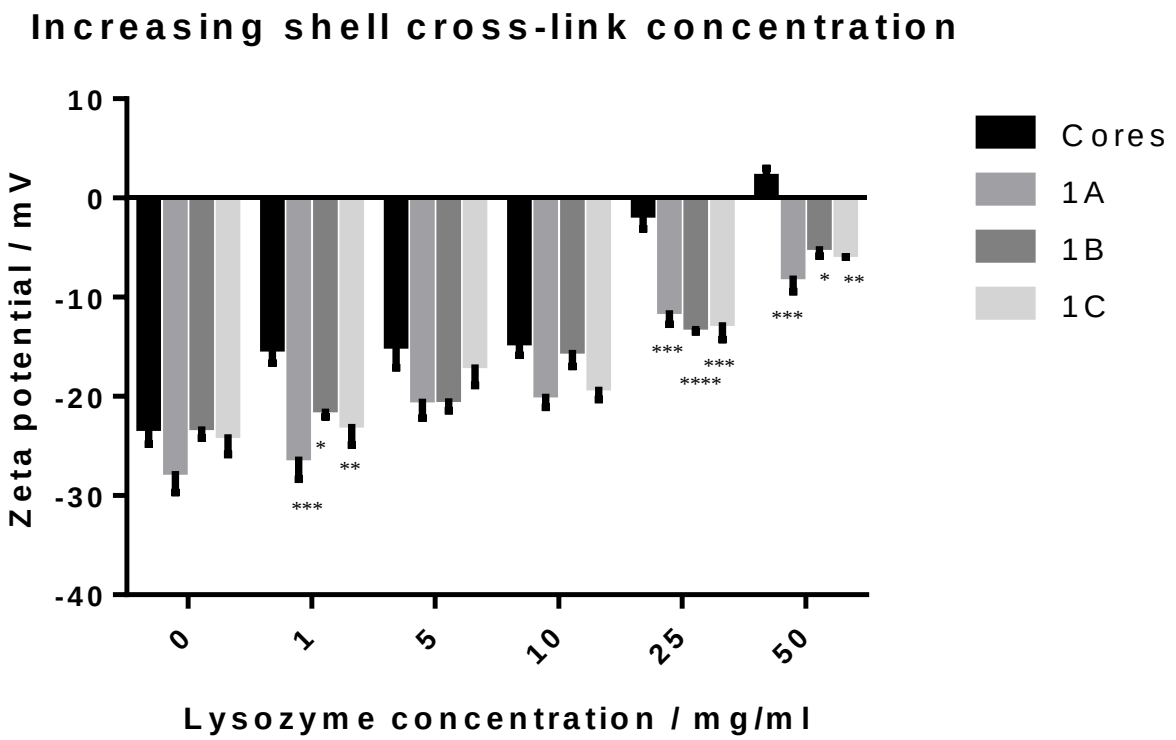

Figure 6-7 A graph showing the zeta potentials of latex particles with increasing shell cross-link concentration, as adsorbed lysozyme increases with the statistical significance level indicated

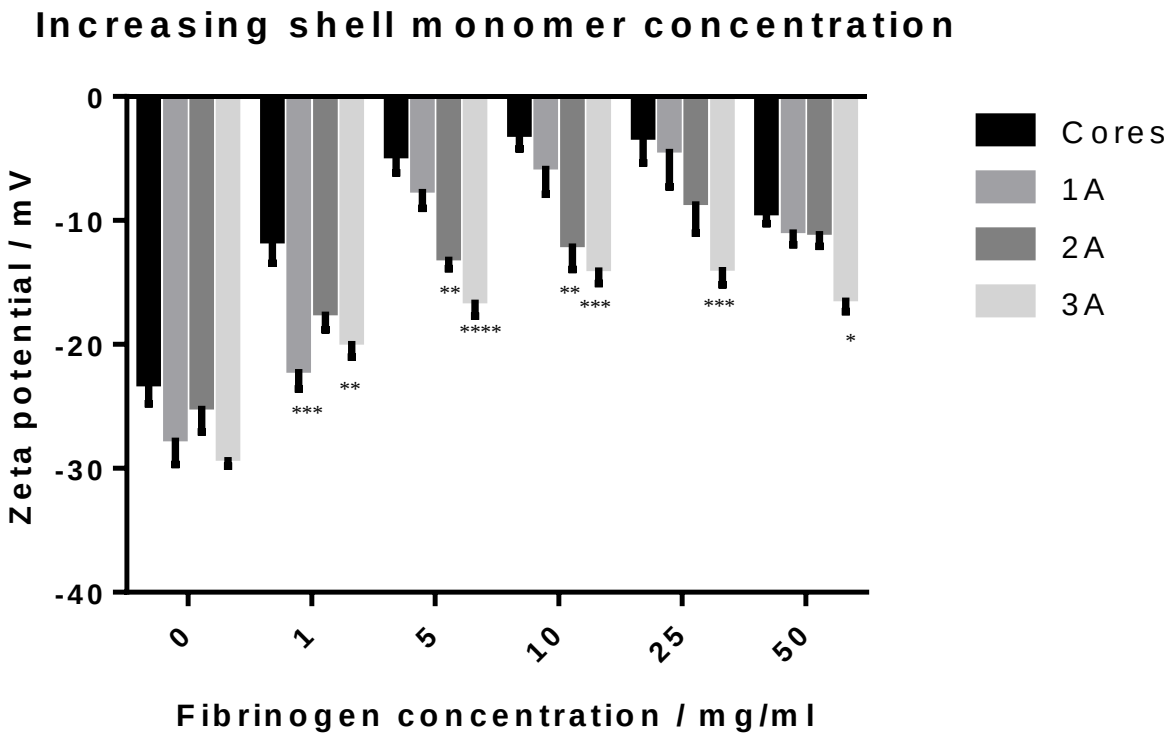

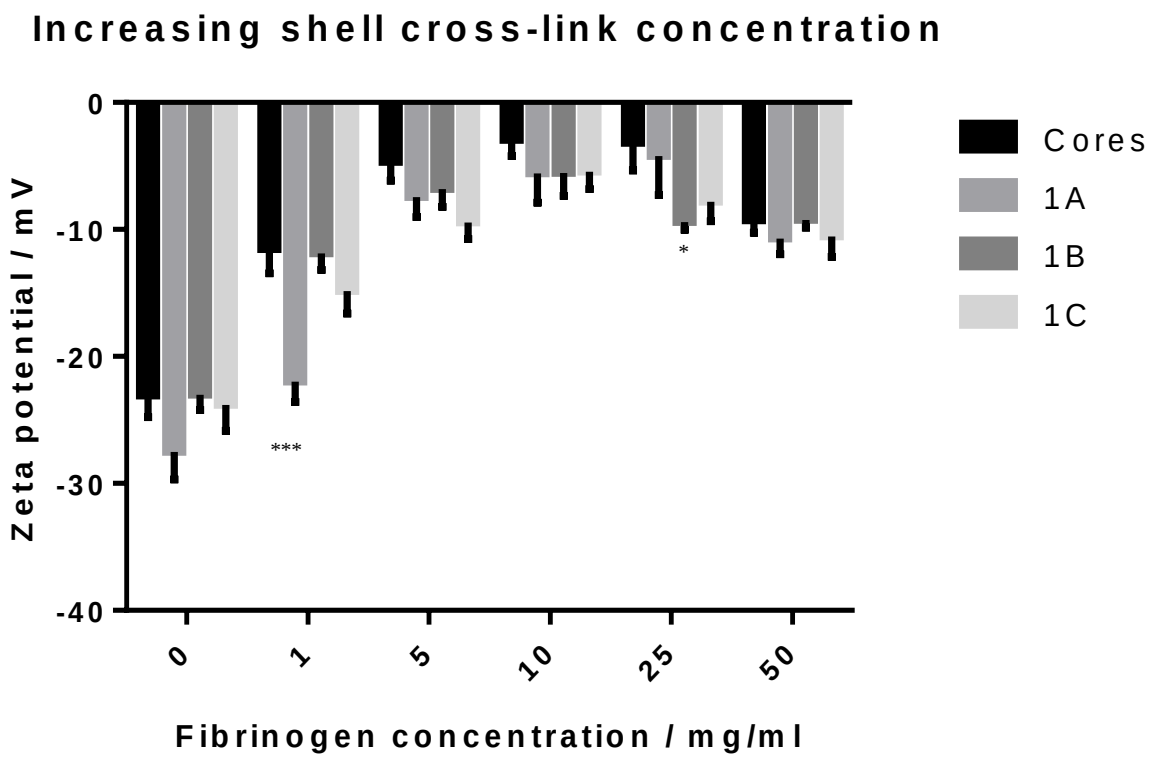

Figure 6-9 A graph showing the zeta potentials of latex particles as adsorbed fibrinogen increases, as shell cross-link concentration is increased with the statistical significance level indicated

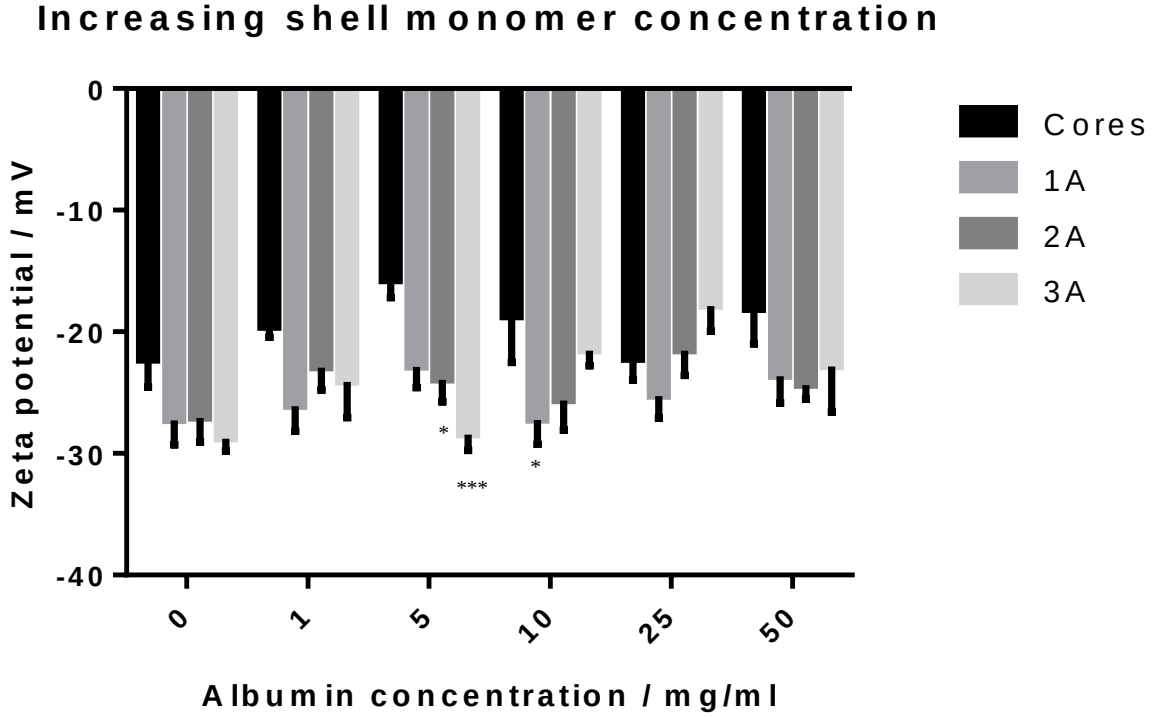

Figure 6-10 A graph showing the zeta potentials of latex particles as adsorbed albumin increases, as shell monomer concentration is increased with the statistical significance level indicated

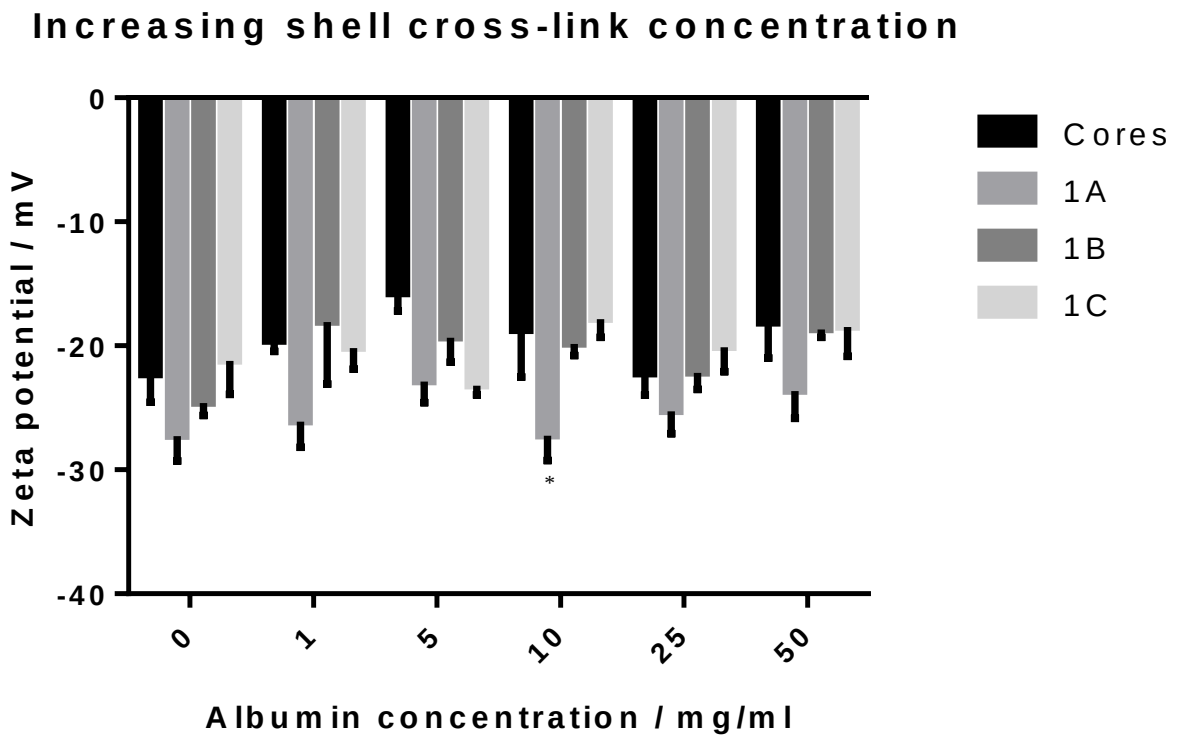

Figure 6-11 A graph showing the zeta potentials of latex particles as adsorbed albumin increases, as shell cross-link concentration is increased with the statistical significance level indicated

The above graphs show that for lysozyme and fibrinogen, adsorption of protein from higher concentrations of protein solution has caused a marked change in zeta potential with the charge presented by the particle becoming much less negative. Varying the concentration of the albumin solution had little significant effect on the zeta potential of the core-shell latex particles when compared to the bare cores. This is due to the charge on the individual protein molecules at the pH of the experiment (approx. 7.2) Lysozyme has an isoelectric point (pI) pH 10-11, fibrinogen has pI pH of approx. 5.5 and albumin approx. 4.9. This means that the individual protein molecules of lysozyme should be positively charged and would reduce the negative charge shown by the particles. Albumin and fibrinogen would be slightly negatively charged and should therefore reduce the negative charge on the particles but by a lesser degree. This observation is seen in the trends of the particles. Higher concentrations of protein solution have a larger effect on the change of the charge seen on

the particles. This is due to the availability of more protein molecules to adsorb onto the surface of the particles. These effects are highlighted in the following table of the zeta potentials (in mV) of the stock protein solutions.

		PROTEIN CONCENTRATION (MG/ML)				
		1	5	10	25	50
PROTEIN	Lysozyme	1±0.3	2±1	5±0.5	11±1	14±1
	Fibrinogen	-10±0.3	-12±0.3	-10±0.7	-5±1	-5±0.7
	Albumin	-22±2	-15±1	-12±1	-14±0.7	-12±1

Table 6-8 A table of zeta potential for the stock protein solutions

In order to assess the significance of the trends, the above data was analysed using two-way ANOVA and the significance of the change in charge of the core-shell particles, relative to the bare cores is presented on the graphs with stars (**) according to the level of significance.

The data presented above figures shows the statistical significance of the zeta potential readings recorded for the core-shell particles with adsorbed lysozyme. Particles with no protein adsorbed to the surface show no significant difference in zeta potential when compared to the core particles. The above shows that at high concentrations of lysozyme (50 – 25 mg/ml) there is a significant difference in the zeta potentials of the core-shell particles, compared to the bare cores. This is due to the higher number of positive lysozyme molecules adsorbed to the surface of the shells. This has raised the zeta potential. From Figure 6-6 A graph showing the zeta potentials of latex particles with increasing shell monomer concentration, as adsorbed lysozyme increases with the statistical significance level indicated above, it can be seen that the highest increase of zeta potential was felt by the core particle which actually became positively charged. This is likely due to its smaller

surface volume compared to the CS particles, which means that the same volume of protein interacted with a smaller surface giving a higher apparent charge. This large increase in zeta potential remains higher at 25 mg/ml lysozyme concentration but the effect is not as strong. As the protein concentration is decreased, the zeta potential then reaches a consistent level of around -15 mV. This could indicate an equilibrium adsorption level at lower concentrations. The CS particles observe a similar behaviour, there is little significance across the increasing shell monomer concentration set at lower protein concentrations, with some increase in zeta potential but at the higher concentrations, the relative increase is more pronounced. However, this increase is significantly less than is seen on the cores. This is perhaps due to the larger surface areas which the CS particles have, meaning that the charged protein molecules are able to distribute over a larger area. Figure 6-6 also shows that for most of the protein concentrations, the zeta potential increase effect decreases as shell monomer increases, particularly at the highest concentration. This effect is likely down to the particles increasing in size as the monomer concentration increases, meaning that charged proteins are distributed over a greater surface area.

Similar effects are seen as shell cross-link concentration is increased, however the zeta potential values for this set of particles are more positive than for the increasing shell monomer concentration set. This is again likely down to these particles being smaller than the particles with more shell monomer which gives them larger shells. This means that the protein molecules are spread over a smaller area, giving a higher overall charge. At all protein concentrations, there is little if any significant difference in zeta potential as cross-link concentration increases indicating that protein adsorption is independent of the stiffness or the shell and that shell size is the predominant factor.

When fibrinogen is adsorbed to the surface of the CS particles, zeta potential is increased, this is again particularly apparent at higher concentrations. At the highest concentration of fibrinogen, the change in zeta potential is less than the next highest concentration. This is different to what is seen for lysozyme. This is probably due to the fact that fibrinogen is a much larger protein. Lysozyme is approximately 14 kDa whereas fibrinogen is 340 kDa. This suggests that for relatively smaller particles such as the cores or 1A particles there could be some steric interference occurring between adsorbed protein molecules, meaning that a maximum concentration of particles on the surfaces had been reached. This would be between 25 and 50 mg/ml.

Again there is little to no significant difference between the effect of the protein on increasing zeta potential and the increasing shell cross-link concentration but all concentrations of protein increased zeta potential more for the more crosslinked particles than it did for the particles with larger shells. As shell size is increased, the increase in zeta potential becomes less, this effect is seen across all concentrations of protein and suggests again that the dominant effect is one of protein charge: adsorption area ratio. The increase in zeta potential of fibrinogen on the core molecules is less than for lysozyme. This could be due to the larger proteins trying to fit around the cores or possibly due to the fact that fibrinogen has a more negative charge. The particles with no proteins are negatively charged and therefore there could be a degree of repulsion between the particles and the proteins as well as some steric hindrance. Also the magnitude of the charge of the fibrinogen is less than lysozyme which gives a lower cumulative effect on the overall zeta potential.

Across the whole data set, there is little if any difference in zeta potential for CS particles with adsorbed albumin. This is likely due to the zeta potential of free albumin in solution

being close to the zeta potential of the unadsorbed particles as shown in Table 6-8. This means that the degree of adsorption cannot be readily determined by zeta potential. Different methods would be required to quantify the protein adsorbed to these particles, such as direct visualisation of the particles with electron microscopy.

6.3.4 BCA assay

The BCA assay measures total protein content in the samples, serving as a comparison to the effect on surface charge caused by protein adsorption shown in the zeta potential experiment above. The following figures show the total amounts of protein which were adsorbed onto the CS particle surfaces.

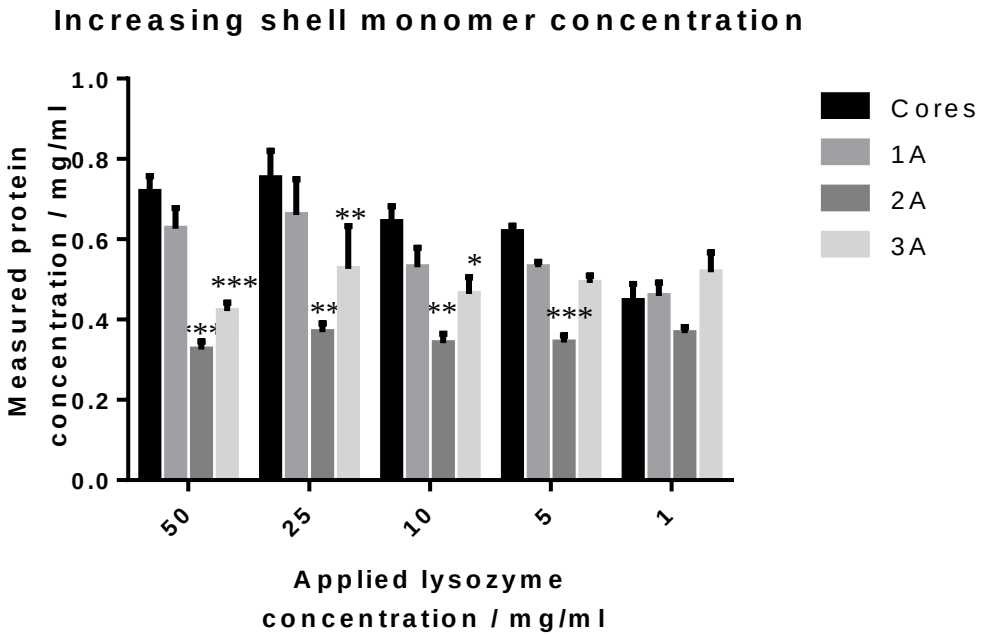

Figure 6-12 A graph of total measured lysozyme adsorbed to the surface of CS particles as shell monomer concentration increases

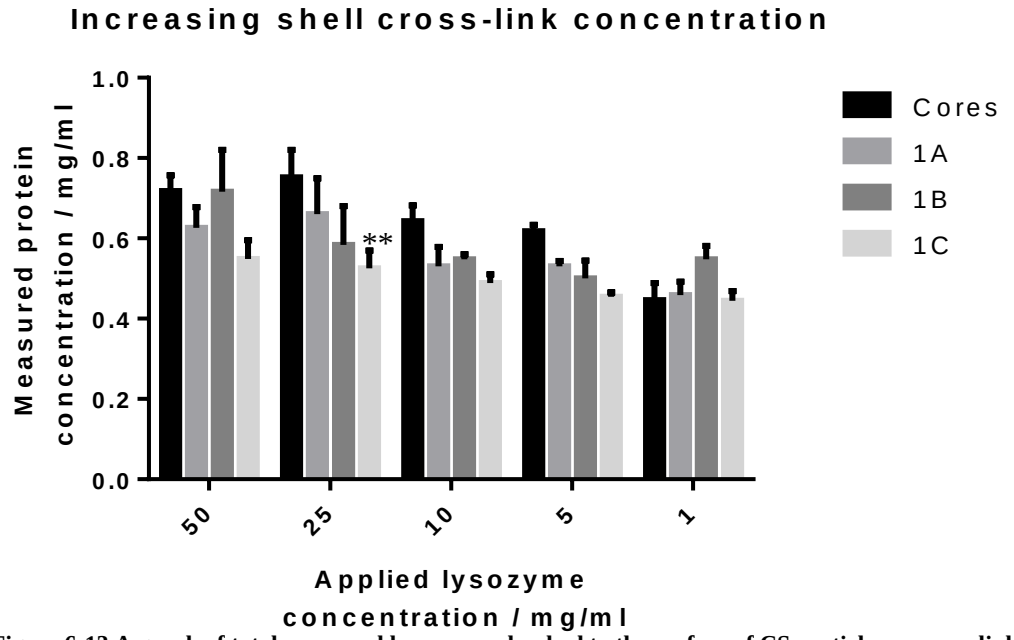

Figure 6-13 A graph of total measured lysozyme adsorbed to the surface of CS particles as cross-link concentration increases

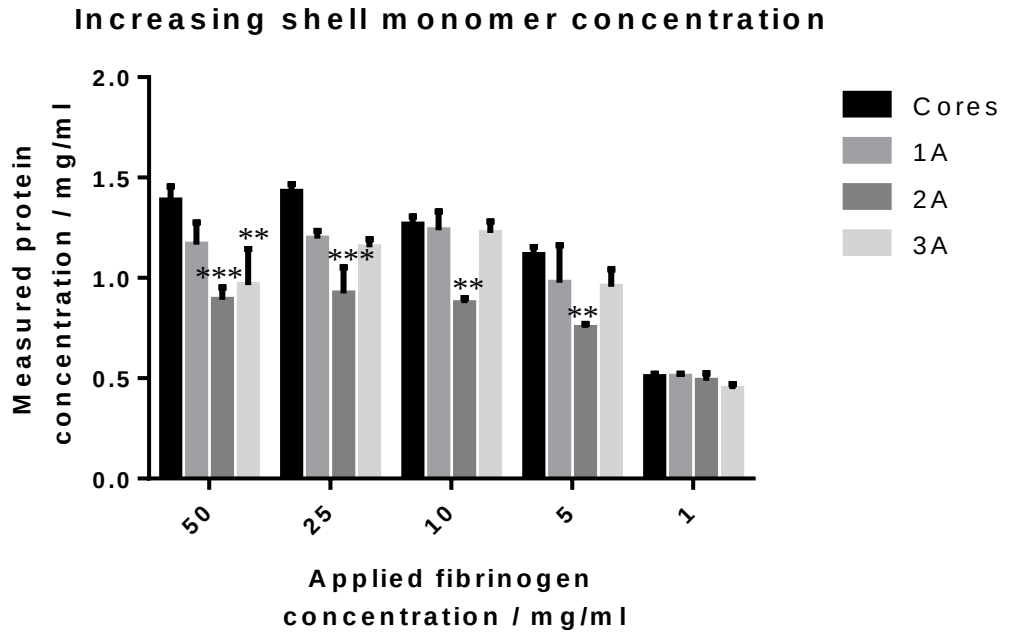

Figure 6-14 A graph of total measured fibrinogen adsorbed to the surface of CS particles as shell monomer concentration increases

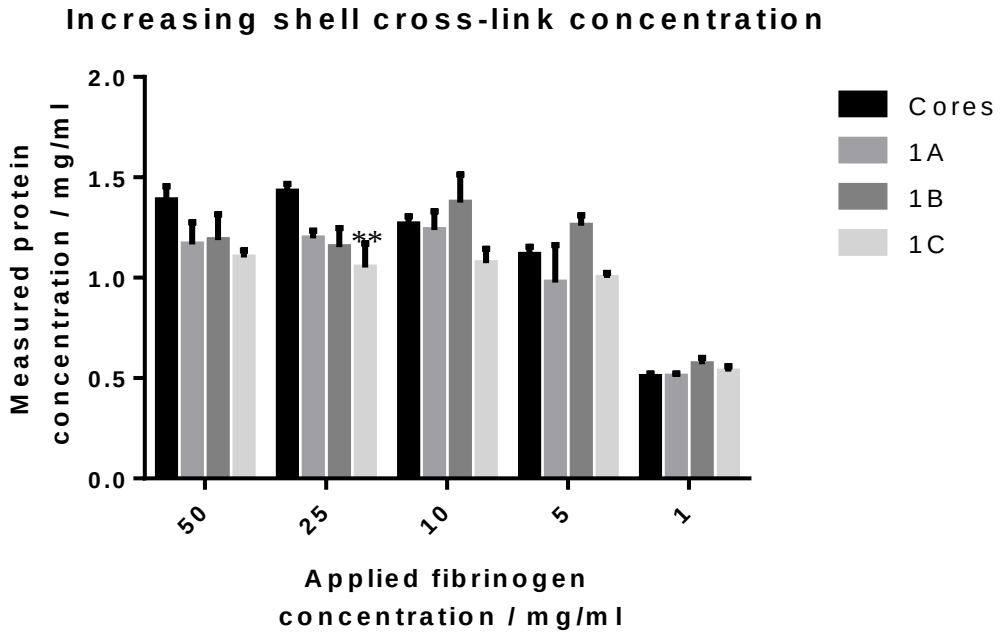

Figure 6-15 A graph of total measured fibrinogen adsorbed to the surface of CS particles as cross-link concentration increases

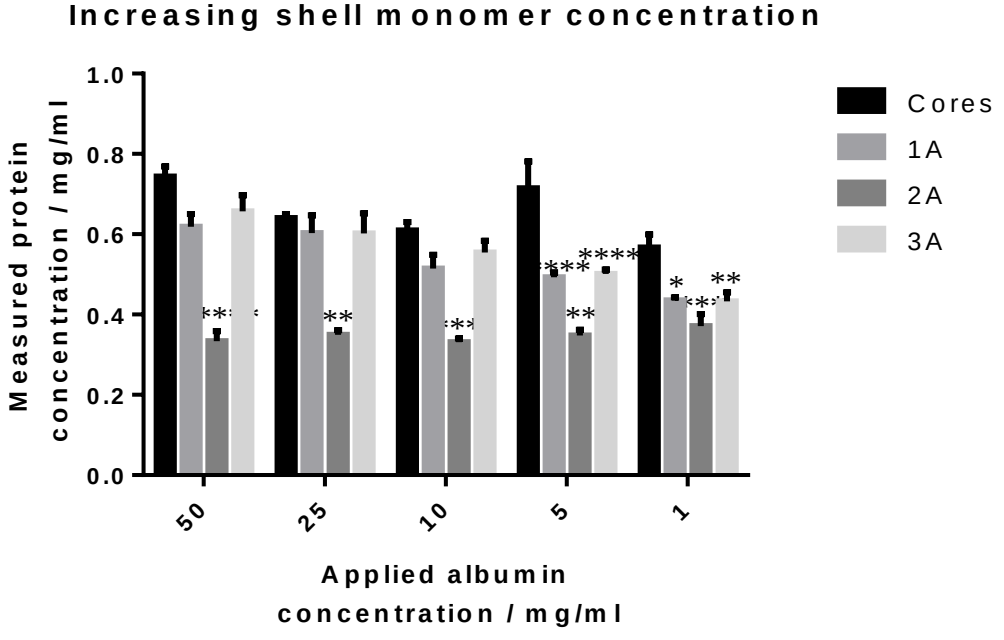

*

Figure 6-16 A graph of total measured albumin adsorbed to the surface of CS particles as shell monomer increases

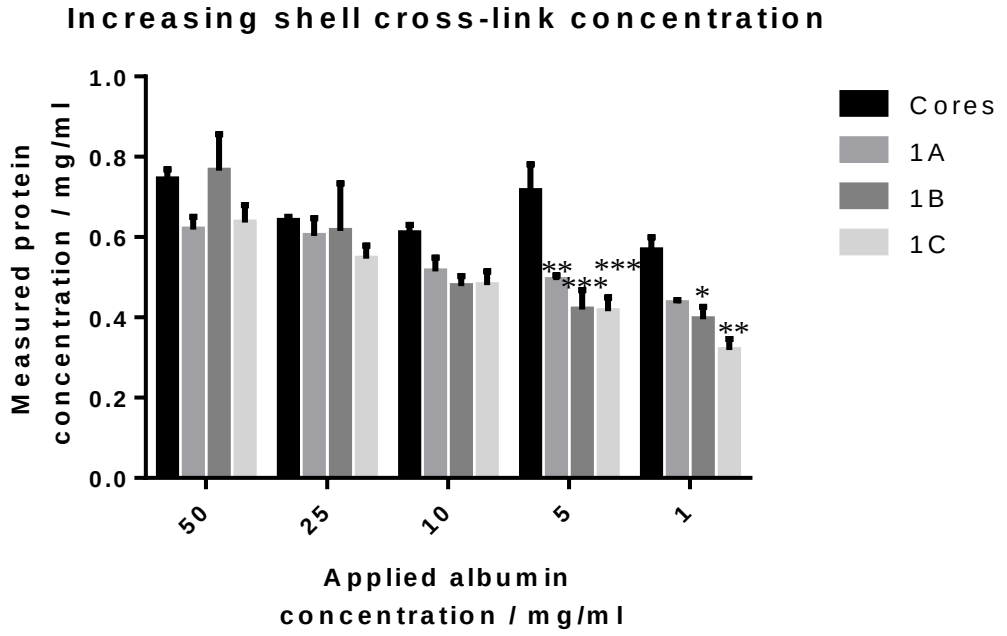

Figure 6-17 A graph of total measured lysozyme adsorbed to the surface of CS particles as cross-link concentration increases

The above graphs show the results of the total protein analysis of the core shell particles. The levels of significance as calculated via two-way ANOVA by the programme GraphPad Prism are indicated on the graphs using stars (**).

Particles with adsorbed lysozyme (figs 12-13) showed the highest amount of protein was adsorbed onto the cores at all concentrations of applied protein, with the exception of 1 mg/ml. The total amounts adsorbed onto the particles were small – all less than 1 mg/ml in total. This shows that the charges of the proteins were having a larger effect on the particles than the amounts adsorbed. Increasing shell monomer concentration reduced the total amount of protein adsorbed to the particles, falling to the lowest levels for particles 2A. The difference of these levels were highly significant as indicated on the graphs. This matches well with the zeta potential data which shows the adsorbed protein had the highest effect

on the bare core particles and that increasing the shell size reduces this effect. All of the CS particles showed protein adsorbed onto their surfaces. But the amounts adsorbed do not link directly with the results of the zeta potential experiment which indicates that the size of the particles is the dominant effect and small amounts of adsorbed protein can have a large effect on the electrophoretic mobility of these particles.

Overall, a larger amount of fibrinogen adsorbed onto the CS particles and cores than did lysozyme or albumin, but the effect on zeta potential was less than for lysozyme this is due to the reduced charge of the protein compared to lysozyme.

Again a larger volume of protein adsorbed to the cores than for the particles with shells and there appeared to be little significant difference as the cross-link concentration increased. At concentrations higher than 1mg/ml the amount of protein adsorbed to the particles remains roughly the same but significantly less fibrinogen again adsorbed onto the 2A particles.

Albumin adsorbed onto the particles in roughly similar amounts compared to lysozyme but had less of an effect on the zeta potential as mentioned previously. The BCA assay has confirmed that the protein is present on the particle surfaces on all particles and all concentrations, this shows that the largest effect that the protein has on the particles is to alter their charge show in the differences of zeta potential. Again the 2A particles adsorbed significantly less protein than the other particles. For the set of particles with increasing cross-link concentration in the shells, as the amount of protein adsorbed increased as the concentration of the protein solution increased slightly whereas the amounts of protein adsorbed to the particles with increasing shell monomer concentration remained roughly the same. At higher concentrations, above 5 mg/ml the amounts of albumin adsorbed onto the particles were not significantly different from the amounts adsorbed onto the cores,

indicating that the size and crosslink concentration has little effect on the ability to adsorb protein and also that very small differences in adsorbed protein amount can have large effects on zeta potential.

6.4 Conclusion

In this chapter the synthesis and analysis of some of the properties of core-shell particles has been described. The cores were synthesised using common emulsion polymerisation techniques and a protected shell monomer, previously synthesised in-house was grafted to the core.

The resulting core-shell particles showed increased particle size upon deprotection due to the exposure of hydrophilic moieties on the particle surfaces swelling with solvent. This is a key property of a hydrogel so these CS particles could be thought of as being nanoscale particle hydrogels.

The deprotected particles were shown to adsorb protein molecules to their surface which was shown by a change in the zeta potential – the charge on the surface of a particle. A larger overall effect was seen when adsorbing the positive protein lysozyme compared to a more negatively charged protein fibrinogen. The effects of the protein albumin were inconclusive due to the similar zeta potential of the protein and particles. The BCA assay showed that protein was adsorbed onto the surface of the particles and that it is directly measurable. The assay also shows that relatively small amounts of protein can have large effects on changing the zeta potential of the particles.

Protein adsorption is a useful characteristic to analyse as it gives an indication that these particles can have biological activity. When encountering a biological system, materials frequently become protein fouled. This can be from a variety of sources which include immune responses. Materials which show little or no protein adsorption can have very little

effect on a biological system. CS particles have shown to have use in drug delivery and in controlled release of bioactive molecules and these particles could show promise in this area. Further work could look towards investigating the size: adsorption ratio and whether this would have a link to a release pattern for a bioactive molecule.

7 Culturing fibroblasts on hydrogel surfaces

7.1 Introduction

7.1.1 Fibroblasts

Fibroblasts are a cell type found throughout the body of animals. They are responsible for synthesising components of the extracellular matrix (ECM) including collagens. They have an important role in wound healing, both in initial ECM repair and in the remodelling of damaged tissues, often contributing towards scar formation. [147, 148] Fibroblasts are the most common form of cell comprising connective tissues in animals and along with keratinocytes, make up some of the key cell types responsible for generating healthy skin in humans they are usually to be found in the basement membrane of skin. They are bi-or multipolar cells and grow in an elongated morphology. In cell culture they are adherent

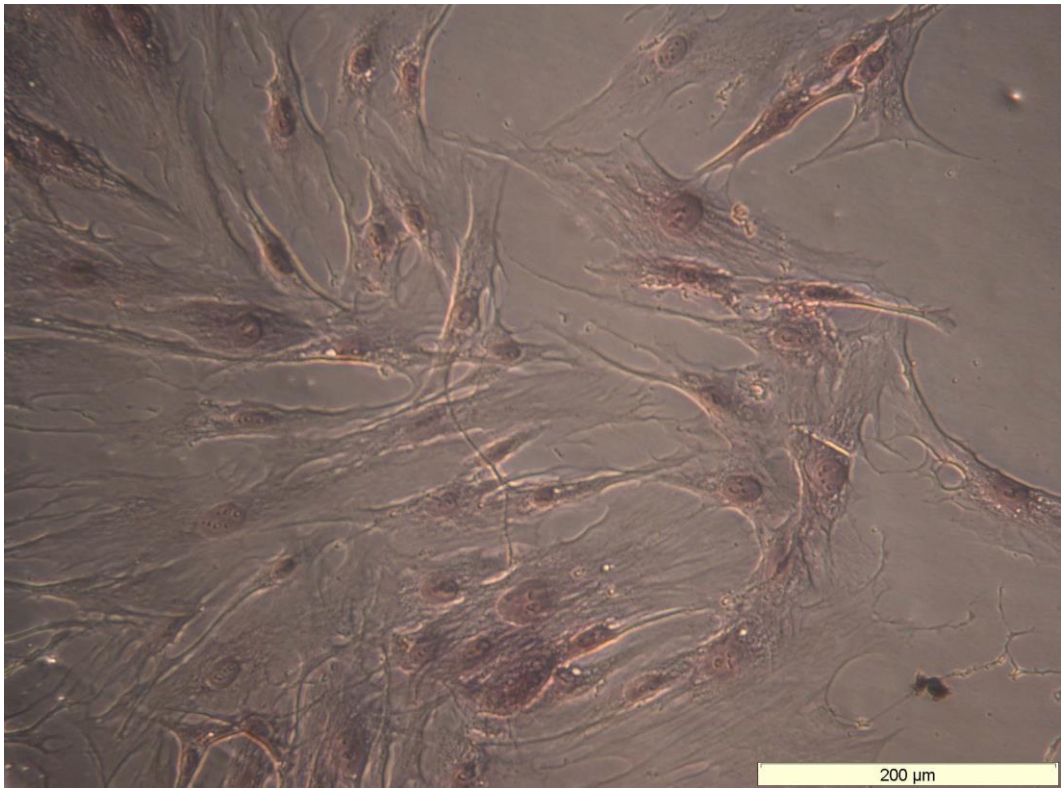

Figure 7-1 A light micrograph of NHDF cells grown on TCP stained with PicoSirius red

cells. The image below is of fibroblasts grown on tissue culture plastic (TCP) under normal conditions in our lab.

The cells have been stained with PicoSirius red, a stain which highlights collagen fibres present in the cell cytoskeleton. Also noticeable is the prominent cell nucleus, roughly central in the cells. Previous work in the group has shown that PGMMA hydrogels produced in previous chapters are not cytotoxic to normal human dermal fibroblasts (NHDF). [149]

7.1.2 Alamar Blue assay

The Alamar blue assay is a viability assay used in *in vitro* cell culture. There are a number of advantages to its use, the first being that it is toxic to the cells and the user, it is added directly to the culture medium towards the end of the incubation period and requires no additional reagents. It comprises no radioactive materials, such as some other assays used for viability or proliferation, for example [^{3}H] thymidine and so requires no special handling or disposal methods. Finally, it can be used over long culture times (up to 72 hours). All of

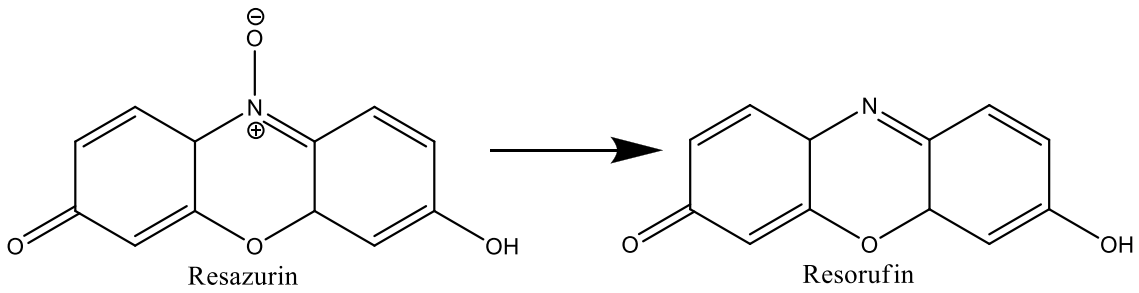

Figure 7-2 Chemical structures of resazurin and resorufin

these advantages make it an inexpensive assay with wide application, whether it is for small or large scale. [150-153] During active metabolism, cells take up the blue coloured resazurin molecule, reducing it to the red-pink coloured resorufin, which is also fluorescently

active.[154] This reaction is easily observed visually or measured using absorbance or fluorescence.

7.1.3 Polymerisation using benzoyl peroxide and dimethylaminopyridine

A different method of radical polymerisation was used in this chapter to produce new forms of the bare, latex particle free PGMMA hydrogel used as a control. This new polymerisation uses benzoyl peroxide (BPO) as the radical initiator and dimethylaminopyridine (DMAP). The polymerisation reaction can be conducted at the lower temperature of 30°C and

BPO/DMAP acts as a redox initiator system. This initiator system has been used previously in our group in the synthesis of silyl enol ethers.[155]

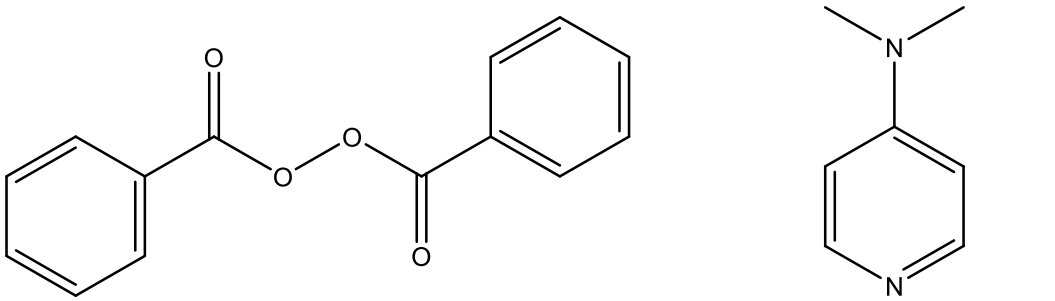

Benzoyl peroxide Dimethylaminopyridine

Figure 7-3 Chemical structures of BPO and DMAP

7.2 Experimental

7.2.1 Hydrogels

The hydrogel materials used were those described previously; formulations **1** (100 nm particles), **2** (250 nm particles) and **3** (720 nm particles). Each formulation comprising of gels with 50%, 25% & 1% w/w latex: GMMA for a total of 9 gels. As a control bare PGMMA hydrogels were also used. In addition to the bare PGMMA gels produced previously, two new formulations of bare gels were produced to examine whether any chemical effects resulting from the use of the potassium persulphate initiator, had any effect on cell adhesion. The new formulations were as follows.

7.2.1.1 Alternative PGMMA formulations

7.2.1.1.1 Materials

GMMA was obtained from Cognis and used without further purification. GDMA was obtained from sigma and used without further purification. Reagent grade ethanol and isopropyl alcohol (IPA) was obtained from Fisher scientific. Benzoyl peroxide (BPO), dimethylaminopyridine (DMAP), azobisisobutyronitrile (AIBN) and dimethyl sulphoxide (DMSO) were obtained from Sigma and used without further purification.

7.2.1.1.2 Thermal polymerisation

GMMA (4g) and GDMA (0.2g) were mixed in ethanol or DMSO, Two soda glass plates were lined with PET sheets and a PTFE spacer (250µm thickness) was placed between the sheets, the apparatus was held in place with bulldog clips. BPO (0.133g) and DMAP (0.133g) were mixed then added to the polymerisation mixture which was mixed well. As mentioned previously, any bubbles that appeared were removed by brief sonication. The polymerisation mixture was injected between the sheets and cured at 30°C for 16- 24 hours.

The resulting gels were removed from the sheets, washed and stored in ethanol. The ethanol in the DMSO gel was replaced several times over the course of a week in order to displace and remove any residual DMSO left in the gel as this would be particularly toxic to cells.

As well as the preparations described above, alternative formulations with differing ratios of BPO/DMAP initiator (100:1, 30:1 GMMA:BPO/DMAP), different initiators (AIBN), or different solvents (IPA) were tested but these formulations either failed to cure fully (lower BPO/DMAP ratios) or phase separated during curing (AIBN, IPA) and these gels were discontinued.

7.2.1.2 Preparation of hydrogels

All of the latex hydrogels and the bare PGMMA gels had been disinfected by storage in ethanol, they were removed from the ethanol under sterile conditions, allowed to dry slightly and cut into disks approximately 4.5mm in diameter, using a borer for the seeding experiment. The disks were then equilibrated with Dulbecco's modified Eagle's media (DMEM) containing 10% FBS and 1% penicillin/streptomycin (pen-strep) and media with 1% pen-strep and no serum.

This produced two sets of gels: serum (SER) and non-serum (NSER). The two sets served as a way of investigating whether serum proteins became deposited on the hydrogel surfaces during the equilibration process and aided in cell adhesion.

To equilibrate the gels, they were washed with media, agitated in the media and allowed to sit for 30 minutes then the media was replaced. This was repeated every 30 minutes for 4 hours. When not used, the gels were sealed in sterile sample tubes and stored in the fridge.

When the hydrogels were required for cell seeding experiments, they were removed from their media, blotted dry on sterile filter paper and placed in to low adherent 48 well plates (ProCell Falcon, 48 well plates, non- tissue culture treated), in triplicate, they were then allowed to air dry in the flow cabinet in order to dry them slightly for approximately 1 hour, during this time, the well plates were loosely covered to prevent infection. This made it easier for the cells to adhere to the surface when added during the experiment.

7.2.2 Normal human dermal fibroblast cell culture

7.2.2.1 Cell culture media materials

Dulbecco's modified Eagle's media (DMEM), foetal bovine serum (FBS), pen-strep ethylene diamine tetracetic acid (EDTA) and trypsin solution were obtained from Sigma, used without further purification and handled under aseptic conditions. Complete cell culture media (10% FBS, 1% pen-strep) was stored in the fridge until needed and warmed to 37°C when required.

7.2.2.2 Culturing NHDF cells

Normal human dermal fibroblast (NHDF) cells were obtained from ProCell and were cultured to confluence in 100ml Nunc brand flasks, obtained from Fisher Scientific. Cells were incubated at 37°C, 5% CO_2. Cells were cultured lying flat in 20ml complete DMEM media, described above. Media was changed every 3-4 days. Cells were passaged when they reached approximately 90% confluence, which was roughly every 7 days.

7.2.2.3 Passaging NHDF cells

When they became approximately 90% confluent the NHDFs were passaged. To achieve this, the media in the flasks was aspirated off and 5 ml trypsin/EDTA solution was added to the flask and the cells were left for 5 minutes to detach from the base of the flask. After 5, the flask was tapped vigorously to remove any remaining cells and the resulting solution was centrifuged at approx. 2000 RPM for 6 minutes to form a pellet. When this was complete the supernatant was quickly removed and depending on the next process for the cells, media was replaced. If the cells were returning to culture and increase in number in the incubator, the cell pellet was resuspended in media and split between the desired number of flasks, usually 4, and the total media volume was made up to 20 ml. If the cells were being used for seeding as part of the experiment, they were counted using a haemocytometer, adjusted to the appropriate concentration using further media and seeded as required.

7.2.3 Culturing NHDFs on hydrogels

The cells were lifted from the flasks as described above and counted using a haemocytometer, the cell concentration was adjusted to 2.5 $x10^5$ cells/ml with fresh media and the cells were concentrated and seeded at a total cell number of 1.25 $x10^4$ cells, in 25 µl on each gel. This small volume of more concentrated cells was based on seeding 50 µl of 2.5 $x10^5$ cells/ml NHDF but it was found that 50 µl was slightly too much liquid and it didn't all absorb into the gel resulting in some of the cells being washed off the gels when more media was added. The cell solution was allowed to soak into the gels for an hour before 300 µl of fresh media (containing serum) was added to each well and the well plates were

covered and placed in the incubator for 48 hours. The same volume of cells was also seeded on to tissue culture plastic (TCP) and topped up with 300 µl media

After 36 hours, the plates were removed from the incubator and the gels were carefully removed from their wells and added to fresh wells in new plates, 300 µl fresh media was added to each well. 30.3 µl of Alamar blue solution was added at this point and the new wells were returned to the incubator.

This removal of the gels to fresh plates was to use the Alamar blue assay to count only the cells growing on the gel surfaces and not any that had migrated or been washed off the gels and adhered to the well plate surface.

7.2.3.1 Assessing cell number using the Alamar blue assay

The Alamar blue assay is a means of assessing cell number by the metabolic activity of the cells, the blue dye Resazurin is reduced by the cells to a red dye, the resulting change in the absorption peak, read by a plate reader can be calibrated to give an accurate number of active cells present in a sample.

7.2.3.1.1 Materials

Resazurin dye was obtained from sigma as a powder and diluted 1mg/ml in sterile phosphate buffered saline (PBS) also obtained from sigma. The resulting solution known as Alamar blue solution was stored in the fridge in the dark and used as required.

7.2.3.1.2 Alamar blue assay

At the required time, the plates were removed from the incubator, 10% volume of Alamar blue solution was added (32.5 µl) and the solution was gently mixed with the media and the plates were returned to the incubator for a further 12 hours. At the same time known concentrations of cells were seeded on to TCP in wells in a 96 well plate to construct a

standard curve. The volumes were 3 x10^5, 2.5 x10^5, 1 x10^5, 5 x10^4, 1 x10^4, 5 x10^3 cells/ml, in triplicate, concentrated in 25 µl as mentioned previously. 25 µl of media was also added to a separate well as a blank. After an hour the wells were topped up with 300 µl fresh, warmed media. The well plates were returned to the incubator for 11 hours.

At the end of the experiment, 100 µl of Alamar blue containing media was removed to a fresh 96 well plate and its absorbance was read at 570 and 600 nm using a BioTech ELx800 plate reader.

7.2.3.2 Fixation of cells

At the end of the experiment, the media was aspirated from each of the wells and 10% formalin (Sigma) was added to fix the cells, the wells were covered and left for 24 hours. At the end of 24 hours, the formalin solution was removed and the cells were stained.

7.2.3.3 Staining and imaging of cells

The nuclei of the NHDF cells were stained with Giemsa stain and collagen in the cytoskeleton was stained with PicoSirius red

7.2.3.3.1 Materials

Giemsa stain was obtained from Sigma and used as supplied. Sirius red stain was obtained from Sigma (supplied as Direct Red 80), and diluted in saturated aqueous picric acid solution (Sigma) to make a 0.1% solution. Care must be taken with picric acid that it doesn't dry out as dry picric acid is a high explosive. Glacial acetic acid was obtained from Sigma and diluted 5 ml in 1L of deionised water, this acidified water was stored and used as required.

7.2.3.3.2 Staining method and imaging.

Giemsa stain was added in a few drops onto the hydrogels in each well as well as the wells in the TCP control. The wells were left for approximately 10-15 minutes before being washed well with water. Care must be taken not to wash the hydrogels too vigorously or they will break or cells may be washed from their surface. Care must also be taken throughout the fixing, staining, washing and imaging steps that the gels do not dry out fully as they will shrink and cause the cells on their surfaces (if any) to distort or lift off completely.

After washing, thoroughly PicoSirius red was added and left to stain for one hour before being removed and the wells washed twice with acidified water. Most of the water was removed and the gels were placed on a glass slide and imaged using an Olympus upright microscope. The TCP wells were imaged using an Olympus inverted microscope with phase contrast. The microscope images were recorded using Cell^{B} software. The best images were obtained from the gels if they were blotted dry with filter paper but not allowed to dry out fully as they then begin to curl making imaging very difficult.

7.3 Results and discussion

7.3.1 Hydrogels

The new gels made with BPO/DMAP and DMSO or Ethanol (written following as 0-DM or 0-ET) appeared visually similar to the hydrogels produced previously and both were clear, flexible gels. The DMSO hydrogel had a slightly brown tinge to it which did not wash out over time but appeared to have no notable effect on the gel properties, this is likely from incorporation of DMAP into the gel structure. The DMSO gel was also stickier than any of the other gels, requiring washing with ethanol to remove it from the PET films onto which it

had polymerised during the curing. This gel was also slightly stickier than any of the other gels following washing, but to a much lesser degree than when it was drier, and stuck more strongly to the forceps used to manipulate the gels and the well plates into which it was placed, requiring slightly more force to manipulate it. The initial stickiness may be explained by the presence of diols not involved in hydrogen bonding with the solvent. Following multiple washes, the gels became less sticky and tended more to adhere well to surfaces when slightly drier. When swollen with ethanol or media it behaved as the other gels do with no noticeable differences.

The ethanol BPO/DMAP gel appeared visually and functionally the same as the gels made previously using potassium persulphate.

The equilibrium water content for these gels were as follows: 0-DM 80.21 ± 3.3% 0-ET 78.00 ± 4.1% which is very similar to the EWC reported previously for the potassium persulphate gels

When all of the hydrogels were equilibrated in the media they took on the purplish pink tinge of the media showing that they had absorbed the media into their structure. Full equilibration with media, as well as washing away any possible residual cytotoxic chemicals left over from the polymerisation steps, also acts as a useful indicator of the sterility of the hydrogel samples. The indicator present in the media will turn yellow if bacterial or fungal cells are present and metabolising and therefore producing acidic metabolites. Whilst the polymerisation of the hydrogels is conducted with rather toxic organic chemicals and often at high temperatures, as well as the gels being stored in ethanol which not only allows them to maintain a degree of swelling, but also acts as a disinfectant, there are a number of possible points at which an opportunistic pathogen may infect the gels. The gels were

handled according to aseptic technique and stored in sterile sample tubes, the media in which they were equilibrated and stored retained its pink-purple colouring indicating that they remained free from infection.

When the gels were ready to be used for a cell seeding experiment, they were dried slightly, this decision was made following preliminary experiments which showed that gels fully hydrated with media prior to addition of media containing cells did not absorb any more media meaning that any cells contained in this new media often washed off the surface when moved or when new media was added, giving an unclear indication of the ability of the fibroblasts to adhere to the hydrogels. Following partial drying and then rehydration with the media containing the cells, many more cells were seen on the surface of the gels, some did still get washed off when fresh media was added or migrated on their own to the surface of the well plates but a large number of cells remained on the gels. The readiness of the cells to be washed from the surfaces of the gels suggests initially poor adhesion to the gels. Stronger adhesion sites on the substrates would have made washing the cells from the surfaces more difficult. When the gels were moved to fresh wells, very few cells, if any were then washed off or migrated, indicating better adhesion to the gels at later stages.

7.3.2 NHDF cell culture

NHDF cells grew well in culture and multiplied relatively quickly, reaching confluence following passaging in roughly a week. A T75 flask of cells would yield roughly 1 x10^5 cells/ml in 10 ml of media. The cells remained viable until roughly passage 12-14, wherein they began to senesce, stopped proliferating and began to die off.

When the cells were cultured on the hydrogels, they appeared to adhere well and remain viable which was indicated by the Alamar blue assay, data of which follows. Towards the end of the experiment when the gels were transferred to fresh plates, much care was needed as the gels were fragile and prone to snapping when manipulated out of the narrow wells. For the most part the gels survived intact and any that did break did not appear to lose any significant number of adhered cells. The decision to transfer the gels was made due to the observation of fibroblasts adhering to the bases of the wells they had either migrated there or been washed off the hydrogel surfaces during the initial stages of the experiment. This is despite the plates being advertised as low adherence plates, which stands as an indication of the adherent ability of these cells.

7.3.3 Assessing cell number using the Alamar blue assay

The Alamar blue assay gave a clear and quantifiable representation of the viability and the number of cells present in the wells. When first added the media was dyed dark blue and over time turned pink so at a glance, it is easy to assess the relative success or failure of an experiment. The assay is affected by the metabolic activity of bacteria so care must be taken to ensure sterility throughout the experiment so as to only measure the activity of the desired cells. The assay gives a linear relationship between cell number and observed optical density as is shown, as an example, in the calibration curve below. Errors in the optical density readings can come from a variety of sources such as differing cell metabolic activity between wells or bubbles appearing or disappearing as a result of the mechanical shaking of the plate whilst it is in the reader. This is particularly troublesome as there is little that can be done to stop this once the plate has gone into the machine. Also minute differences in the volumes of media extracts used in the assay can have a pronounced effect on the optical density reading given, this differences are imperceptible to the human eye but can be a considerable source of error in the readings.

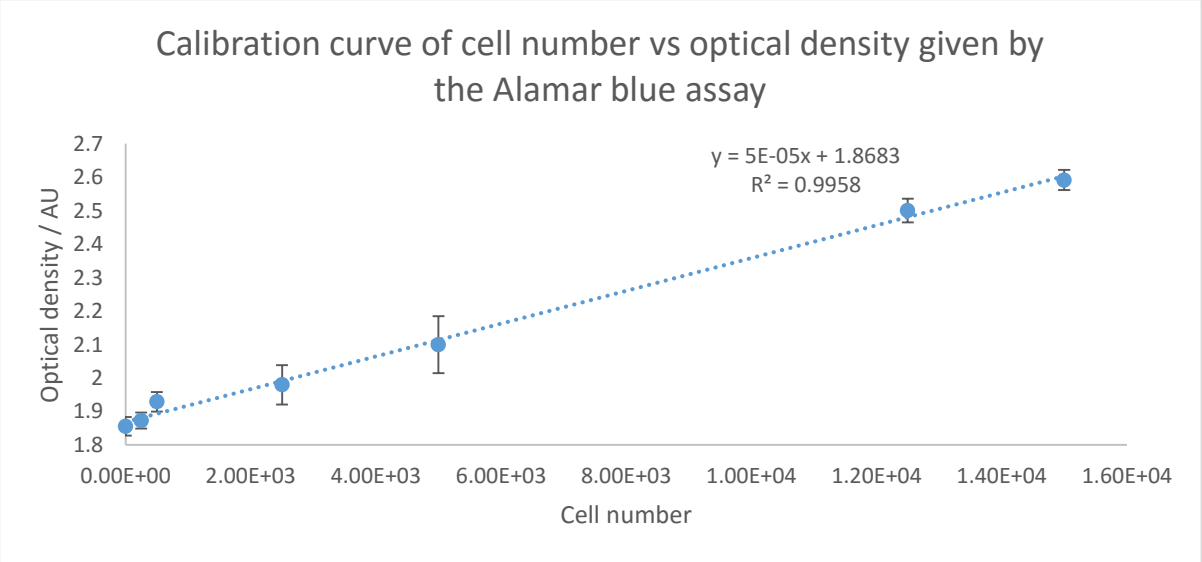

Figure 7-4 A calibration curve of cell number vs optical density given by the Alamar blue assay

As can be seen in the above graph, the assay is not very accurate in the lower end of the curve, corresponding to low cell numbers this is because, the assay measures the metabolic activity of all of the cells present so lower cell numbers have a lower overall total metabolic activity and therefore give a reduction in the observed colour change.

Using the assay and the above calibration, it was possible to calculate the number of metabolically active cells present on the surface of the gel after 48 hours. The following figures show a graphical representation of the number of cells on each of the gels, presented as an average of three gels, the error bars are the standard error where n=3

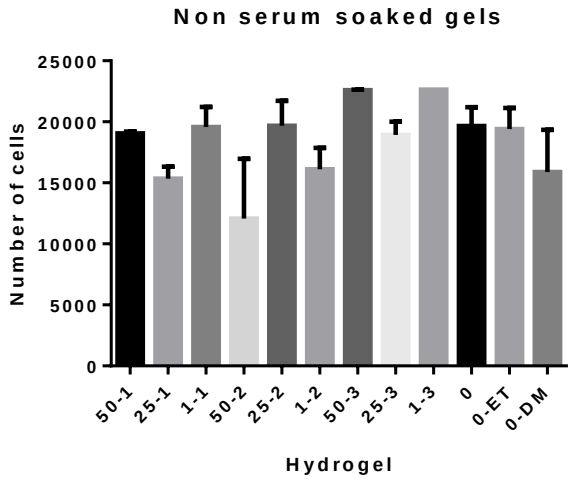

Figure 7-5 A graph of the number of cells recorded by the Alamar blue assay on the surface of NSER hydrogels after 48 hours

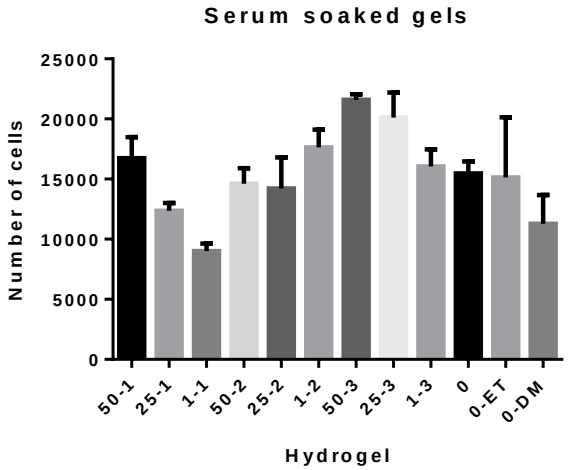

Figure 7-6 A graph of the number of cells recorded by the Alamar blue assay on the surface of SER hydrogels after 48 hours

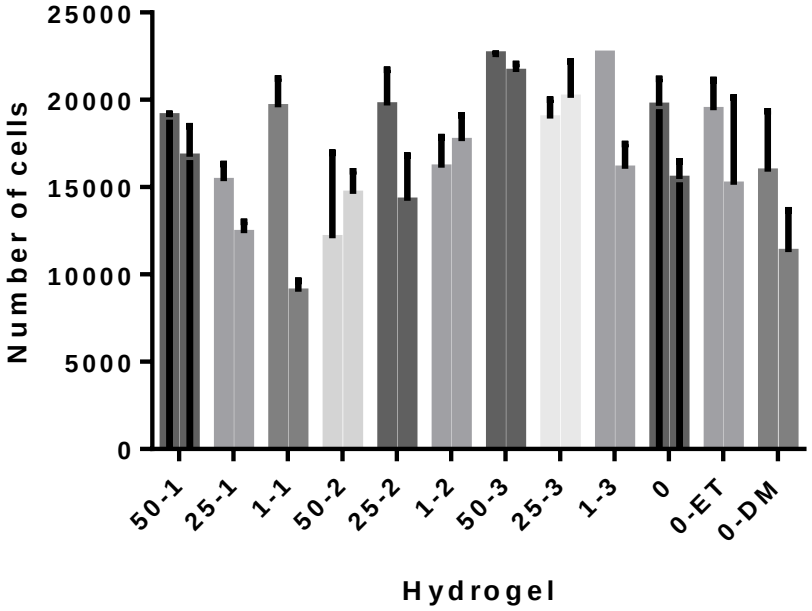

Figure 7-7 A combined graph of the number of cells recorded by the Alamar blue assay on the surface of NSER and SER hydrogels after 48 hours

The above graphs show a representation of the number of cells present on the surface of the hydrogels at the end of the experiment, the first graph, Figure 7-5 shows the cell counts for the NSER hydrogels and Figure 7-6 for SER hydrogels. The third graph Figure 7-7 is the previous two combined for clarity where the left hand bar in each set is the NSER gels and the right is SER. The cell numbers have also been presented in the following table.

	NUMBER OF CELLS	
HYDROGEL	**NSER**	**SER**
50-1	19000 ± 150	16700 ± 1730
25-1	15300 ± 970	12400 ± 640
1-1	19600 ± 1650	9000 ± 620
50-2	12000 ± 4890	14600 ± 1290
25-2	19700 ± 2030	14200 ± 2580
1-2	16100 ± 1740	17600 ± 1500
50-3	22600 ± 33	21600 ± 460
25-3	18900 ± 1070	20100 ± 2090
1-3	22600 ± 0	16000 ± 1400
0	19700 ± 1540	15500 ± 1000
0-ET	19400 ± 1740	15100 ± 4990
0-DM	15900 ± 3470	11300 ± 2400
TCP	16600 ± 1230	

Table 7-1 A table of the number of cells recorded by the Alamar blue assay on the NSER and SER hydrogels

The data presented above (Table 7-1 A table of the number of cells recorded by the Alamar blue assay on the NSER and SER hydrogels shows that in almost all cases the number of cells present on the gels at the end of 48 hours incubation has increased from the number

of cells seeded at the start of the experiment (12500 cells). This number is only the cells that remained on the gels and does not include any cells that were washed off or migrated off the gels over the course of the 48 hour incubation. Where the cell number is below this count, a larger number of the original cells seeded must have been washed off the gels leaving the remaining number to continue on the gel.

As the cell numbers have increased, this suggests that the cells are able not only to adhere to the hydrogels but also to proliferate on the hydrogel surface which shows that the hydrogels are not only non-cytotoxic but also are a suitable surface for the growth of cells.

Statistical analysis of the cell numbers using ANOVA showed that there was no significance between the number of cells present on any of the gels of the NSER hydrogels ($p=0.0623$). For the SER hydrogels, ANOVA showed that there was a statistical significance between the number of cells on the hydrogel over all ($p=0.0159$) but when analysed with Sidak's multiple comparison test, as calculated by the Graphpad Prism statistical software, the only significance was found between the 1-1 gel and 50-3. The number of cells found on the 1-1 gel appears to be anomalously low and this significance could therefore be discounted. The low number of cells could be contributed to cells being washed off the surface during the experiment or by being physically knocked off the surface by the mechanical handling of the gel during the transfer to a fresh plate. The images in the following section show that cells are indeed present on the surface of the gel.

Figure 7-7 above, showing the combined graphs, shows that for nearly all of the gels, the number of cells counted on the surface of the gels suggests that more cells are present on the surface of the gels which were equilibrated in media that did not contain FBS. However when analysed using ANOVA, there is no statistical significance between any of the gels,

apart from the 1-1 gels but this is the result of the anomalous reduced cell number observed on the 1-1 SER gel which is explained above. This indicates that the cells deposit sufficient proteins to enable adhesion to the gels and that these proteins do not deposit from the cell culture media. Whilst statistically insignificant, there is a slight trend for some of the gels particularly those containing few or no particles to have larger numbers of cells present on the surfaces. This could be an indication that serum proteins contained in the media used to swell the gels may have an effect on the swelling properties of the gel. This would need to be investigated further.

The above data also shows that the cells grew on the hydrogels in similar numbers to those which grew on the tissue culture plastic in the controls indicating that under these conditions, the hydrogels perform at least as well as the well-established TCP as a cell culturing platform.

7.3.4 Imaging cells

Following fixation and staining, the cells were imaged using reflected light on an upright microscope. This microscope setup was used due to the hydrogels being opaque meaning that the more commonly used set up of an inverted microscope could not be used. The hydrogels themselves presented challenges to image for a number of reasons. Hydrogels swell differently in different liquids e.g. water and ethanol and it is thought also between formalin solution and PBS which are used in the washing and fixing steps, as well as the various dyes and washes used in the staining steps. Formalin used in fixation may also increase the number of cross-links present in the gels. Slight changes in hydrogel size could result in cells lifting from the surface of the hydrogel which would give a lower appreciation of number of cells that were present on the surfaces during the cell culturing experiments.

Another problem with imaging hydrogels is the actual liquid content of the hydrogel. Whilst culturing with cells, this property is indispensable, when it comes to imaging, highly swollen hydrogels present a challenge. Hydrogels that are too wetted retain a small film of water on the surface which is observed to be above any attached cells or hydrogel surface features, which obscures the visual identification of any cells or features. Using a glass coverslip presents a similar problem as it seems to obscure any visual information and any residual liquid on the gel surface pools between the contours on the gel and the cover slip, further obscuring the imaging. Mountants such as glycerol/PBS when used with coverslips also show this problem as well as beginning to lift the cells off the surface after relatively short contact times. Fully drying out the hydrogels after dehydrating with ethanol did allow for a somewhat effective imaging method, if they hydrogels dried flat. Curved or slanting hydrogels led to differing focal points when examined using the microscope, making actually taking acceptable images much more challenging. The main problem with the dehydration and drying method was that the gels shrank considerably from their size during culture and some cells were sloughed off the surface, while patches of cells would appear buckled and irregular.

The usual protocol for imaging the cells was to remove most of the liquid that the gel had been stored in, usually PBS, blot dry on both sides using filter paper then carefully place the gel onto a microscope slide and image. When imaging it was desirable to be quick as the hydrogels quickly begin to dry out, and as they dry they begin to curve which changes the overall plane of focus making for partly blurry images. The drying problem was compounded by the microscope itself which, due to its setup, shines the illumination required to see the analysed sample, down the objective lens. Therefore for higher magnifications, this light spot is more highly focused and magnified which creates local heating points, drying out the

gel and causing it to change shape. Higher light intensities caused rapid drying and curling of the gels as well as a large amount of glare in the image, making viewing difficult whereas at lower light intensities, details were difficult to identify. A balance was therefore struck which was towards the lower light intensity end of the scale allowing slightly longer time to image a sample before it inevitably dried out. The following figures are of the hydrogels with adhered NHDF cells.

Figure 7-9 A-X Light micrographs of NSER hydrogels with adhered cells

Figure 7-8 A-X Light micrographs of SER hydrogels with adhered cells

LABEL	GEL
A,B	**50-1**
C,D	**25-1**
E,F	**1-1**
G,H	**50-2**
I,J	**25-2**
K,L	**1-2**
M,N	**50-3**
O,P	**25-3**
Q,R	**1-3**
S,T	**0**
U,V	**0-ET**
W,X	**0-DM**

NSER

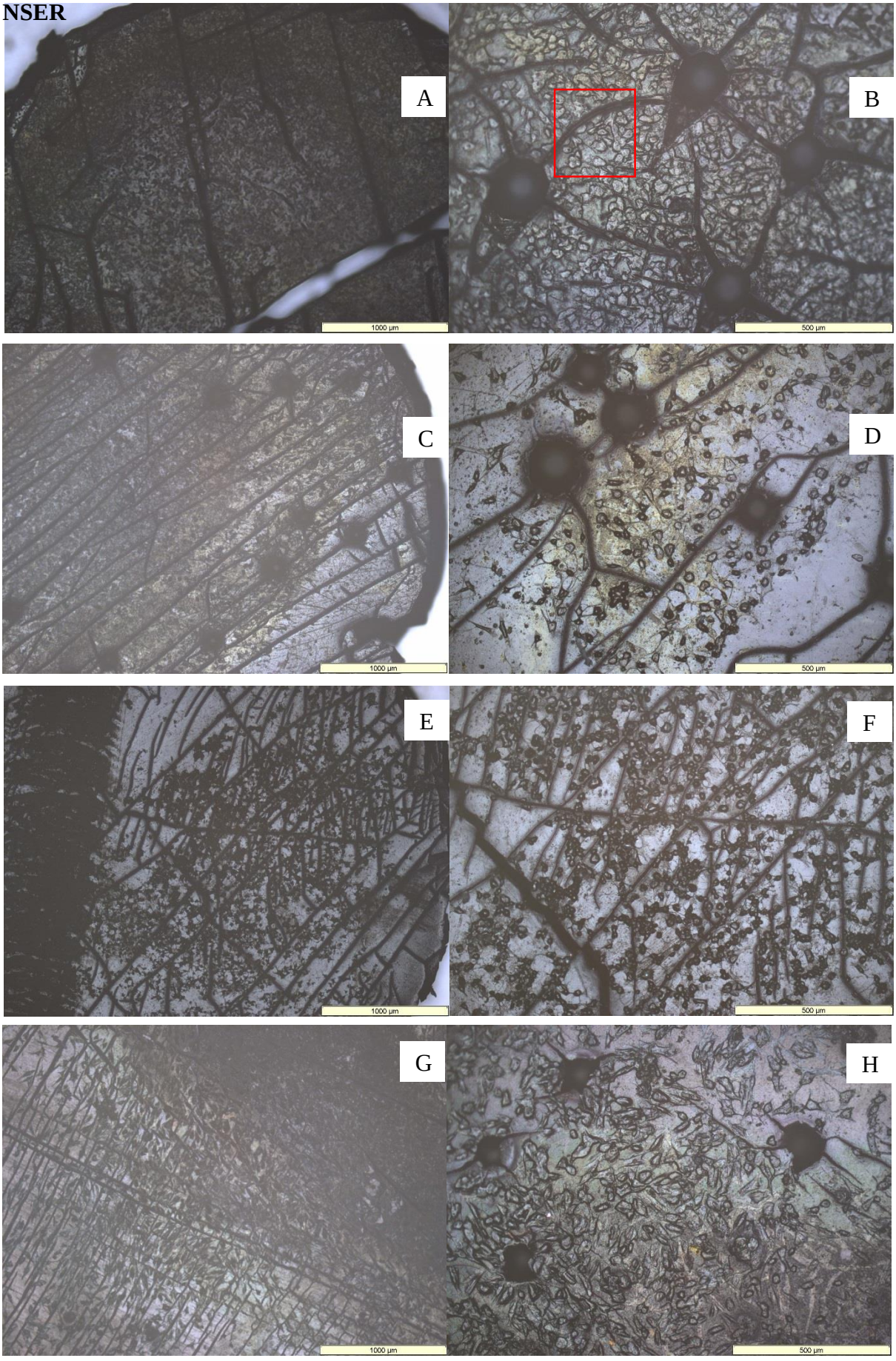

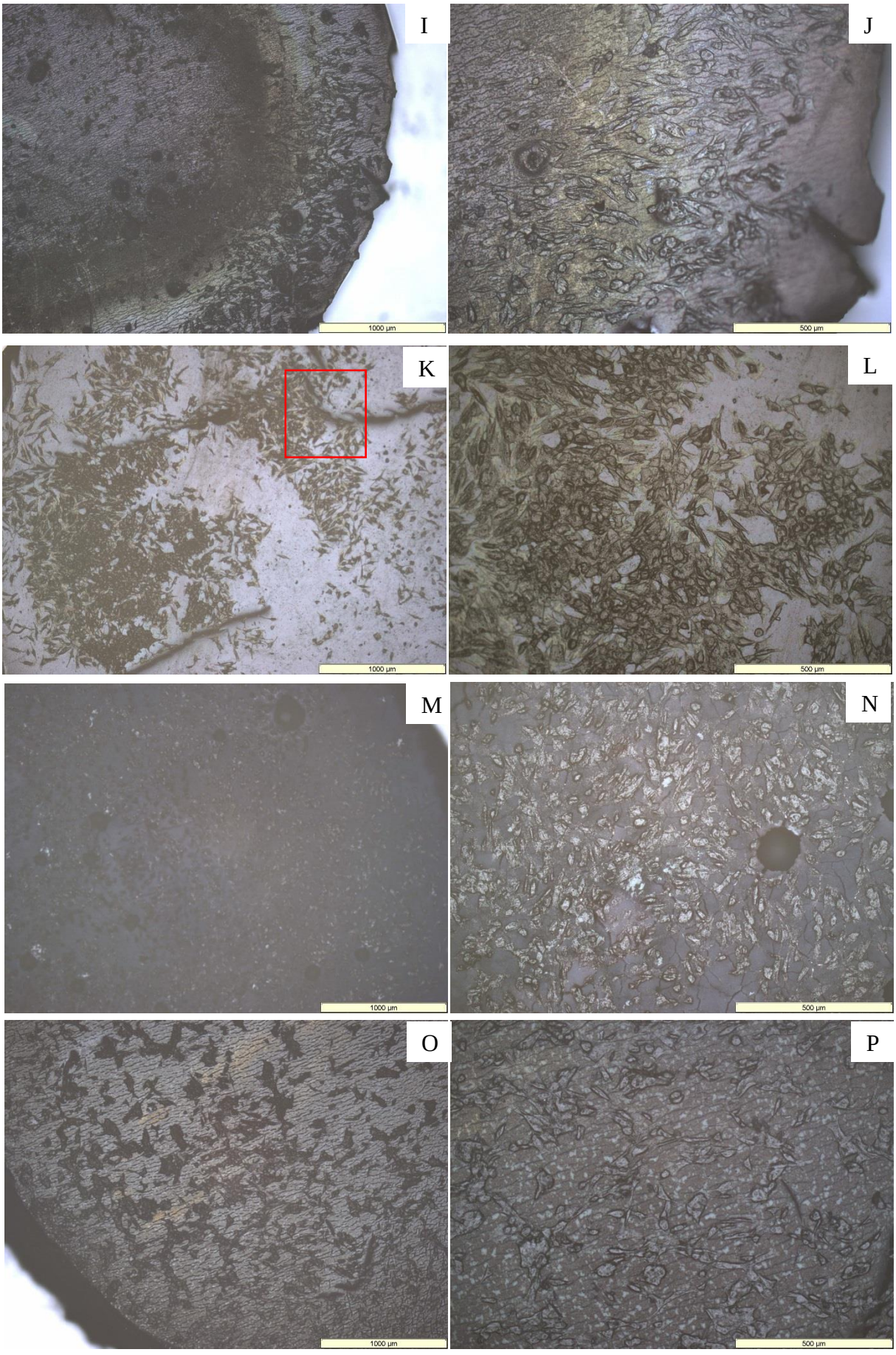
I
1000 µm
J
500 µm
K
1000 µm
L
500 µm
M
1000 µm
N
500 µm
O
1000 µm
P
500 µm

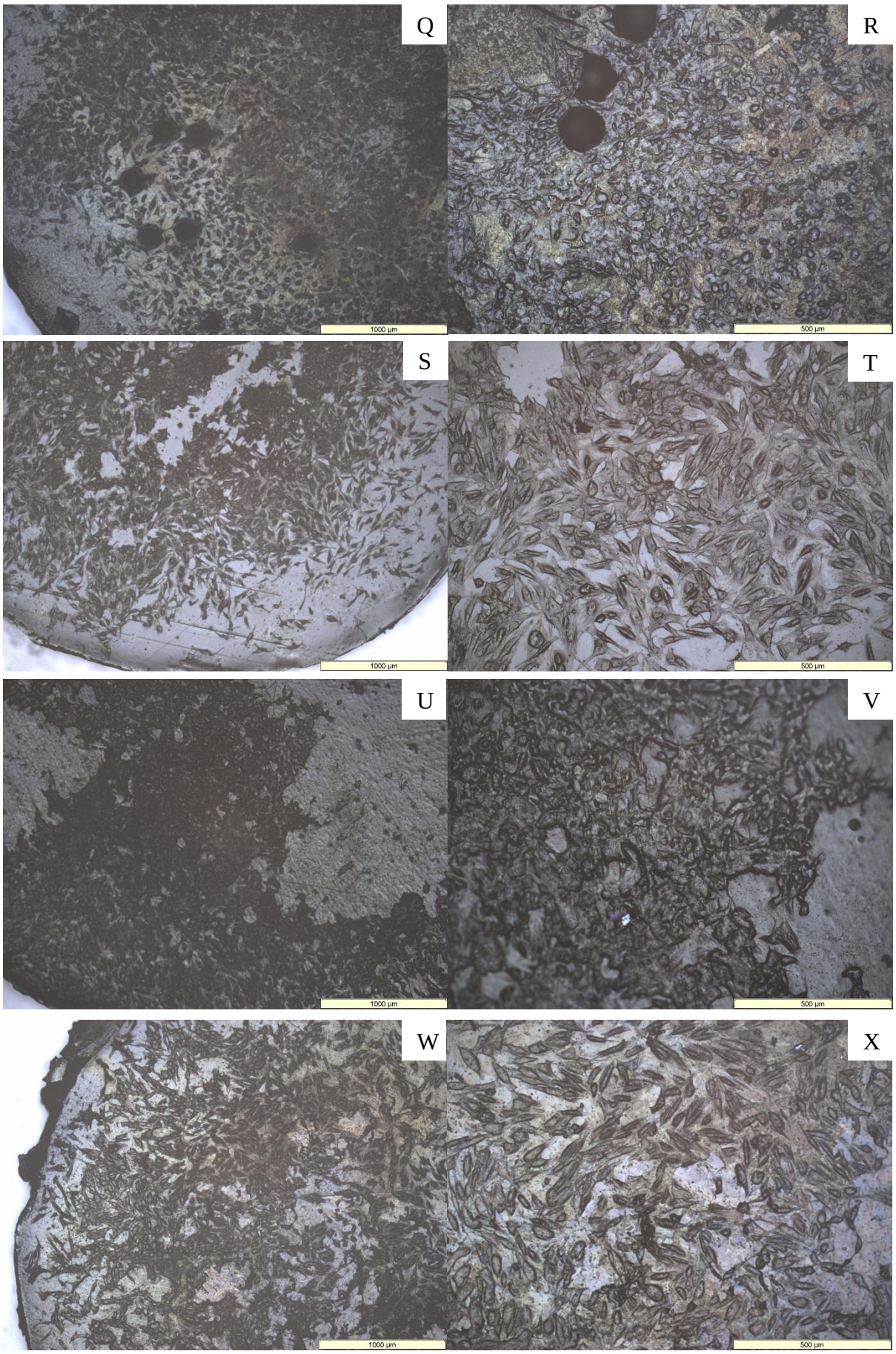
Q
1000 µm
R
500 µm
S
1000 µm
T
500 µm
U
1000 µm
V
500 µm
W
1000 µm
X
500 µm

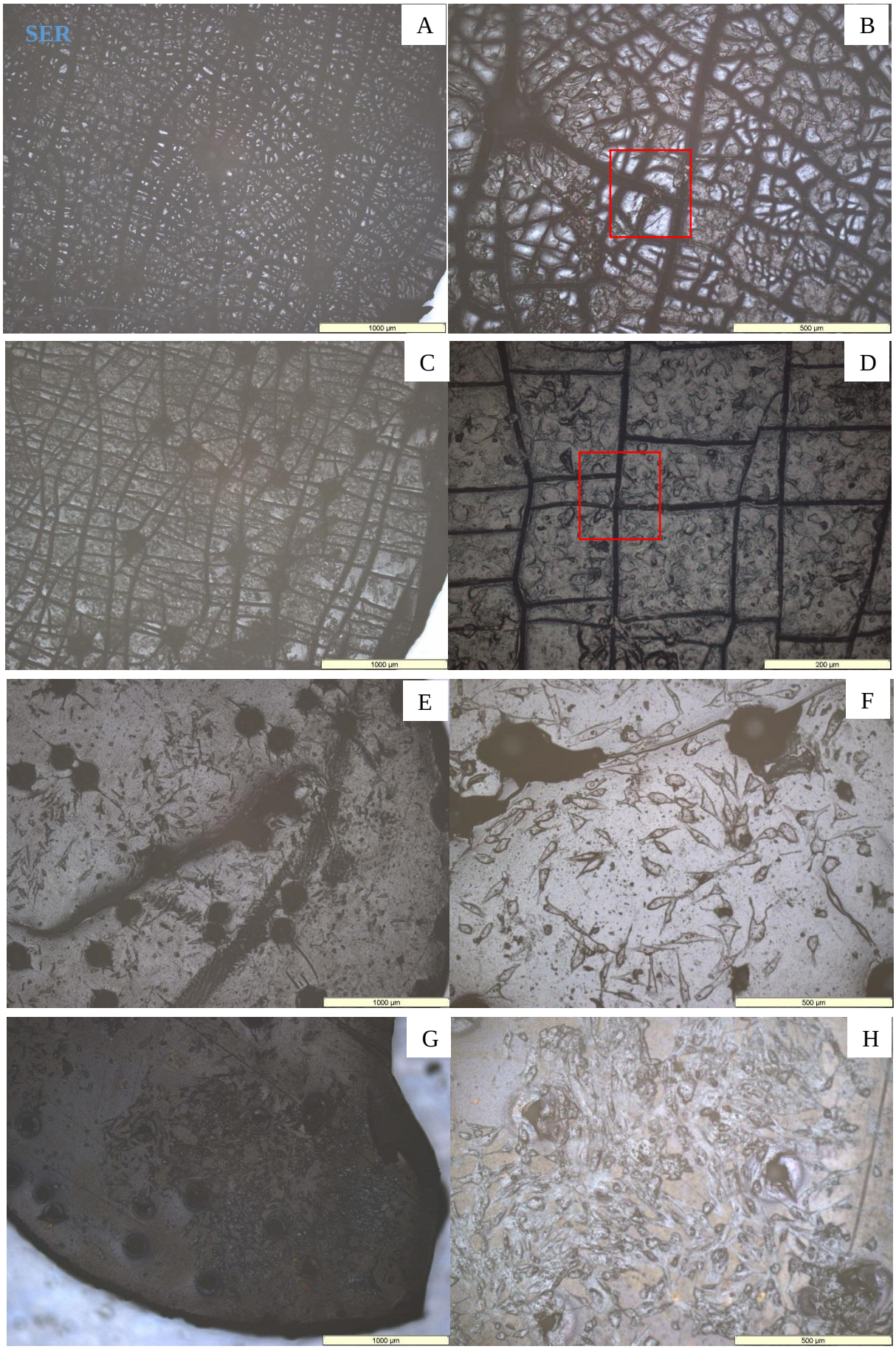
SER
A
1000 µm
B
500 µm
C
1000 µm
D
200 µm
E
1000 µm
F
500 µm
G
1000 µm
H
500 µm

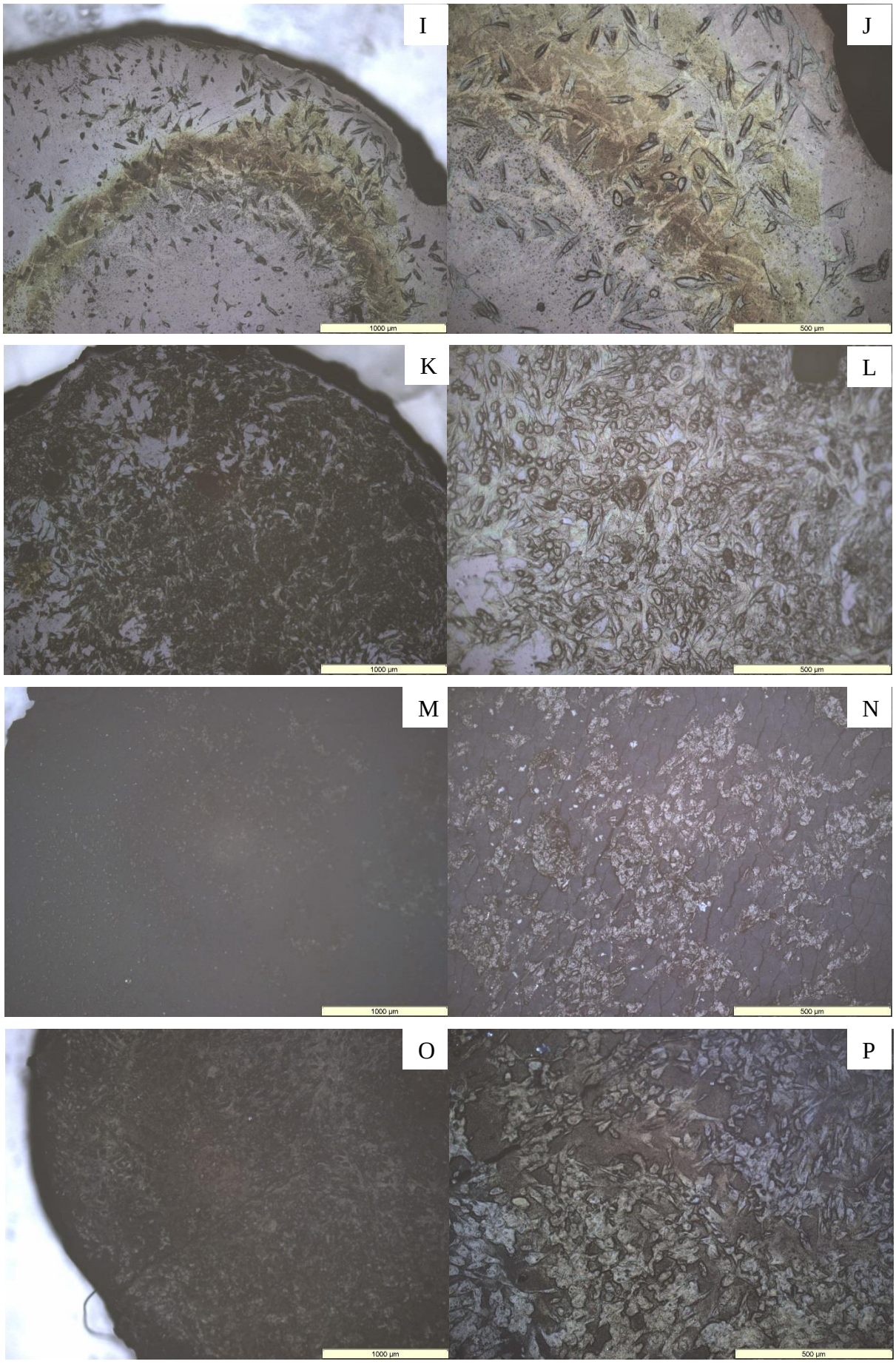
I
1000 µm
J
500 µm
K
1000 µm
L
500 µm
M
1000 µm
N
500 µm
O
1000 µm
P
500 µm

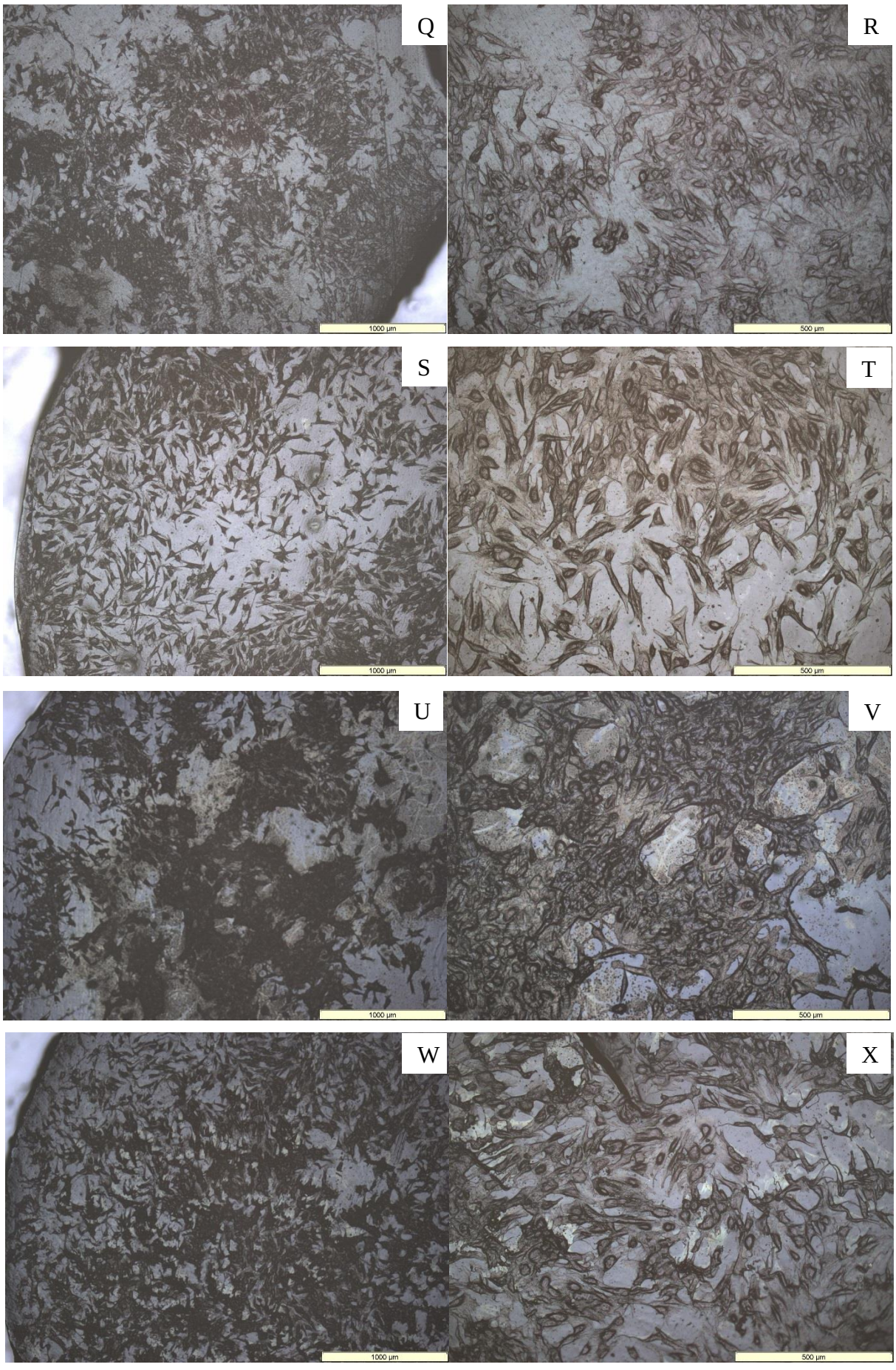
Q
1000 µm
R
500 µm
S
1000 µm
T
500 µm
U
1000 µm
V
500 µm
W
1000 µm
X
500 µm

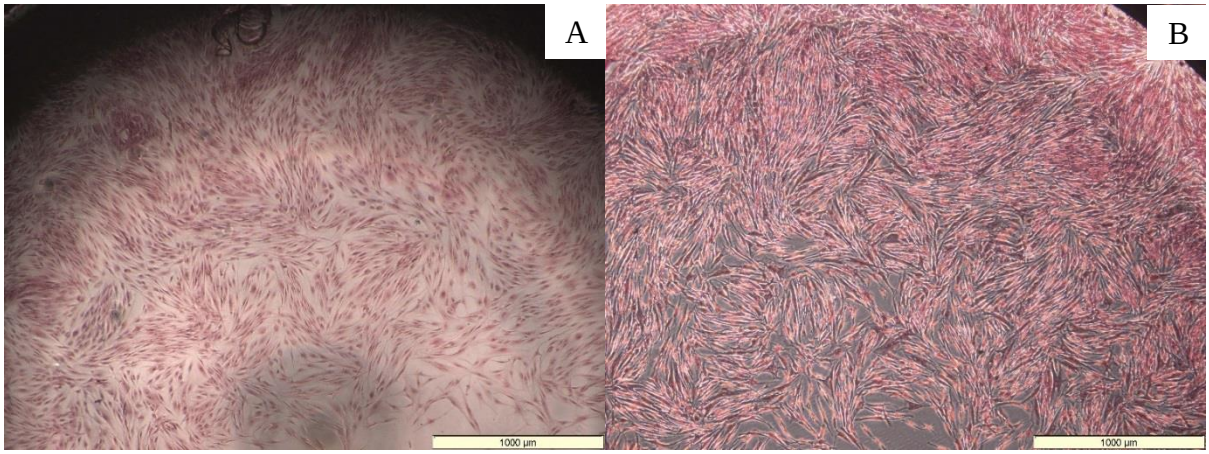

Figure 7-10 A-F Light micrographs of TCP controls with adhered cells

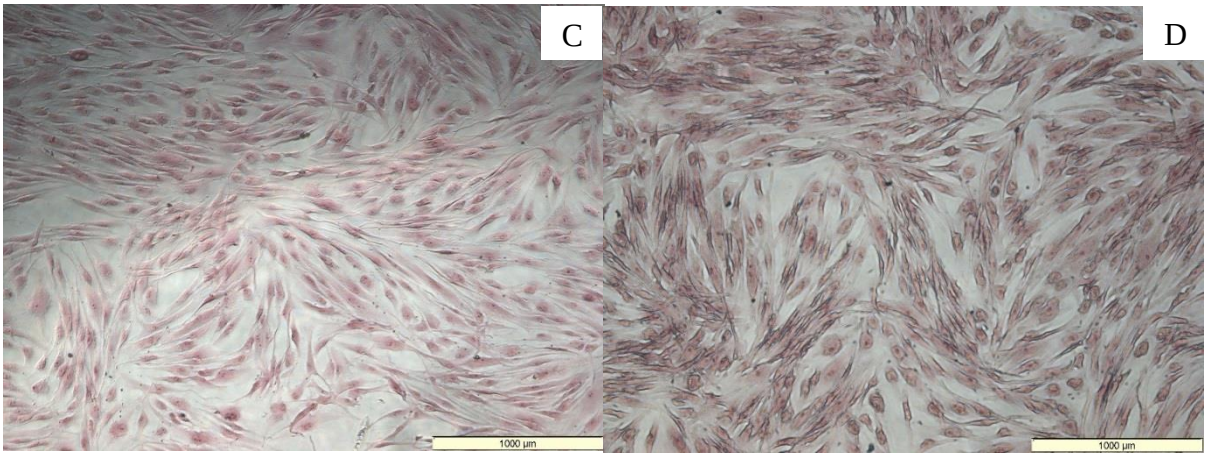

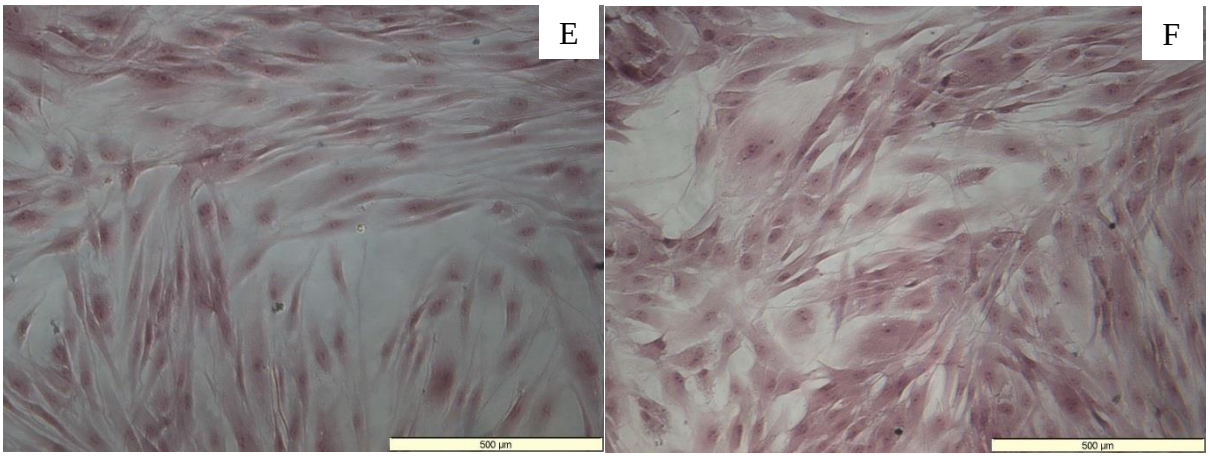

From the images above it is possible to see that NHDF cells have adhered to all of the hydrogel surfaces, including the PGMMA surfaces of the 0- series hydrogel. This could be seen as surprising as previously shown results with 3T3 cells and work in our group had shown that similar PGMMA hydrogels were essentially non cell adhesive with the same cell type. [149] This is possibly due to the partially dried hydrogels presenting a better surface for cells to initially encounter and enabling a better profile for the deposition of proteins onto which the cells can adhere. As with the cell number data calculated using the Alamar blue assay, it is not possible to determine visually whether the cells show a preference for a particular hydrogel and relying on manually counting cells imaged on the surfaces would lead to inaccuracies due to the tendencies of the cells to lift from the hydrogels or otherwise be washed off during the processing steps required to stain them, as has been discussed previously. This is highlighted in the apparently few cells observed on hydrogels 25%-2 (Figure 7-8 I&J, Figure 7-9 I&J) for both the NSER and SER groups. The Alamar blue assay recorded relatively high cell numbers on both of these gels. On most of the gels imaged, the cells appeared spread over most of the surface with some clustering in one area. This is likely the spot onto which they were first added as part of the droplet pipetted at the start of the experiments. This effect is highlighted in the following figures (Figure 7-11 Figure 7-12) which are composite images of SER 1%-1 and 0-1 made from recreations of the images shown above and from two other microscope images taken at the same time. These two images highlight that although the fibroblasts have adhered to the surfaces, they have not spread across the entire hydrogel surface available. Perhaps, given enough culture time, they would spread and proliferate over the entire surface.

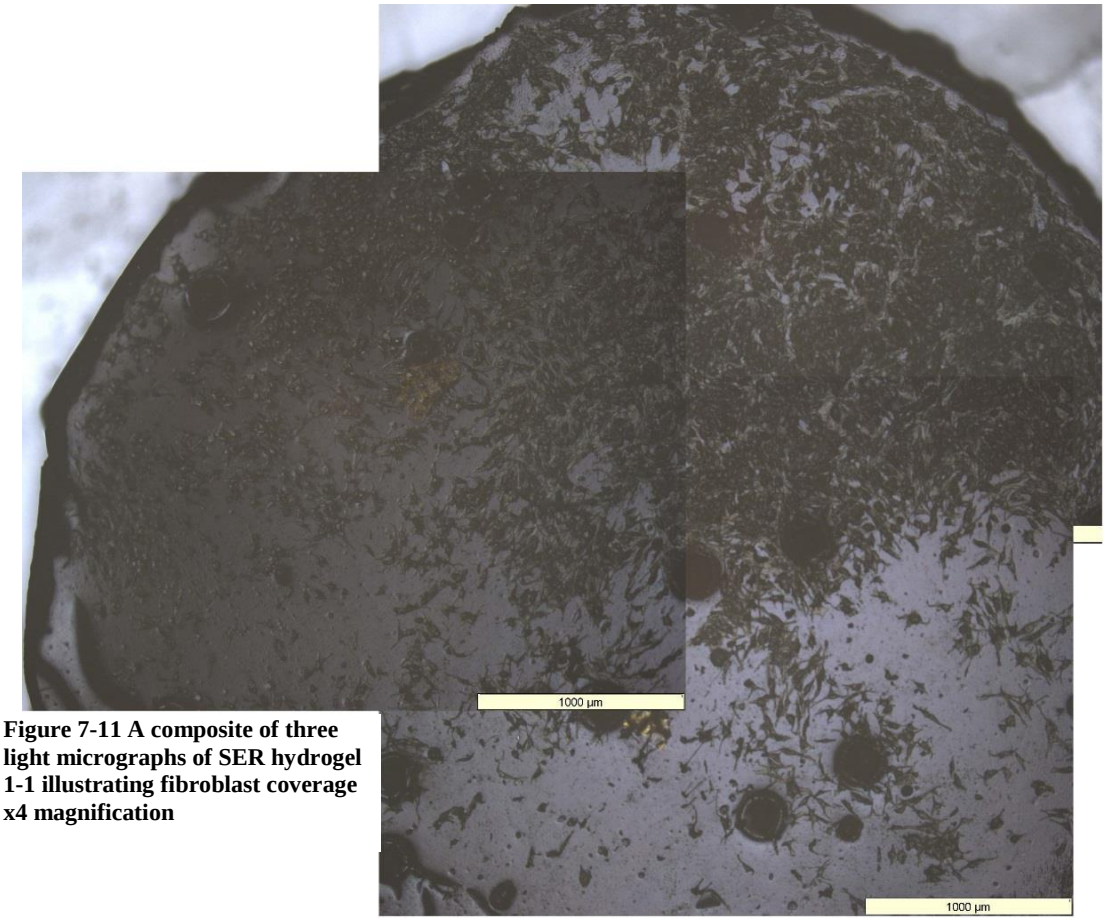

Figure 7-11 A composite of three light micrographs of SER hydrogel 1-1 illustrating fibroblast coverage x4 magnification

Figure 7-12 A composite of three light micrographs of SER hydrogel 1-1 illustrating fibroblast coverage x4 magnification

Many of the images presented above show that where the NHDF cells are present in higher densities, they appear to be growing in confluence with one another which is an indicator of the cells acceptance of the surface on which they are adhered. Indeed the images above that show individual cells or cells in lower densities, are flattened looking and have spread out projections onto the surface which enables them to grip onto the surface and is a key visual indicator of adherence. Examples of this can be seen in the images for NSER hydrogel images of 50-1 & 1-2 (Figure 7-8 I&K) SER hydrogels 50-1, 25-3 (Figures 7-9 L & P) and particularly the 0 gels from both sets.

The TCP controls show similar numbers of cells adhered to the base of 96 well plate wells but these cells appear to be less densely packed than for the hydrogels shown above. This is likely due to the fibroblasts in the controls enjoying slightly longer adherence times. The cells which were transported on to the hydrogels were contained in a small drop of media, this drop was then absorbed into the hydrogel matrix which aided greatly in the cells' over all adherence. It may also have meant that as the cells fell under gravity to the surface of the gel, the volume of available media was decreasing so they had to attach where they landed. For the cells in the controls, this small drop was not constrained and the cells would have been free to adhere to a surface then migrate to a new location if they required. When the remainder of the media required for the experiment was added after an hour, any non-adhered cells would have been washed from the surface of the hydrogel, perhaps to fall on another part of the gel or on the base of the well but the observed cell densities which are higher in some areas of the hydrogels than others suggest that once this new media was added, the cells were already established and were neither washed off or felt the need to migrate significant distances.

The cells visible in the TCP controls (Figures 7-10 A&F) also show much better staining than those seen on the hydrogels. The red colouration is stained collagen in the fibroblasts' cytoplasm and the darker circles are the cell nuclei. Much of this colouration is not seen on the hydrogel samples due to the hydrogels themselves absorbing much of the colour from the staining solutions. The gels themselves were then stained a dark colour, which appears blueish under the microscope. This due to the Giemsa and PicoSirius red stains used. This can make initial identification of cells difficult when looking down the microscope but the cells themselves have absorbed enough stain to be seen in contrast to the hydrogel's darkened backgrounds. The stain in the gels can be removed with exhaustive washing but the repeated handing of the gels or the turbulence caused by the washing steps can run the risk of breaking up the hydrogels as they are rather fragile when wet, or washing any adhered cells from the surface of the gels. The hardest gels to image were the 50% 3 hydrogels which, before staining were the most opaque. These gels had the highest concentration of the largest particles and when the gels had absorbed the stains, made for particularly dark looking images. The cells present on these gels, however, appeared to reflect some light slightly which made them easier to identify.

The large dark circles and black lines seen in some of the images above for example hydrogels NSER 50-1 (Figure 7-8**Error! Reference source not found.** A) and SER 25-1 (Figure 7-9 C) are features left by air bubbles and cracks in the hydrogels. The circular holes are caused when air bubbles are formed during the curing process of the hydrogels and the cracks form as part of the hydrogel sheets dry or are moved. Both of these features are random and unavoidable despite steps taken to reduce their incidence. These features however, appear to have little impact on the NHDF cells interaction with the hydrogels apart from representing a physical barrier. In some cases, highlighted with a red box in Figures 7-8

B&K, 7-9 B&C (representing hydrogels NSER 50-1, 1-2 and SER 50-1, 25-1) cells can be seen bridging these small gaps. This shows that the cells are moving around their environment and growing and proliferating on the surfaces.

7.4 Conclusion

In this chapter, it has been shown that all of the hydrogels produced previously are potentially suitable biomaterials for adherent cells to grow on their surfaces. They are non-cytotoxic to human fibroblast cells on contact and the cells themselves appear able to survive and proliferate on the surface of the gels for at least 48 hours. At the end of 48 hours, all of the cells were still viable, as measured using the Alamar blue assay.

It was not possible to gain a statistically significant understanding of which, if any of the hydrogels were a better surface for cell adhesion and growth, in part due to the assay used. Future experiments could look to using different assays such as CyQuant or PicoGreen which measure DNA content of the cells. These assays are independent of the measurement of metabolic activity of the cells and give direct correlation to the proliferative ability of the cells. The Alamar blue assay relies on the metabolism of a dye molecule, which changes colour. The metabolism of the cells is not a guaranteed constant across the lifetime of the cells or even the length of the experiment for example as a response to the stress of simply moving the cells.

Work in this chapter also showed that direct imaging of adhered cells on the hydrogels was possible using an upright microscope with reflected light. A number of potential pitfalls were discovered and made known such as the tendency of the hydrogels to curl under drying or heating conditions caused by the microscopy. Better images could be obtained by using phase contrast on the microscope, or by using a different microscope set up such as

confocal microscopy which would enable better resolution and an understanding of the interaction between the cells and the three dimensional structure of the hydrogels.

8 Culturing THP-1 macrophage-like cells on hydrogel surfaces

8.1 Introduction

8.1.1 THP-1 cells

THP-1 cells were established in 1980 by Tsuchiya and colleagues from the blood of a young boy with monocytic leukaemia.[156] The cells were found to be very similar to primary monocyte cells and were able to undergo differentiation to become a macrophage like cell.[157] When the cells are treated with phorbol-12-myristate-13-acetate (PMA), a phorbal ester, first isolated from plants, they differentiate to a macrophage like phenotype with many similarities in appearance, markers and function to primary macrophages. This has made them a very valuable tool for studying macrophage responses and interactions. [158]

THP-1 cells are a suspension culture cell type, meaning that they float freely in the cell media and are non-adherent. This is due to the cells being monocyte-derived and so in their natural environment, the blood, they are freely floating. THP-1 cells will eventually settle to the bottom of the culture flask but do not adhere. They are easily resuspended with only slight agitation. This culture method differs to static culture, which is more common, seen in a variety of cell types including fibroblasts and keratinocytes. Cells in suspension culture, in some ways are easier to maintain than static culture, particularly when passaging or splitting cells into new cultures, they can be directly removed from the flask and split without the need to use EDTA which stresses and can damage cells over subsequent passages. This means that these cells can reach quite high passage numbers (approximately p25) and remain viable. One key disadvantage of suspension culture is encountered when the cultures require fresh media. In static culture, such as is used with NHDF cells, the used media is simply aspirated away and fresh media is added directly. Suspension culture

requires the cells to be centrifuged into a pellet and resuspended into fresh media, which can cause stress to the cells. THP-1 cells grow best when cultured in a reasonably small environment and in densities between $1x10^5$ and $1x10^6$ cells/ml. This is achieved by supporting the cell culture flask on an angle allowing the cells to grow in a corner of the flask, close to one another. If cultured at densities below $1x10^5$ cells/ml they will not grow very well and are very slow to propagate, whereas if grown about $1x10^6$ cells/ml THP-1 cells will start to senesce and die off.

When viewed under the microscope, undifferentiated THP-1 cells in culture appear round with a large nucleus taking up most of the cell. The following image shows non-adherent, undifferentiated THP-1 cells which resemble monocyte cells in human blood. (Figure 8-1**Error! Reference source not found.**)

When treated with PMA, the cells become more polarised and become to adhere to surfaces.

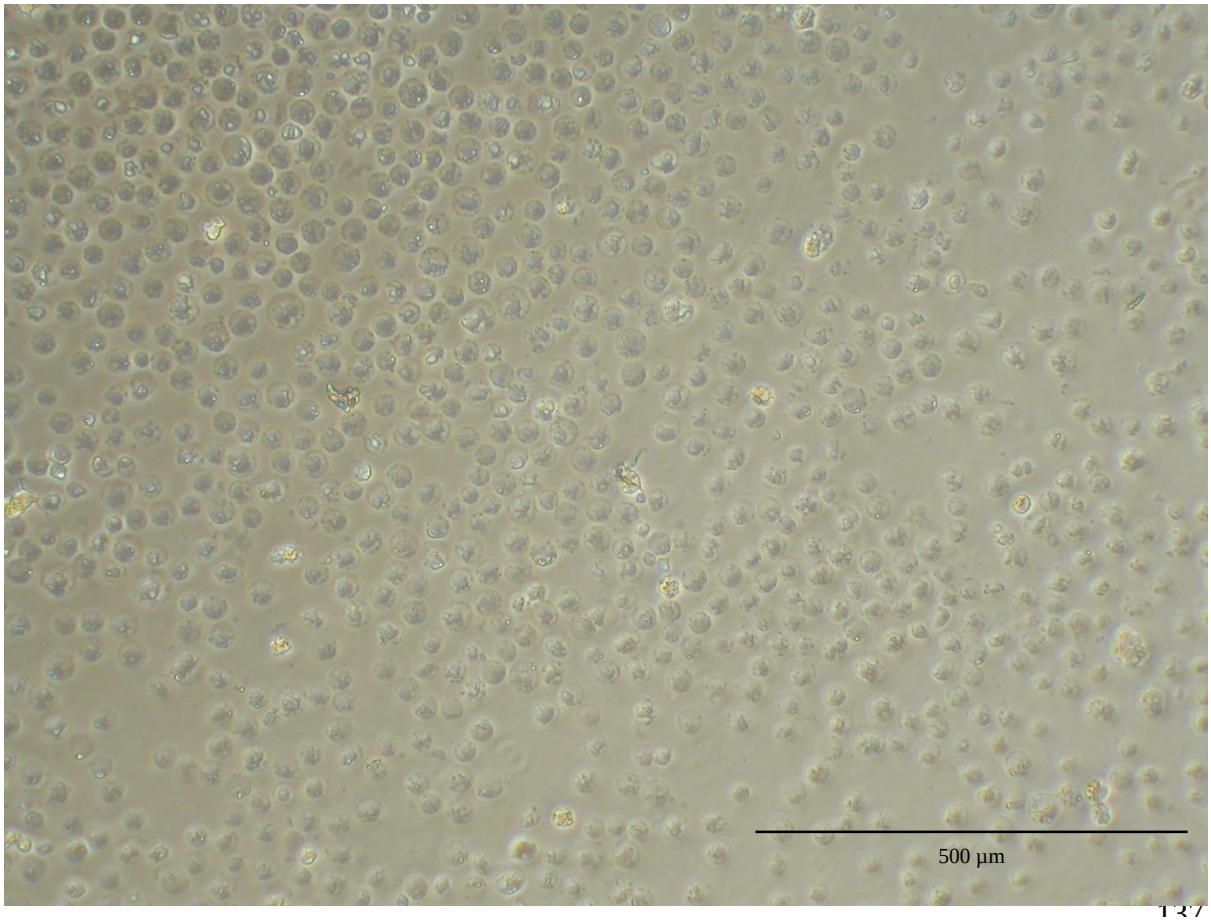

Figure 8-1 A light micrograph of THP-1 cells in normal suspension culture

8.1.2 Culturing THP-1 cells on hydrogels

The first aspect of this experiment is to try to make a hydrogel surface for THP-1 cells to grow on, then to assess whether the THP-1 cells have become activated by the hydrogel and express this by the release of inflammatory cytokines. The cytokines will be collected from culture media extracts and the presence, and levels of the cytokines TNFα and IL-6 will be examined over the course of an experiment using the highly sensitive enzyme-linked immunosorbent assay (ELISA). It has been shown previously that THP-1 cells are capable of expressing these cytokines [159]

8.2 Experimental

8.2.1 THP-1 cell culture

All cell procedures and media manipulations were carried out using aseptic techniques in a type II flow cabinet

8.2.1.1 Preparation of THP-1 cell culture media

RPMI 1640 media and 2-mercaptoethanol, foetal bovine serum (FBS) and L-glutamine (LG) were obtained from Sigma

Heat inactivated FBS (10%) was added to stock solution bottle and mixed well. 10µl 2-mercaptoethanol was added to 1ml stock solution and mixed well using a Vortex Genie 2 instrument. 10µl of this solution was added to 10 ml of stock solution and filter sterilised back into the stock solution bottle, using Acrodisc syringe filters (0.2µm pore size). Stock solution was then sealed and refrigerated, to be used within one month. Remaining solutions and extractions were discarded.

8.2.1.2 Preparation of THP-1 differentiating solutions

Phorbol-12-myristate-13-acetate (PMA), lipopolysaccharide (LPS) were obtained from Sigma. PMA was dissolved in DMSO to give a stock solution of concentration 20 µM, LPS was obtained as a solid and was diluted as required, in cell culture media to give a concentration of 500 ng/ml. PMA was diluted further in cell culture media make 100 nM solutions of PMA.

8.2.1.3 Culturing THP-1 cells

THP-1 human monocyte carcinoma cells were kindly provided by Sam Bullers & Prof. Jenny Southgate (Jack Birch Unit, Dept. of biology, University of York) and cultured in the RPMI media described above. They were grown in suspension culture, upright, or tilted on an angle, at an initial concentration of $1x10^5$ cells/ml in 100ml capacity Nunc brand flasks, obtained from Fisher Scientific. Cells were incubated at 37°C, 5% CO_2. Cell stocks were split or passaged when total concentration reached around $9x10^5$ - $1x10^6$ cells/ml. Cell stocks were typically 25 or 50 ml total volume. Cells were counted using a haemocytometer.

8.2.2 Compatibility testing of hydrogels for THP-1 cells

Initial experiments were undertaken to see whether the hydrogels produced previously would be a suitable material for THP-1 culture and experimentation. A THP-1 adherence experiment was conducted and the cells and gels were stained and mounted in paraffin, following commonly used histological protocols which are described below.

8.2.2.1 Preparation of hydrogels for cell culturing

50-1, 1-1 and 0 hydrogels were chosen for initial testing. When required, the hydrogels were allowed to air dry slightly and were cut into discs of sizes approximately 14mm in diameter. Discs were immersed in the cell culture media described above in sterile sample tubes. The discs equilibrated for 30 minutes, at this point, the media was then removed and replaced

with fresh media. This was repeated for 4 hours, washing with fresh media every 30 minutes. The disks were equilibrated to wash out any residual ethanol that they may have absorbed from their washing and storage, which would kill cells cultured on the gel surfaces. The gels took on the pink colour of the culture media signifying that they had taken up the media.

The media equilibrated hydrogel disks were placed in 24 well plates (Corning® CellBIND® cell culture plates) obtained from Sigma.

In initial experiments, THP-1 cells were seeded directly onto the hydrogels surface at a concentration of $2.5x10^5$ cell/ml and were treated with 100 nm solutions of the differentiating mixtures. LPS was mixed with a separate PMA solution to act as a positive control against PMA on its own. Cell culture media was used as a negative control against the differentiating solutions. Bare tissue culture plastic (TCP) was used as a positive control against the hydrogels.

500µl of cell solution was added to each well and 500µl differentiating solution or cell culture media was then added, giving a total volume of 1ml. The well plate was covered and placed in an incubator for 48 hours.

8.2.2.2 Fixing cells

At the end of the experiment the cell media was aspirated from all the wells and 500 µl Phosphate buffer solution (PBS) was added, each well was mixed well and the PBS was again aspirated off. 1 ml of 10% formalin was then added to each well and the plate was covered and left for 24 hours at room temperature. After 24 hours the formalin was removed and the wells were topped up with 70% ethanol. The wells were sealed and stored in a refrigerator.

8.2.2.3 Staining and imaging cells

Following fixation ethanol was removed from the wells and haematoxylin (obtained from Sigma) was added to each well and left for approximately two minutes and rinsed well with tap water. Stained cells were imaged with a dissection microscope.

8.2.2.4 Embedding, sectioning and mounting hydrogel samples

The resolution available on the dissection microscope was insufficient to resolve any cellular details so the hydrogels were processed for histological sectioning.

Following fixation the cells were placed in 70% ethanol for 2 hours and then cut in half. This was so they had a flat surface on which to stand. Each half was then placed in a cassette and incubated in fresh 100% ethanol for 2 hours at room temperature. They were then washed with fresh 100% ethanol for 10 minutes. Cassettes were then placed in a warmed polyester wax, ethanol mixture (1:1, warmed at 37° overnight), for 1 hour. Following this, the cassettes were placed in two warmed beakers of a decreasing ratio of ethanol to wax for 30 and 15 minutes respectively and finally in a warmed beaker of pure wax for 15 minutes. The cassettes finally emptied of wax and a small amount of fresh wax was added to help secure the hydrogel halves in the correct orientation (flat side down). The cassettes were placed on a cold stone to speed up setting and then topped up with more fresh wax. A lid was placed on top and they were allowed to set at room temperature for 24 hours.

The wax blocks were sectioned with a microtome instrument using a diamond tipped 7µm blade and the sections were placed on glass slides for imaging, staining and dewaxing.

8.2.3 Culturing and fluorescent imaging of THP-1 cells on hydrogels

In order to determine the correct concentration of phalloidin dye to be used to view cytoskeletal structures, titrations of various concentrations were performed using a Cytospin instrument.

8.2.3.1 Materials

THP-1 cells in culture media were used in 150µl aliquots. The Cytospin divider cassette containing glass slides were assembled according to instructions. Texas Red-X Phalloidin was obtained from Invitrogen and was subsequently diluted with lab grade PBS. Cells were fixed with formalin and permeabilised with Triton-X solution as described above.

Following initial experimentation with THP-1 and 3T3 cells described previously, the following procedure was developed to culture and fluorescently image THP-1 cells on hydrogels.

50% and 1% hydrogels of all three latex formulations and PGMMA hydrogels prepared previously. These gels were chosen to represent the extremes in concentration of particles in the gels. The hydrogels were equilibrated in media and placed into wells of a 24 well plate. Steel seeding rings were placed into the individual wells, on top of the gels. TCP was used as a control. The hydrogel set up was duplicated so one set could be treated with PMA and one with just cell culture media to test whether the surface of the hydrogel surfaces themselves encouraged differentiation and activation of the THP-1 cells.

8.2.3.2 Cell culture

THP-1 cells were seeded at a density of $5x10^5$ cells/ml and a volume of 200µl into each seeding ring in each well. The rings were either topped up with 200µl of 100nM PMA

treatment or 200µl culture media. The plate was then covered and incubated for 48 hours. At the end of 48 hours, the cells were fixed with formalin as before.

8.2.3.3 Epifluorescent imaging of THP-1 cells on hydrogel surface

The protocol for staining the THP-1 cells was the same as that for the 3T3 cells described previously. The protocol is repeated below.

Following fixation the gels in the wells were treated with a 0.1% Triton-X solution in PBS. The Triton-X solution was used to permeabilise the cell membranes allowing Hoechst to enter and stain the nuclei. The wells were covered and placed on a rocker plate for 15 minutes. After 15 minutes, the solution was removed and the wells were treated with a 1 in 10000 (v/v) solution of Hoechst stain in PBS and placed on a rocker for 10 minutes. Following this the solution was removed and the gels were washed with PBS and again placed for 3x5 minutes on the rocker. After washing the gels were removed from the wells and mounted on glass microscope slides, a few drops of an antifade solution and a cover slip was placed on top.

The gels were imaged using a mercury burner lamp in the blue fluorescent channel using an upright microscope. The ImagePro plus software was used to obtain images of cell nuclei on the surface of the hydrogel. The cells were imaged using a non-oil lens.

8.2.3.4 Assessing required phalloidin concentration using the Cytospinning Method

In order to gain images of the shape of the cells adhered to the hydrogels, a fluorescent cytoskeletal dye was selected. In order to determine the correct concentration of phalloidin to be used a titration was done against THP-1 cells. The Cytospin 4 instrument (Thermo Scientific) was used to form a thin layer of THP-1 cells on a glass slide.

150µl aliquots of cell solution were added to the dividing lanes in Cytospin cassettes, four of these cassettes, each containing three aliquots were placed in the Cytospin centrifuge device and run at 1300 RPM for 4 minutes. After three minutes the cassettes were dismantled, excess liquid was removed and the cells now affixed to the surface of the glass slide were fixed using formalin (5ml per well) for 10 minutes before being washed well with PBS. The slides were dried well and each cell containing lane was bordered with hydrophobic ink lines drawn using a PAP pen. Phalloidin was titrated into concentrations of 1:25, 1:50, 1:100, 1:250, 1:500, 1:1000, and 1:10000 v/v in PBS respectively. These concentrations of phalloidin were added to the Hoechst solution during the permeabilisation stage described in the previous section and the cells were treated as described above. The slides were imaged using a mercury burner lamp in the blue fluorescent channel using an upright microscope. The ImagePro plus software was used to obtain images of cell nuclei on the slides.

8.2.3.5 Epifluorescent imaging of cytoskeletal features of THP-1 cells on hydrogels.

Following the determination of the appropriate phalloidin concentration (1in 500 v/v in PBS), the cell culturing experiment was repeated. Following fixation of the cells, the phalloidin solution was added with the Triton-X and PBS solution and the remainder of the fluorescent staining protocol was followed, as described in the previous section.

8.2.4 THP-1 adherence on hydrogels

Epifluorescence imaging was found to be unsuitable for these hydrogel materials so the protocol was altered as follows. At the end of the experiment, an assessment of the cells'

activation and or their expression of the inflammatory cytokines TNF-α, IL1-β and IL-6 will be conducted by use of ELISA on extracts from the culture media.

8.2.4.1 Materials

Hydrogels 50-, 25-&1- from all three formulations were used in this experiment, as well as the original bare PGMMA hydrogel as a control. A further material control was used, discs cut from the PET sheet used to cover the glass sheets used in the polymerisation, described in previous chapters was also used. This PET sheet was cut, washed in ethanol, dried well and added to the wells used for this experiment. The hydrogels were cut into smaller sizes of approx. 4.5 ml diameter and equilibrated in culture media as before.

Differentiating media was produced for the cells in 500 ml stock bottles as described previously. Solutions used were PMA (200 nM), PMA & LPS (200 nmol & 500 ng/ml respectively) and normal cell culture media was used as a control.

Alamar blue solution was made up as 1mg/ml resazurin (Sigma) in sterile PBS and was stored in a sealed sample tube, in the refrigerator, in the dark. 10% formalin solution was obtained from Sigma and used without further dilution. Mini ELISA kits containing antibodies specific for TNF-α and IL-6 were obtained from Peprotech.

8.2.4.2 Method

The hydrogels were cut into approx. 4.5 mm diameter discs using a borer and blotted dry using sterile filter paper. The gels were then placed into wells of a 48 well plate (ProCell Falcon plates, 48 well, non TC treated), in triplicate, one plate for each time point (0, 4, 8, 12, 24 hours). This was one set of plates. Each differentiating mixture, described in the

previous section was given its own set of plates for a total of 15 plates. The sets were labelled PMA, LPS and MED.

The gels were loosely covered and allowed to air dry in the laminar flow hood for 1 hour.

When the THP-1 cells were ready to be seeded, they were removed from their culture flasks, centrifuged to remove old media and fresh media was added. The cells were counted using a haemocytometer and their viability was assessed using the Trypan blue exclusion assay. The cell concentration was adjusted to 5 $x10^5$ cells/ml with fresh media and the cells were concentrated and seeded at a total cell number of $2.5x10^4$ cells, in 25 µl on each gel. This small volume of more concentrated cells was based on seeding 50 µl of $5x10^5$ cells/ml but from preliminary experiments, it was found that 50 µl was slightly too much liquid and it didn't all absorb into the gel resulting in some of the cells likely being washed off the gels when fresh media was added. The cell solution was allowed to soak into the gels for an hour before 500 µl of fresh media, containing the relevant differentiating solution, was added to each well and the well plates were covered and placed in the incubator for 48 hours. The same volume of cells was also seeded on to tissue culture plastic (TCP) and topped up with 300 µl media.

After 40 hours had been completed, the plates used for time point T_0 (one for each of PMA, LPS & MED) were removed from the incubator, 50.3 µl of Alamar blue solution was added at this point, mixed gently and the plates were returned to the incubator.

After a further 8 hours, all of the plates were removed from the incubator, the media for the plates used for T_0 was aspirated off and stored in Ependorf tubes, in the freezer for ELISA. 100 µl of media was transferred to a fresh 96 well plate for Alamar blue analysis. The hydrogels and cells at T_0 were then fixed with 10% formalin solution for one hour then formalin was removed and PBS was added to the wells. The media in the remaining plates

was removed and discarded and fresh media of the corresponding type was then added (PMA, LPS, MED) and the plates were returned to the incubator. This time point was recorded as T_0, following this, at time points corresponding to hours elapsed from T_0, (T_4, T_8, T_{12}, T_{24}) one plate for each of PMA, LPS and MED was removed, media extracted and stored in Ependorf tubes, 100 µl of media was transferred to 96 well plates for Alamar blue analysis using a plate reader (BioTech ELx800). When the media had been removed, the cells were fixed with formalin, as before for 1 hour then wells were topped up with PBS. Cells grown at the same densities on tissue culture plastic were used as controls at the same time points. Hydrogels were stored in PBS and imaged using an Olympus upright microscope using reflected light.

8.2.4.3 Alamar blue analysis

The media extracts were analysed with the Alamar blue assay against cells seeded at densities of $6x10^5$, $5x10^5$, $2\ x10^5$, $1\ x10^5$, $5\ x10^4$, $1\ x10^4$, $5\ x10^3$ and media. These cells were seeded on to tissue culture plastic and removed at the same time points as the hydrogels. The plates were read using a BioTech ELx800 plate reader.

8.2.4.4 Imaging of cells on hydrogels

The hydrogels were imaged using an Olympus upright microscope. The cells were not stained due to time constraints and were imaged directly on the hydrogels.

8.2.4.5 Enzyme-Linked Immunosorbent Assay of cytokines

The cytokine contents of media extracts were analysed using mini enzyme-linked immunosorbent assay (ELISA) development kits according to the protocols provided. ELISA microplates were prepared with capture antibody (100µl per well). The wells were sealed and incubated at room temperature overnight. The wells were then aspirated and washed

4x using wash buffer (0.005% Tween-20 in PBS) and blotted on paper towels. 300 µl block buffer (1% BSA in PBS) was then added to each well. This was incubated for at least 1 hour. A standard curve was generated from provided standards, concentrations ranged from 2 ng to zero. 100µl of each sample and standard were added to wells and incubated at room temperature for 2 hours. The wells were washed 4x and detection antibody was added (100 µl per well). The wells were sealed and incubated for 2 hours. Following this, the wells were washed 4x and an Avidin-Horseradish peroxidase (HRP) conjugate was added (1:2000 dilution, total volume 11 ml). 100µg was added to each well and incubated at room temperature for 30 minutes. The wells were 4x washed and ABTS substrate (100 µg per well) was added to indicate colour change. The plates were read using a plate reader at 405 nm with correction set at 650 nm.

8.3 Results and discussion

8.3.1 Compatibility testing of hydrogels and THP-1 cells

THP-1 cells were cultured on the surface of the hydrogels for 48 hours and treated with PMA, PMA & LPS and media.

LPS is a lipopolysaccharide, usually found on the surface of bacterial capsules, they are highly conserved in bacteria in nature and are one of the immune system's chief means of recognising bacterial infection. Therefore when encountered by immune cells, the cells become activated and seek to quickly remove the source of the LPS, in macrophages, this is represented by an inflammatory response.

TCP and cell culture media were used as positive and negative controls. At the end of the experiment, the cells and hydrogels were fixed with formalin. This kills the cells, stopping all cellular metabolism and activity, freezing them at that point. It also cross links the cells to the hydrogel. Any cells that are dead are therefore not adhered and at the point of fixation are not cross-linked to the surface. They are subsequently washed off the surface.

Following fixation the cells were stained with hematoxylin, a common histological stain used to highlight cellular components. Due to the opacity of the hydrogels, the usual microscope imaging technique, as would be used on cells cultured on TCP, was ineffective as the cells were unable to be seen through the surface of the gel, using the usual inverted microscope. Therefore the gels were then imaged using a dissection microscope. Unfortunately the resolution available was insufficient to resolve any cellular detail so the gels were processed for histological sectioning. Following the mounting process described above the gels were cut into thin sections using a microtome. These thin sections were hoped to contain many slices of the hydrogel and the cells on them. This is a common technique used often in tissue engineering, particularly when analysing how cells have grown on a biomaterial. When the

waxed samples were sectioned the gels splintered or shattered, leaving small voids where they hydrogels had been in the wax. This method of analysis was deemed unsuitable for these materials and was discontinued. These histological shortcomings suggested that direct imaging was preferable, and so epifluorecence was investigated as an alternative. This method of visual analysis enables direct, non-destructive imaging of the cells on the surface of the hydrogels. The hydrogel samples used in this experiment were destroyed and the experiment was repeated with alterations to the method.

The following images show THP-1 cells in their ordinary state and the TCP controls. The first image Figure 8-2 shows the cells in their ordinary state in suspension culture, in media without any treatment.

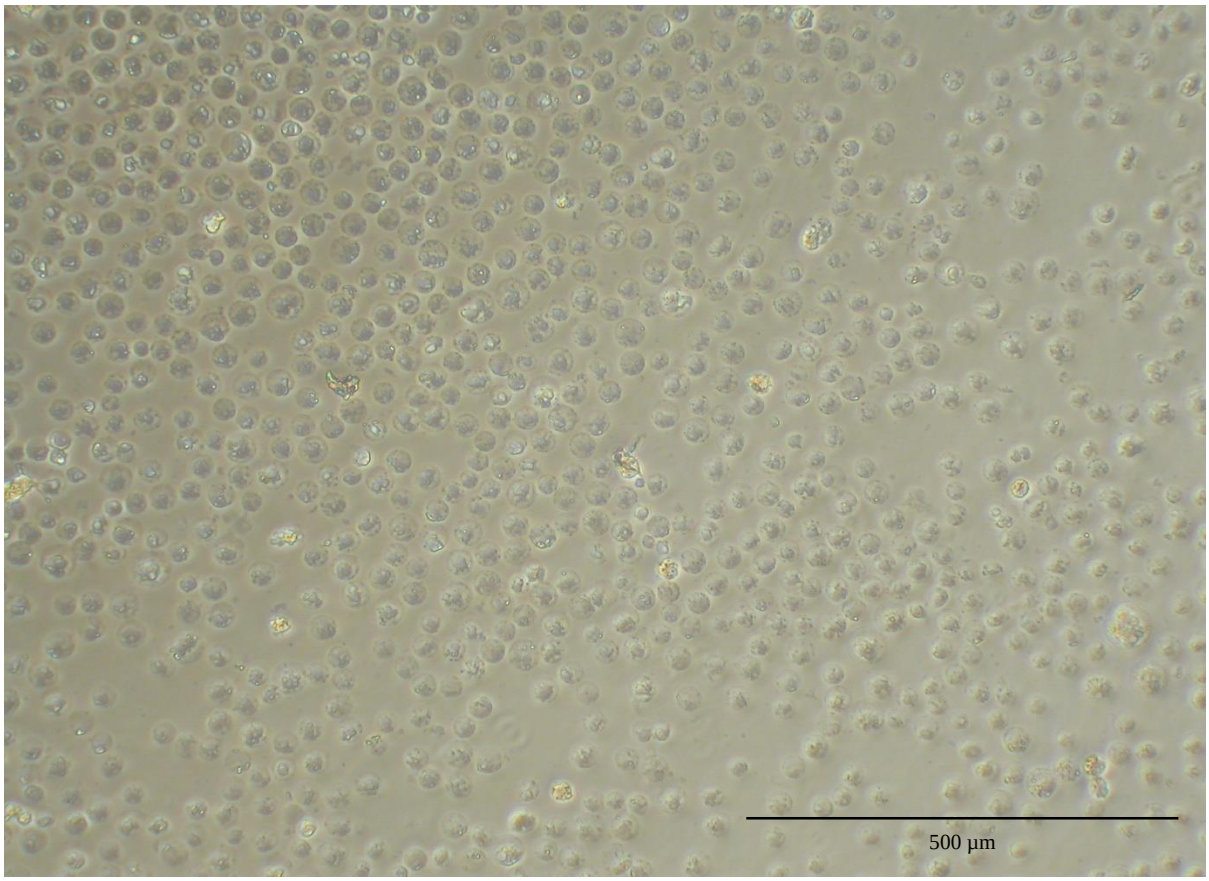

Figure 8-2 A light micrograph of THP-1 cells in ordinary suspension culture

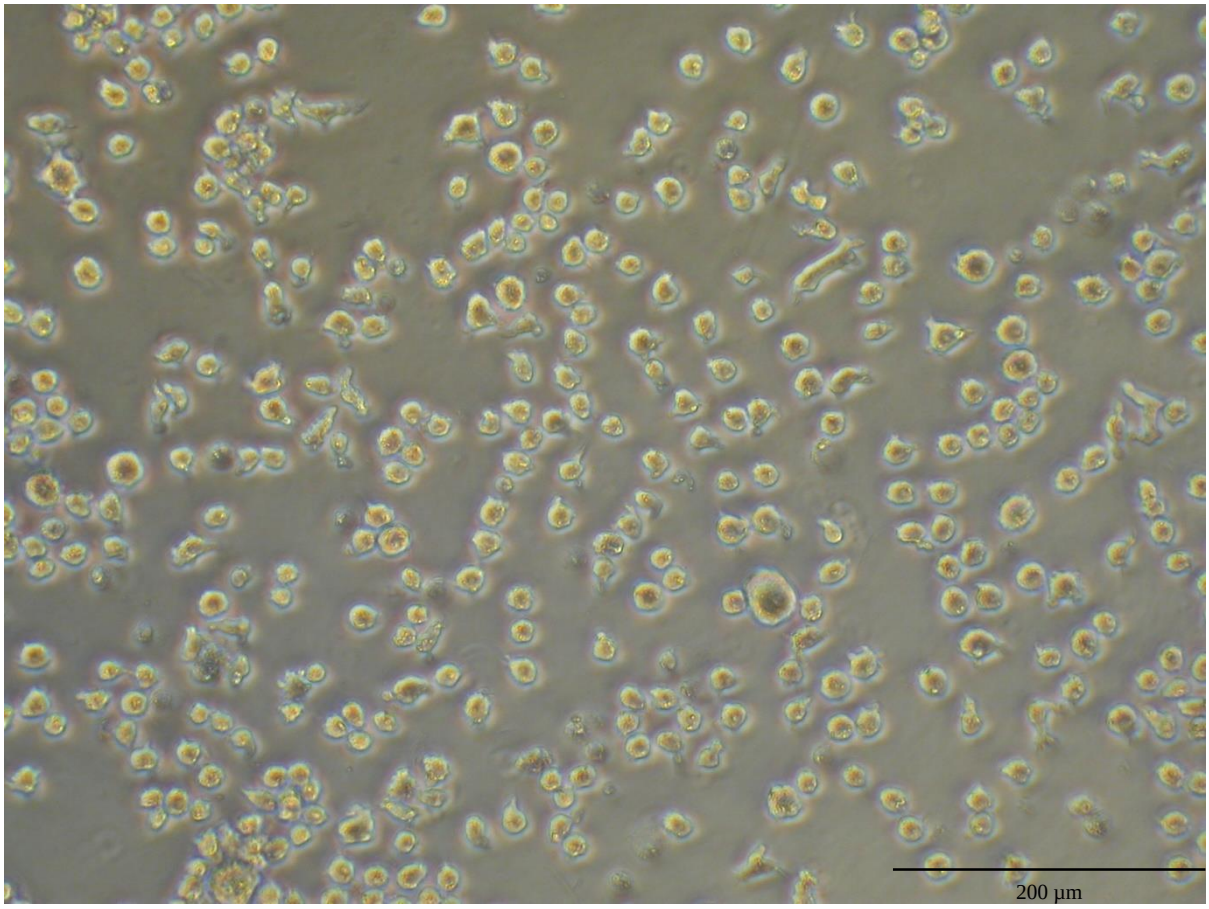

Figure 8-3 Light micrograph of THP-1 cells on TCP treated with PMA

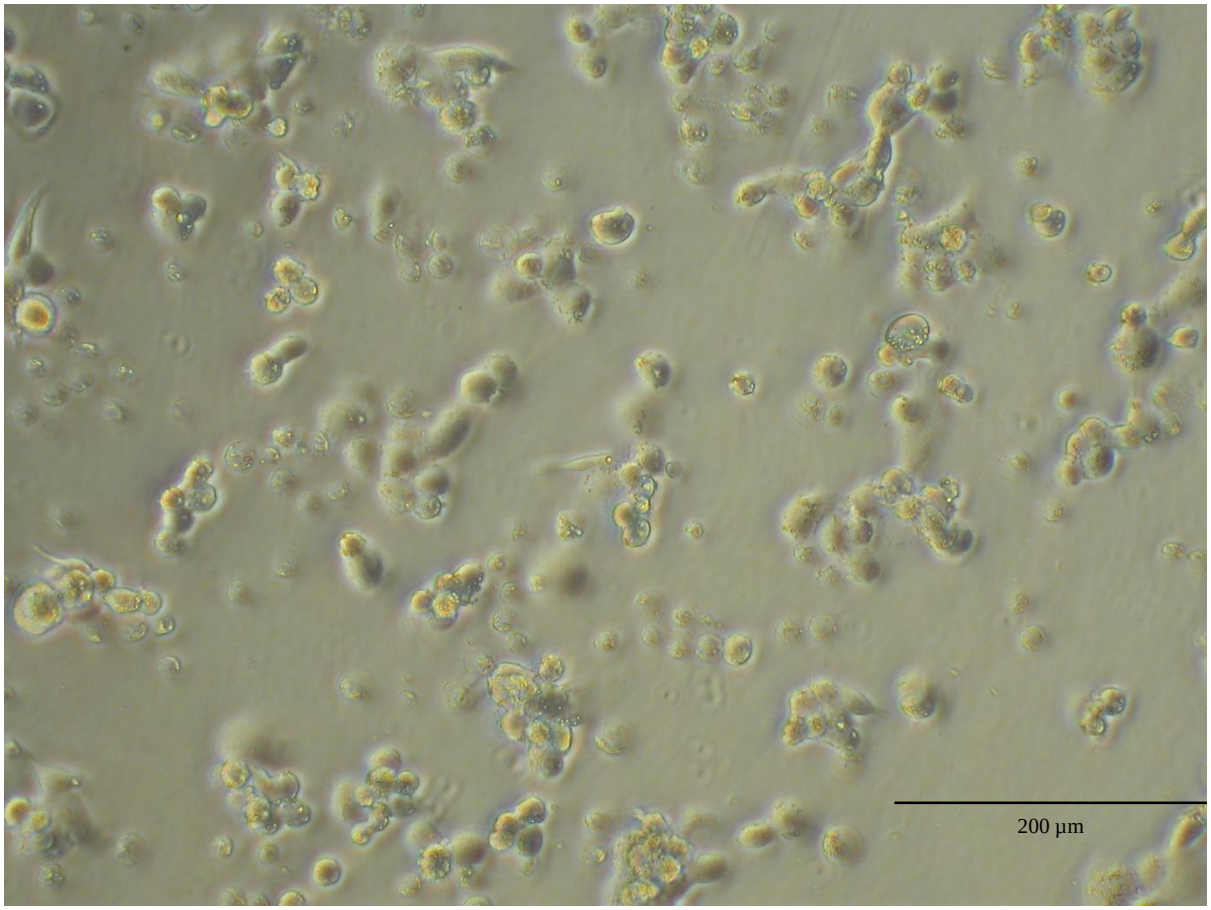

Figure 8-4 A light micrograph of THP-1 cells on TCP treated with PMA & LPS

Figure 8-3 above, shows THP-1 cells which were treated with PMA. They are more irregularly shaped than cells observed in their normal state in suspension culture. This indicates that the cells have differentiated into a macrophage-like cell and begun to adhere to the surface of the TCP using cytoplasmic projections

Figure 8-4 above shows the THP-1 cells treated with PMA & LPS. The combination of differentiation inducing PMA and the immuno-activating molecule LPS has caused a full differentiation and activation of the macrophage-like phase of these cells. In the blood this would be represented by an inflammatory response. The micrographs show that the cells have become much more irregularly shaped with longer projections as they become more activated to inflammatory signals.

8.3.1.1 Staining and imaging cells

Staining with hematoxylin caused the hydrogels to be stained purple, as has been mentioned before but repeated washing removed a good deal of this colouration. When the gels were imaged under the low magnification dissection microscope, it was just possible to make out purple stained dots on the hydrogels which were the stained cells. However due to the resolution available, it was impossible to determine any features of the cells. This was the reason for attempting to embed the gels in paraffin wax.

8.3.1.2 Embedding, sectioning and mounting hydrogel samples.

Following staining with hematoxylin, the hydrogels were split in two. This gave the gels a flat surface, on which to stand whilst they were immersed in paraffin wax which then set around them. The hydrogels, when hydrated, break under the mild force applied by forceps and so are easily bisected with a scalpel. Following the protocol described above, the gels, secured in cassettes, were immersed in solutions of increasing paraffin wax concentration

until they were embedded in pure paraffin. When set around them, the paraffin was cut into 7 μm thick slices using a cryotome with a diamond tipped blade and the slices placed on a microscope slide. When these slices were examined under a microscope, there were holes in the surrounding paraffin where the hydrogel slice had been. This was present in all of the slices examined. The hydrogels had snapped and shattered, leaving nothing to examine using this technique so it was discontinued.

8.3.2 Culturing and fluorescent imaging of THP-1 cells on hydrogels

The culture of THP-1 cells on the hydrogels was repeated using the new procedure described in the experimental section. Steel seeding rings were used to confine the cells and differentiating media into a smaller, definite area. This was adopted to stop the cells spreading and leaking across the whole surface of the hydrogel or spreading to TCP base of the culture well. The TCP is likely to be more favourable for the cells to adhere than the hydrogel surface and were the cells able to reach the TCP it is thought that they would preferentially migrate to and bind to the TCP. The seeding rings were ineffective at stopping the cells and media leaking out of and off of the hydrogels and were not used in further experiments. It appeared that the seeding rings did not form a good seal with the hydrogel possibly from the uneven surface of the hydrogels themselves or from tiny bits of debris trapped under them.

Following 48 hours culture, the cells were fixed and permeabilized and stained, then imaged using the fluorescent microscope. The cells were cultured separately with PMA and without in order to determine whether the surface of the hydrogel had an activating effect on the THP-1 cells The following images (Figure 8-5 &Figure 8-6) show the presence of THP-1 nuclei on the surface of the hydrogels. There is strong background autofluorescence from the embedded PS particles.

The images show that the cells are present the surfaces of the hydrogels but do not give an indication of whether the cells are activated as the Hoechst stain used is a nuclear stain and does not give an indication as to the general morphology of the cells. A cytoskeletal stain would give this indication. The cytoskeletal dye phalloidin, which binds to and fluorescently labels actin filaments in cells was originally a green stain, however the colour of the dye and the features that it highlighted was found to be completely swamped by the natural autofluorescence of the PS nanoparticles embedded in the structure of the hydrogel so Texas red-X phalloidin which operates at a different, less autofluorescence dominated wavelength was chosen for the following experiment.

The following are micrographs of hydrogel surfaces with nuclear stained THP-1 cells present. There seems to be no discernible difference in the adherence of THP-1 cells to the surface of the PGMMA hydrogel, shown below. This could indicates that the surface of the gel itself causes a differentiation from the monocyte-like cell phase to the macrophage-like cell phase enabling adherence to the surface. But it unclear whether the cells have properly adhered to the surface of the gel or are rounded up cells, loosely bound to the surface on fixing.

The above micrographs show that there is no discernible difference between the adherence of the THP-1 cells on the surface of the bare PGMMA hydrogel, with or without treatment with PMA. There are few cells observable and these micrographs are a typical

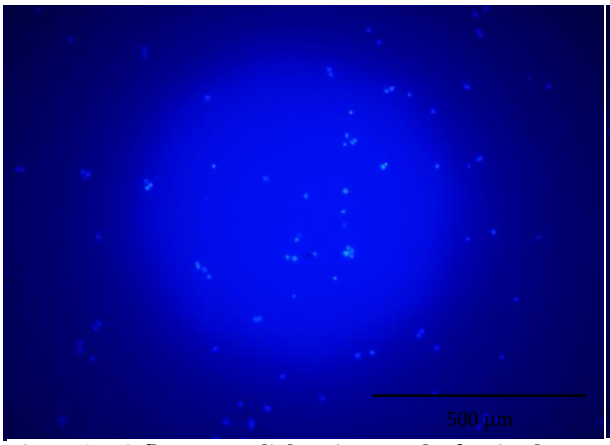

Figure 8-5 A fluorescent light micrograph of stained THP-1 nuclei on hydrogel 0 treated with PMA

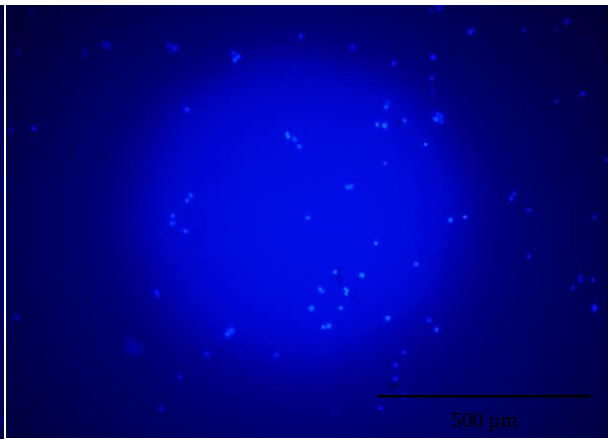

Figure 8-6 A fluorescent light micrograph of stained THP-1 nuclei on hydrogel 0 treated with media

representation of the cellular presence on the surface of the gels. The number of THP-1 cells seen is much lower than the 3T3 cells used previously, which were cultured and imaged under similar conditions. This suggests that the THP1 cells are much less adherent than 3T3 cells, which was expected, but the fact that there are cells present means that it is possible for the cells to adhere to the hydrogel surface.

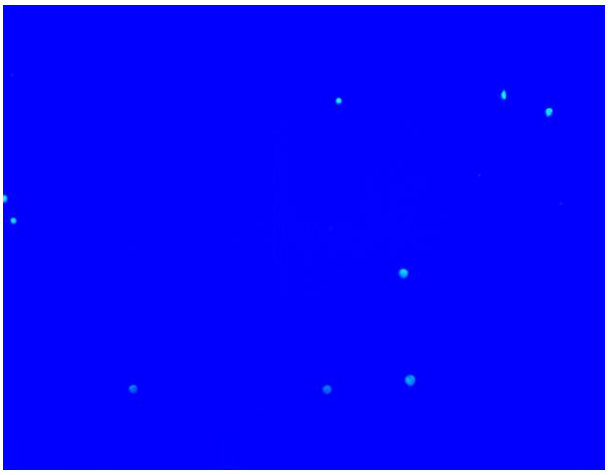

Figure 8-7 A fluorescent light micrograph of stained THP-1 nuclei on hydrogel 50-1 treated with PMA

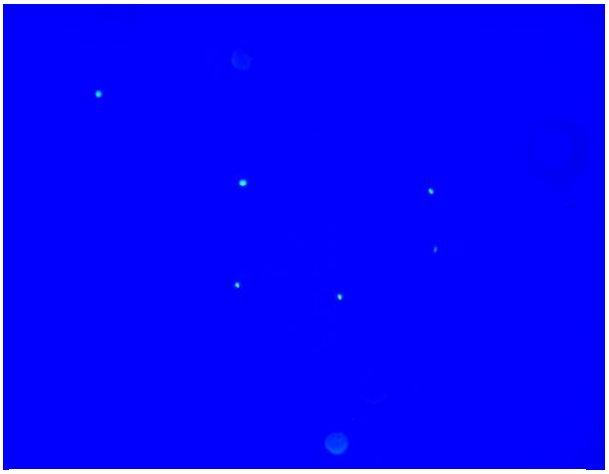

Figure 8-8 A fluorescent light micrograph of stained THP-1 nuclei on hydrogel 50-1 treated with media

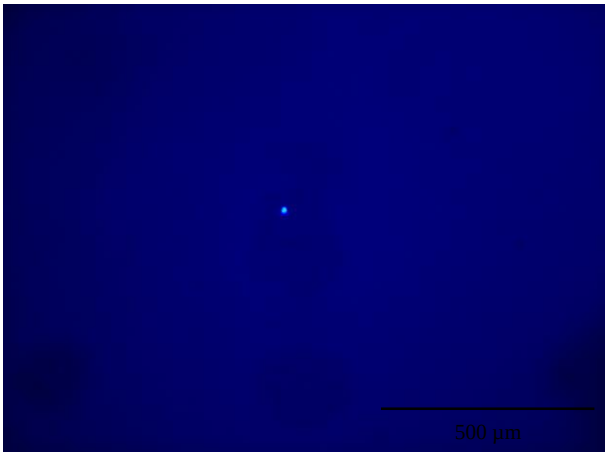

Figure 8-9 A fluorescent light micrograph of stained THP-1 nuclei on hydrogel 1-1 treated with PMA

Very few cells were observed on the 50% and 1% PS hydrogels and those that were, were very sparsely populated across the surface. No cells were observed on the 1% gels treated without PMA. IT is possible that during the processing for fluorescence, the cells were washed off the surface or perhaps the THP-1 cells failed to fully differentiate into an adherent cell type during culture.

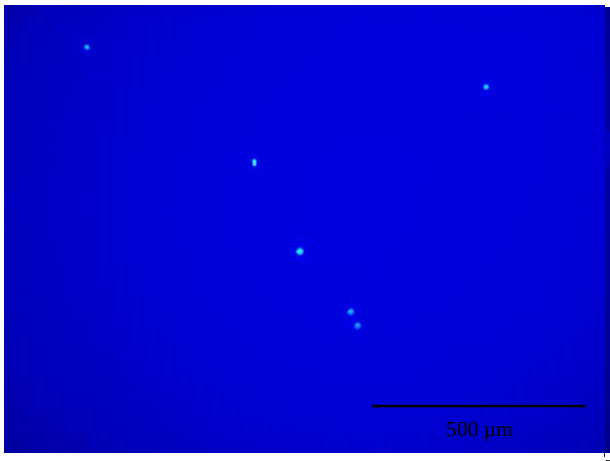

Figure 8-10 A fluorescent light micrograph of stained THP-1 nuclei on hydrogel 50-2 treated with PMA

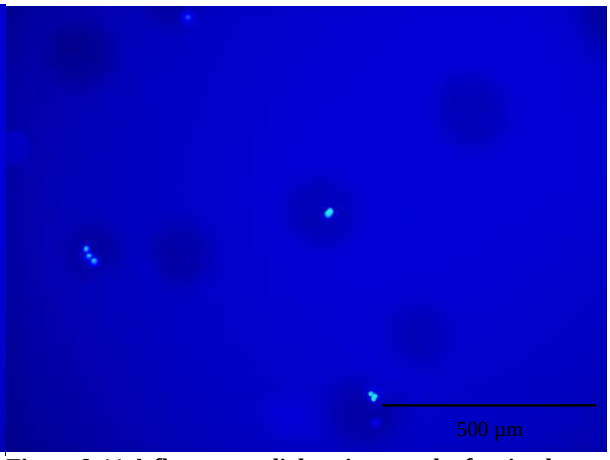

Figure 8-11 A fluorescent light micrograph of stained THP-1 nuclei on hydrogel 50-2 treated with media

Again the above images show very few cells, sparsely populated across the surface of the gel. This could indicate that the make-up of the particles, both individually and as a surface may be having an effect on the adherent properties of the THP-1 cells or that the entire culture batch simply did not respond strongly to the PMA and did not differentiate much. The gel which was not treated with PMA appears to have cells only in the holes in the gels. These holes are from bubbles that appeared randomly in the liquid monomer during curing. The cells appear to prefer these defects to the bulk surface of the gel. As these bubbles were stabilised in the hydrogel during polymerisation, it is likely that they presented a more hydrophobic environment. It is possible that these holes would have a higher concentration of particles in them, this more hydrophobic environment may present a better site for protein adsorption and therefore may allow for better cell adherence. The bubbles do not penetrate all the way through the surface of the gel as these cells would have remained on

the bottom of the culture well following fixation and the removal of the gels from the well or they provided protection for the cells when the rest of the cells cultured on the gel were washed off at the end of the experiment. There were no cells found on this sample of the 1-2 gel.

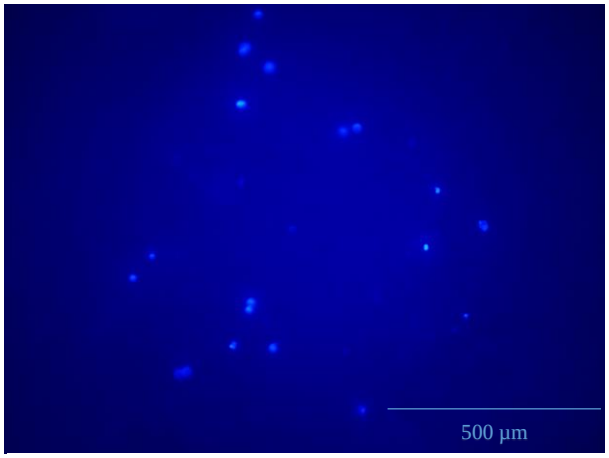

Figure 8-12 A fluorescent light micrograph of stained THP-1 nuclei on hydrogel 50-3 treated with PMA

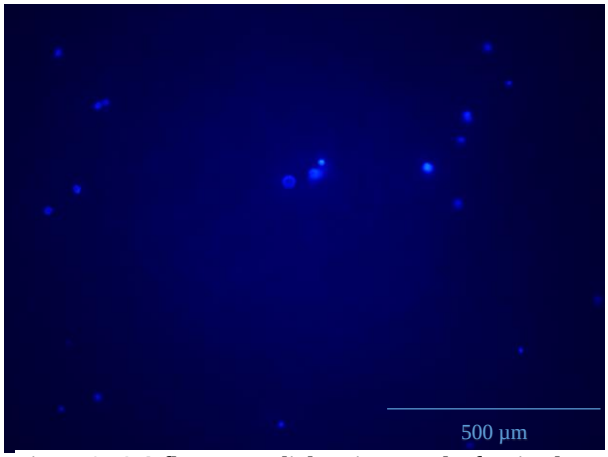

Figure 8-13 A fluorescent light micrograph of stained THP-1 nuclei on hydrogel 50-3 treated with media

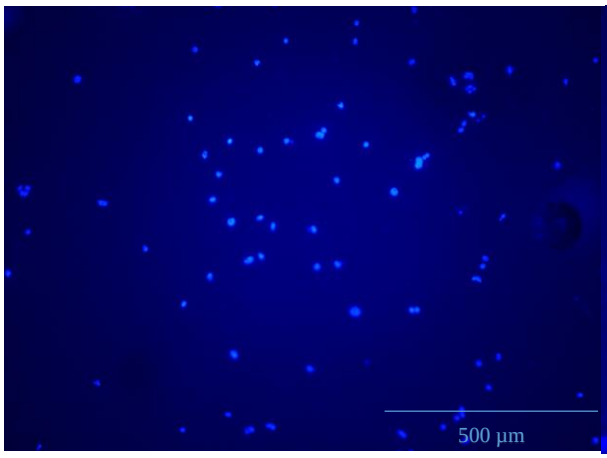

Figure 8-14 A fluorescent light micrograph of stained THP-1 nuclei on hydrogel 1-3 treated with PMA

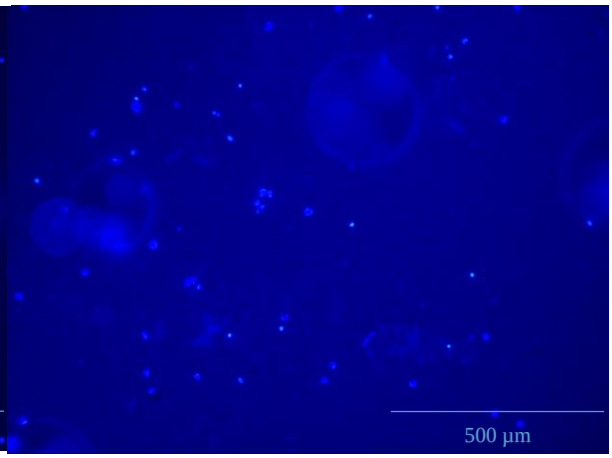

Figure 8-15 A fluorescent light micrograph of stained THP-1 nuclei on hydrogel 1-3 treated with media

The adherence of THP-1 cells to hydrogels containing particles from formulation 3 (approx. 750 nm) appear to be higher than those observed with smaller particle sizes. This could be due to the cells more strongly recognising the surface of individual particles due to their larger sizes or are finding the clefts in between individual particles useful for anchoring

points for adherence. Again there appears to be no discernible differences in the number of cells present on the surfaces treated with PMA and those that were not treated.

All of the above images do show cells on the surface of the hydrogels, however it is not possible to determine whether the cells are activated and adhered or just loosely attached. Nor is it possible to conclude if individual gels have any different differentiating or activating inducing properties. Noteworthy of all the micrographs is the low number of cells observable. Similar concentrations of cells were seeded onto the surface in preliminary 3T3 experiments, shown previously, yet far fewer cells are observable on the surfaces of the gels used in the THP-1 experiments. Some of this difference will be due to the differing adherent properties of THP-1 and 3T3 cells but many THP-1 cells are simply not adhering.

A drawback of this analysis method is the inability to see cell morphology and so assess how well the cells are adhering, whether they are truly sticking down by sending out cytoplasm projections to grip the surface of the hydrogels, or if they are rounded up, dead or dying, or in a state of dormancy, loosely attached to the surface.

8.3.3 Cytospinning THP-1 cells for phalloidin titration

The cells fixed to the surface of the glass sides by the Cytospin instrument, were stained using Hoechst (nuclear stain) and phalloidin, a cytoskeleton stain which binds to actin filaments. Texas Red phalloidin was used as it was found that the PS latex embedded hydrogels gave off a strong autofluorescence in the yellow channel used by the fluorescence microscope but less autofluorescence in the red channel. This meant that any cells imaged in this channel were less likely to be swamped by background autofluorescence. The following images show the titrations of phalloidin concentration. The Hoechst nuclear stain and the exposure time of the images recorded by the software are constant throughout.

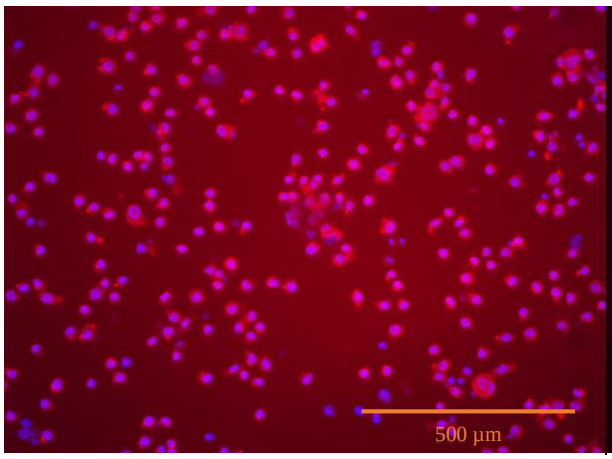

Figure 8-17 A composite red and blue fluorescence light micrograph of stained THP-1 nuclei 1:25 phalloidin concentration

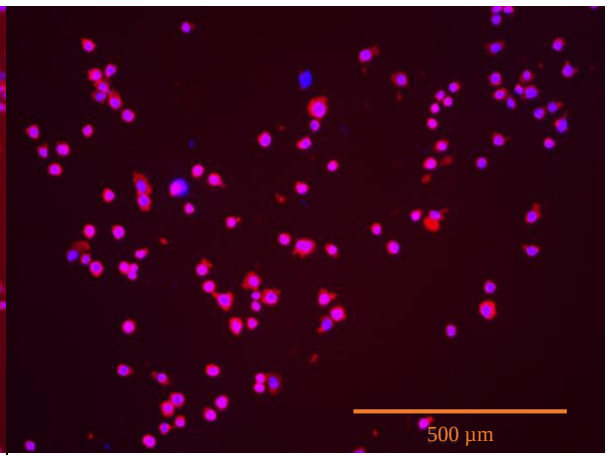

Figure 8-18 A composite red and blue fluorescence light micrograph of stained THP-1 nuclei 1:50 phalloidin concentration

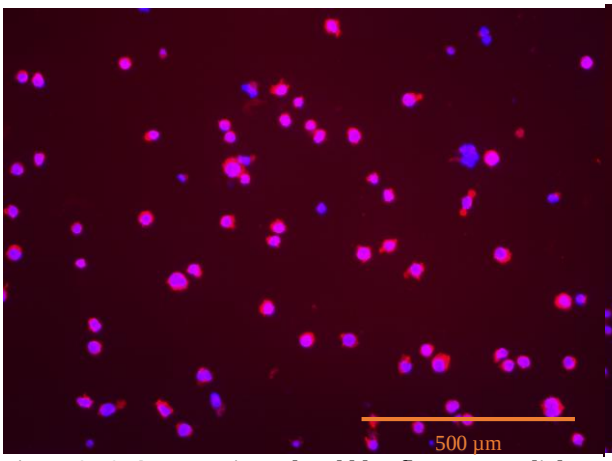

Figure 8-19 A composite red and blue fluorescence light micrograph of stained THP-1 nuclei 1:100 phalloidin concentration

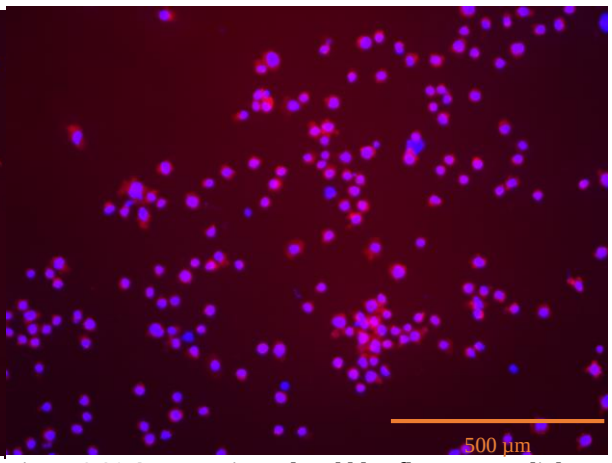

Figure 8-20 A composite red and blue fluorescence light micrograph of stained THP-1 nuclei 1:250 phalloidin concentration

Figure 8-21 A composite red and blue fluorescence light micrograph of stained THP-1 nuclei 1:500 phalloidin concentration

Figure 8-22 A composite red and blue fluorescence light micrograph of stained THP-1 nuclei 1:1000 phalloidin concentration

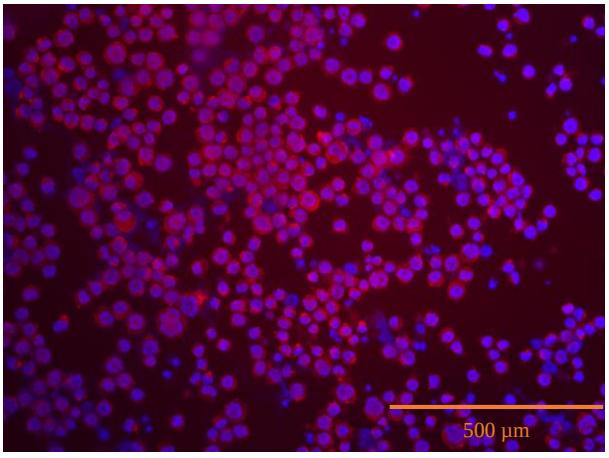

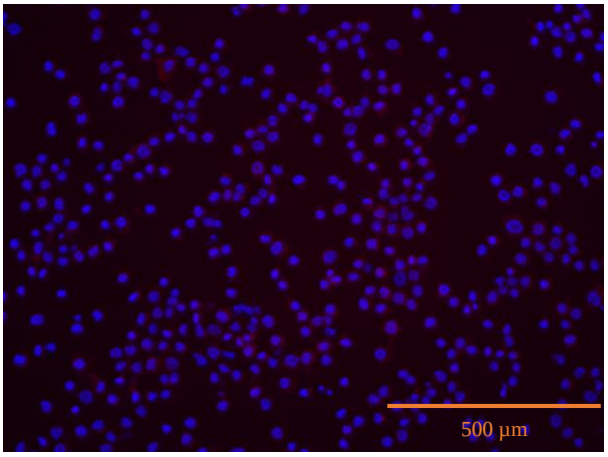

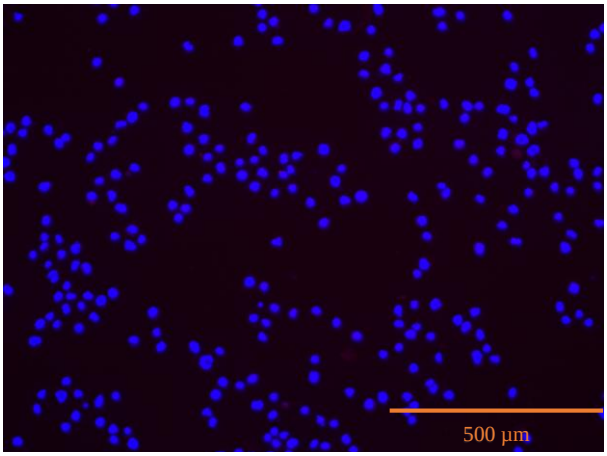

Figure 8-23 A composite red and blue fluorescence light micrograph of stained THP-1 nuclei 1:10000 phalloidin concentration

The concentration of 1 in 500 v/v phalloidin in PBS was found to give the bests feature resolution at the lowest concentration and was chosen to be used in future experiments.

The concentration of the nuclear stain was maintained throughout the experiment and the phalloidin concentration decreased incrementally. The images presented above are overlaid images taken in the blue and red channels of the fluorescence microscope and show the blue dyed nucleus of the THP-1 cells and the red dyed actin filaments in the cytoskeleton. All of these cells appear rounded because they were forced onto the surface of the glass slides very quickly by centrifugation, rather than being allowed to adhere naturally during culture. Nevertheless it is possible to see this rounded shape and distinguish it from the background and the colouring of the nucleus. As the phalloidin concentration decreases it becomes harder to discern morphological features of cells, particularly in the 1 in 1000 and 1 in 10000 dilutions, Figure 8-22 Figure 8-23. It was therefore concluded that the 1 in 500 dilution (Figure 8-21) was the optimal balance of possible resolution of cellular features, lowest background interference and least volume of phalloidin used.

8.3.4 Epifluorescence imaging of cytoskeletal features of THP-1 cells on hydrogels

The cell culturing procedure was repeated, following this, the hydrogels were imaged using the cytoskeletal dye. From the resulting images, it was found that there was a very large degree of autofluorescence in the red channel which caused the cell structure, as shown by the phalloidin, to be much obscured or completely swamped by background autofluorescence. This is likely due to the gel becoming saturated with low levels of phalloidin dye binding non-specifically to the gel and the combined autofluorescence swamping the fluorescence caused by the dye binding specifically to the actin filaments in the cell cytoskeleton. Washing the gel in PBS for a long period of time (up to two weeks) showed a reduced autofluorescence but any cells present on the surface of the gel were either washed off the surface or, during this time, had naturally lost the fluorescence conferred from the dyes present. The following figure is an image of THP-1 cells on a PS latex embedded hydrogel, stained with phalloidin and imaged at the same magnification and exposure time as the above micrographs used for the phalloidin titrations. Careful examination of the image reveals that cellular features can be discerned (some are ringed) however it is very difficult to make out anything other than their presence from this image, it is harder still when using the microscope in the initial analysis as the autofluorescence is very intense. Due to this inability to discern any details of the THP-1 cell features, the epifluorescence aspect of the project was discontinued

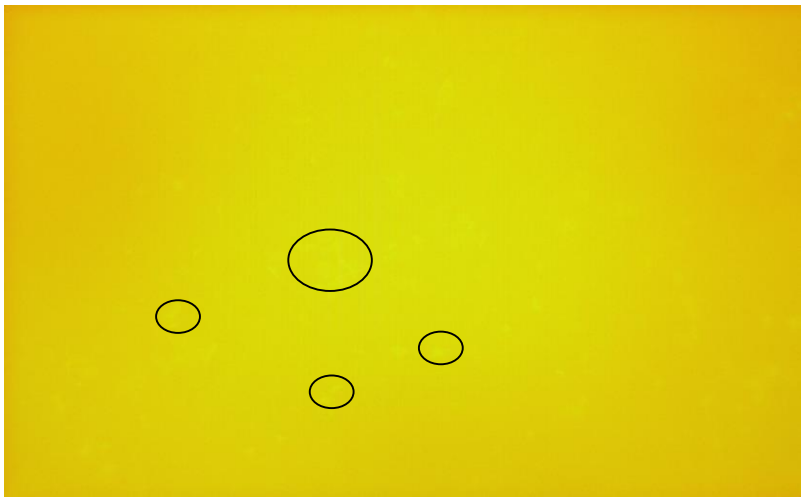

Figure 8-24 A composite red and blue fluorescence light micrograph of stained THP-1 cells on hydrogel 50-1 1:500 phalloidin concentration

8.3.5 THP-1 adherence on hydrogels

The THP-1 cells were seeded onto the hydrogels in a small concentrated volume as this was found, in previous experiments to give a good chance for the cells to adhere to the surface of the hydrogels, instead of being washed off the surface immediately, which could be an explanation for the low observed number of cells present on the hydrogels described in the results of the preliminary experiments in this chapter. Smaller hydrogels were also used, this was partly to save materials and also to allow more experiments to be run in parallel more efficiently using fewer well plates. The gels were cut to the same size as the hydrogels used for the fibroblasts experiments. This size was chosen as it is approximately the same size as the base of a 96 well plate well.

THP-1 cells were introduced to the surfaces of the hydrogel materials, allowed time to settle on the surface and treated with differentiating media. The cells were then left to differentiate for 48 hours and their ability to adhere to the surfaces was investigated. Whether there was any resulting activation of the cells caused by the hydrogel surface or to what extent this activation was displayed was investigated. After 48 hours the media was changed and the replacement media was extracted from the gels at time points of 4, 8, 12 and 24 hours. The media extracted after 48 hours culturing time was recorded as time point 0. Media was then stored and to be analysed for cytokines produced by the cells using the enzyme linked immunoabsorbant assay (ELISA).

Preliminary experiments found that it took the THP-1 cells around 36-48 hours to fully differentiate into a macrophage-like cell type and fully adhere to a surface. This was why 48 hours was chosen as time point T_0. However when the well plates were removed from the incubator, the wells which had been treated with Alamar blue solution all remained blue instead of the expected pink-red colour. This was an indicator that the cells had either died

off or had become dormant and were undergoing little cellular metabolism. The following images are of the TCP control wells which were treated with PMA, onto which, the cells should have adhered the best.

Figure 8-25 A light micrograph of THP-1 cells on TCP at T_0 treated with PMA

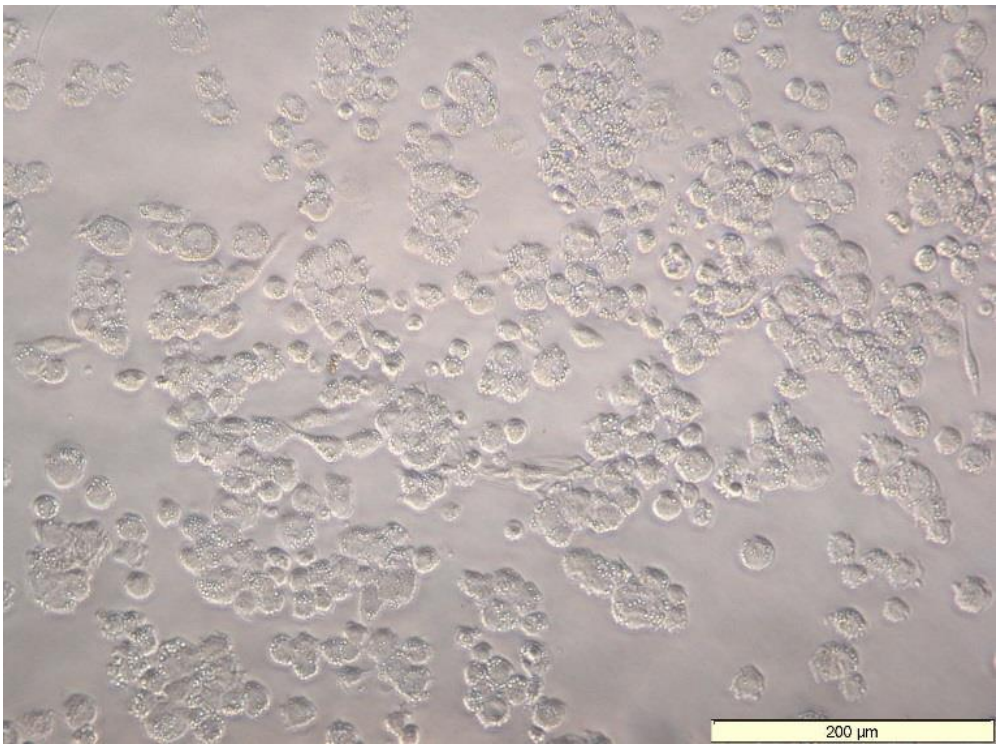

Figure 8-26 A light micrograph of THP-1 cells on TCP at T_0 treated with PMA

Figure 8-25 above shows the cells in the TCP wells, at first glance many of them look to be irregularly shaped which would be a good indicator of THP-1 activation and adherence. However, higher magnification (Figure 8-26) revealed that most, if not all of the cells had a number of round features inside them. These are likely cell blebs which indicates that the cells are undergoing apoptosis, a form of programmed cell death and are therefore dead or dying. This could be confirmed immunohistochemically by using apoptosis markers such as cytochrome C or caspases.

It was not possible to form a calibration curve from the Alamar blue data at any of the time points as the optical density readings for each well that was analysed using Alamar blue was too similar. Even where differing numbers of cells had been seeded into the wells. At later time points, the optical densities did increase slightly compared to T_0, suggesting that there were a few cells present that were metabolising but it was still not possible to draw a calibration curve to assess these numbers.

Figure 8-27A-V light micrographs of THP-1 cells on hydrogels treated with PMA

The following images show the cells that were found on the hydrogels at T_0.

LABEL	GEL
A,B	**50-1**
C,D	**25-1**
E,F	**1-1**
G,H	**50-2**
I,J	**25-2**
K,L	**1-2**
M,N	**50-3**
O,P	**25-3**
Q,R	**1-3**
S,T	**0**
U,V	**PET**

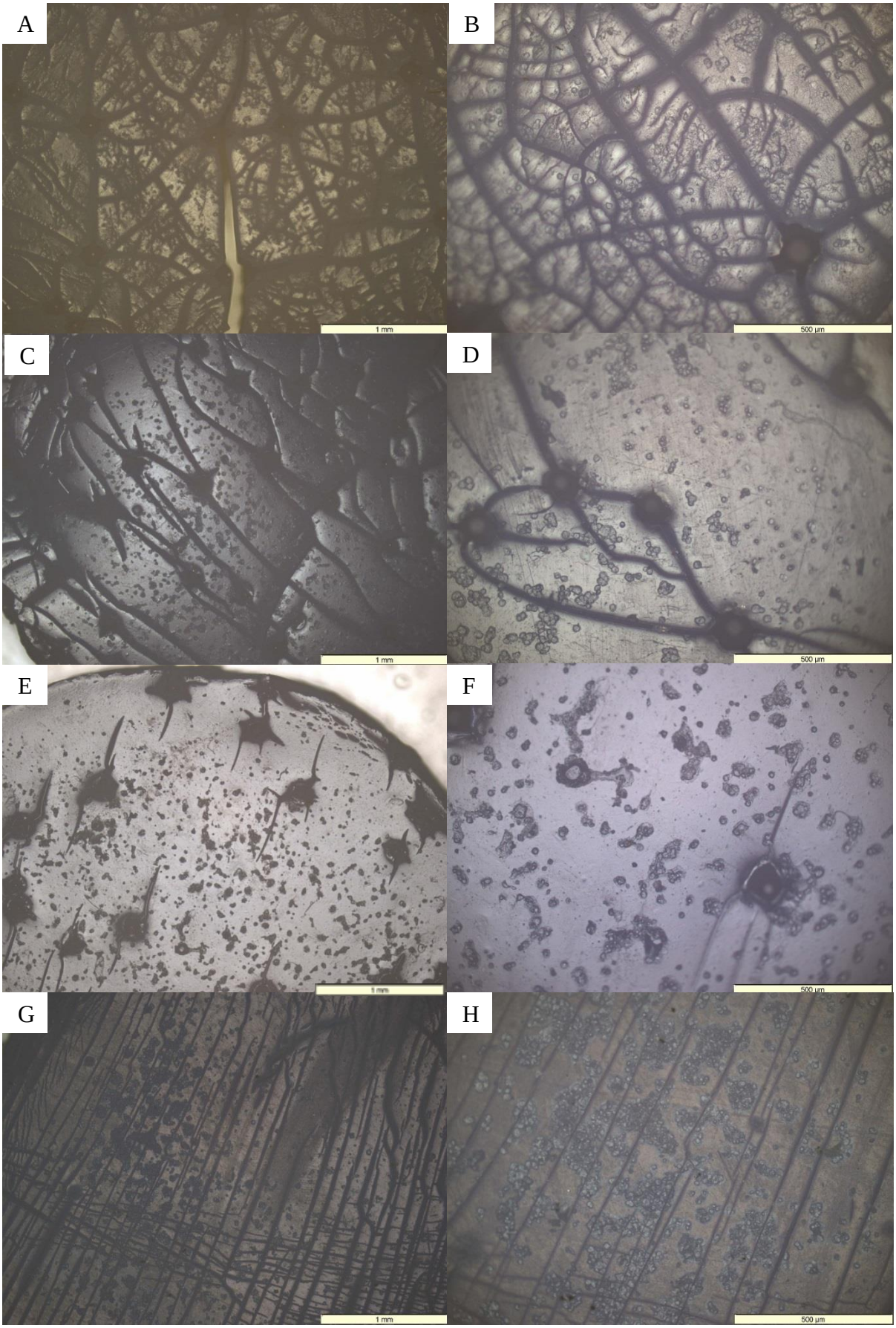
A
1 mm
B
500 µm
C
1 mm
D
500 µm
E
1 mm
F
500 µm
G
1 mm
H
500 µm

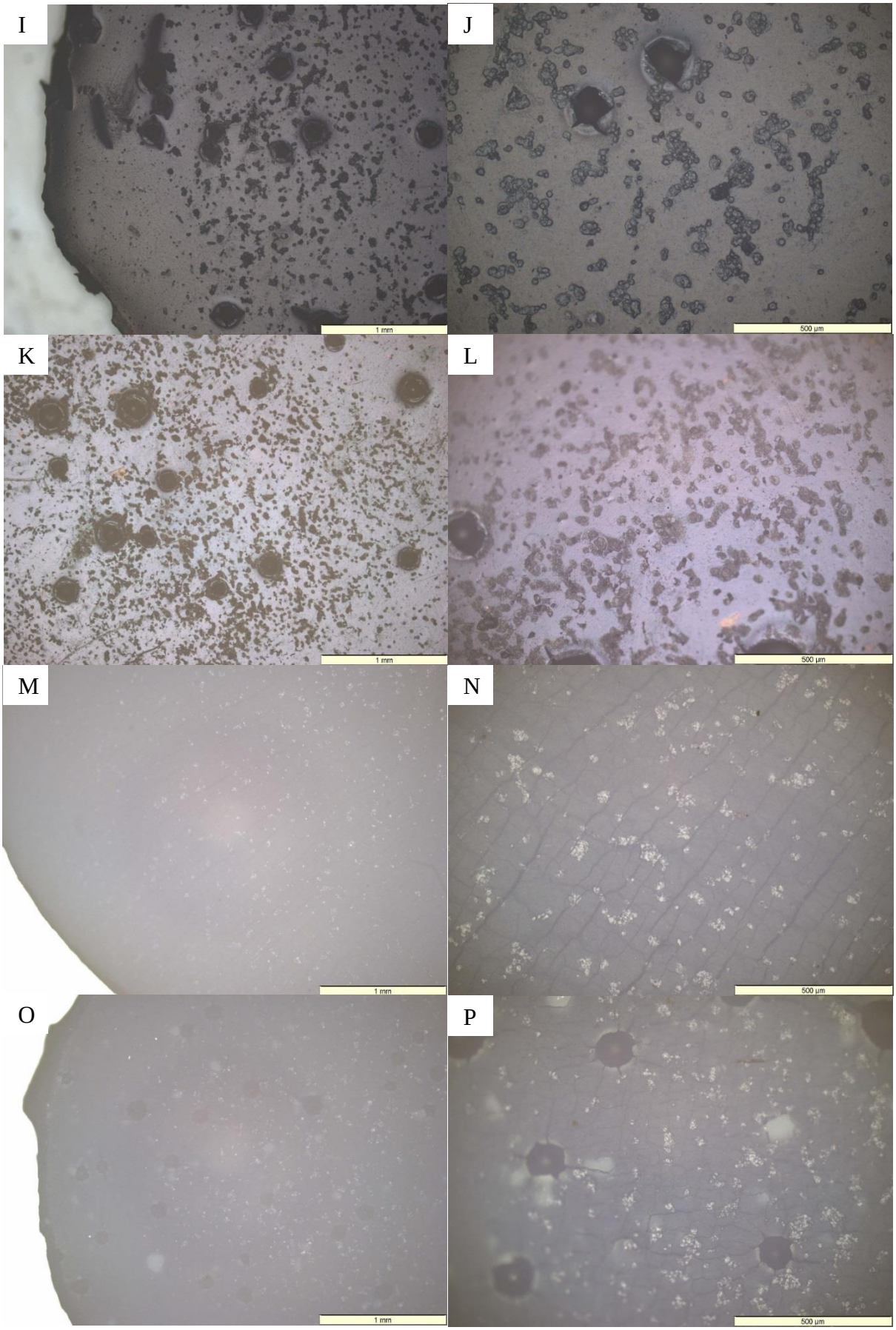
I
J
K
L
M
N
O
P
1 mm
500 µm

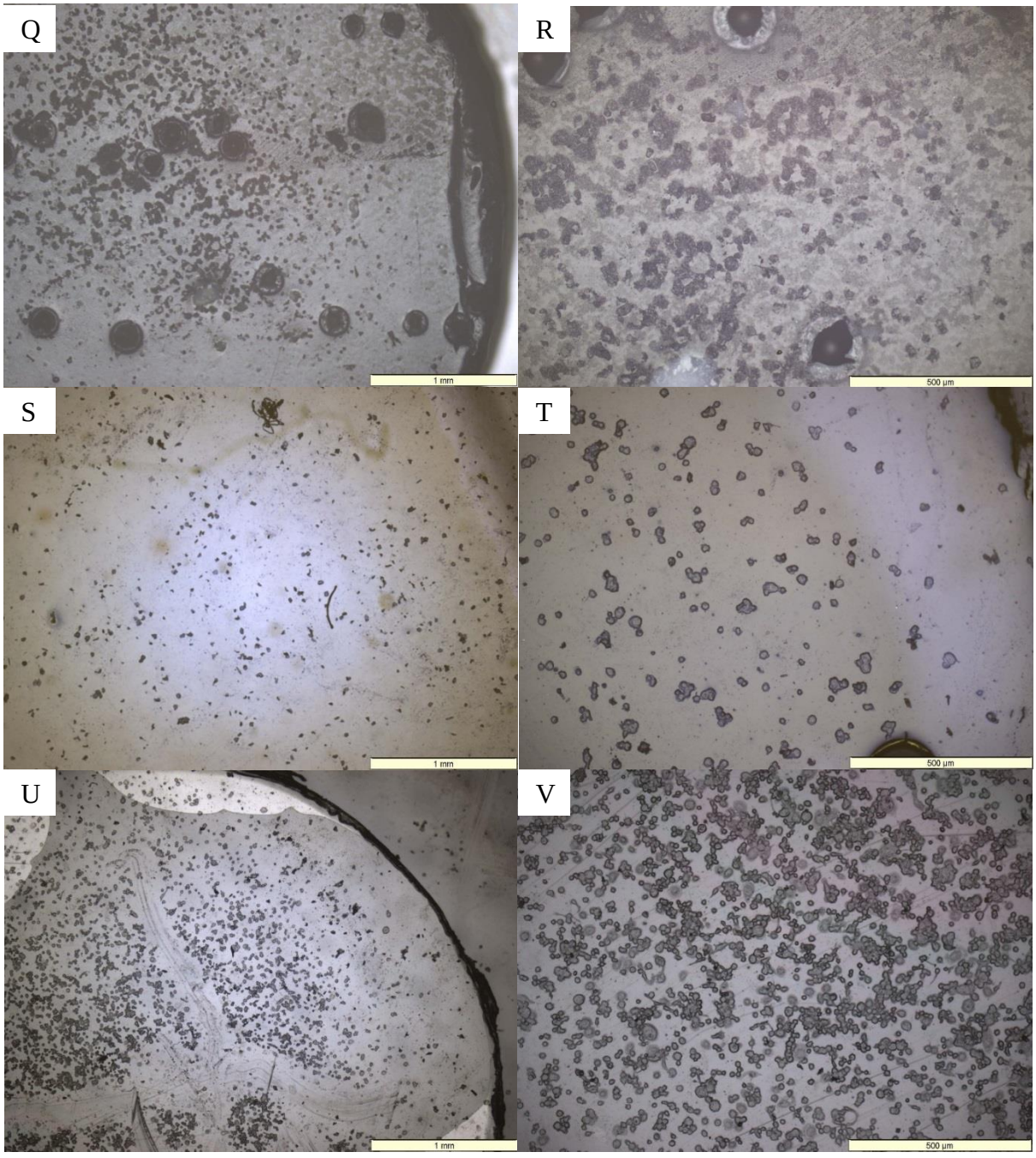
Q
1 mm
R
500 µm
S
1 mm
T
500 µm
U
1 mm
V
500 µm

The above images are all from the PMA treated set of hydrogels. The sets treated with LPS and MED look very similar, with many cells present but rounded and not very healthy looking. These images have not been presented.

The cells present on the gels are almost all rounded looking and many look unhealthy, particularly in Figure 8-27 R**Error! Reference source not found.** of hydrogel 1-3. This coupled with the lack of indication of any significant cellular metabolism from the cells according to the Alamar blue assay leads to the conclusion that this experiment was not successful. The cells could be either dead, dying or are in a state of low metabolic dormancy and it is therefore not possible to conclude whether they have reacted to the hydrogel surfaces and give no indication of activation.

The images shown in Figure 8-27 U&V above, of the PET disks are somewhat interesting. It was not thought that cells would be able attach to these surfaces at all. However there appears to be a large number of cells present on this plastic disk. Unfortunately the cells themselves, whilst present are mostly rounded looking and unhealthy and so again, a conclusion cannot be drawn to ascertain whether the THP-1 cells would be responding to this surface in an inflammatory manner or if they found favourable conditions on which to settle during the initial part of the experiment. A future experiment could look to this case and assess whether THP-1 cells are capable or even willing to adhere to this surface.

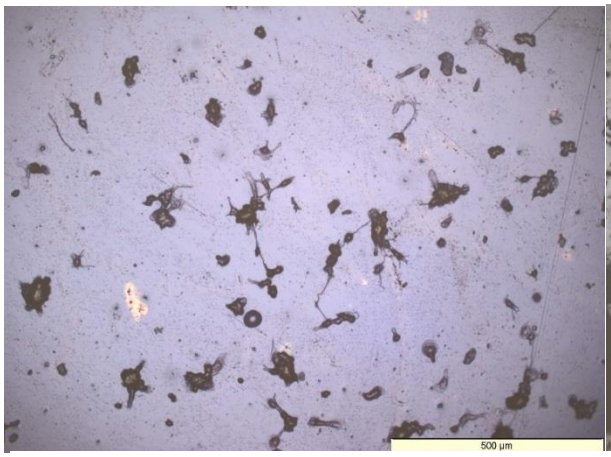

Figure 8-28 A light micrograph of THP-1 cells on hydrogel 0 treated with PMA

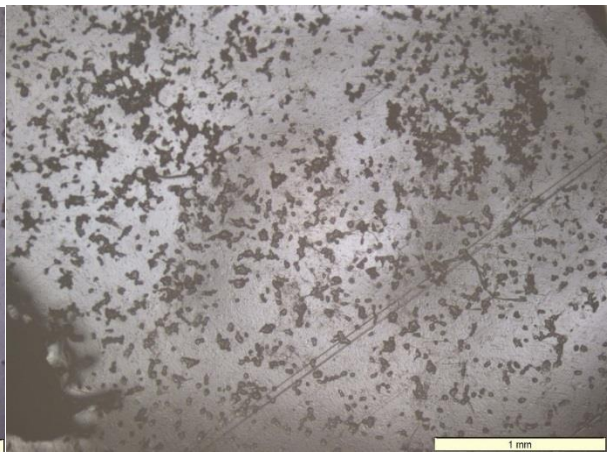

Figure 8-29A light micrograph of THP-1 cells on hydrogel 1-1 treated with PMA

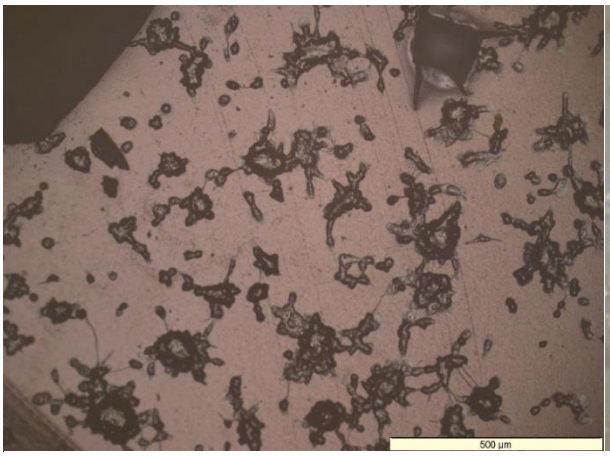

Figure 8-30 A light micrograph of THP-1 cells on hydrogel 25-2 treated with PMA x10 magnification

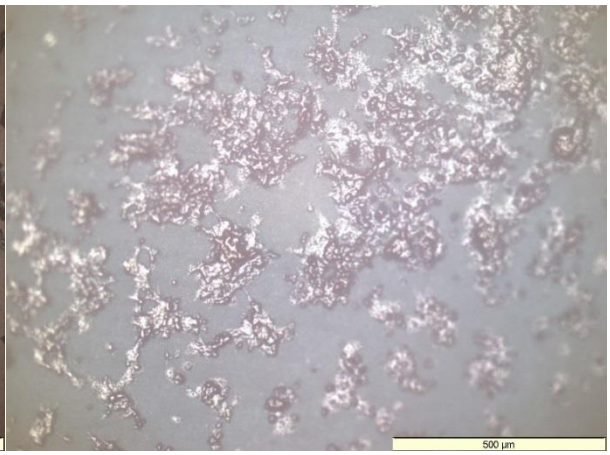

Figure 8-31 A light micrograph of THP-1 cells on hydrogel 50-3 treated with PMA x10 magnification

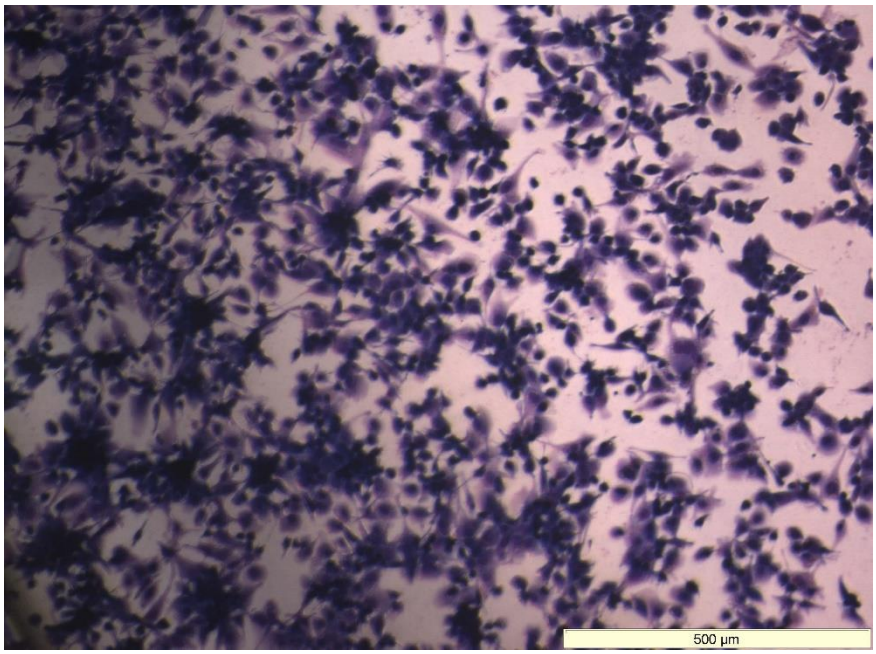

Figure 8-32 A light micrograph of Giemsa stained THP-1 cells on TCP treated with PMA

Smaller scale preliminary experiments prior to this experiment did show that it was possible to culture THP-1 cells on hydrogel surfaces and visual analysis appears to show that these cultured cells were adhered to the surface due to their spreading appearance, shown above in Figure 8-28 - Figure 8-32. Numbers of adhered cells were unable to be quantified by this experiment.

The above images, Figure 8-28 - Figure 8-32 illustrate the visual appearance of THP-1 cells adhered to examples of the gels used in this experiment.

8.3.6 Enzyme-linked Immunosorbent Assay of cytokines

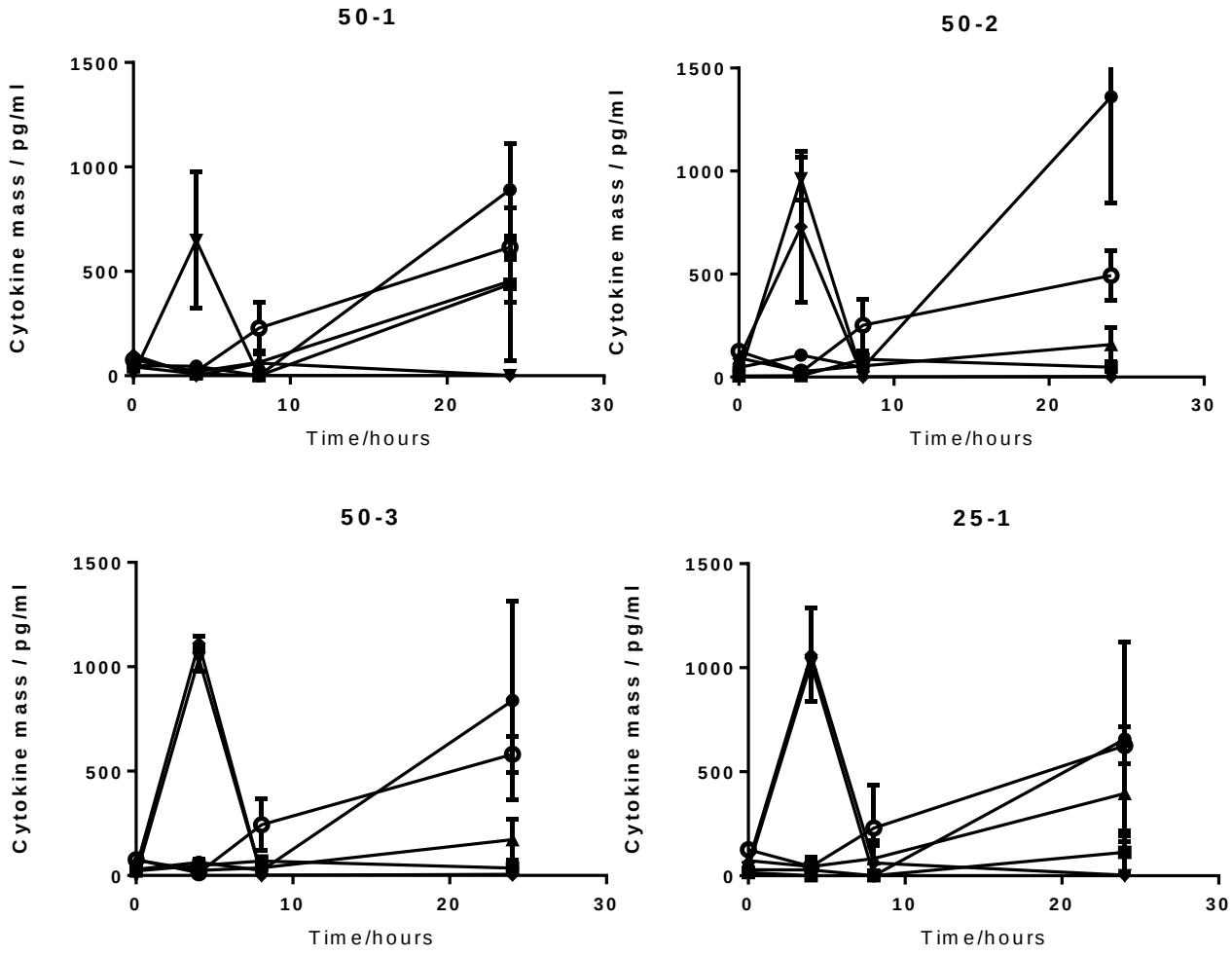

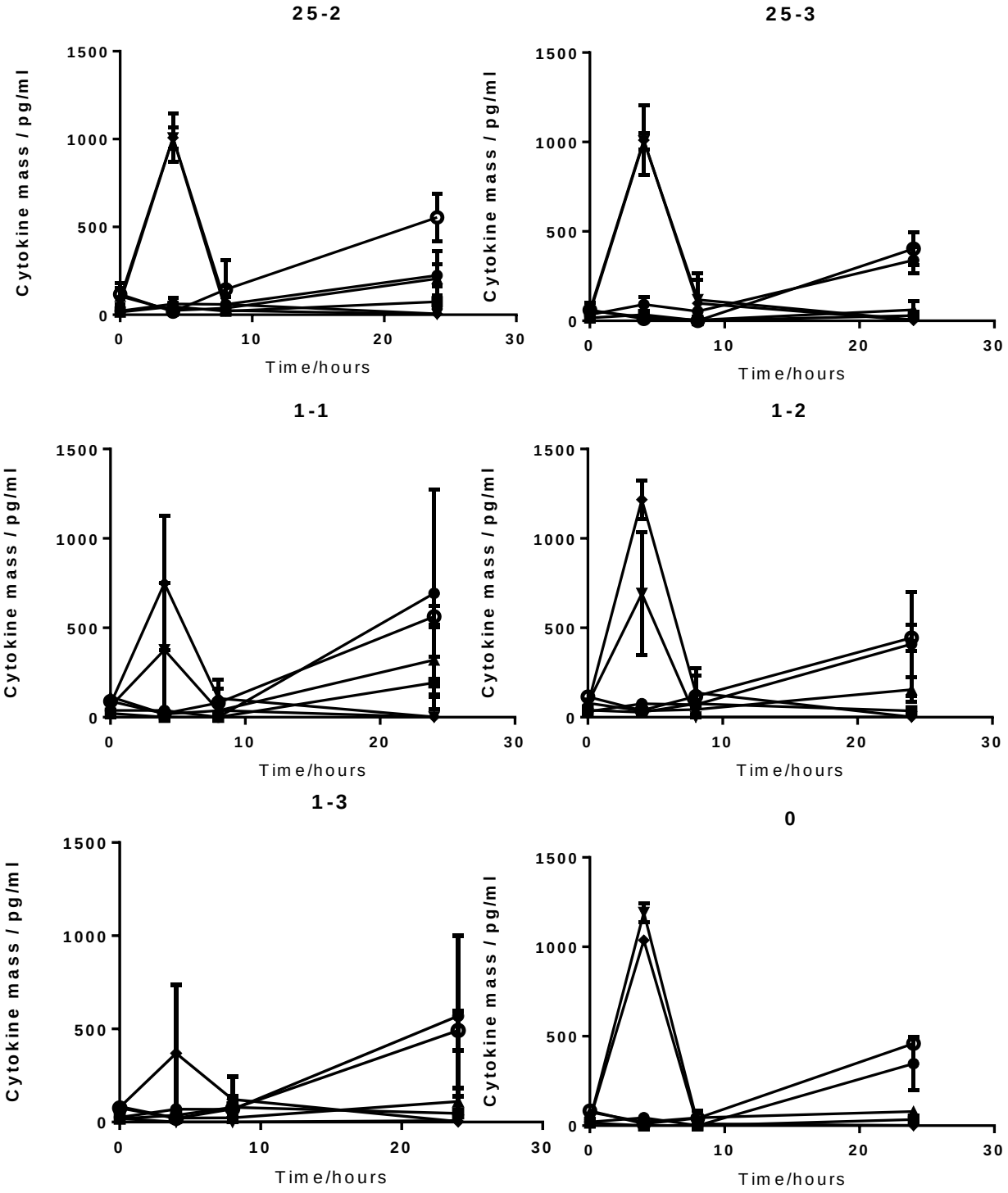
25-2
25-3
1-1
1-2
1-3
0
Cytokine mass / pg/ml
Time/hours
1500
1000
500
0
0
10
20
30

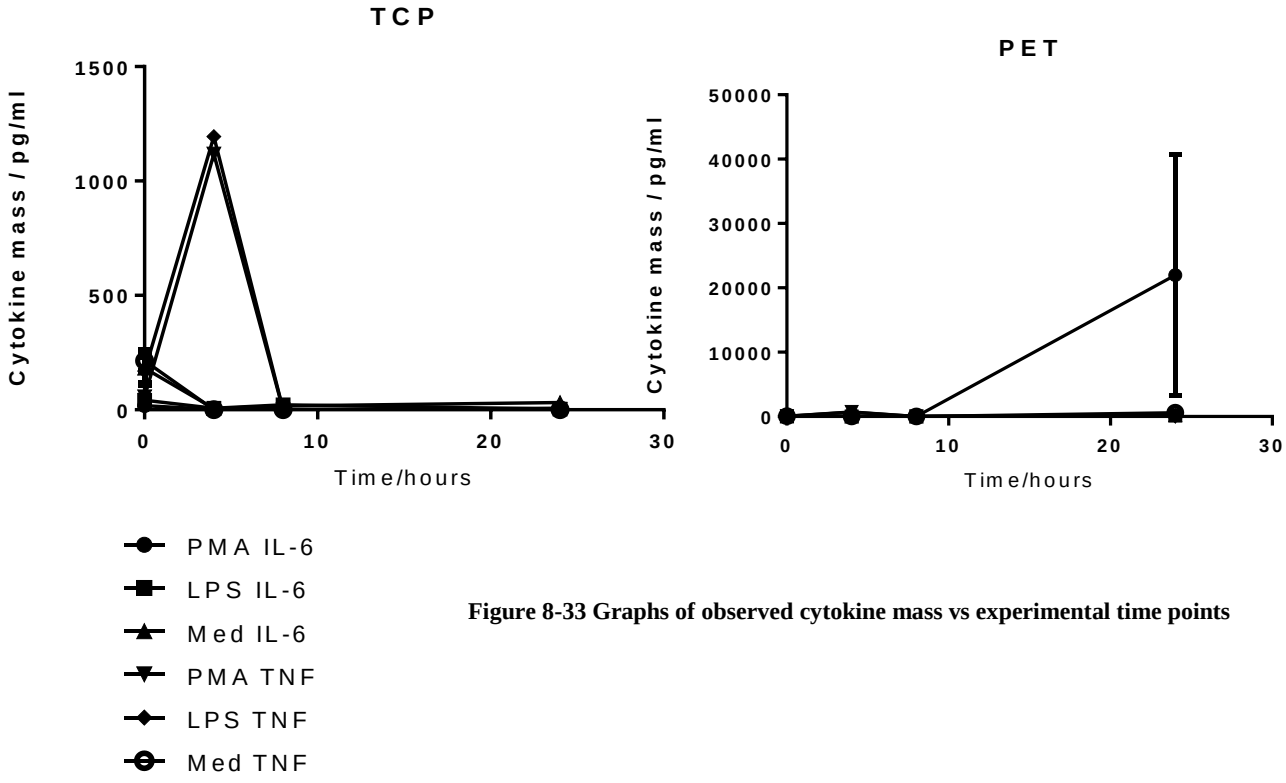

Figure 8-33 Graphs of observed cytokine mass vs experimental time points

The amounts of cytokines measured using the ELISA are presented above in figure 8-33. They were produced using GraphPad Prism. The error bars are the standard error where n=3. Tables of statistical significance for each graph comparing each of the points within data sets is included in the appendix. The significance was computed using ANOVA and Tukey's multiple comparison test.

A general trend across all data sets is that the very low levels of cytokines released, typically less than 1000 pg/ml of either cytokine. IL-6 appears to have been released in greater quantities than TNF-α. Cytokine production, particularly IL-6 appears to peak at 4 hours after the start of the experiment. Production then decreases to low levels and rises again at

the final time point but to levels lower than that seen at 4 hours. These trends appear to be consistent as particle size and particle concentration are increased.

There is little significance between the cells treated with LPS with PMA, compared to those treated with PMA in isolation. It was expected that the cells treated with PMA & LPS would have produced much higher levels of inflammatory cytokines, but this may be an indication of the low level of success in differentiating the cells using PMA. Indeed most of the samples do not show any significant difference between those cells treated with PMA which should have caused a differentiation to an inflammatory phenotype, and those which were treated with media and acted as a control.

The fact that there is measurable cytokine production in the samples indicates that the cells are capable of producing cytokines and do, however the very low levels, varied data and lack of any particular statistical significance makes it difficult to ascertain if the cytokines produced are a result of the differentiating solution, LPS or the gel surfaces causing an inflammatory response.

Comparing the rough surface gels to the surface of TCP which was shown in preliminary experiments to be a suitable and favourable surface for the THP-1 cells to adhere to, seems to show little difference at the 4 hour time point, however there is no indication of a cytokine response across any of the treatments as the time points progress. This would suggest that the THP-1 cells may have become settled on the surface of the TCP and after an initial inflammatory response have ceased to be inflamed. On the rough surfaced gels, most of the samples show an upsurge of cytokine production at 24 hours, this shows that after an initial inflammatory response, the cells settled for approximately 20 hours then once again become inflamed. This could possibly indicate that the THP-1 cells were not completely

settled on the gel surfaces but instead were merely resting there later detaching and resettling then becoming inflamed again.

The THP-1 cells should not have proliferated in this time as differentiated cells of this type do not proliferate. The results of the AlamarBlue assays presented previously show no measurable difference between the numbers of cells at each of the time points which indicated very low levels of cellular activity, if any, this would support the low levels of cytokines produced across all of the samples. This however does not allow a conclusion regarding the successful differentiation of the THP-1 cells by PMA as there is no significance between the numbers of active cells and the amounts of cytokines produced when the treated cells are compared to the media controls.

The PET control showed very little response by the THP-1 cells apart from a small increase in cytokine production at 4 hours and a much larger production of IL-6 at 24 hours. The aberrant nature of this response compared to all others and the huge degree of error (approx. ±20000 pg/ml) indicate that this is an erroneous result and should be discarded.

The lack of any noticeable difference between cells treated with PMA and LPS indicates that the cells were sparingly differentiated by PMA or that they were inactive throughout.

50-1

For the 50-1 gels the largest degree of significant difference in cytokine productions is found on the cells treated with PMA. There were much higher amounts of IL-6 released after 24 hours and no significant difference at earlier time points. This production indicates that the cells required 24 hours post treatment in order to become inflamed by their surfaces. The lack of activity prior to this matches the AlamarBlue data which showed little overall cell activity so the sudden jump at T24 is surprising. It is likely due to the cells in this sample slowly settling to; then acclimatising to their surface and only becoming active when this

had completed. The same cells showed a spike of TNF-α after 4 hours which would show that the cells were settled sooner and became inflamed quickly then either detached from the surface for approx. 20 hours before settling again and releasing il-6 or became dormant on the surface for this time.

The cells treated with LPS showed little difference across the time points but spiked slightly at T8 with IL-6, then died off again. There was no appreciable difference in TNF-α release across the time points. This could show that these cells became settled and differentiated some time before 8 hours and then were initially inflamed but then this response died off over the remaining 16 hours of the experiment. There should have been a larger response from the cells treated with LPS as it is a known inflammatory agent so this low activity agrees with the AlamarBlue data and likely shows that the cells failed to fully differentiate.

There is no appreciable difference in the release of IL-6 from the cells treated with cell culture media which is to be expected as these cells should not have differentiated. However there is some increase in production of TNF-α from 8-24 hours which could show that after this time, the cells settled on the gels via gravity then differentiated themselves and became inflamed slightly by the rough surfaces.

50-2

For the 50-2 gel, the only significant change in cytokine production is seen in the cells treated with PMA, these cells released IL-6 after approx. 24 hours. The cells showed little other cytokine production apart from a small amount of TNFα being produced by the LPS and PMA treated cells at 4 hours. This TNF α production was not significant. The low overall production is likely a result of these cells failing to differentiate during the experiment and remaining in a dormant state throughout as indicated by the AlamarBlue results. The error bar for PMA IL-6 is clipped at the axis limit.

50-3

Both groups of cells treated with PMA and LPS showed an increase of production of TNFα after 4 hours indicating that the cells had differentiated somewhat and adhered to the surface of these larger particles and the surrounding gels. This adhesion had led to an in initial increase in TNF α production. The only IL-6 production at significant levels was at T24. This matches with some of the previous experiments indicating that the cells release TNF-α as an early indication of inflammation then IL-6 as an indicator of more prolonged inflammation.

25-1

The information shown above indicates that as the particle size increased the amount of cytokines produced slightly increased. The levels produced by the now less concentrated particles appears to be at approximately the same level as the amounts recorded produced by cells on the largest particles. This perhaps shows that fewer particles have a more pronounced effect on the inflammatory response of the cells.

Again the production of TNF-α appears to quickly spike after 4 hours then tail off, in both cells treated with LPS and PMA. This is followed by an increase of IL-6 towards 24 hours. This again shows that some of the cells may have differentiated and are being irritated by the surfaces but appear to have a period of lesser activity after approx. 4 hours where they lie dormant and are either not activated by the surface or are inactive all together as is suggested by AlamarBlue.

25-2

The profile for these large particles is the same as those shown in the previous data set. With very similar levels of IL—6 released. TNF levels are lower however. Also for the media controls, the cytokine production shows an increase as time elapses, further showing that

the cells may be differentiating on the surfaces of the gels and becoming increasingly inflamed.

25-3

The largest particles show the same activation profile as the previous particle size indicating there is little difference to the cells from smaller to larger particle sizes. The amounts of cytokines released appear relatively similar also. There is little production of IL-6 which shows that the cells were probably inactive.

1-1

The profiles of cytokine release for the most dilute particle gels are similar to those shown previously however a large degree of variance in the data means that these profiles are not significant. This is due to the cells not showing any noticeable differentiation or activity during the experiments.

1-2

Again there is little significance in the IL-6 results due to the variability of the data. The very small amounts of cytokines released mean that small fluctuations have a pronounced affect. The PMA and LPS treated cells do show some increase in TNF-α production at T4 as has been shown previously but at similar to lower levels, possibly due to less inflammation being induced by a less rough surface.

1-3

Again for this gel set, the variability of the data has led to little meaningful conclusions. This is due to the lack of success with differentiating the cells and their inactivity.

0 – bare hydrogel

The bare gels with no particles show very similar cytokine release profiles to those seen previously. This is surprising as these gels should have caused low levels of inflammation compared to those containing particles. This shows that the cells are becoming inflamed independent of the surface roughness modification or that the low levels of cytokine release are independent of surface differences possibly due to the low levels of activity of the cells or the lack of success of the experiment.

TCP

The TCP controls showed that the cells were somewhat inflamed by the TCP surface, this is surprising as the material itself is designed to be attractive to cells and would as such should not elicit an inflammatory response. The lack of difference between the cells treated with PMA and LPS suggest that at these low levels, the cells are not responding to external inflammatory agents and are likely functioning in a very low activity state.

An interesting observation is that most of the groups of cells showed a higher that previously seen initial activation at T0. This is possibly due to the cells being disturbed by the change in conditions of the experiment. Possibly having being settled on the well surface previously and then being lifted and quickly resettling.

The lack of any significant difference between this control and the other experiments again shows that the whole experiment was rather unsuccessful.

PET

The PET samples acted as a material control and were not supposed to be a particularly attractive surface for which the cells could adhere. This is supported by the very low levels of cytokine production across all of the samples and treatments. The only significance in this data comes from two results from T24 IL-6. As mentioned previously, it is fair to assume that

these points are erroneous and can be disregarded. They are more likely to be the result of an error or contamination of the ELISA measurement procedure than a particularly strong inflammatory response to the surfaces.

The lack of cytokine activity on these samples could indicate that this surface is indeed a poor surface for THP-1 cells to adhere to, but due to the overall low activity of cells in all experiments, It would be difficult to say for sure that the low activity was caused by the surface or the temperamental nature of the cells across the whole experiment.

8.4 Conclusion

Unfortunately, this experiment was unable to be repeated due to time constraints and the exhaustion of funding and hydrogel materials, however it has been shown in this chapter that it is possible to culture THP-1 macrophage like cells on hydrogel materials. The cells have been shown to be adhered to all forms of the hydrogels, under some conditions, more than others. In this chapter, various methods of preparing and optimising the hydrogels were examined and the useful aspects of these protocols were maintained. It was discovered that the hydrogels are not suitable materials for typical histological processing and analysis due to their tendency to snap or shatter when cut with a microtome blade. The hydrogels are also unsuitable for microscopy using fluorescent stains as they have a tendency to absorb the fluid containing the stain, undergoing non-specific binding with the stain and producing strong autofluorescence which swamps any legitimate observations that could be made. On a more positive note, it has been found that the hydrogels can be easily imaged using an upright microscope using reflected light to yield very reasonable pictures without using phase contrast or staining the cells.

ELISA demonstrated that the cells were producing very low levels of cytokines, which were measurable. However no particular meaningful trends between differing hydrogel types could be determined. The cytokine data further agreed with the Alamar blue data and visual examination of the cells indicating that they were in a very low activity state or otherwise non-active.

Future work in this area could look towards building upon the areas optimised in this chapter and assessing what the THP-1 cell response is to the hydrogel surface by cytokine analysis. With this data, it would be possible to see if any responses could be moderated by changing certain aspects of the hydrogels such as altering physical characteristics such as the flexibility of the hydrogel, by changing the cross-link density of the gels or changing a chemical functionality such as incorporating peptides into the hydrogel structure which could increase cell adhesion properties.

9 Conclusions and further work

In this thesis it was demonstrated that hydrogel biomaterials made from glycerol methacrylate could be easily synthesised and in potentially large quantities. These hydrogels were shown to have good water contents, of 75-80%. Polystyrene latex particles were synthesised using emulsion polymerisation with good control of particle size. It was also shown that it was relatively simple to incorporate these particles into the structure and surface of the hydrogels to give hydrogel materials with rough surfaces but identical chemistry. The latex hydrogels were also shown to be non-cytotoxic and could act as viable biomaterials. 3T3 fibroblast cancer cells were shown to adhere to the surfaces and it normal human dermal fibroblast cells were shown to be able to proliferate on the hydrogels. THP-1 macrophage like cells were shown to be able to adhere to the surface but quantification of this and an investigation to the cell's reaction to the surface using cytokine analysis was unsuccessful.

While the hydrogels do act as functioning biomaterials, their innate fragility when wetted meant that they were difficult to work with. A future experiment could look to curing the hydrogels directly into the wells of the cell culture plates which would eliminate many of the problems faced when handling the gels. Also it would remove the need to transplant the hydrogels from one plate to another as seen in the NHDF chapter. It was required to move the gels in this instance because the fibroblast cells used showed either a willingness to migrate off the hydrogel surfaces on which they had been placed, or that they were washed off during an earlier stage of culturing. If the gels were adhered to the bottom of a culture well, there would be no room for cells to get around or underneath the gels and easy quantification of the cell numbers could be accomplished. It was shown that the benzoyl peroxide/ dimethylaminopyridine polymerisation method produced equivalent PGMMA

hydrogels to those made using potassium persulphate as an initiator. This polymerisation, however was accomplished at a lower temperature which would be advantageous if curing hydrogels directly into a well plate as there would be less potential thermal damage done to the plates.

The latex hydrogels showed good abilities to absorb liquids which is a key hydrogel feature but they also showed an interesting property where droplets of liquids placed on the surface would remain in droplet form for some time and is illustrated in the following image. The hydrogel on the left of the image is 50-1 and the right is bare PGMMA. The image was taken on the bench in our lab. The red liquid is distilled water containing a red dye

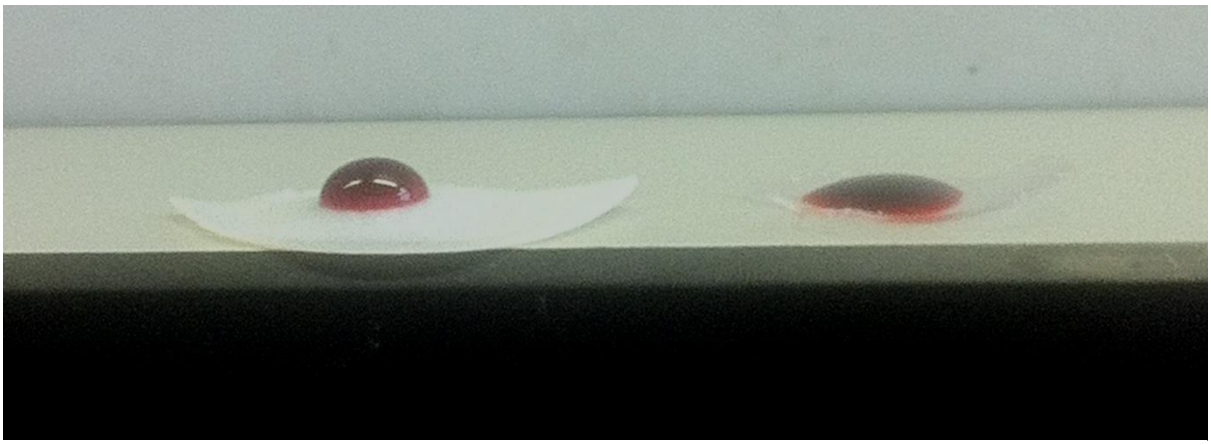

Figure 9-1 A photograph of water droplets on the surface of hydrogels 50-1 and 0

This property was exploited when seeding cells in small volumes of media onto the hydrogels as the droplet was contained on the surface of the gel until it had time to soak into the hydrogel, which typically took less than an hour. Future experiments could look to quantifying this property as a function of contact angle of the applied drop. Preliminary contact angle studies were not very successful as when dried the hydrogels absorbed the drop too quickly for accurate measurements to be taken. A future experiment could look to

using the technique of captured bubble contact angle measurement which is conducted under water with an air bubble. This technique was not available to me during the course of this project and time was exhausted before further investigations could be made.

THP-1 culture was very variable and the cells quite temperamental, processes that worked one day, when repeated in exactly the same way two days later would have no effect. In the final experiment presented, the THP-1 cells all appeared either dead or inactive on the surfaces of the hydrogels and controls. For this to happen to every single well or sample analysed there must have been an environment wide issue befall them. This could have been over stressing of the cells when setting up and conducting the experiment but this is unlikely as there would surely be one or two wells which behaved as expected. One possible cause is a problem with the incubator, a minor fault with CO_2 regulation overnight for example might have been enough to kill or inactivate the cells or a loss of incubator moisture may have had a similar effect. A future experiment could look to repeating my experimental set up successfully and assessing the cell's responses to the surfaces by looking at the cytokines they produced over the course of the experiment. This was the key aim of the project which was sadly not met. Another possible experiment would be to look at cell surface markers present on the THP-1 cells, which are expressed upon adhesion. Using immunohistochemistry, it would be possible to definitively show that they THP-1 cells had properly adhered to the surfaces of the hydrogels.

Some of the most promising work in this project was the core-shell work. In this chapter, protected CS particles were produced simply in water using emulsion polymerisation. They were easily washed and purified, then deprotected. The particles then swelled with water to far greater particle diameters than they had shown previously. This was a key indicator of hydrogel functionality, so the particles could be thought of as microgel particles. The CS

particles showed that they could adsorb protein molecules and therefore show promise as a potential carrier for biologically active molecules. Future experiments could look at their encapsulation and release of biologically active molecules, or possibly at their incorporation into hydrogels in a similar manner to the latex particles and see if this presented a different sort of hydrogel surface, onto which a cell could adhere. If the particles are shown to have good release profiles, then hydrogels containing particles or immobilised particles could find application in advanced wound dressings.

10 Appendix

Tables of significance showing the results of Tukey's multiple comparison tests on cytokine data. Significance levels are denoted by stars (**). No significance by NS.

50-1 PMA IL-6

Time	**0**	**4**	**8**	**24**
0		NS	NS	****
4	NS		NS	****
8	NS	NS		****
4	****	****	****	

50-1 LPS IL-6

Time	**0**	**4**	**8**	**24**
0		NS	NS	NS
4	NS		NS	NS
8	NS	NS		*
24	NS	NS	*	

50-1 MED IL-6

Time	**0**	**4**	**8**	**24**
0		NS	NS	NS
4	NS		NS	NS
8	NS	NS		NS
24	NS	NS	NS	

50-1 PMA TNF

Time	0	4	8	24
0		**	NS	NS
4	**		**	**
8	NS	**		NS
24	NS	**	NS	

50-1 LPS TNF

Time	0	4	8	24
0		NS	NS	NS
4	NS		NS	NS
8	NS	NS		NS
24	NS	NS	NS	

50-1 MED TNF

Time	0	4	8	24
0		NS	NS	*
4	NS		NS	**
8	NS	NS		NS
24	*	**	NS	

50-2 PMA IL-6

Time	0	4	8	24
0		NS	NS	**
4	NS		NS	**
8	NS	NS		**
24	**	**	**	

50-2LPS IL-6

Time	0	4	8	24
0		NS	NS	NS
4	NS		NS	NS
8	NS	NS		NS
24	NS	NS	NS	

50-2 MED IL-6

Time	0	4	8	24
0		NS	NS	NS
4	NS		NS	NS
8	NS	NS		NS
24	NS	NS	NS	

50-2 PMA TNF

Time	0	4	8	24
0		NS	NS	NS
4	NS		NS	NS
8	NS	NS		NS
24	NS	NS	NS	

50-2 LPS TNF

Time	0	4	8	24
0		NS	NS	NS
4	NS		NS	NS
8	NS	NS		NS
24	NS	NS	NS	

50-2 MED TNF

Time	0	4	8	24
0		NS	NS	NS
4	NS		NS	NS
8	NS	NS		NS
24	NS	NS	NS	

50-3 PMA IL-6

Time	0	4	8	24
0		NS	NS	****
4	NS		NS	****
8	NS	NS		****
24	****	****	****	

50-3 LPS IL-6

Time	0	4	8	24
0		NS	NS	NS
4	NS		NS	NS
8	NS	NS		NS
24	NS	NS	NS	

50-3 MED IL-6

Time	0	4	8	24
0		NS	NS	NS
4	NS		NS	NS
8	NS	NS		NS
24	NS	NS	NS	

50-3 PMA TNF

Time	0	4	8	24
0		****	NS	NS
4	****		****	****
8	NS	****		NS
24	NS	****	NS	

50-3 LPS TNF

Time	0	4	8	24
0		****	NS	NS
4	****		****	****
8	NS	****		NS
24	NS	****	NS	

50-3 MED TNF

Time	0	4	8	24
0		NS	NS	**
4	NS		NS	**
8	NS	NS		NS
24	**	**	NS	

25-1 PMA IL-6

Time	0	4	8	24
0		NS	NS	****
4	NS		NS	****
8	NS	NS		****
24	****	****	****	

25-1 LPS IL-6

Time	0	4	8	24
0		NS	NS	NS
4	NS		NS	NS
8	NS	NS		NS
24	NS	NS	NS	

25-1 MED IL-6

Time	0	4	8	24
0		NS	NS	*
4	NS		NS	**
8	NS	NS		*
24	*	**	*	

25-1 PMA TNF

Time	0	4	8	24
0		****	NS	NS
4	****		****	****
8	NS	****		NS
24	NS	****	NS	

25-1 LPS TNF

Time	0	4	8	24
0		****	NS	NS
4	****		****	****
8	NS	****		NS
24	NS	****	NS	

25-1 MED TNF

Time	0	4	8	24
0		NS	NS	****
4	NS		NS	****
8	NS	NS		**
24	****	****	**	

25-2 PMA IL-6

Time	0	4	8	24
0		NS	NS	*
4	NS		NS	NS
8	NS	NS		NS
24	*	NS	NS	

25-2 LPS IL-6

Time	0	4	8	24
0		NS	NS	NS
4	NS		NS	NS
8	NS	NS		NS
24	NS	NS	NS	

25-2 MED IL-6

Time	0	4	8	24
0		NS	NS	NS
4	NS		NS	*
8	NS	NS		NS
24	NS	*	NS	

25-2 PMA TNF

Time	0	4	8	24
0		****	NS	NS
4	****		****	****
8	NS	****		NS
24	NS	****	NS	

25-2 LPS TNF

Time	0	4	8	24
0		****	NS	NS
4	****		****	****
8	NS	****		NS
24	NS	****	NS	

25-2 MED TNF

Time	0	4	8	24
0		NS	NS	****
4	NS		NS	****
8	NS	NS		****
24	****	****	****	

25-3 PMA IL-6

Time	0	4	8	24
0		NS	NS	****
4	NS		NS	**
8	NS	NS		***
24	****	**	***	

25-3 LPS IL-6

Time	0	4	8	24
0		NS	NS	NS
4	NS		NS	NS
8	NS	NS		NS
24	NS	NS	NS	

25-3 MED IL-6

Time	0	4	8	24
0		NS	NS	NS
4	NS		NS	NS
8	NS	NS		NS
24	NS	NS	NS	

25-3 PMA TNF

Time	0	4	8	24
0		****	NS	NS
4	****		****	****
8	NS	****		NS
24	NS	****	NS	

25-3 LPS TNF

Time	0	4	8	24
0		****	NS	NS
4	****		****	****
8	NS	****		NS
24	NS	****	NS	

25-3 MED TNF

Time	0	4	8	24
0		NS	NS	****
4	NS		NS	****
8	NS	NS		****
24	****	****	****	

1-1 PMA IL-6

Time	0	4	8	24
0		NS	NS	NS
4	NS		NS	NS
8	NS	NS		*
24	NS	NS	*	

1-1 LPS IL-6

Time	0	4	8	24
0		NS	NS	NS
4	NS		NS	NS
8	NS	NS		NS
24	NS	NS	NS	

1-1 MED IL-6

Time	0	4	8	24
0		NS	NS	NS
4	NS		NS	NS
8	NS	NS		NS
24	NS	NS	NS	

1-1 PMA TNF

Time	0	4	8	24
0		NS	NS	NS
4	NS		NS	NS
8	NS	NS		NS
24	NS	NS	NS	

1-1 LPS TNF

Time	0	4	8	24
0		*	NS	NS
4	*		NS	*
8	NS	NS		NS
24	NS	*	NS	

1-1 MED TNF

Time	0	4	8	24
0		NS	NS	NS
4	NS		NS	NS
8	NS	NS		NS
24	NS	NS	NS	

1-2 PMA IL-6

Time	0	4	8	24
0		NS	NS	NS
4	NS		NS	NS
8	NS	NS		NS
24	NS	NS	NS	

1-2 LPS IL-6

Time	0	4	8	24
0		NS	NS	NS
4	NS		NS	NS
8	NS	NS		NS
24	NS	NS	NS	

1-2 MED IL-6

Time	0	4	8	24
0		NS	NS	NS
4	NS		NS	NS
8	NS	NS		NS
24	NS	NS	NS	

1-2 PMA TNF

Time	0	4	8	24
0		***	NS	NS
4	***		***	***
8	NS	***		NS
24	NS	***	NS	

1-2 LPS TNF

Time	0	4	8	24
0		****	NS	NS
4	****		****	****
8	NS	****		NS
24	NS	****	NS	

1-2 MED TNF

Time	0	4	8	24
0		NS	NS	NS
4	NS		NS	*
8	NS	NS		NS
24	NS	*	NS	

1-3 PMA IL-6

Time	0	4	8	24
0		NS	NS	*
4	NS		NS	*
8	NS	NS		*
24	*	*	*	

1-3 LPS IL-6

Time	0	4	8	24
0		NS	NS	NS
4	NS		NS	NS
8	NS	NS		NS
24	NS	NS	NS	

1-3 MED IL-6

Time	0	4	8	24
0		NS	NS	NS
4	NS		NS	NS
8	NS	NS		NS
24	NS	NS	NS	

1-3 PMA TNF

Time	0	4	8	24
0		NS	NS	NS
4	NS		NS	NS
8	NS	NS		NS
24	NS	NS	NS	

1-3 LPS TNF

Time	0	4	8	24
0		NS	NS	NS
4	NS		NS	NS
8	NS	NS		NS
24	NS	NS	NS	

1-3 MED TNF

Time	0	4	8	24
0		NS	NS	NS
4	NS		NS	*
8	NS	NS		NS
24	NS	*	NS	

0 PMA IL-6

Time	0	4	8	24
0		NS	NS	****
4	NS		NS	****
8	NS	NS		****
24	****	****	****	

0 LPS IL-6

Time	0	4	8	24
0		NS	NS	NS
4	NS		NS	NS
8	NS	NS		NS
24	NS	NS	NS	

0MED IL-6

Time	0	4	8	24
0		NS	NS	NS
4	NS		NS	NS
8	NS	NS		NS
24	NS	NS	NS	

0 PMA TNF

Time	0	4	8	24
0		****	NS	NS
4	****		****	****
8	NS	****		NS
24	NS	****	NS	

0 LPS TNF

Time	0	4	8	24
0		****	NS	NS
4	****		****	****
8	NS	****		NS
24	NS	****	NS	

0 MED TNF

Time	0	4	8	24
0		NS	NS	****
4	NS		NS	****
8	NS	NS		****
24	****	****	****	

TCP PMA IL-6

Time	0	4	8	24
0		NS	NS	NS
4	NS		NS	NS
8	NS	NS		NS
24	NS	NS	NS	

TCP LPS IL-6

Time	0	4	8	24
0		NS	NS	NS
4	NS		NS	NS
8	NS	NS		NS
24	NS	NS	NS	

TCP MED IL-6

Time	0	4	8	24
0		****	****	***
4	****		NS	NS
8	****	NS		NS
24	***	NS	NS	

TCP PMA TNF

Time	0	4	8	24
0		****	NS	NS
4	****		****	****
8	NS	****		NS
24	NS	****	NS	

TCP LPS TNF

Time	0	4	8	24
0		****	****	****
4	****		****	****
8	****	****		NS
24	****	****	NS	

TCP MED TNF

Time	0	4	8	24
0		****	****	****
4	****		NS	NS
8	****	NS		NS
24	****	NS	NS	

PET PMA IL-6

Time	0	4	8	24
0		NS	NS	**
4	NS		NS	**
8	NS	NS		**
24	**	**	**	

PET LPS IL-6

Time	0	4	8	24
0		NS	NS	NS
4	NS		NS	NS
8	NS	NS		NS
24	NS	NS	NS	

PET MED IL-6

Time	0	4	8	24
0		NS	NS	NS
4	NS		NS	NS
8	NS	NS		NS
24	NS	NS	NS	

PET PMA TNF

Time	0	4	8	24
0		NS	NS	NS
4	NS		NS	NS
8	NS	NS		NS
24	NS	NS	NS	

PET LPS TNF

Time	0	4	8	24
0		NS	NS	NS
4	NS		NS	NS
8	NS	NS		NS
24	NS	NS	NS	

PET MED TNF

Time	0	4	8	24
0		NS	NS	NS
4	NS		NS	NS
8	NS	NS		NS
24	NS	NS	NS	

11 References

[1] Langer R, Vacanti JP. Tissue engineering. Science 1993;260:920-6.
[2] Viola J, Lal B, Grad O. The emergence of tissue engineering as a research field. National Science Foundation 2003.
[3] MacNeil S. Progress and oportunities for tissue engineered skin. Nature 2007;445:874-80.
[4] Harrison CA, MacNeil S. The mechanism of skin graft contraction: an update on current research and potential future therapies. Burns 2008;34:153.
[5] Kopeck J. Hydrogels: From soft contact lenses and implants to self-assembled nanomaterials. J Pol Sci, Part A: Polymer Chemistry 2009;47:5929-46.
[6] Eves P, Layton C, Headley S, Dawson RA, Wagner M, Morandini R, et al. Characteristics of an *in-vitro* model of human melanoma invasion based on reconstructed human skin. Br J Dermatol 2000;142:210-5.
[7] Harrison CA, Layton CM, Hau Z, Bullock AJ, Johnson TS, MacNeil S. Transglutaminase inhibitors induce hyperproliferation and parakeratosis in tissue engineered skin. Br J Dermatol 2007;156:247.
[8] Sahota PS, Burn JL, Heaton M, Freelander E, Suvarna SK, Brown NJ, et al. Development of a reconstructed human skin model for angiogenesis. Wound Rep Regen 2003;11:275.
[9] Eaglstein WH, Falanga V. Tissue engineering and the development of Apligraf®, a human skin equivalent. Clinical Therapeutics 1997;19:894-905.
[10] Steinberg JS, Edmonds M, Hurley Jr DP, King WN. Confirmatory data from EU study supports Apligraf for the treatment of neuropathic diabetic foot ulcers. J Am Pod Med Assoc 2010;100:73-7.
[11] Bhargava S, Chappell CR, Bullock AJ, Layton C, MacNeil S. Tissue engineered buccal mucosa for substitution urethroplasty. Br J Urol 2004;93:207.
[12] Schlotmann K, Kaeten M, Black AF, Damour O, Waldmann-Laue M, Forster T. Cosmetic efficacy claims *in-vitro* using a three dimensional human skin model. Int J Cosmetic Sci 2008;23:309-18.
[13] Damour O, Augustin C, Black AF. Applications of reconstructed skin models in pharmaco-toxological trials. Med & bio eng & computing 1998.
[14] Mackaness GB. THE IMMUNOLOGICAL BASIS OF ACQUIRED CELLULAR RESISTANCE. J Exp Med 1964;120:105-20.
[15] Gordon S. Alternative activation of macrophages. Nat Rev Immunol 2003;3:23-35.
[16] Dalton DK, Pitts-Meek S, Keshav S, Figari IS, Bradley A, Stewart TA. Multiple defects of immune cell function in mice with disrupted interferon-gamma genes. Science 1993;259:1739-42.
[17] Van Epps HL. Macrophage activation unveiled. J Exp Med 2005;202:884-.
[18] Mosser DM. The many faces of macrophage activation. J leukoc Biol 2003;73:209-12.
[19] MacMicking J, Xie Q-w, Nathan C. NITRIC OXIDE AND MACROPHAGE FUNCTION. Annu Rev Immunol 1997;15:323-50.
[20] Monney L, Sabatos CA, Gaglia JL, Ryu A, Waldner H, Chernova T, et al. Th1-specific cell surface protein Tim-3 regulates macrophage activation and severity of an autoimmune disease. Nature 2002;415:536-41.
[21] Chizzolini C, Rezzonico R, De Luca C, Burger D, Dayer J-M. Th2 Cell Membrane Factors in Association with IL-4 Enhance Matrix Metalloproteinase-1 (MMP-1) While Decreasing MMP-9 Production by Granulocyte-Macrophage Colony-Stimulating Factor-Differentiated Human Monocytes. J Immunol 2000;164:5952-60.
[22] Wroblewskia JM, Copplea A, Batsona LP, Landersb CD, Yannelli JR. Cell surface phenotyping and cytokine production of Epstein–Barr Virus (EBV)-transformed lymphoblastoid cell lines (LCLs). Cell Immunol 2000;204:19-28.

[23] Laskin DL. Macrophages and Inflammatory Mediators in Chemical Toxicity: A Battle of Forces. Chem Res Toxicol 2009;22:1376-85.
[24] Woodard BH, Rosenberg SI, Farnham R, Adams DO. Incidence and nature of primary granulomatous inflammation in surgically removed material. . Am J Surgical Path 1982;6:119-29.
[25] Adams DO. The granulomatous inflammatory response. A review. Am J Path 1976;84:164-91.
[26] Goerdt S, Politz O, Schledzewski K, Birk R, Gratchev A, Guillot P, et al. Alternative versus Classical Activation of Macrophages. Immunity 1999;10:137-42.
[27] Stein M, Keshav S, Harris N, Gordon S. Interleukin 4 potently enhances murine macrophage mannose receptor activity: a marker of alternative immunologic macrophage activation. J Immunol 1992;176:287-92.
[28] Crawford RM, Finbloom DS, Ohara J, Paul WE, Meltzer MS. B cell stimulatory factor-1 (interleukin 4) activates macrophages for increased tumoricidal activity and expression of Ia antigens. J Immunol 1987;139:135-41.
[29] Raes G, De Baetselier P, Noel W, Beschin A, Brombacher F, Hassanzadeh Gh G. Differential expression of FIZZ1 and Ym1 in alternatively versus classically activated macrophages. J Leukoc Biol 2002;71:597-602.
[30] Fadok VA, Bratton DL, Konowal A, Freed PW, Westcott JY, Henson PM. Macrophages That Have Ingested Apoptotic Cells In Vitro Inhibit Proinflammatory Cytokine Production Through Autocrine/Paracrine Mechanisms Involving TGF-beta, PGE2, and PAF. J Clin Invest 1998;101:890-8.
[31] te Velde AA, Klomp JP, Yard BA, de Vries JE, Figdor CG. Modulation of phenotypic and functional properties of human peripheral blood monocytes by IL-4. J Immunol 1988;140:1548-54.
[32] Anderson CF, Mosser DM. A novel phenotype for an activated macrophage: the type 2 activated macrophage. J leukoc Biol 2002;72:101-6.
[33] Doyle AG, Herbein G, Montaner LJ, Minty AJ, Caput D, Ferrara P, et al. Interleukin-13 alters the activation state of murine macrophages *in vitro*: Comparison with interleukin-4 and interferon-gamma. Eur J Immunol 1994;24:1441-5.
[34] McInnes A, Rennick DM. Interleukin 4 induces cultured monocytes/macrophages to form giant multinucleated cells. J Exp Med 1988;167:598-611.
[35] Fenton MJ, Buras JA, Donnelly RP. IL-4 reciprocally regulates IL-1 and IL-1 receptor antagonist expression in human monocytes. J Immunol 1992;149:1283-8.
[36] Doherty TM, Kastelein R, Menon S, Andrade S, Coffman RL. Modulation of murine macrophage function by IL-13. J Immunol 1993;151:7151-60.
[37] Mantovani A, Locati M, Vecchi A, Sozzani S, Allavena P. Decoy receptors: a strategy to regulate inflammatory cytokines and chemokines. Trends in Immunology 2001;22:328-36.
[38] Atochina O, Da'dara AA, Walker M, Harn DA. The immunomodulatory glycan LNFPIII initiates alternative activation of murine macrophages *in vivo*. immunology 2008;125:111-21.
[39] Reese TA, Liang H-E, Tager AM, Luster AD, Van Rooijen N, Voehringer D, et al. Chitin induces accumulation in tissue of innate immune cells associated with allergy. Nature 2007;447:92-6.
[40] Ho VW, Sly LM. Derivation and characterization of murine alternatively activated (m2) macrophages. Methods Mol Biol 2009;531:173-85.
[41] Fruchon S, Poupot M, Martinet L, Turrin C-O, Majoral J-P, Fournie J-J, et al. Anti-inflammatory and immunosuppressive activation of human monocytes by a bioactive dendrimer. J leukoc Biol 2009;85:553-62.

[42] Porcheray F, Viaud S, Rimaniol AC, Léone C, Samah B, Dereuddre-Bosquet N, et al. Macrophage activation switching: an asset for the resolution of inflammation. Clin Exp Immunol 2005;142:481-9.
[43] Rutschman R, Lang R, Hesse M, Ihle JN, Wynn TA, Murray PJ. Cutting Edge: Stat6-Dependent Substrate Depletion Regulates Nitric Oxide Production. J Immunol 2001;166:2173-7.
[44] Modolell M, Corraliza IM, Link F, Soler G, Eichmann K. Reciprocal regulation of the nitric oxide synthase/arginase balance in mouse bone marrow-derived macrophages by TH 1 and TH 2 cytokines. Eur J Immunol 1995;25:1101-4.
[45] Gratchev A, Schledzewski K, Guillot P, Goerdt S. Alternatively Activated Antigen-Presenting Cells: Molecular Repertoire, Immune Regulation, and Healing. J Scand Immunol 2001;53:386-92.
[46] Song E, Ouyang N, Hörbelt M, Antus B, Wang M, Exton MS. Influence of Alternatively and Classically Activated Macrophages on Fibrogenic Activities of Human Fibroblasts. Cellular Immunology 2000;204:19-28.
[47] Hesse M, Modolell M, La Flamme AC, Schito M, Fuentes JM, Cheever AW, et al. Differential Regulation of Nitric Oxide Synthase-2 and Arginase-1 by Type 1/Type 2 Cytokines In Vivo: Granulomatous Pathology Is Shaped by the Pattern of L-Arginine Metabolism. J Immunol 2001;167:6533-44.
[48] Goerdt S, Walsh LJ, Murphy GF, Pober JS. Identification of a novel high molecular weight protein preferentially expressed by sinusoidal endothelial cells in normal human tissues. J Cell Biol 1991;113:1425-37.
[49] Topoll HH, Zwadlo G, Lange DE, Sorg C. Phenotypic dynamics of macrophage subpopulations during human experimental gingivitis. J periodontal Res 1989;24:106-12.
[50] Flavell RA. The relationship of inflammation and initiation of autoimmune disease: role of TNF super family members. Curr Top Microbial Immunol 2002;266.
[51] Szekanecz Z, Haines G, Lin T, Harlow L, Goerdt S, Rayan G, et al. Differential distribution of ICAM-1, ICAM-2 and ICAM-3, and the MS-1 antigen in normal and diseased human synovia. Arthritis Rheum 1994;37.
[52] Rimmer S, Wilshaw S-P, Pickavance P, Ingham E. Cytocompatibility of poly(1,2 propandiol methacrylate) copolymer hydrogels and conetworks with or without alkyl amine functionality. Biomaterials 2009;30:2468-78.
[53] Djemadji-Oudjieln N, Goerdt S, Schmuth M, Orfanos C. Immunohistochemical identification of type II alternatively activated dendritic macrophages (RM 3/1+++, MS-1± 25F9−) in psoriatic dermis. Arch Dermatol Res 1996;288:757-64.
[54] Mantovania A, Sozzanic S, Locatie M, Allavenaf P, Antonio Sica S. Macrophage polarization: tumor-associated macrophages as a paradigm for polarized M2 mononuclear phagocytes. Trends Immunol 2002;23:549-55.
[55] Bryers JD, Giachelli CM, Ratner BD. Engineering biomaterials to integrate and heal: The biocompatibility paradigm shifts. Biotech and Bioeng 2012;109:1898-911.
[56] Gerber JS, Mosser DM. Reversing Lipopolysaccharide Toxicity by Ligating the Macrophage Fc{{gamma}} Receptors. J Immunol 2001;166:6861-8.
[57] Lentz AJ, Horbett TA, Hsu L, Ratner BD. Rat peritoneal macrophage adhesion to hydroxyethyl methacrylate-ethyl methacrylate copolymers and hydroxystyrene-styrene copolymers. J Biomed Mater Res 1985;19:1101-15.
[58] Smetana K, Vacik J, Souckova D, Krocova Z, Sulc J. The influence of hydrogel functional groups on cell behaviour. . J Biomed Mater Res 1990;24:463-70.
[59] Smetana K, Lukas J, Paleckova V, Bartunkova J, Liu FT, Vacik J, et al. Effect of chemical structure of hydrogels on the adhesion and phenotypic characteristics of human

monocytes such as expression of galectins and other carbohydrate-binding sites. Biomaterials 1997;18:1009-14.
[60] Fukano Y, Usui ML, Underwood RA, Isenhath S, Marshall AJ, Hauch KD, et al. Epidermal and dermal integration into sphere-templated porous poly(2-hydroxyethyl methacrylate) implants in mice. J Biomed Mater Res - Part A 2010;94:1172-86.
[61] Collier TO, Anderson Jm, Brodbeck Wg, Barber T, Healy KE. Inhibition of macrophage development and foreign body giant cell formation by hydrophilic interpenetrating polymer network. . J Biomed Mater 2004;69A:851-9.
[62] Kao WJ, Hubbell JA, Anderson JM. Protein-mediated macrophage adhesion and activation on biomaterials: a model for modulating cell behavior. J Mater Sci: Materials in Medicine 1999;10:601-5.
[63] Jenny CR, Anderson JM. Effects of surface coupled polyethylene glycol hydrogels grated with RGD and PHSRN separated by interpositional spaces of various lengths. . J Biomed Mater Res 1999;44:206-16.
[64] Brown BN, Ratner BD, Goodman SB, Amar S, Badylak SF. Macrophage polarization: An opportunity for improved outcomes in biomaterials and regenerative medicine. Biomaterials 2012;33:3792-802.
[65] Ma J, Chen T, Mandelin J, Ceponis A, Miller N, E., Hukkanen M, et al. Regulation of macrophage activation. Anglais 2003;60:2334-46.
[66] Kao WJ. Evaluation of protein-modulated macrophage behavior on biomaterials: designing biomimetic materials for cellular engineering. Biomaterials 1999;20:2213-21.
[67] Godek ML, Michel R, Chamberlain LM, Castner DG, Grainger DW. Adsorbed serum albumin is permissive to macrophage attachment to perfluorocarbon polymer surfaces in culture. J Biomed Mater Res- Part A 2009;88:503-19.
[68] Zolnik BS, Gonzalez-Fernsndez A, Sadrieh N, Dobrovolskaia MA. Minireview: Nanoparticles and the immune system. Endocrinology 2010;151:458-65.
[69] Jiang D, Liang J, Noble PW. Hyaluronan in tissue injury and repair. An Rev Cell Devel Bio 2007. p. 435-61.
[70] Sant S, Poulin S, Hildgen P. Effect of polymer architecture on surface properties, plasma protein adsorption, and cellular interactions of pegylated nanoparticles. J Biomed Mater Res-Part A 2008;87:885-95.
[71] Xia Z, Huang Y, Adamopoulos IE, Walpole A, Triffitt JT, Cui Z. Macrophage-mediated biodegradation of poly(DL-lactide-co-glycolide) in vitro. J Biomed Mater Res - Part A 2006;79:582-90.
[72] Sosnik A, Carcaboso AM, Glisoni RJ, Moretton MA, Chiappetta DA. New old challenges in tuberculosis: Potentially effective nanotechnologies in drug delivery. Advanced Drug Delivery Reviews 2010;62:547-59.
[73] El-Sherbiny IM, McGill S, Smyth HDC. Swellable microparticles as carriers for sustained pulmonary drug delivery. J Pharm Sci 2010;99:2343-56.
[74] Jain V, Singh R. Dicyclomine-loaded eudragit®-based microsponge with potential for colonic delivery: Preparation and characterization. Trop J Pharm Res 2010;9:67-72.
[75] Sabokbar A, Pandey R, Athanasou NA. The effect of particle size and electrical charge on macrophage-osteoclast differentiation and bone resorption. J Mater Sci Mater Med 2003;14:731-8.
[76] Jones KS. Assays on the influence of biomaterials on allogeneic rejection in tissue engineering. Tissue Engineering - Part B: Reviews 2008;14:407-17.
[77] Pamula E, Dobrzynski P, Szot B, Kretek M, Krawciow J, Plytycz B, et al. Cytocompatibility of aliphatic polyesters - In vitro study on fibroblasts and macrophages. J Biomed Mater Res- Part A 2008;87:524-35.

[78] Schmidt DR, Kao WJ. Monocyte activation in response to polyethylene glycol hydrogels grafted with RGD and PHSRN separated by interpositional spacers of various lengths. J Biomed Mater Res- Part A 2007;83:617-25.
[79] Anderson JM, Jones JA. Phenotypic dichotomies in the foreign body reaction. Biomaterials 2007;28:5144-20.
[80] T. A H, A. S H. Bovine Plasma Protein Adsorption onto Radiation-Grafted Hydrogels Based on Hydroxyethyl Methacrylate and *N*-Vinylpyrrolidone. Appl Chem Protein Int: ACS; 1975. p. 230-54.
[81] Alexander H, Brunski JB, Cooper SL, Hench LL, Hergenrother RW, Hoffman AS, et al. CHAPTER 2 - Classes of Materials Used in Medicine. In: Ratner BD, Lemons ASHJSE, editors. Biomaterials Science. 2 ed. San Diego: Academic Press; 1996. p. 197.
[82] Liu WF, Chen CS. Engineering biomaterials to control cell function. Materials Today 2005;8:28-35.
[83] Brandl F, Sommer F, Goepferich A. Rational design of hydrogels for tissue engineering: Impact of physical factors on cell behavior. Biomaterials 2007;28:134-46.
[84] García AJ. Get a grip: Integrins in cell-biomaterial interactions. Biomaterials 2005;26:7525-9.
[85] Tang L, Ugarova TP, Plow EF, Eaton JW. Molecular determinants of acute inflammatory responses to biomaterials. Journal of Clin Invest 1996;97:1329-34.
[86] Flick MJ, Du X, Witte DP, Jirou, x, kov, et al. Leukocyte engagement of fibrin(ogen) via the integrin receptor αMβ2/Mac-1 is critical for host inflammatory response in vivo. J Clin Invest 2004;113:1596-606.
[87] Horbett TA, Ratner BD, Schakenraad JM, Schoen FJ. CHAPTER 3 - Some Background Concepts. In: Ratner BD, Lemons ASHJSE, editors. Biomaterials Science. San Diego: Academic Press; 1996. p. 133-64.
[88] Li D, Zheng Q, Wang Y, Chen H. Combining surface topography with polymer chemistry: exploring new interfacial biological phenomena. Polym Chem 2014;5:14-24.
[89] Brock A, Chang E, Ho CC, LeDuc P, Jiang X, Whitesides GM, et al. Geometric determinants of directional cell motility revealed using microcontact printing. Langmuir 2003;19:1611-7.
[90] Jiang X, Bruzewicz DA, Wong AP, Piel M, Whitesides GM. Directing cell migration with asymmetric micropatterns. Proc Nat Acad Sci USA 2005;102:975-8.
[91] Curtis A, Wilkinson C. Topographical control of cells. Biomaterials 1997;18:1573-83.
[92] Sridharan R, Cameron AR, Kelly DJ, Kearney CJ, O'Brien FJ. Biomaterial based modulation of macrophage polarization: a review and suggested design principles. Mater Today 2015;18:313-25.
[93] Adutler-Lieber S, Zaretsky I, Platzman I, Deeg J, Friedman N, Spatz JP, et al. Engineering of synthetic cellular microenvironments: Implications for immunity. J Autoimmunity 2014;54:100-11.
[94] McWhorter FY, Wang T, Nguyen P, Chung T, Liu WF. Modulation of macrophage phenotype by cell shape. Proc of the Nat Acad Sci USA 2013;110:17253-8.
[95] Sussman EMH, M.C. Muster, J. Moon, R.T., Ratner, B.D. Porous Implants Modulate Healing and Induce Shifts in Local Macrophage Polarization in the Foreign Body Reaction. Ann Biomed Eng 2014;42:1508-16.
[96] Fryling CF, Harrington EW. Emulsion Polymerization. Ind & Eng Chem 1944;36:114-7.
[97] Harkins WD. A General Theory of the Mechanism of Emulsion Polymerization. JACS 1947;69:1428-44.
[98] Smith WV, Ewart RH. KINETICS OF EMULSION POLYMERIZATION. J Chem Phys 1948;16:592-9.

[99] Smith WV. The Kinetics of Styrene Emulsion Polymerization1a. JACS 1948;70:3695-702.
[100] Song C, Labhasetwar V, Cui X, Underwood T, Levy RJ. Arterial uptake of biodegradable nanoparticles for intravascular local drug delivery: Results with an acute dog model. J Controlled Rel 1998;54:201-11.
[101] Viota JL, Carazo A, Munoz-Gamez JA, Rudzka K, Gómez-Sotomayor R, Ruiz-Extremera A, et al. Functionalized magnetic nanoparticles as vehicles for the delivery of the antitumor drug gemcitabine to tumor cells. Physicochemical in vitro evaluation. Mater Sci Eng: C 2013;33:1183-92.
[102] Jain NK, Mishra V, Mehra NK. Targeted drug delivery to macrophages. Expert Opinion on Drug Delivery 2013;10:353-67.
[103] Panyam J, Labhasetwar V. Biodegradable nanoparticles for drug and gene delivery to cells and tissue. Advanced Drug Delivery Reviews 2012;64, Supplement:61-71.
[104] Moghimi SM, Hunter AC, Murray JC. Long-circulating and target-specific nanoparticles: Theory to practice. Pharmacol Rev 2001;53:283-318.
[105] Goodman SB. Wear particles, periprosthetic osteolysis and the immune system. Biomaterials 2007;28:5044-8.
[106] Goodman SB, Ma T. Cellular chemotaxis induced by wear particles from joint replacements. Biomaterials 2010;31:5045-50.
[107] Mark WT, Kristi SA. Hydrogels as extracellular matrix mimics for 3D cell culture. Biotech and Bioeng 2009;103:655-63.
[108] Sun T, Jackson S, Haycock JW, MacNeil S. Culture of skin cells in 3D rather than 2D improves their ability to survive exposure to cytotoxic agents. J Biotech 2006;122:372-8.
[109] Smith LM, Dobson CC. Absolute displacement measurements using modulation of the spectrum of white light in a Michelson interferometer. Appl Opt 1989;28:3339-42.
[110] Leach R, Haitjema H. Bandwidth characteristics and comparisons of surface texture measuring instruments. Meas Sci & Tech 2010;21.
[111] Baryshev SV, Zinovev AV, Tripa CE, Erck RA, Veryovkin IV. White light interferometry for quantitative surface characterization in ion sputtering experiments. Appl Surf Sci 2012;258:6963-8.
[112] Krupička A, Johansson M, Wänstrand O, Hult A. Mechanical response of ductile polymer coatings to contact and tensile deformation. Prog Org Coat 2003;48:1-13.
[113] Kurtz SM, van Ooij A, Ross R, Malefijt JD, Peloza J, Ciccarelli L, et al. Polyethylene wear and rim fracture in total disc arthroplasty. Spine 2007;7:12-21.
[114] Henke M, Brandl F, Goepferich AM, Tessmar JK. Size-dependent release of fluorescent macromolecules and nanoparticles from radically cross-linked hydrogels. Eur J Pharm Biopharm 2010;74:184-92.
[115] Goldberg M, Langer R, Jia XQ. Nanostructured materials for applications in drug delivery and tissue engineering. J Biomater Sci-Polym Ed 2007;18:241-68.
[116] Hoffman AS. Applications of thermally reversible polymers and hydrogels in therapeutics and diagnostics. J Control Rel 1987;6:297-305.
[117] Langer R. Drugs on Target. Science 2001;293:58-9.
[118] Langer R, Vacanti JP. Tissue engineering. Science 1993;260:920-6.
[119] Laroui H, Dalmasso G, Nguyen HTT, Yan YT, Sitaraman SV, Merlin D. Drug-Loaded Nanoparticles Targeted to the Colon With Polysaccharide Hydrogel Reduce Colitis in a Mouse Model. Gastroenterology 2010;138:843-U77.
[120] Lim SM, Oh SH, Lee HH, Yuk SH, Im GI, Lee JH. Dual growth factor-releasing nanoparticle/hydrogel system for cartilage tissue engineering. J Mater Sci-Mater Med 2010;21:2593-600.

[121] Lv S, Liu L, Yang W. Preparation of Soft Hydrogel Nanoparticles with PNIPAm Hair and Characterization of Their Temperature-Induced Aggregation. Langmuir 2009;26:2076-82.
[122] Paulino AT, Guilherme MR, Mattoso LHC, Tambourgi EB. Smart Hydrogels Based on Modified Gum Arabic as a Potential Device for Magnetic Biomaterial. Macromol Chem Phys 2010;211:1196-205.
[123] Wang CM, Wang DA. An injectable, nanoaggregate-based system for mesenchymal stem cell (MSC) delivery: enhancement of cell adhesion and prevention of cytotoxicity. J Mater Chem 2010;20:3166-70.
[124] Atabaev TS, Lee JH, Lee JJ, Han D-W, Hwang Y-H, Kim H-K, et al. Mesoporous silica with fibrous morphology: a multifunctional core–shell platform for biomedical applications. Nanotech 2013;24:345603.
[125] Bonner DK, Leung C, Chen-Liang J, Chingozha L, Langer R, Hammond PT. Intracellular Trafficking of Polyamidoamine–Poly(ethylene glycol) Block Copolymers in DNA Delivery. Bioconjugate Chem 2011;22:1519-25.
[126] Son SU, Jang Y, Park J, Na HB, Park HM, Yun HJ, et al. Designed Synthesis of Atom-Economical Pd/Ni Bimetallic Nanoparticle-Based Catalysts for Sonogashira Coupling Reactions. JACS 2004;126:5026-7.
[127] Wei S, Wang Q, Zhu J, Sun L, Lin H, Guo Z. Multifunctional composite core-shell nanoparticles. Nanoscale 2011;3:4474-502.
[128] Loo C, Lin A, Hirsch L, Lee MH, Barton J, Halas N, et al. Nanoshell-enabled photonics-based imaging and therapy of cancer. Tech cancer res & treat 2004;3:33-40.
[129] Hu PP, Zheng LL, Zhan L, Li JY, Zhen SJ, Liu H, et al. Metal-enhanced fluorescence of nano-core-shell structure used for sensitive detection of prion protein with a dual-aptamer strategy. Analytica Chimica Acta 2013;787:239-45.
[130] Gowd GS, Patra MK, Mathew M, Shukla A, Songara S, Vadera SR, et al. Synthesis of Fe3O4@Y2O3:Eu3+ core-shell multifunctional nanoparticles and their magnetic and luminescence properties. Optical Materials 2013;35:1685-92.
[131] Borthakur LJ, Jana T, Dolui SK. Preparation of core-shell latex particles by emulsion co-polymerization of styrene and butyl acrylate, and evaluation of their pigment properties in emulsion paints. J Coat Tech Res 2010;7:765-72.
[132] Ribeiro T, Baleizao C, Farinha JPS. Synthesis and Characterization of Perylenediimide Labeled Core-Shell Hybrid Silica-Polymer Nanoparticles. J of Phys Chem C 2009;113:18082-90.
[133] Cheng F, Lorch M, Sajedin SM, Kelly SM, Kornherr A. Whiter, Brighter, and More Stable Cellulose Paper Coated with TiO2 /SiO2 Core/Shell Nanoparticles using a Layer-by-Layer Approach. ChemSusChem 2013;6.
[134] Wang GJ, Kang CS, Jin RG. Synthesis of acrylic core–shell composite polymers and properties of plastisol–gels. Progress in Organic Coatings 2004;50:55-61.
[135] Lu M, Keskkula H, Paul DR. Thermodynamics of solubilization of functional copolymers in the grafted shell of core-shell impact modifiers: 2. Experimental. Polymer 1996;37:125-35.
[136] Majewski AP, Stahlschmidt U, Jérôme V, Freitag R, Müller AHE, Schmalz H. PDMAEMA-Grafted Core–Shell–Corona Particles for Nonviral Gene Delivery and Magnetic Cell Separation. Biomacromolecules 2013;14:3081-90.
[137] Verma NK, Crosbie-Staunton K, Satti A, Gallagher S, Ryan KB, Doody T, et al. Magnetic core-shell nanoparticles for drug delivery by nebulization. J Nanobiotech 2013;11.
[138] Darwish MSA, Kunz U, Peuker U. Preparation and catalytic use of platinum in magnetic core/shell nanocomposites. J Appl Pol Sci 2013;129:1806-11.

[139] Pelton R, Hoare T. Microgels and Their Synthesis: An Introduction. Microgel Suspensions: Wiley-VCH Verlag GmbH & Co. KGaA; 2011. p. 1-32.
[140] Rimmer S, Mohd. Ramli AN, Lefèvre S. Preparation of polystyrene-poly (styrene-g-N-isopropylacrylamide) core-shell particles: copolymerization of oligo (N-isopropylacrylamide) macromonomers and styrene onto polystyrene seed particles and stability of the resultant particles. Polymer 1996;37:4135-9.
[141] Atkin R, Bradley M, Vincent B. Core-shell particles having silica cores and pH-responsive poly(vinylpyridine) shells. Soft Matter 2005;1:160-5.
[142] Yun Y, Li H, Ruckenstein E. Hydrophobic Core/Hydrophilic Shell Amphiphilic Particles. J Colloid Interface Sci 2001;238:414-9.
[143] Hoare T, Pelton R. Highly pH and Temperature Responsive Microgels Functionalized with Vinylacetic Acid. Macromolecules 2004;37:2544-50.
[144] Liu S, Weaver JVM, Save M, Armes SP. Synthesis of pH-Responsive Shell Cross-Linked Micelles and Their Use as Nanoreactors for the Preparation of Gold Nanoparticles. Langmuir 2002;18:8350-7.
[145] Chen XY, Armes SP, Greaves SJ, Watts JF. Synthesis of Hydrophilic Polymer-Grafted Ultrafine Inorganic Oxide Particles in Protic Media at Ambient Temperature via Atom Transfer Radical Polymerization: Use of an Electrostatically Adsorbed Polyelectrolytic Macroinitiator. Langmuir 2004;20:587-95.
[146] Mori H, Hirao A, Nakahama S. Protection and polymerization of functional monomers. 21. Anionic living polymerization of (2,2-dimethyl-1,3-dioxolan-4-yl)methyl methacrylate. Macromolecules 1994;27:35-9.
[147] Jackson W, Nesti L, Tuan R. Mesenchymal stem cell therapy for attenuation of scar formation during wound healing. Stem Cell Research & Therapy 2012;3:20.
[148] Martin P. Wound Healing--Aiming for Perfect Skin Regeneration. Science 1997;276:75-81.
[149] Rimmer S, Wilshaw SP, Pickavance P, Ingham E. Cytocompatibility of poly(1,2 propandiol methacrylate) copolymer hydrogels and conetworks with or without alkyl amine functionality. Biomaterials 2009;30:2468-78.
[150] Fumarola L, Spinelli R, Brandonisio O. In vitro assays for evaluation of drug activity against Leishmania spp. Res Microbio 2004;155:224-30.
[151] Corral MJ, González E, Cuquerella M, Alunda JM. Improvement of 96-well microplate assay for estimation of cell growth and inhibition of Leishmania with Alamar Blue. J Microbio Meth 2013;94:111-6.
[152] Nakayama GR, Caton MC, Nova MP, Parandoosh Z. Assessment of the Alamar Blue assay for cellular growth and viability in vitro. J of Immunol Meth 1997;204:205-8.
[153] Zhou X, Holsbeeks I, Impens S, Sonnaert M, Bloemen V, Luyten F, et al. Noninvasive real-time monitoring by alamarBlue® during in vitro culture of three-dimensional tissue-engineered bone constructs. Tissue Engineering - Part C: Methods 2013;19:720-7.
[154] González-Pinzón R, Haggerty R, Myrold DD. Measuring aerobic respiration in stream ecosystems using the resazurin-resorufin system. J Geophys Res: Biogeosciences 2012;117:G00N6.
[155] England RM, Rimmer S. Synthesis of chain end functionalized linear and branched polymers by radical polymerisation in the presence of a silyl enol. Chem Comms 2010;46:5767-9.
[156] Tsuchiya S, Yamabe M, Yamaguchi Y, Kobayashi Y, Konno T, Tada K. Establishment and characterization of a human acute monocytic leukemia cell line (THP-1). Int J Cancer 1980;26:171-6.
[157] Qin Z. The use of THP-1 cells as a model for mimicking the function and regulation of monocytes and macrophages in the vasculature. Atherosclerosis 2012;221:2-11.

[158] Auwerx J. The human leukemia cell line, THP-1: A multifacetted model for the study of monocyte-macrophage differentiation. Experientia 1991;47:22-31.
[159] Jeon J-W, Jung J-G, Shin E-C, Choi HI, Kim HY, Cho M-L, et al. Soluble CD93 Induces Differentiation of Monocytes and Enhances TLR Responses. J Immunol 2010;185:4921-7.